Development of new barrier materials using microfibrillated cellulose

Sébastien Raynaud

Communauté
UNIVERSITÉ Grenoble Alpes

THÈSE

Pour obtenir le grade de

DOCTEUR DE LA COMMUNAUTE UNIVERSITE GRENOBLE ALPES

Spécialité : **Matériaux, Mécanique, Génie Civil, Electrochimie**

Arrêté ministériel : 7 août 2006

Présentée par

Sébastien RAYNAUD

Thèse dirigée par **Alain DUFRESNE**,
et codirigée par **David GUERIN**

préparée au sein du **Laboratoire Génie des Procédés Papetiers**

dans **l'École Doctorale Ingénierie - Matériaux, Mécanique, Energétique, Environnement, Procédés, Production (I-MEP2)**

Développement de nouveaux matériaux barrières utilisant des microfibrilles de cellulose

Thèse soutenue publiquement le **14 Février 2017**
devant le jury composé de :

Dr. Jose-Maria LAGARON
Directeur de recherche, Spanish National Research Council, président
Dr. Hélène ANGELLIER-COUSSY
Maître de conférences, Université de Montpellier II, rapporteur
Pr. Yves GROHENS
Professeur, Université de Bretagne Sud, rapporteur
Dr. Laurent HEUX
Directeur de recherche CNRS, Université Grenoble Alpes, membre
Pr. Alain DUFRESNE
Professeur, Université Grenoble Alpes, membre
Dr. David GUERIN
Ingénieur de recherche, Centre Technique du Papier, membre

Homies help homies. Always.

- Finn

Remerciements

Merci.

À mes encadrants, Pr. Alain Dufresne et Dr. David Guérin, ainsi qu'aux membres du jury Dr. Jose-Maria Lagaron, Dr. Hélène Angellier-Coussy, Pr. Yves Grohens, et Dr. Laurent Heux.

Aux autres, aussi. Du CTP, du LGP2, ainsi que de ni l'un ni l'autre.

Ça fait assez sobre, comme ça, mais je suis vraiment reconnaissant envers pas mal de personnes.

Bonne lecture !

Table of Contents

List of abbreviations

α	Mass fraction of poly(vinyl alcohol) in a composite
$\Delta H_f(T_m)$	Heat of fusion of poly(vinyl alcohol)
$\Delta H_f^\circ(T_m^\circ)$	Heat of fusion of 100% crystalline poly(vinyl alcohol)
λ	Wavelength of X-ray
χ_c	Degree of crystallinity
AKD	Alkyl ketene dimer
AZC	Ammonium zirconium carbonate
AZR	Azetidinium ring
a_w	Water activity
C	Cloisite-Na
C	Concentration of diffusing substance
CA	Citric acid
CNC	Cellulose nanocrystals
CMC	Carboxymethyl cellulose
CNF	Cellulose nanofibrils
CTP	Centre Technique du Papier
D	Diffusion coefficient
DMA	Dynamic mechanical analysis
DSC	Differential scanning calorimetry
d_{001}	Inter-layer spacing
e	Thickness
EVOH	Ethylene vinyl alcohol
FTIR	Fourier transform infrared spectroscopy
J	Rate of transfer of diffusing substance per area unit of section
K	Kaolinite
L	Laponite
LbL	Layer by layer
M_∞	Quantity of water vapour that has entered the material at equilibrium
m_d	Mass of sample equilibrated at 0% relative humidity
MFC	Microfibrillated cellulose
MFC 0-5P	MFC from kraft birch pulp with 0 to 5 passes in the homogeniser

MFC D	MFC from Domsjö pulp (sulfite softwood)
MFC KB	MFC from kraft birch pulp
MFC UM	Commercial MFC from the University of Maine
MMT	Montmorillonite
M_t	Quantity of water vapour that has entered the material at time t
m_w	Mass of sample equilibrated at given relative humidity
N	Nanofil 116
OP	Oxygen permeability
OTR	Oxygen transmission rate
p	Partial pressure of diffusing substance
P	Permeability coefficient
p_0	Water vapour saturation pressure
PA	Polyamide
PAA	Poly(acrylic acid)
PAE	Polyamidoamine epichlorohydrin
PE	Polyethylene
PEN	Poly(ethylene naphtalate)
PET	Poly(ethylene terephtalate)
PS	Polystyrene
PVC	Poly(vinyl chloride)
PVDC	Polyvinylidene chloride
PVOH	Poly(vinyl alcohol)
RH	Relative humidity
S	Solubility coefficient
$Sorp$	Water vapour sorption
SEM	Scanning electron microscopy
t	Time
TEM	Transmission electron microscopy
TEMPO	2,2,6,6-tetramethylpiperidine-N-oxyl
TGA	Thermogravimetric analysis
TR	Transmission rate
V	Volume
vol%	Volume fraction
wt%	Mass fraction
WVP	Water vapour permeability
WVTR	Water vapour transmission rate

$WVTR_{10 \text{ or } 65}$	WVTR normalised to a basis weight of 10 or 65 g/m²
x	Space coordinate measured normal to the section
XRD	X-ray diffraction

General Introduction

General Introduction

Every human eats. Some may harvest or hunt their own food, but most of them shop for it. Food thus needs to be stored and transported in a convenient way, which is achieved by the use of packaging. Packaging can also be there to protect food against different degradation mechanisms, in order to increase the shelf life of the products and limit food spoilage. This protection against gases, water, aroma, or mineral oils for example, is obtained thanks to barrier materials capable of hindering the mass transport of such substances through the packaging. Barrier properties may also be required to protect the packaging against its contents, e.g. in the case of fatty products. For these reasons, food packages are mainly made of plastics and aluminium. Papers and boards are permeable; they do not have barrier properties on their own, but can be used as a base for the application of a thin barrier top-coating. Such complex has the mechanical resistance of the base and the barrier of the top-layer. In addition to plastics and aluminium, this top-layer can be made by coating water-based emulsions/dispersions or wax.

These coating materials are mainly produced from non-renewable resources or can present issues in terms of end-of-life, giving the opportunity of developing more sustainable barrier solutions for food packaging applications. In order to achieve this, the use of biosourced and/or biodegradable polymers as a top layer on paper or board is investigated. Among biopolymers, cellulose is the most widely available and can be converted into microfibrillated cellulose (MFC) by mechanical defibrillation of cellulose fibres down to the nanometre scale. Due to the fine dimensions of its elements, MFC is able to form dense films having oxygen and grease barrier properties capable of competing with the aforementioned barrier packaging materials. MFC as a top-layer on paper or board allows producing fully biobased and biodegradable barrier packages, but its application is limited by several factors. MFC is sensitive to water and moisture, limiting its barrier performance in humid conditions. It is also highly viscous at low solid content. The high amount of water in the suspension affects the base paper network upon contact, and the low solid content makes the layer technically and economically difficult to dry on industrial coaters while reaching relevant dry coat weights.

In this framework, a PhD thesis has been performed at Centre Technique du Papier (CTP) by Guezennec (2012), investigating the use of MFC for water-based barrier coating on board. In order to address the issue of high viscosity of MFC dispersions at low solid content, MFC has been mixed with hydrosoluble barrier polymers, leading to suspensions having a final solid content acceptable for the industry. Laboratory and pilot trials highlighted the potential of MFC to be used for improving the drying behaviour of a hydrosoluble barrier polymer. Poly(vinyl alcohol) (PVOH) led to more ductile layers with a better barrier towards water vapour than starches. These layers still lack of water and moisture resistance, thus requiring an additional water and water vapour barrier layer obtained from commercial petro-sourced latex. Improving the behaviour of PVOH:MFC layers in humid conditions may enable their use as barrier top-layer without requiring an additional water or water vapour barrier layer. Also, the biobased fraction of such layer is low due to the presence of MFC as filler. It could be changed by developing a process for which MFC would be the main component, provided that its high viscosity and water content are overcome.

This thesis takes place in the framework of the development of more sustainable barrier coatings for papers and boards by the use of MFC. Two different kinds of materials were considered:

100% MFC barrier layers laminated on board, and composite barrier layers consisting of MFC as filler with application to water-based coating. The role of MFC fibrillation on the barrier performance of these two materials was studied. Strategies to overcome issues caused by the hydrophilicity of such materials, by crosslinking and addition of layered silicates, were set up and compared. Finally, the potential improvements imparted by MFC in terms of drying behaviour and dispersion of layered silicates in water based composite coatings were identified and quantified.

First, the context of barrier food packaging is more precisely described, along with the state of the art on MFC and MFC-based composite formulations with application to barrier coating (Chapter I). Then, the materials and methods used in this thesis are described (Chapter II). The degree of fibrillation of different MFC grades is described by indirect methods on suspensions and self-standing films, along with their barrier properties and application to wet lamination on board (Chapter III). The next chapter focuses on PVOH:MFC composites with application to water-based barrier coating, investigating the influence of the different MFC grades and different PVOH grades on the barrier properties, the influence of MFC on PVOH layer formation using a laboratory drying bench, and the potential of improving the behaviour of PVOH and MFC films in wet and humid conditions by crosslinking (Chapter IV). Finally, lamellar mineral fillers have been introduced in PVOH:MFC layers to improve the barrier properties, especially in humid conditions, as self-standing films and coatings on board (Chapter V). The manuscript ends with general conclusions and perspectives.

Chapter I: Literature Review

Chapter I: Literature Review

The objective of this study is to develop more sustainable barrier packaging solutions using microfibrillated cellulose (MFC). The use of biosourced and/or biodegradable polymers as barrier layers for more sustainable food packaging applications is currently widely studied. Among them, cellulose is largely available and can be converted into MFC by mechanical defibrillation of cellulose fibres down to the nanometre scale. It gives promising opportunities for using it as part of a suspension with application to water-based barrier coating, contrary to thermoplastic biopolymers that would more likely be applied by extrusion-coating or lamination.

Packaging is part of our daily life and represents a huge market. In 2011 in the European Union (UE-27), 135 kg of packaging has been consumed per capita, excluding wood, for a total of 68 million tonnes (EUROPEN, 2014). It involves a large consumption of resources and generation of wastes at a time when the consumer is more and more concerned by sustainable development, defined as a development that meets the needs of the present without compromising the ability of future generations to meet their own needs (Brundtland, 1987). The industry is also taking it into consideration for its evolution. DuPont (2012) sent a survey to 500 industry professionals related to packaging, asking to select among sustainability, food safety/security, performance, and cost, the two trends that most impact their work today and the two trends that would most impact their work in ten years. Sustainability has been selected only 32% times for North America today and 20% times for Europe today, but it rose up to 48% and 53% as expectation for ten years after for North America and Europe, respectively (DuPont Packaging & Industrial Polymers and Packaging World, 2012). This evolution requires innovation in the sector of packaging and alternatives to current methods in terms of materials, favouring renewable sources. The end-of-life also has to be taken into account, avoiding non-recyclable materials and favouring biodegradable materials when wastes can be accidentally disposed in nature by consumers.

The first section of this literature review chapter is dedicated to the context of food packaging and barrier properties. The second section focuses on microfibrillated cellulose (MFC) suspensions and films as biosourced and biodegradable barrier solutions with application to coating. The third part focuses on the use of MFC as filler in a hydrosoluble barrier polymer, and the further addition of layered silicates for reducing permeability. Finally, the fourth part describes the potential to improve the previously mentioned materials behaviour in wet contact or humid conditions using crosslinking.

I.1. In the context of barrier food packaging

I.1.1. Protecting food from spoilage

Food can be affected by its environment. Upon storage, its organoleptic properties (flavour, smell, appearance, texture) usually deteriorate progressively until it can no longer be consumed. There are several mechanisms responsible for food spoilage depending on the type of food. A variation in moisture content will affect the crispiness of cookies and pastries or, on the other hand, will lead to the desiccation of cakes. Oxygen is responsible for oxidative phenomena turning grease rancid and leading to vitamin degradation. It is also responsible for the development of aerobic bacteria (Khwaldia et al., 2010). Light is responsible for photo-catalysed oxidation leading to colour fading in meat, making it unattractive (Feldmeier, 2009). Examples of food spoilage mechanisms can be found in Table 1.

Cause of spoilage	Mechanism of spoilage	Food concerned	Protection required
Taste - rancidity	Photo-catalytic oxidation of fat	Cheese	Oxygen and light barrier
	Enzymatic hydrolysis of triglycerides	Milk	Oxygen barrier
Odour - putrid	Decomposition of proteins and amino-acids by anaerobic bacteria	Meat	Gas barrier*
Colour - browning	Oxidation of myoglobin in oximyoglobin at low O_2 pressure	Meat	Gas barrier*
Texture - softening	Hydration	Biscuits, coffee	Water vapour barrier
Packaging degradation	Grease leak	Ready-cooked dish	Grease barrier

Table 1 - Example of food spoilage mechanisms. Adapted from Huis in't Veld (1996) and Locre (2016).
*Gas barrier: oxygen, nitrogen, and carbon dioxide when under vacuum or modified atmosphere.

One role of packaging is to protect the content of the package, and in the case of food packaging it can also mean protection from these undesirable effects. In order to control the causes of spoilage, the exposure of food to light, water vapour, oxygen, and other gases has to be monitored. Concerning gases it generally consists in avoiding permeation through the package by the use of a gas barrier layer. This is the protection from permeation, i.e. mass transport though the package. Two other interactions are generally described: migration, i.e. mass transport from the package to the food, and scalping, i.e. mass transport from the food to the package. As the main contamination of a package by food is generally due to the water or grease present in the food, the package therefore requires an inner water or grease barrier layer. Regulation (EC) No 1935/2004 on materials and articles intended to come into contact with food (European Parliament, 2004) states in its Article 3 that “Materials and articles, including active and intelligent materials and articles, shall be manufactured in compliance with good manufacturing practice so that, under normal or foreseeable conditions of use, they do not transfer their constituents to food in quantities which could: (a) endanger human health; or (b) bring about an unacceptable change in the composition of the food; or (c) bring about a deterioration in the organoleptic characteristics thereof.” This article, called the principle of inertia, applies to all materials.

Some materials also benefit from harmonised European regulations, e.g. plastic materials with Commission Regulation (EU) No 10/2011 on plastic materials and articles intended to come into contact with food (European Parliament, 2011), in which a positive list authorises certain monomers and additives to be used in the manufacturing of these materials, while setting overall and specific migration limits to avoid the transfer of contaminants in too high amounts. Paper, while not regulated at European level and rarely at national levels, still have recognised recommendations available with positive lists and limits for the content and/or transfer of its constituents, e.g. BfR Recommendation on Food Contact Materials XXXVI. Paper and Board for Food Contact (Bundersinstitut für Risikobewertung, 2016). Despite these regulations, the migration of some non-intentionally added substances (NIAS) could appear such as issues linked to mineral oils (Biedermann and Grob, 2010).

I.1.2. Permeability

The protection of food by a packaging of low permeability may be necessary to avoid food spoilage. The objective of this section is to describe the theory behind permeation, and to link it to the measurement of the barrier properties of materials for food packaging application.

I.1.2.1. Theory of mass transfer

Diffusion is the result of random molecular motion, or random walk. A single molecule undergoes collisions that make it go sometimes towards a region of higher, sometimes of lower, concentration, without a preferred direction. However, considering a surface separating two regions of high and low concentration, the average amount of molecules exiting from the high concentration region will be higher than the average amount of molecules exiting from the low concentration region. As a result, on average, diffusion occurs towards regions of lower concentration (Crank, 1975).

Diffusion has been put in equation by Fick in 1855 $(Eq.1)$, based on the proportionality between the rate of transfer of the diffusing substance through a unit area of a section, and the concentration gradient measured normal to the section, i.e.

$$J = -D\frac{\partial C}{\partial x} \quad (Eq.1)$$

where J is the rate of transfer per unit area of section (in quantity of gas per unit of area and unit of time), C the concentration of diffusing substance (in quantity of gas per unit of volume), x the space coordinate measured normal to the section (in unit of distance), and D the diffusion coefficient (in squared unit of distance per unit of time) (Crank, 1975).

The case of gas diffusion through a membrane will now be considered, with a concentration C in mol/m^3. Assuming that the diffusion coefficient is independent of the coordinate normal to the section, Fick's law becomes:

$$J = D\frac{C_A - C_B}{e} \quad (Eq.2)$$

where C_A and C_B are the concentrations (mol/m^3) at both sides of a membrane of thickness e (m), considering that J (mol/(m².s)) represents the transfer from A to B.

According to Henry's law $(Eq.3)$, the gas concentration on side A and B can be linked to the gas partial pressure at the surface of the membrane:

$$C = Sp \quad (Eq.3)$$

where p is the gas partial pressure (Pa) on the side corresponding to the gas concentration C (mol/m^3), and S is Henry's solubility (mol/(m^3.Pa)). Fick's law becomes:

$$J = DS\frac{p_A - p_B}{e} \quad (Eq.4)$$

where J is expressed in mol/(m².s), and p_A and p_B are the partial pressure of gas (Pa) at both sides of the membrane.

The permeability is expressed as the product of the diffusion and the solubility coefficients:

$$P = DS \quad (Eq.5)$$

It corresponds to an intrinsic property of the membrane obtained by normalisation of the gas flow to the membrane thickness and differential pressure, expressed in mol.m/(m².s.Pa). Combining $(Eq.4)$ and $(Eq.5)$, the expression of permeability generally used for transmission experiments is:

$$P = \frac{Je}{p_A - p_B} \quad (Eq.6)$$

I.1.2.2. Measuring gas permeability

This thesis focuses on oxygen and water vapour permeability, presenting significant differences and being measured by different techniques. The most common experiment for determining a material's permeability is by applying a difference in gas partial pressure Δp, also called driving force, between the two sides of the samples of thickness e and surface S_f, and using an indicator to follow the transfer from the high partial pressure side (side A) to the low partial pressure side (side B).

In the case of oxygen permeability, the indicator of mass transfer can be a direct measure of the amount of molecules permeating through the membrane as described in standard ASTM F1927-14. The membrane separates a chamber (side A), where an oxygen flow is set up, and a coulometric sensor (side B). Each oxygen molecule permeating through the membrane is carried to the sensor by a nitrogen flow and detected. The indicator can also be the increase of the oxygen partial pressure at side B. The membrane separates a first chamber (side A), where the oxygen partial pressure is known, and a second chamber (side B), that has been flushed with nitrogen to obtain an oxygen-free atmosphere. Side B is equipped with a fluorescence sensor; at regular intervals, the sensor is excited with light from an optical fibre and answers by fluorescence depending on the oxygen concentration that can thus be determined.

In the case of water vapour permeability the main indicator used is the mass of water, using the "cup method" as described in standard ISO 2528. A cup is sealed with the membrane after being filled with a desiccant, i.e. a substance absorbing humidity, so that all water vapour inside the cup (side B) is captured by the desiccant. The cup is placed in a climatic chamber of known humidity (side A) and weighted at regular intervals. An increase in mass occurs by ambient water vapour permeating through the membrane and being confined by the desiccant. The cup can also be filled with water, instead of desiccant, leading to saturation inside the cup (100% relative humidity). In this case, permeation goes towards the exterior of the cup and the loss of mass is followed.

For all techniques a gas flow J is obtained in quantity of gas per unit of surface and of time, similar to the one described in the previous section. The transmission rate (TR) is the flow normalised to the driving force (differential pressure):

$$TR = \frac{J}{\Delta p} \equiv \frac{quantity\ of\ gas}{surface \cdot time \cdot differential\ pressure} \quad (Eq. 7)$$

Many units can be found for expressing the permeability, as the quantity of gas can be expressed in mol or cm^3(STP), cm^3(STP) corresponding to the volume of gas in standard temperature and pressure conditions. In the case of water vapour, the quantity of gas can also be expressed in g due to the measurement method. The driving force can be expressed in Pa, hPa, kPa, bar, atm, or mmHg, while the surface is generally expressed in m^2 and the time in s, h, or d.

In addition, the normalisation to the driving force is not always specified, especially concerning water vapour. For oxygen transmission, the oxygen content and gas pressure side A is generally known while side B is oxygen-free. For water vapour transmission, the driving force must generally be calculated according to the vapour pressure at the temperature of the experiment and the difference in relative humidity between side A and side B.

The transmission rate depends on the thickness of the planar material. The value obtained after normalisation to the sample thickness is the permeability (P) and is intrinsic to the material, assuming that the material is continuous and homogeneous:

$$P = TR * e \equiv \frac{quantity\ of\ gas \cdot thickness\ of\ sample}{surface \cdot time \cdot differential\ pressure} \quad (Eq. 8)$$

Once again, many units can be found in the literature. In addition to the previous discussion, the thickness of the sample can be expressed in mm or µm. It can also be expressed in m leading to a simplification with the surface in m^2, e.g. from mol.m/(m^2.s.Pa) to mol/(m.s.Pa), but doing so the physical sense of the unit is partially lost.

In this first chapter of literature review the barrier properties have been converted, if needed and if possible, into cm^3(STP).µm/(m².d.bar) in the case of oxygen permeability and g.µm/(m².d.hPa) in the case of water vapour permeability. From now on, for ease of reading, cm^3(STP) will only be written as cm^3 in oxygen permeability units. These units have been chosen because they are in the order of magnitudes for practical work and application: film of 10 to 100 µm, measurements over a few days, partial pressure of oxygen in air close to 1 bar and water vapour around 20 hPa. These units also generally give results between 10^{-3} and 10^{3}, which is more convenient for the understanding than results around 10^{-13} as can be found concerning water vapour permeability in g/(m.s.Pa) for example. Concerning multi-layer materials such as coating on board, results will mostly be expressed in terms of transmission, i.e. without normalisation to the thickness. This is due to the fact that the assumption of a continuous and homogeneous material is lost, the thickness of the coated layer is not necessarily known, and also because this unit is meaningful for papermakers.

Another aspect that has to be mentioned is the relative humidity (RH) at which the permeability is measured. In addition to have a direct effect on the differential water vapour pressure, an increased humidity can plasticise hydrophilic materials such as cellulose and affect gas permeation. For this reason, it is necessary to precise the relative humidity during the transmission experiment. However, the sample is not always perfectly equilibrated at a certain relative humidity due to a potential difference between side A and side B. This is especially the case for water vapour as a difference in humidity between the two sides is a requirement for obtaining a transmission. In this thesis, and especially in the literature review, the relative humidity associated with permeability measurements will always be the highest humidity between side A and side B in order to avoid heavy descriptions. For example, if a water vapour transmission experiment is done by decrease of the mass of a cup filled with water, sealed by the sample, and put in a climatic chamber at 50%RH, the relative humidity of the experiment is considered 100% corresponding to the equilibrium inside the cup. In this case, assuming that the experiment takes place at 23°C giving a saturation vapour pressure of $p_v(sat)$ of 28.13 hPa, the driving force is:

$$\Delta p = p(H_2O)_A - p(H_2O)_B = (100\% - 50\%) \cdot p_v(sat) = 14.07\ hPa \quad (Eq.9)$$

If the water vapour transmission experiment is done by increase of the mass of a cup filled with a desiccant, sealed by the sample, and put in a climatic chamber at 23°C 50%RH, the relative humidity of the experiment is considered 50% corresponding to the equilibrium in the climatic chamber. In this case, the relative humidity inside the cup is 0% and the driving force is also 14.07 hPa.

I.1.3. Different materials for different barriers

Different foods have different spoilage mechanisms and therefore have different packaging requirements. Cheese usually requires a slightly higher moisture barrier than meat, and cookies require a much lower oxygen barrier (Feldmeier, 2009). Carton pizza boxes require a grease barrier in order to avoid being contaminated by food, but the moisture and oxygen barrier is not important considering the short lifetime of the packaging. Meat can also be kept under a modified atmosphere

comprising 80% oxygen for preserving its red colour and 20% carbon dioxide for hindering bacteria development. In this case, in addition to oxygen, a CO_2 barrier is required (Modified Atmosphere Packaging.com, 2012).

Gas barrier is usually obtained with the use of aluminium or a polymer. The polymer to choose depends on the type of barrier required: some can protect against water vapour but are permeable to oxygen, such as polyethylene (PE) as shown in Table 2, some can protect against oxygen but are permeable to water vapour, such as ethylene vinyl alcohol (EVOH), and some do not protect against either oxygen or water vapour, such as polystyrene (PS). Polymers with a low permeability towards both water vapour and oxygen exist, such as polyvinylidene chloride (PVDC), but at a higher price. Most oxygen barrier polymers such as poly(vinyl alcohol) (PVOH), EVOH, or polyamide (PA), are affected by humidity and have to be sandwiched between two layers of low permeability towards water vapour. Thus, a low water vapour and oxygen transmission material can be obtained by association of different polymers into a multi-layer material such as polypropylene (PP)-EVOH-PE (Coexpan, n.d.). Aluminium is usually used as a sheet of a few micrometres or a layer in the nanometre range that is obtained by metallisation. It can be used in a multi-layer system poly(ethylene terephthalate) (PET)-Aluminium-PE for example, leading to almost no permeability for both oxygen and water vapour (Lange and Wyser, 2003). The protection against oxygen can be further improved by the use of oxygen scavengers, consuming the gas that would permeate in the packaging (Anthierens et al., 2011).

		Oxygen permeability $cm^3.\mu m/(m^2.d.bar)$		Water vapour permeability $g.\mu m/(m^2.d.hPa)$
Polymer	Full name	23°C 50%RH	23°C 0%RH	23°C 85%RH
PET	Poly(ethylene terephtalate)	1,000 - 5,000		21 - 84
PP	Polypropylene	50,000 - 100,000		8 - 17
PE	Polyethylene	50,000 - 200,000		21 - 84
PS	Polystyrene	100,000 - 150,000		42 - 167
PVC	Poly(vinyl chloride)	2,000 - 8,000		42 - 84
PEN	Poly(ethylene naphtalate)	500		29
PA	Polyamide		100 - 1,000	21 - 418
PVOH	Poly(vinyl alcohol)		20	1,255
EVOH	Ethylene vinyl alcohol		1 - 10	42 - 125
PVDC	Poly(vinylidene chloride)		10 - 300	4

Table 2 - Oxygen and water vapour permeability of polymers commonly used in packaging (Lange and Wyser, 2003). Upon unit conversion from original publication, oxygen permeabilities have been rounded to one significant figure.

I.1.4. Processes for producing paper-based barrier packaging

Paper is a porous and hydrophilic material that is permeable to oxygen, water vapour, water, grease, aromas, and light. In order to be an effective food packaging, its properties have to be enhanced with the addition of a barrier material. Coating is widely used in the papermaking industry

and consists in the application of a thin layer of coating material on a lignocellulosic fibres base. The deposition of the layer can be made from a melt polymer by extrusion coating, from polymer or aluminium sheets by lamination, or from a solution or suspension by water-based barrier coating.

I.1.4.1. Extrusion coating and lamination

Extrusion coating and lamination are the two main off-line processes for paper or board coating. Extrusion coating consists in the application of a polymer layer on a paper or board thanks to an extrusion device and subsequent cooling down with a chill-roll, as shown in Figure 1. Polyethylene is the most commonly used polymer along with PP, PET, or PA for example. Lamination is another process for producing a multi-layer material by association of a base (paper, board, or polymer) with a polymer or aluminium film. An adhesive is applied on the base and the film can undergo a corona treatment, after which the base and the film are glued together.

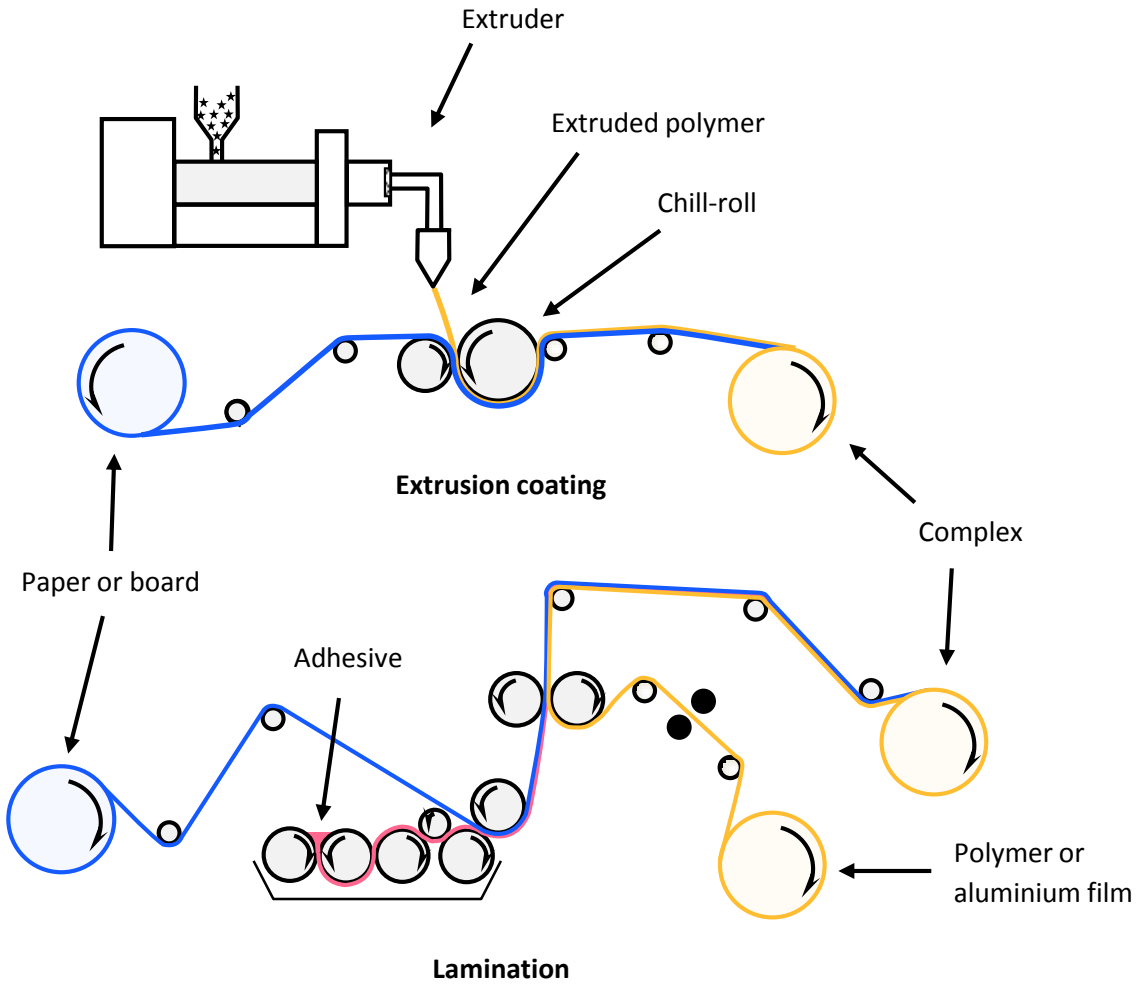

Figure 1 - Extrusion coating (top) and lamination (bottom) processes. Adapted from Girard (2011).

I.1.4.2. Water-based coating

In the case of water-based coating, the coating material at wet state is called “coating colour”. In papermaking, the water based coatings can be applied either with a decorative purpose, e.g. making the surface white, or with a functional purpose, e.g. barrier, anticorrosion, with improved printability, or anti-slip. In the case of water based barrier coatings, the coating colours are mainly polymer-based. For example, grease barrier coating colours could consist of a mixture of hydrosoluble polymer (starch) with fluorinated resin, and water or water vapour barrier colours mainly consist of a mixture of latex, based on polymers or copolymers of styrene, butadiene, acrylate, methacrylate, or vinyl acetate (Plackett, 2011), sometimes added with micro emulsioned wax.

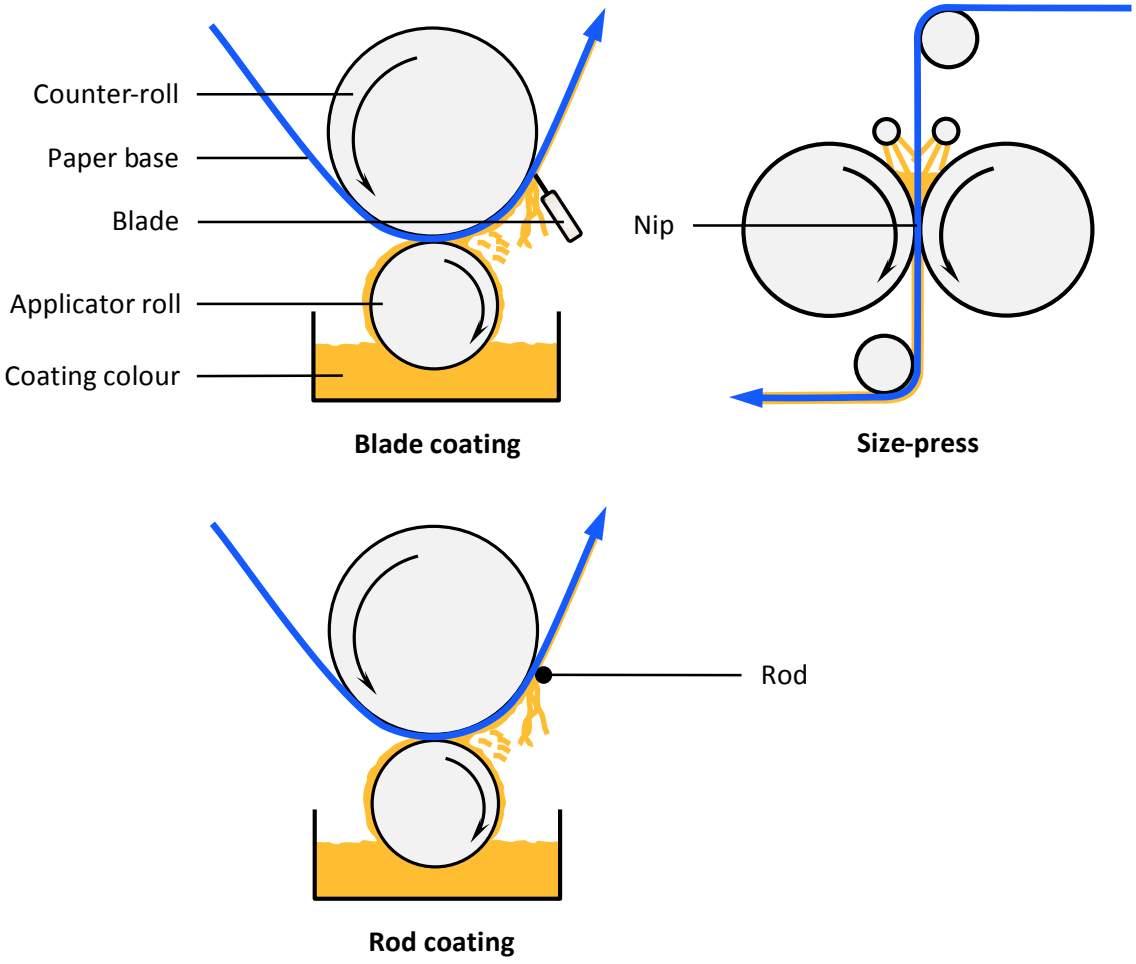

Figure 2 - Process blade coating, rod coating, and size-press. Adapted from Girard (2011).

There are plenty of processes used in papermaking to apply a water based colour onto paper: size press, metering size press, blade (stiff, bent, or bevelled), rod, curtain, slot-die, spray, or gravure coating. The most spread for barrier coating are described in Figure 2, and an example of industrial coating machine is presented in Figure 3. Size-press coating consists in an impregnation of the paper

going into a pond of coating colour delimited by two soft covered rolls under pressure, so that the base can be coated on both sides. In barrier coating, this process is mainly used to develop grease and water barrier, but is not able to form a continuous film at the surface of the paper and thus is not appropriate for gas barrier. Both blade coating and rod coating consist in the deposition of an excess of coating colour on the base, thereafter levelled at the desired coat weight by either a blade or a rod. The rod coating process offers a wider range of possible coat weights: 5 to 50 wet g/m², compared to blade coating: 5 to 20 wet g/m². Rod coating, thanks to the continuous rotation of the rod, leads to less generation of streaks and scratches caused by fibres peeled off the paper and stuck behind the metering element (e.g. the blade). However, the rod coating process is less efficient to get a full coverage of the paper and to produce a smooth surface. In addition, the development of high gas barrier coating on paper requires getting defect-free barrier layers. This is generally done in several steps, the first one being a preparation of the board substrate, using a metering size press coating, in order to prevent the further penetration of the upcoming water based coating into the substrate. This is followed by a double coating associating, first, a rod (smooth or grooved) coating, and then a blade coating on the same side in order to apply the mineral coating of aesthetic and printability purpose. A rod coating is also performed on the back side in order to ensure the flatness of the material in the end. The back side treatment can also be used in order to bring some barrier, but with limited performances since a single treatment is not leading to excellent barriers. The barrier functionality is thus generally brought by additional off-line coatings, except on the most recent machine started up in Kotka mills during summer 2016 (Hämäläinen, 2016) where barrier coating is done on-line.

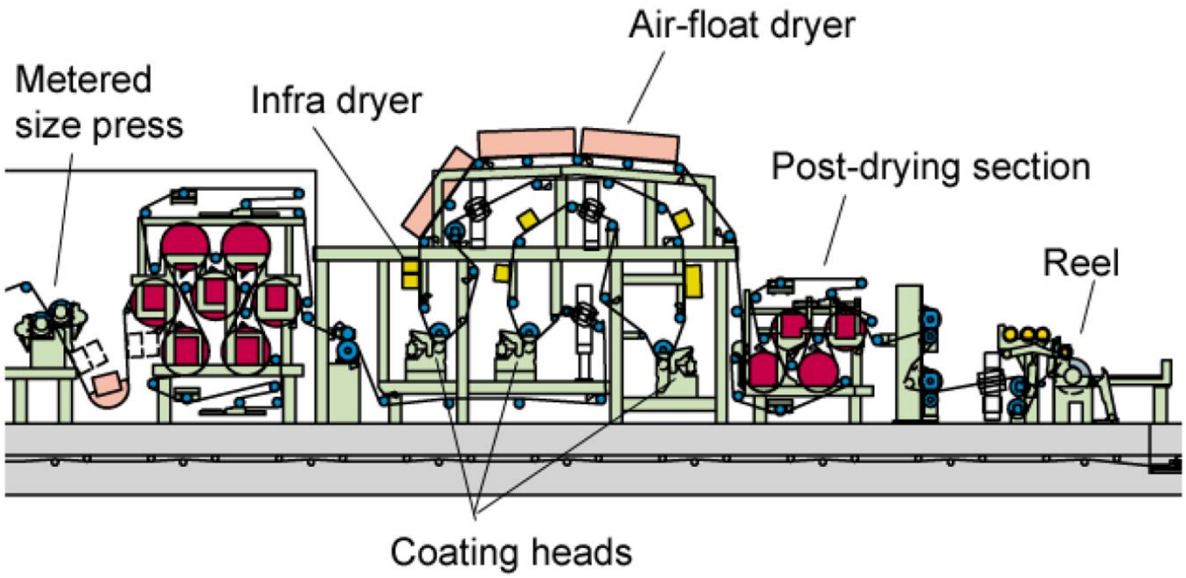

Figure 3 - Coating section of a folding boxboard machine. VTT Industrial Systems. Knowpap 8.0. Vantaa: Prowledge Oy 2006. Reprinted from Keski-Orvola (2007).

I.1.5. Life cycle of food packages

Food packaging requires barrier properties that are mainly obtained with the use of plastic packaging or complexes of paper or board with plastics, aluminium, wax, or fluorinated products.

These materials are mostly obtained from non-renewable resources or can present issues in terms of end-of-life.

According to the European Waste Hierarchy described in the Waste Framework Directive 2008/98/EC (European Parliament & Council, 2008), the preferred end-of-life solutions are :

1. Prevention: measures, taken before a material has become waste, that reduce the quantity and impact of the generated waste.
2. Preparing for re-use: checking, cleaning, or repairing recovery operations by which a material that has become waste is prepared so that it can be re-used without any other pre-processing.
3. Recycling: recovery operations by which waste materials are reprocessed into materials, whether for the original or other purposes.
4. Other recovery: other operations the principal result of which is waste serving a useful purpose by replacing other materials (e.g. energy recovery, biodegradation)
5. Disposal: any operation that is not recovery, i.e. not resulting in waste serving a useful purpose (e.g. landfill, release to sea or ocean).

As the re-use of food packaging is not a common option, except for returnable bottles, recycling should be the main end-of-life target. In the European Union (UE-27), despite a satisfying increase in recycling rate from 25% in 2005 to 34% in 2011, plastic packaging is still far below the 83% of paper and board (EUROPEN, 2014). The lower fraction of paper and board packaging ending up to incineration and landfill is also in the favour of paper and board being more sustainable (Guezennec, 2012). In a context of sustainable development, it is necessary to develop alternatives to current plastic packaging solutions and the use of paper-based packaging would be positive in terms of material source and end-of-life. It is also necessary to find alternatives to some paper-based solutions such as the non-recyclable wax paper or the use of fluorinated products that can be hazardous for human health.

I.1.6. Perspectives

More and more consumers consider the environmental impact of a product important in purchasing decisions. As a consequence, companies tend towards including environment as part of their business strategy (Tetra Pack, 2015). Using biopolymer is an interesting strategy for the replacement of non-renewable polymers. Many biopolymers directly originated from the biomass can have application in paper coating thanks to their grease or gas barrier, such as caseinates, whey protein isolate, isolated soy protein, wheat gluten, corn zein, chitosan, carrageenan, alginate, and starch (Khwaldia et al., 2010).

Among biopolymers, microfibrillated cellulose (MFC), coming from the fibrillation of lignocellulosic fibres, has been recently found to be an interesting lead thanks to its renewable source, biodegradability, and high oxygen barrier. It can be used as films, e.g. sandwiched between two bioLDPE moisture-barrier films, to form a fully biobased transparent heat-sealable barrier flexible packaging (Qvintus and Kangas, 2015). They can also be used as nanofiller in a matrix, e.g. with PLA for the extrusion of bottles or food containers with improved properties (Scalzo et al.,

2014), or as part of water-based coating colours for the formation of an oxygen-barrier layer on top of paper or board (Aulin et al., 2010).

As examples of industrial alternatives for producing barrier packaging, BASF includes Ecovio (partially made of poly(lactic acid)) in a fully-compostable anti-migration formulation, or as water-barrier for paper cups (Blum and Diehl, 2015). Mondi (2015) developed an aluminium-free film for dried instant products, specifying that thanks to this technology one of their customer was able to reduce its carbon footprint by 25%. This also led to the development of new companies proposing alternatives such as Xylophane with their Skalax: a coating material made from hemicelluloses, a carbohydrate present in wood, that is barrier to oxygen, grease, and mineral oil (Xylophane, 2014).

I.2. Microfibrillated cellulose (MFC)

I.2.1. Cellulose and nanocellulose

Cellulose is a renewable and biodegradable resource that is widely available on Earth. It is a linear polysaccharide made of a repeat unit, called cellobiose, that is a combination of two anhydroglucose rings joined via a β-1,4 glycosidic bond (Siqueira et al., 2010), as shown in Figure 4. It exists in four polymorphs (I, II, III, and IV). This study will be focused on cellulose I, namely native cellulose, which can be found mostly in wood, annual plants, and vegetables. As each anhydroglucose unit bears three hydroxyl groups, cellulose has the ability to form a strong hydrogen bond network. With this highly cohesive nature, cellulose has a fibrous structure, no melting point, and does not readily dissolve in typical aqueous solvents (Eichhorn et al., 2010).

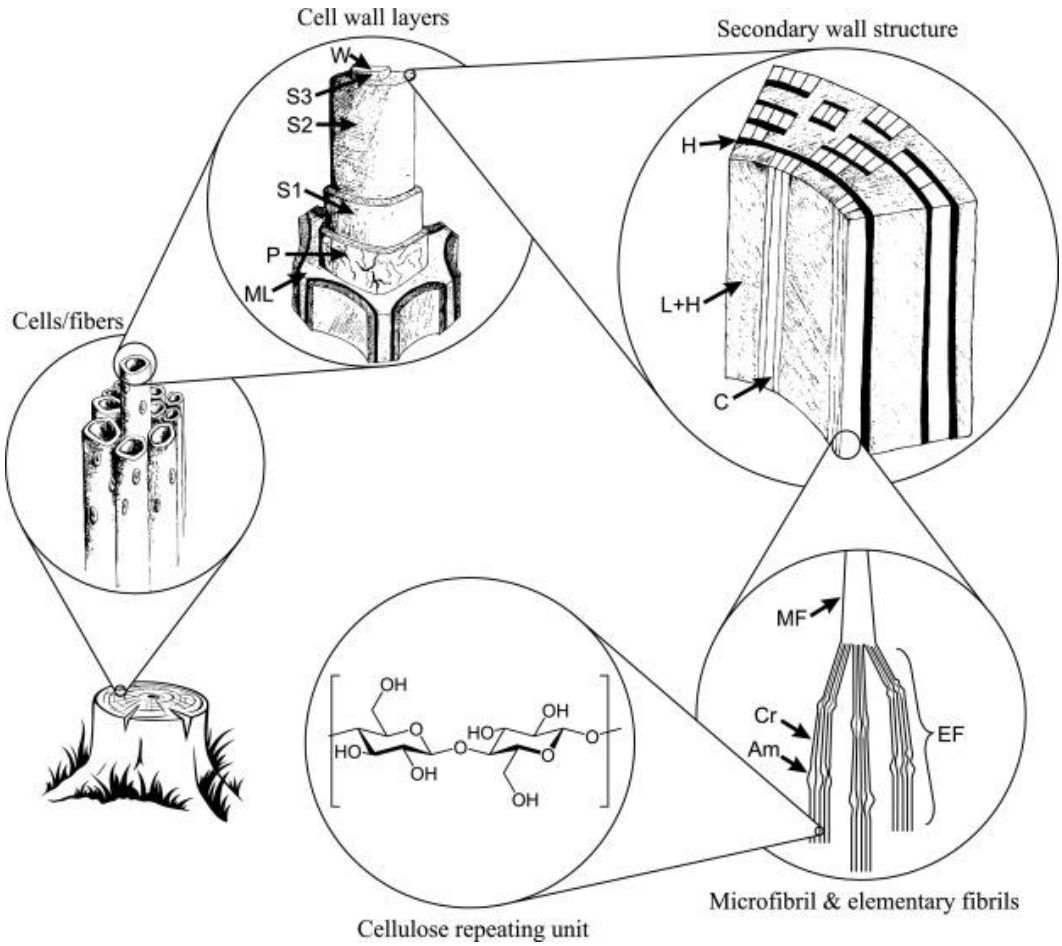

Figure 4 - Hierarchical structure of wood biomass and the characteristic of cellulose microfibrils (Nechyporchuk et al., 2016a). MF: microfibril, EF: elementary fibril, Cr: crystalline part, Am: amorphous part.

Cellulose fibres can have various dimensions depending on the source. The two main categories of wood fibres are hardwood fibres and softwood fibres that have different dimensions and chemical compositions. In the paper industry, these macroscopic fibres are often refined: the

pulp passes between two refining discs where a high shear is applied so that fibrillation occurs. This reduces the size of the fibres by cutting them and peeling them like bananas, releasing fine fibres of smaller dimensions.

Cellulose molecules are the building blocks of wood. As shown in Figure 4, they are packed into 30 to 40 chains forming individual microfibrils of about 5 to 10 nm in diameter. These microfibrils aggregate into bundles, the latter forming the cell wall of wood fibres (Isogai et al., 2011). This layout is very solid thanks to the interactions between these small elements, but a strong mechanical treatment such as several passes of a pulp suspension at high pressure (600 to 1,500 bar) in a homogenizer can break the bonds, and makes possible the individualisation of the microfibrils and microfibrils bundles (Spence et al., 2011a). The fibrous micro- or nano-scale elements present in the resulting pulp will thereafter be named "Microfibrillated Cellulose" (MFC).

MFC is made of alternately crystalline and amorphous parts. The ordered crystallites are small rods of 10 per 100 nm (Bras et al., 2010) linked together by disordered domains giving MFC its flexibility. A strong acid hydrolysis of wood pulp is able to remove all the amorphous cellulose, giving a suspension of nano-sized crystals called Cellulose Nano-Crystals (CNC) (Siqueira et al., 2009). In the literature, cellulose nano-crystals can also be found under the names of whiskers, cellulose whiskers, nano-whiskers, or crystalline cellulose nanoparticles. MFC and CNC are the two main varieties of nanocelluloses, after which can be added bacterial cellulose - very pure MFC produced by bacteria - and all sub-genres of MFC and CNC distinguished by their production process and their possible chemical modification, e.g. TEMPO-mediated oxidation (Isogai et al., 2011) or carboxymethylation (Wågberg et al., 2008).

Microfibrillated cellulose is a general term that is neither globally approved nor precisely defined for the moment. The most generally accepted terms at the moment are CNF (cellulose nanofibres) or MFC (microfibrillated cellulose), but a wide range of other names can be found in the literature referring to this material: cellulose microfibrils, cellulose nanofibrils, nanocellulose, nanofibrillar cellulose, cellulose nanofibres, cellulose filament, cellulose nanoparticles, or TEMPO-oxidised cellulose nanofibres. This may aim at being more precise about the dimensions, structure, or preparation method. There are indeed numerous grades of MFC depending on the cellulose source and the physical and chemical treatments used to produce them.

I.2.2. Production of microfibrillated cellulose

MFC can be produced from a wide range of cellulose-containing products such as wood, annual plants, fruits and vegetables, marine animals, or green algae. Concerning wood, chemical composition is of major influence in the processing of the fibres. It differs depending on the wood species and the pulping technique. Iwamoto and co-workers (2008) showed that the hemicellulose content had an important role in nanofibrillation, especially concerning dried pulp. Hemicelluloses act as inhibitors of the coalescence of microfibrils during drying, and a high content in a once-dried pulp results in a fibrillation as easy as for never-dried pulp, using a grinding technique (Iwamoto et al., 2008). A chemical treatment can be applied to the pulp before fibrillation in order to reduce the interfibrillar interactions and make the mechanical treatment more efficient, leading to smaller microfibril dimensions and a lower energy consumption (Tapin-Lingua, 2013).

I.2.2.1. Mechanical defibrillation

The main mechanical treatments used for MFC production are performed with a high pressure homogenizer, detailed thereafter, or a micro-grinder. Micro-grinder consists in fibrillation by high shear induced by a small gap between two rotating serrated disks (Taniguchi and Okamura, 1998). Other treatments can be found, such as cryocrushing (Chakraborty et al., 2005; Surip et al., 2012), sonication (Fukuzumi et al., 2009; Zhao et al., 2007), or simple stirring at low solid content in the case of chemically modified pulp (Isogai et al., 2011). This thesis focuses on MFC produced by high-pressure homogenisation.

The production of microfibrillated cellulose was born in the 80s using the high-pressure homogenization technique (Turbak et al., 1985). A pulp suspension of 2 wt% consistency is pumped through a valve that opens and closes in rapid succession so that the fibres are subjected to large pressure drops, typically of about 600 to 1,500 bars under high shearing forces, as shown in Figure 5.

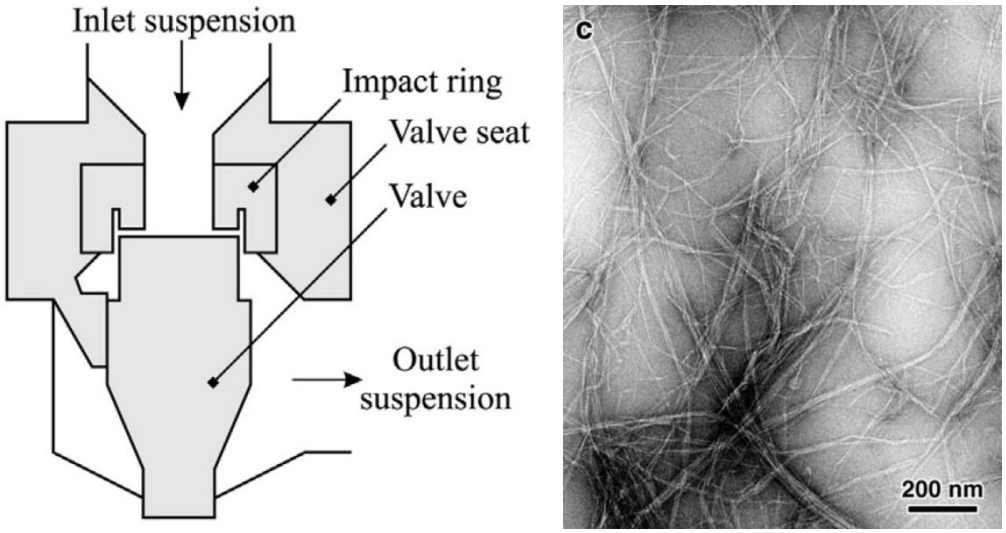

Figure 5 - Process of homogenisation (Nechyporchuk et al., 2016a) (left) and TEM picture of a MFC suspension (Velásquez-Cock et al., 2016) (right).

Most of the times, the pulp has to be mechanically treated several times to obtain a satisfying MFC suspension. Few studies report the production of homogeneous nanofibres with no resulting macro-elements, for example with a single pass through a micro-grinder after several pre-treatments (Abe et al., 2007). In the case of homogenizers, a previous reduction of the fibres dimensions is required in order to avoid clogging the apparatus, as the suspension has to flow through a small orifice (Andresen et al., 2006). It is usually performed by refining (Spence et al., 2010b) or blending (Bhattacharya et al., 2008).

Guezennec (2012) compared the morphological properties of MFC suspensions produced by homogenization and grinding, homogenized MFC were composed of thinner elements while ground MFC had a better homogeneity. These techniques can be also combined: Hassan and co-workers (2012) used a grinding treatment for a first fibrillation and then performed a high-pressure homogenization that resulted in smaller and more homogenous MFC.

I.2.2.2. Pre-treatment of the pulp

The mechanical fibrillation of cellulose fibres requires a high amount of energy and very harsh conditions. A pre-treatment can be applied in order to reduce the interactions between nanofibres and make the defibrillation easier. The main pre-treatments for the production of microfibrillated cellulose are enzymatic pre-treatment (detailed thereafter), or chemical pre-treatments such as TEMPO-mediated oxidation or carboxymethylation. TEMPO-mediated oxidation consists in oxidising the C6 primary alcohol group of cellulose to aldehyde and carboxyl groups, inducing repulsion between the fibrils. Carboxymethylation consists in substituting the hydrogen in the cellulose C6 primary alcohol group by a carboxymethyl group CH_2-COOH, inducing repulsion between the fibrils and steric effect. Other chemical pre-treatments are reported in the literature, such as periodate-chlorite oxidation, sulfonation, or quaternisation (Nechyporchuk et al., 2016a).

Cellulase refers to a group of enzymes that catalyse the cellulolysis, i.e. the hydrolysis of cellulose. The main sorts of cellulases are endoglucanase, exoglucanase and β-glucosidase. A schematic diagram of their impact on cellulose can be found in Figure 6. Endoglucanase randomly hydrolyses β-1,4-glucosidic bonds, exoglucanase releases soluble cellobiose or glucose from the chain termini, and β-glucosidase hydrolyses cellobiose to glucose (Dufresne, 2012). The use of a monocomponent endoglucanase is preferred for an enzymatic pre-treatment as it allows a selective hydrolysis of the non-crystalline cellulose and promotes cell wall delamination, while exoglucanase and β-glucosidase would rather be responsible of the release of glucose units and depolymerisation (Nechyporchuk et al., 2015; Pääkkö et al., 2007). After refining the pulp in order to increase the accessibility for the enzymes, the latter are added in the pulp suspension at controlled pH and temperature, under stirring, and neutralized after the desired time for example by increase of temperature (Henriksson et al., 2008). After washing, the mechanical treatment can be applied.

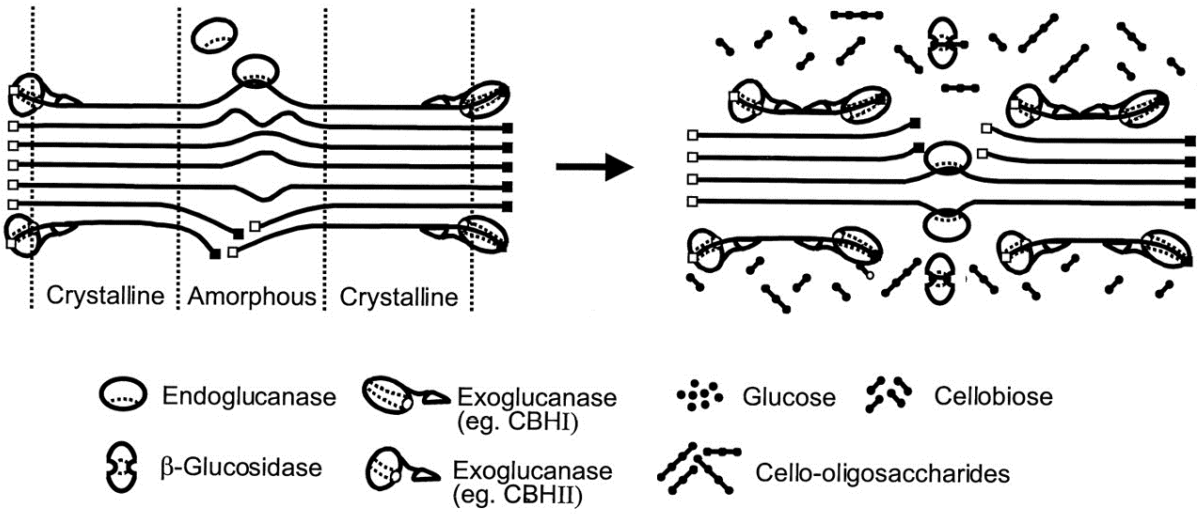

Figure 6 - Schematic diagram of different cellulase impacts on cellulose. Adapted from Lynd and co-workers (2002).

I.2.3. Applications

MFC have promising applications in numerous fields thanks to their high mechanical properties, biocompatibility, ability to form a strong network, and high viscosity at low solid content.

Bacterial cellulose (BC) has potential uses in food for colour and flavour change, or as thickening, gelling, stabilizing, water-binding, or packing material (Shi et al., 2014). It could also be used in pharmaceutics for example as part of a wound-healing patch for application to traumatic tympanic membrane perforation (Kim et al., 2013). MFC can be combined with inorganic particles such as metal ions and oxides, carbon nanotubes, or conductive polymers, in order to produce a biocompatible material for microelectronic devices. Such material has possible application in matrix or scaffold for stimulated drug release devices, implantable biosensors, and neuronal prostheses (Shi et al., 2013). Because of strong interactions and dense network, films of high transparency and haze can be produced with possible application as low cost top-layer for solar panels (Fang et al., 2014).

With MFC it is possible to create low density materials such as aerogels that can absorb up to 96 times their own dry weight in oils or organic solvent (Zheng et al., 2014); such hydrophobic and oleophilic foams can be used for water cleaning. With a higher but still low density, MFC foams of low thermal conductivity can be produced in combination with starch for insulation (Yildirim et al., 2014). CelluComp (2013) has pointed out the use of MFC in paints and coatings for rheology modification, better film forming, and better film resistance. Its use in CMC-containing pigment coating formulations has been investigated by Aalto University and Omya International AG (Dimic-Misic et al., 2013). It can in particular increase the crack resistance, as patented in the case of acrylic paints and coatings (Van Engelen et al., 2014a), and demonstrated in the case of PVOH:MFC coating with the reduction of the blistering effect upon drying (Guezennec, 2012). The rheology of MFC suspensions is also adapted to allow its use as drilling fluid (Van Engelen et al., 2014b).

Microfibrillated cellulose is also studied for the production of anti-bacterial materials. A recent PhD surveyed this field and demonstrated the ability of tight MFC networks to increase the efficiency and duration of an anti-bacterial molecule release (Lavoine, 2014). Other publications deal with the association of MFC with anti-bacterial metals by electrostatic assembly, such as silver nanoparticles and titanium (Xiao et al., 2013), or ZnO nano-particles (Martins et al., 2013), for application in food packaging. Another promising property of microfibrillated cellulose is its ability to form films of low permeability, in particular towards oxygen. A direct application of this property is the design of barrier materials, which are of great interest in the field of food packaging. MFC are studied as self-standing film or part of a multi-layer material, e.g. by coating (Aulin et al., 2010). Another application is the production of membranes with controlled permeation such as selective permeation of hydrogen molecules (Fukuzumi et al., 2013) or membranes for water cleaning in order to remove impurities, such as dysentery or cholera, by filtration (Ma et al., 2013), or dyes, arsenic, heavy metal ions by filtration and adsorption (Mathew et al., 2014). Finally, the most studied application of MFC is the production of materials with improved mechanical properties by using MFC as reinforcement in a polymer matrix (Siqueira et al., 2010).

MFC has many applications in a wide number of fields. As a result, and in combination with the regular improvement in terms of MFC production processes, the interest in the industrial production of this material is increasing. The global nanocellulose production capacity increased from 9 t/y (ton per year) in 2009 to more than 1,000 t/y in 2014. It is expected to continue to grow up to about 10,000 t/y by 2024 considering an optimistic forecast (Future Markets, 2014). Nowadays many pilot scale MFC production facilities have developed with a production capacity of 3 to 100 t/y, such as FCBA/CTP (France), Innventia (Sweden), or Nippon Paper (Japan). In the recent years, MFC production at commercial scale saw the day with a capacity of about 150 t/y for the US Forest

Service/University of Maine and 350 t/y for CelluForce, Inc./Domtar. This development continues towards industrialisation, with Borregaard investing about 25 M€ for a MFC production plant having a capacity of 1,000 t/y (Borregaard, 2014).

I.2.4. Properties of MFC suspensions

The properties of MFC suspensions strongly depend on their degree of fibrillation and their eventual chemical modification. A chemical pre-treatment such as TEMPO-mediated oxidation leads to the formation of anionic groups and thus repulsion between the nanofibrils allowing an easier fibrillation. As a consequence, such MFC suspensions have very few residual macro-fibres and appear as translucent gels. Non-modified MFC suspensions appear as white gels being more or less smooth depending on the fraction of residual macro-fibres and fines, observable by scanning electron microscopy (SEM), as shown in Figure 7.

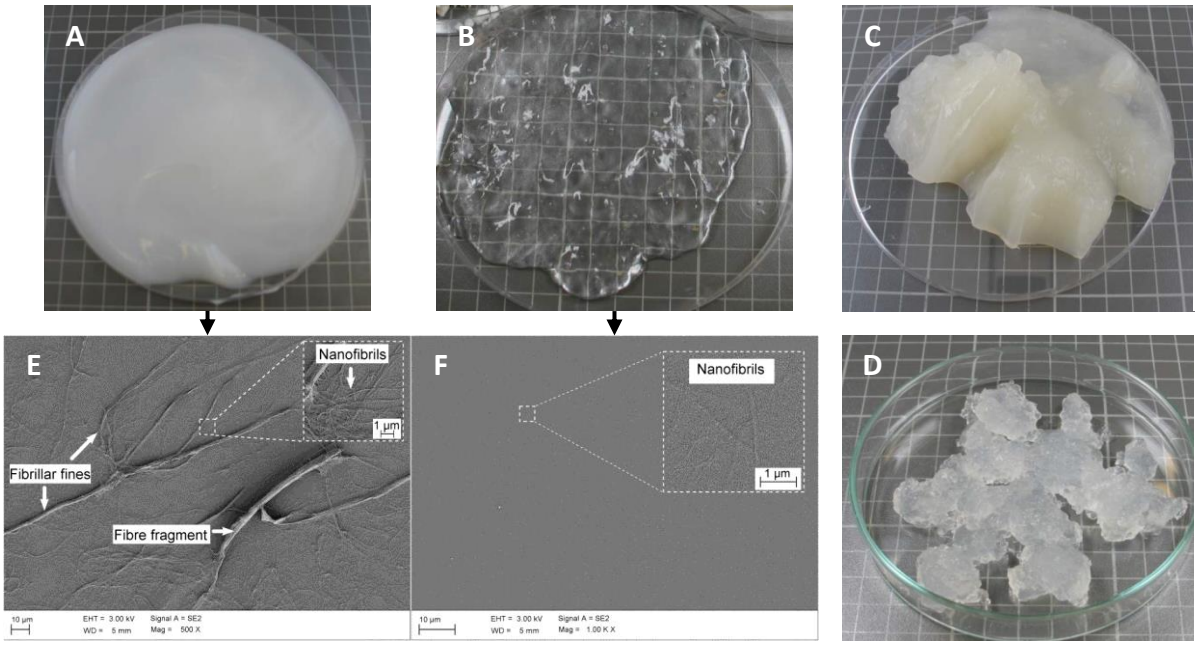

Figure 7 - Visual appearance of non-modified (A) and chemically pre-treated MFC suspensions. Pre-treatments are TEMPO-mediated oxidation (B), carboxymethylation (C), and quaternisation (D) (Pöhler et al., 2010). SEM pictures of MFC suspensions dried on glass slides without chemical pre-treatment (E), picture width 235 µm, and with a TEMPO-mediated oxidation pre-treatment (F), picture width 115 µm (Chinga-Carrasco, 2011).

I.2.4.1. Degree of fibrillation

To our knowledge, no standard conditions are used to determine the diameter of the microfibrils. In addition, the production of MFC often leads to the obtaining of a fraction of macro-fibres residues that can eventually be eliminated by filtration (Fukuzumi et al., 2009). Chinga-Carrasco and co-workers (2014) studied the effect of macrofibres residue removal and observed a reduction in surface roughness of cast films from 1 µm to 0.5 µm by fractionation.

Lignin acts as binding agent in wood fibres and has been found to interfere with defibrillation. Spence and co-workers (2010a) produced MFC with several pulps by refining and subsequent treatments with a homogenizer. They observed an increase in average microfibril diameter from 79 nm for a 0.80 wt% lignin bleached softwood pulp to 265 nm for a 14 wt% lignin unbleached softwood pulp. The same trend was observed for hardwood pulps. As a matter of comparison the same treatment has been applied to a 31 wt% lignin thermo-mechanical pulp, resulting in fibrils of about 1 µm average diameter. For this reason, most of the works on MFC films are performed using bleached pulps (Spence et al., 2010a).

Arola and co-workers (2013) studied the influence of another wood component on the MFC network formation: hemicelluloses. Bleached kraft hardwood pulp has been mechanically treated with a microfluidizer and films have been produced with or without an enzymatic treatment comprising xylanase for hemicellulose removal. This treatment allowed removing 32% to 36% of the xylan, corresponding to the accessible fraction located on the microfibrils, and resulted in an increase in film density, evidencing a tighter network (Arola et al., 2013). Similar results have been observed on a non-microfibrillated pulp, along with a reduction of the pores dimensions upon removal of hemicellulose (Oksanen et al., 1997). As previously mentioned, hemicelluloses act as inhibitors of the coalescence of microfibrils during drying and facilitate the nanofibrillation of once-dried pulp (Iwamoto et al., 2008).

The characterisation of the degree of fibrillation of MFC by a direct measurement of size distribution is difficult due to their high length compared to small diameter and due to their possible multi-scale distribution: nano-elements mixed with residual macro-sized fibres. The fibrillation is usually measured by indirect methods such as rheology, specific surface area, or the mechanical properties of resulting films (Kangas et al., 2014). A recent patent also propose the monitoring of a MFC suspension quality by analysis of turbidity (Nuopponen et al., 2016).

I.2.4.2. Rheology

The rheology of MFC suspensions has been recently reviewed by Nechyporchuk and co-workers (2016b), who distinguish two main types of microfibrillated cellulose: MFC with or without a chemical modification. Without chemical modification they possess a highly flocculated structure, while with chemical modification they possess better colloidal stability and do not evidently flocculate (Nechyporchuk et al., 2016b).

MFC suspensions have a high viscosity at low concentration (usually 1 or 2 wt%) due to their high specific surface area and ability to form hydrogen bonds. This is positive for an application as rheology modifier, but it is a drawback for an application in water-based barrier coating. The application of a MFC suspension at 2 wt% as water-based barrier coating is not convenient as it requires evaporating the 98 wt% of water. It limits the achievable coat weight due to limits in industrial coating machines drying capacities, capable of drying from 130 kg/(h.m) (kilogram of water per hour and per meter in width), for a small board machine, up to 260 kg/(h.m) for a large and modern machine (Guezennec et al., 2014). In practice, it limits the dry MFC coat weight below 0.5 g/m².

Guezennec increased the solid content of MFC suspensions by centrifugation and by inverted dialysis. Suspensions of up to 6.3% and 10.9% have been obtained, respectively, but there are few benefits in using this concentrated material for coating. The increase in solid content led to an increase in viscosity of at least one order of magnitude that puts it out of the viscosity range required for coating processes. In addition, centrifugation may result in a loss of the smallest elements that could stay in the aqueous phase thrown out, and inverted dialysis induced a strong aggregation of the microfibrils (Guezennec, 2012). The possibility of using such concentrated suspensions by reducing their viscosity, e.g. using a surfactant (Iotti et al., 2010), is a current problematic but will not be discussed in the framework of this thesis.

An alternative to the low solid content is the use of MFC as filler in a composite formulation. Adding MFC to a hydrosoluble polymer solution will affect its viscosity but it can be controlled by monitoring the fraction of MFC present in the composite. Keeping a low amount of MFC may enable its use in a water-based formulation for coating while having a higher solid content of 15 wt% in the case of poly(vinyl alcohol) for example (Guezennec, 2012).

I.2.5. Properties of MFC films

It has been seen in the previous section that there are interests in using MFC in the wet state, e.g. for rheology modification, but most of the applications are related to the ability of MFC to form a dense network upon drying. Therefore, dry MFC films, also called nanopaper (Sehaqui et al., 2014), have been studied and produced using various techniques and conditions. Other dry MFC materials can be produced, such as aerogels by freeze-drying (Pääkkö et al., 2008), filaments by wet-spinning (Lundahl et al., 2016) or even complex structures by 3D-printing (Sydney Gladman et al., 2016), but will not be detailed here because they do not apply to the formation of barrier layers.

I.2.5.1. Production of MFC films

The most popular film production method is solvent casting, where a MFC suspension of a few tenth of wt% is stored at monitored temperature (23 to 65°C) and humidity (mostly 50%RH or ambient) so that free-drying occurs. This process is based on the slow evaporation of the solvent, which is water in most of the cases, and takes from 1 to 5 days (Arola et al., 2013; Rodionova et al., 2012; Spence et al., 2010a; Taniguchi and Okamura, 1998).

The second common method for the production of MFC films makes use of a handsheet former. It includes a first step of filtration of the MFC suspension at a few tenth of wt%, through a nanoporous membrane, in order to increase the consistency to 5 to 15 wt% and obtain a concentrated flat wet MFC cake. After that, the wet cake can freely dry overnight (Arola et al., 2013) or under vacuum at 93°C during 10 minutes (Sehaqui et al., 2010). The hot-pressing at 100°C of filtrated MFC wet cakes has also been investigated, the hot-pressing time having a high influence on the mechanical properties of the resulting MFC films (Österberg et al., 2013).

I.2.5.2. Structure of MFC films

Microfibrillated cellulose films are homogeneous, strong, translucent, biodegradable, and smooth to a submicrometer level (Taniguchi and Okamura, 1998). Upon drying, the microfibrils get closer to each other and form a dense network thanks to strong electrostatic interactions. This network tends to have a layered structure, as observed on fracture surfaces in Figure 8, and pores in the nanometre range: 3 to 200 nm using microfibrils of 30 to 90 nm in diameter (Sehaqui et al., 2014).

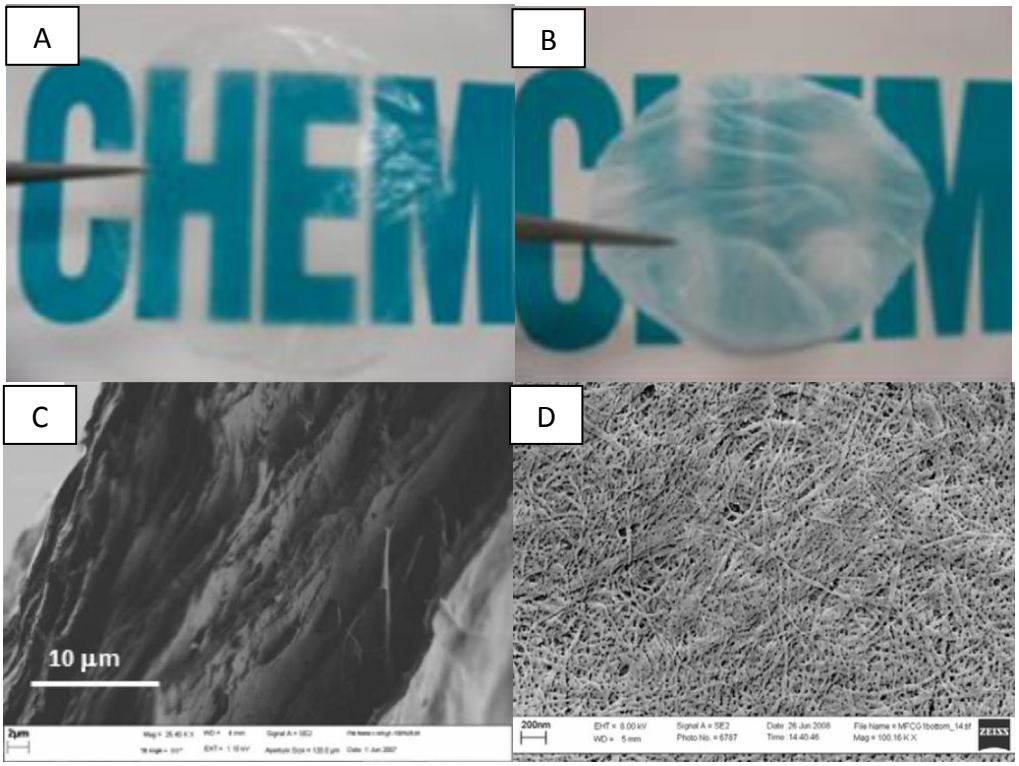

Figure 8 - MFC films from spruce (A) and eucalyptus (B) (Rodionova et al., 2012), MFC film section (C) (Plackett et al., 2010) and top surface (D) (Minelli et al., 2010).

The term microfibrillated cellulose includes a vast number of grades with different chemical compositions, treatments, and morphologies, among others. They will have a different behaviour concerning network formation and film properties, with in addition the influence of the drying conditions. These differences can be firstly observed in terms of density. As a matter of comparison, the density of reference materials are given: 1.48 g/cm^3 for amorphous cellulose (Chen et al., 2004), 1.63 g/cm^3 for crystalline cellulose I_β (Diddens et al., 2008), and 0.21 g/cm^3 for a film cast from untreated bleached softwood pulp (Spence et al., 2010a).

MFC films have a crystallinity of 50% to 75% (Fukuzumi et al., 2009; Sehaqui et al., 2014), thus fixing the theoretical density of non-porous pure cellulose microfibrils networks at 1.56 to 1.59 g/cm^3. According to Table 3, films with a density close to these target values are obtained along with lower values below 0.90 g/cm^3. This highlights the large differences that can be found between different MFC grades.

Pre-treatment	Source	Diameter (nm)	Density (g/cm^3)
Only mechanical	(Spence et al., 2010a)	1,006	0.51
		140	0.78
		265	0.79
		79	0.86
		62	0.90
		85	0.97
	(Sehaqui et al., 2014)	62	0.51
	(Syverud and Stenius, 2009)	-	1.07
	(Arola et al., 2013)	-	1.20
	(Belbekhouche et al., 2011)	52	1.33
Enzymatic pre-treatment	(Guezennec, 2012)	-	0.76
		-	1.16
	(Henriksson et al., 2008)	-	1.20
	(Minelli et al., 2010)	24	1.35
TEMPO-mediated oxidation	(Rodionova et al., 2012)	-	0.85
		-	1.43
	(Fukuzumi et al., 2009)	4	1.45
	(Fujisawa et al., 2011)	-	1.47
		-	1.51
Carboxymethylation	(Minelli et al., 2010)	9	1.10
	(Aulin et al., 2010)	8	1.57

Table 3 - Diameter of MFC in suspension and density of the resulting films.

I.2.5.3. Mechanical properties

MFC films are reported to be tough and high barrier to gases, as could be expected for such a dense and highly crystalline material. High Young's moduli of 6 to 15 GPa and tensile strengths of 100 to 200 MPa are commonly reported (Arola et al., 2013; Spence et al., 2010a; Syverud and Stenius, 2009). However, due to the important differences in MFC films structure, a high deviation from these standard values can be observed with for example a Young's modulus of 0.89 GPa for low density films (0.51 g/cm^3) cast in ethanol solvent (Sehaqui et al., 2014), and of 30 GPa for a high density film (1.57 g/cm^3) from carboxymethylated MFC at 5%RH (Aulin et al., 2010). In addition to their structure, as reported in the previous section, humidity plays a major role in the properties of MFC films. The same films that had a 30 GPa modulus at 5%RH get down to 19 GPa at 95%RH. This effect of humidity can be reduced by crosslinking of the nanofibres, which is reported in I.4, page 64. The hot-pressing of MFC films has been reported to lead to hornification, improving the mechanical performance after 2 h soaking in water compared to non-hot-pressed samples (Österberg et al., 2013). Concerning ductility: elongations at break are commonly reported in the range of 3 to 8% (Fukuzumi et al., 2009; Syverud and Stenius, 2009), and higher values of about 13% can be found in the case chemically pre-treated MFC (Siró et al., 2011).

I.2.5.4. Barrier properties

I.2.5.4.1. Oxygen barrier

The effect of humidity on the oxygen barrier of MFC films is even more significant than on the mechanical properties. Liu and co-workers (2011) produced MFC films by vacuum filtration and investigated the oxygen barrier properties at different relative humidity. The oxygen permeability (OP) of the material was of 47 cm^3.µm/(m².d.bar) at 50%RH and increased by a factor 371 at 95%RH, reaching a value of 17,600 cm^3.µm/(m².d.atm). The OP at 0%RH was under the detection limit of the apparatus (Liu et al., 2011). Another work reports an oxygen permeability at 0%RH as low as 1.7 cm^3.µm/(m².d.bar) (Fujisawa et al., 2011). These results are in good accordance with a potential use in food packaging, as it is recommended for modified atmosphere packages to have an oxygen transmission rate below 20 cm^3/(m².d.bar) (Syverud and Stenius, 2009), which could be theoretically reached with a low thickness of material except at high relative humidity.

Cellulose is hydrophilic and its water adsorption at equilibrium increases with relative humidity, as show in Figure 9. A moisture content of 6% to 7% at equilibrium under 50%RH is usually reported. This value can vary depending on the water affinity, which can be influenced by a chemical pre-treatment. For example, Minelli and co-workers (2010) showed that carboxymethylated MFC films (G2) had a higher water uptake compared to enzymatically pre-treated MFC films (G1), as can be observed in Figure 9. Water is a plasticizer for amorphous cellulose and weakens the bonds between microfibrils, decreasing the compact nature of the MFC layer. In presence of water, the microfibrils are less tightly bound, more able to move and to let molecules pass through the network (Minelli et al., 2010). In addition, the presence of water in a MFC film is responsible for an increase in gas solubility (Aulin et al., 2010). For these reasons, the permeability increases with moisture content thus reducing the effectiveness of MFC as barrier material at high relative humidity.

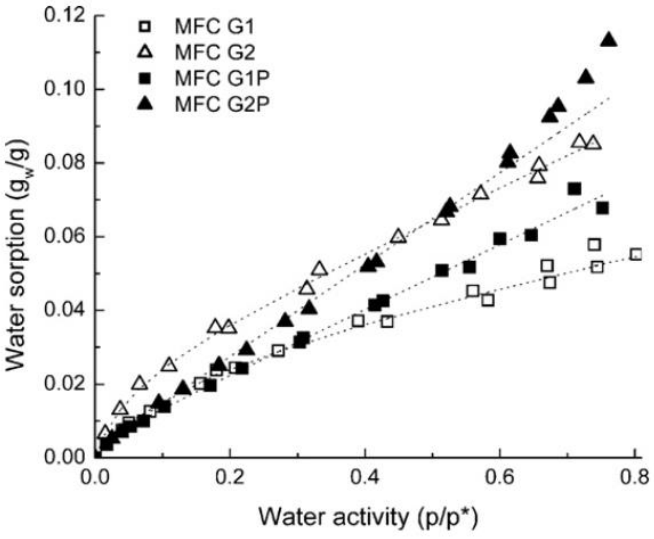

Figure 9 - Water vapour sorption isotherms in MFC films at 35°C (Minelli et al., 2010).
G1: enzymatic pre-treatment. G2: carboxymethylated. P: plasticized with 33 wt% glycerol.

I.2.5.4.2. Water vapour barrier

Due to their hydrophilicity, MFC films are not good barrier to water vapour and few publications deal with their water vapour permeability as self-standing films. The lowest water vapour permeability (WVP) obtained by Spence and co-workers (2010b) is 1,900 g.µm/(m².d.hPa) at 23°C 50%RH. Results in the same order of magnitude have been found for MFC films produced with an enzymatic pre-treatment: 3,280 g.µm/(m².d.hPa), and after a TEMPO-mediated oxidation post-treatment: 7,950 g.µm/(m².d.hPa) (Bardet et al., 2015). The barrier properties of polymers such as polypropylene or polyethylene are in the range of 8 to 17 and 21 to 84 g.µm/(m².d.hPa), respectively, at 23°C 85%RH (Lange and Wyser, 2003), and it has to be noted that the comparison is made at different relative humidities and the WVP of the MFC films is expected to be even higher at 85%RH.

I.2.6. MFC layer for paper coating applications

It has been seen that self-standing MFC films show promising barrier properties. In order to create a new packaging material using the barrier properties of MFC, coating appears to be a fitted technique as it allows having both a thin layer of MFC and a good strength and stiffness thanks to the base. MFC coating can also be used for improving printing quality thanks to its hydrophilic behaviour. An AKD-treatment reduces print-through, but its hydrophobic behaviour is also responsible for a reduction of ink density. A thin layer of MFC coated on an AKD-treated paper helps the drops of ink to spread in a controlled manner and not retract, giving improvement in the ink density in solid fill areas, from 0.74 after AKD sizing and calendering to 0.83 after MFC coating, while the reduction of print-through thanks to AKD is preserved (Luu and Bousfield, 2011).

I.2.6.1. MFC as top-layer

I.2.6.1.1. MFC top-layer obtained by casting or handsheet former

This section will explore the studies where MFC has been used as a coating agent without addition of another material. As the dry content of MFC suspensions is very low, usually about 2 wt%, it is difficult to obtain a satisfying coating weight with common water-based coating techniques. For this reason other techniques have been first considered, such as casting on the base or the production of a MFC top-layer thanks to a dynamic handsheet former.

Fukuzumi and co-workers (2009) formed a thin layer of TEMPO-oxidised MFC on a 25 µm thick PLA film by casting. With a 0.4 µm thick layer of TEMPO-oxidised MFC, the oxygen transmission has been reduced to 100 $cm^3/(m^2.d.bar)$[1]. Another work from Fujisawa and co-workers (2011) studies the coating of TEMPO-oxidised cellulose nanofibres on a polymer. This time it is not a biosourced polymer: the base is PET and the permeability of a 1 µm thick TEMPO-oxidised MFC layer was of 4.9 $cm^3.µm/(m^2.d.bar)$, when the permeability of PET is of 1,550 ($cm^3.µm/(m^2.d.bar)$. Changing the counter-ion of the TEMPO-oxidised MFC to sodium led to a permeability reduced to 0.17 $cm^3.µm/(m^2.d.bar)$ for a 1 µm thick layer (Fujisawa et al., 2011).

[1] This permeability has been converted from the original publication with a similar interpretation as Aulin and co-workers (2010) and Bardet and co-workers (2015), i.e. assuming an original value of 1 $cm^3/(m^2.d.kPa)$ instead of 1 $cm^3/(m^2.d.Pa)$.

Concerning the coating of MFC on a paper base, Syverud and Stenius (2009) used a dynamic handsheet former to produce a layer of MFC on a paper sheet at wet state. First, a 90 g/m² paper sheet is prepared in the former. Once the paper sheet is formed, i.e. after a vacuum filtration step, another sheet of 8 g/m² is prepared using the MFC suspension over the paper sheet that is still at wet state. The addition of this MFC layer decreases the air permeability of the paper from 65,000 nm/(Pa.s) to 360 nm/(Pa.s). As a comparison, a self-supporting MFC film of 17 g/m² produced with the same dynamic sheet former has an air permeability of 13 nm/(Pa.s) (Syverud and Stenius, 2009). An analogous method of wet lamination is described in a recently published patent by Guerin and co-workers (2016a), and reported for the development of a MFC-based oxygen barrier layer as part of a multi-layer material with application to Li-ion battery cell pouches (Guerin et al., 2016b). A diluted MFC suspension is first sprayed on a filtration membrane and drained until having a solid content of 5 to 18 wt%. The wet MFC layer is thereafter reported on a dry cellulosic substrate, and sticks on it upon drying. With 61 to 91% less water to evaporate after filtration compared to a 2 wt% MFC suspension, the drying of the MFC layer becomes more economically viable.

I.2.6.1.2. MFC top-layer obtained by a coating process

Aulin and co-workers (2010) studied the barrier properties of MFC using rod coating. A suspension of homogenized carboxymethylated MFC has been used at 0.85 wt%. Due to the low dry content of MFC suspensions the highest reachable coating weights were as low as 1.0 to 1.8 g/m², but still allowed to obtain an air permeability of 0.2 to 0.3 nm/(Pa.s) upon complete surface coverage, while the paper bases were at 660 to 69,000 nm/(Pa.s) for kraft and greaseproof paper, respectively. These low values are attributed to MFC forming a compact packing with low free-volumes thanks to their morphology and chemistry, along with a high tortuosity due to its high crystallinity (63 ± 9%), knowing that the crystalline parts of a polymer film are non-permeable (Aulin et al., 2010). The influence on the water vapour barrier was also investigated: a 3 g/m² coating of carboxymethylated MFC brought a decrease in water vapour transmission rate (WVTR) at 23°C 50%RH for a greaseproof paper from 90 to 29 g/(m².d), probably thanks to a surface densification and the partial closure of pores. However, the efficiency of this barrier layer is lowered with relative humidity: at 80%RH the WVTR is only halved upon MFC coating, and at 38°C 90%RH it is more than doubled (Aulin and Ström, 2013).

In addition to carboxymethylated MFC, enzymatically pre-treated MFC have also been used. The enzymatically pre-treated MFC demonstrated higher air permeability, as carboxymethylated MFC have smaller dimensions and are able to form a denser network. Rod coating of these MFC grades on a 130 g/m² paper allowed to deposit up to 6 g/m² of MFC, giving an air permeability of 130 nm/(Pa.s) and less than 0.1 nm/(Pa.s) for enzymatically pre-treated and carboxymethylated MFC, respectively. A coating weight below 2 g/m² increases the permeability; this may come from the plasticizing effect of water on the paper, as MFC suspensions are made of 98% water, and a non-homogeneous coverage of the surface by the microfibrils (Nygards, 2011).

Lavoine and co-workers (2014) performed multiple MFC coatings on a 41 g/m² calendered paper, by size-press and rod coating, and had similar issues concerning the high water content of the suspensions. In particular, the size-press technique was ineffective for MFC coating as the suspension is forced inside the paper. Water thus penetrates the paper, weakening the fibres network, and MFC

was unable to form a homogeneous layer at the surface. Results do not show any improvement in mechanical and barrier properties with this coating process. On the other hand, rod coating of MFC is able to increase the barrier properties of the thin paper: 5 and 10 layers of MFC have been coated in order to reach coating weights of 7 and 14 g/m² giving an air permeability of 786 and 256 nm/(Pa.s), respectively, while the base paper had an air permeability of 2,680 nm/(Pa.s). A MFC top-layer is believed to have a positive effect on the mechanical properties of a material, but in the case of paper this strengthening is counterbalanced by the partial destruction of the cohesive fibre network in the paper, induced by the contact with water. The Young's modulus and tensile strength are thus reduced by 20 to 26%. Oxygen permeability tests have been performed and an OTR higher than 1,000,000 cm^3/(m².d.bar) has been found. The MFC coating forms a tight network but pores are remaining on this cellulosic substrate (Lavoine et al., 2014). MFC have also been slot-die coated on board using a roll-to-roll process leading to an especially good grease resistance, with a kit test of 10 and a significant reduction in penetration of an offset ink (Kumar et al., 2016).

The coating of MFC shows encouraging results but the low solid content of MFC suspensions is a major drawback. In addition to be energy-consuming during drying, the high water content during coating has a negative impact on the cellulosic substrate in terms of mechanical properties.

I.2.6.2. Multi-layer structure with application to coating

A MFC layer can bring strong oxygen and grease barrier, but it still lacks of water vapour barrier and its properties drop down in humid conditions. One strategy to overcome this issue is to produce a multi-layer structure by applying a water- and water vapour-barrier material on top of the MFC layer.

This multi-layer approach has been investigated with polyethylene. Carboxymethylated MFC has been produced and 1.2 g/m² has been coated on a 230 g/m² paper. After lamination of 24 g/m² of PE, an OTR of 45 cm^3/(m².d.bar) has been measured, showing a higher barrier than with only the PE layer (Axrup et al., 2011). A bilayer MFC/PE has also been studied in a patent with this time addition of a cationic surfactant, and eventually plasticizers, to MFC produced by homogenization after mechanical pre-treatment. With a higher MFC coat weight of 16 g/m² and 36 g/m² of PE, OTR values of 6 to 25 cm^3/(m².d.bar) have been obtained. As expected, the highest OTR values are measured for samples comprising plasticizers (Iotti, 2014).

Biosourced alternatives to a polyethylene top-layer have been studied with the use of shellac, renewable alkyd resin, beeswax, paraffin, or cooked starch (Aulin and Ström, 2013; Hult et al., 2010; Spence et al., 2011b). Hult and co-workers (2010) used non-chemically modified MFC for application of a 3 g/m² coating on a 60 g/m² paper using a dynamic sheet former. A subsequent rod coating of 11 g/m² of shellac resulted in a significant reduction of WVTR at 23°C 50%RH and of air permeability by more than 80%. A reduction of the OTR at 23°C 0%RH of the same order is observed but the values remain high: more than 4,400 cm^3/(m².d.bar) for the MFC/shellac coated paper. This is attributed to pinholes in the MFC layer, a complete coverage is not obtained. Coating on a paper treated with optical brighteners allowed a more homogeneous coverage resulting in improved air barrier properties (Hult et al., 2010). Alkyd resin has also been investigated as a top-layer for carboxymethylated MFC. Alkyd resin is a polyester whose principal building blocks comprise fatty acids derived from vegetable oils, and it is used as an emulsion in water. The MFC/alkyd resin coating

reduces the WVTR of the substrate down to 0.8 g/(m².d) at 23°C 50%RH for a 6 g/m² MFC coating followed by a 20 g/m² alkyd resin coating. This barrier is lowered at 80%RH but still produces a WVTR as low as 12.7 g/(m².d). After coating of MFC on two different substrates - a greaseproof paper and a paper with a more opened surface - the two bases exhibit the same surface roughness, as shown in Figure 10, with no pinholes or coverage issues reported. This smooth and homogeneous coverage improves the barrier properties of the alkyd resin top-coating: the WVTR at 38°C 90%RH is halved with MFC/alkyd resin compared to only alkyd resin coating, while only MFC coating increases the WVTR (Aulin and Ström, 2013).

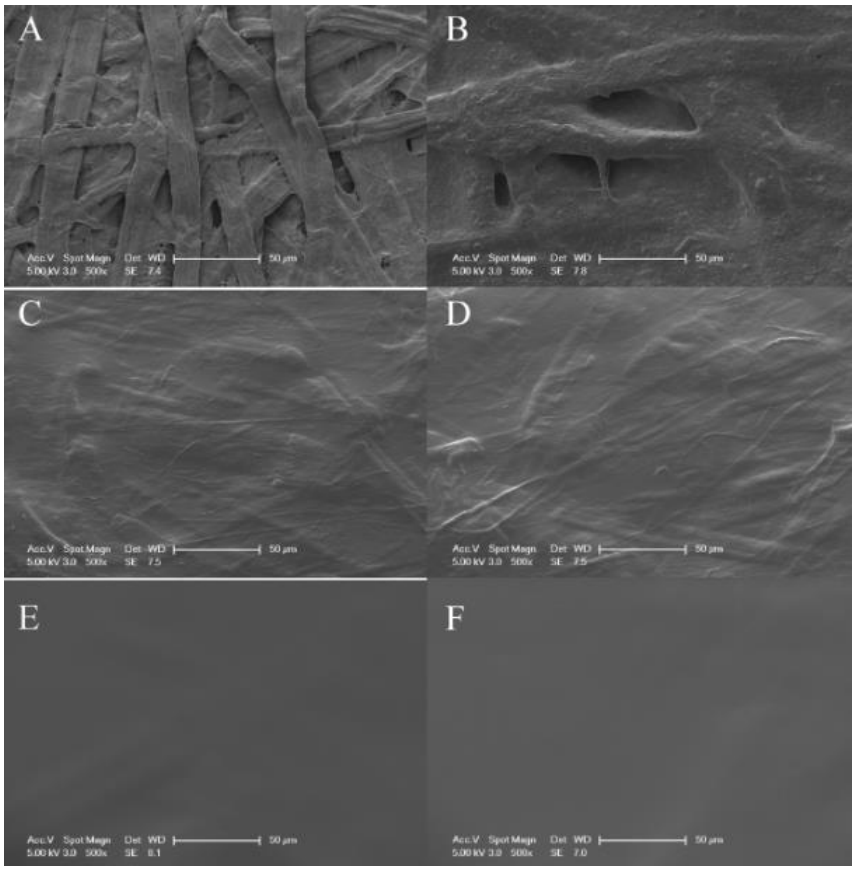

Figure 10 - SEM micrographs of the surface of a standard paper (first column) and a greaseproof paper (second column) as such (first row), coated with 3 g/m² MFC (second row), and coated with 3 g/m² MFC and a 20 g/m² alkyd resin top-layer (third row) (Aulin and Ström, 2013).

I.2.7. Conclusion on microfibrillated cellulose

It has been seen that microfibrillated cellulose is quite a recent material. Highly crystalline, renewable, and biodegradable, it can be extracted mostly from wood and annual plants by various techniques including enzyme activity, chemical modification, and high shear/pressure mechanical treatments. These different techniques, along with the pulp origin and in particular the lignin and hemicellulose fractions, are responsible for various grades of MFC having mostly diameters of 5 to 100 nm and lengths of several micrometres, with possible functionalization. These materials have numerous applications due to their rheological properties, biocompatibility, and ability to form a

tight network resulting in tough barrier films. This network formation is of great interest for the production of barrier layers. Pure MFC films are reported to be translucent, flexible, and to have a layered structure with low porosity and small pores. These properties vary according to the degree of fibrillation, mostly represented by the average diameter of microfibrils, the latter being influenced by quite a number of parameters.

MFC films usually have a high Young's modulus of 6 to 15 GPa and a high tensile strength of 100 to 200 MPa. Values of oxygen permeability of 48 cm^3.µm/(m^2.d.bar) at 23°C 50%RH are reported, meeting the expectations of a material for modified atmosphere packaging. However, due to the differences in structural properties between MFC grades, deviations from these values are observed, going in the way of increased mechanical and barrier properties with an increase in degree of fibrillation. These properties are also influenced by the atmospheric conditions and especially relative humidity. The hydrophilic MFC adsorbs more and more water when the relative humidity increases and gets plasticized by water, allowing a lower packing and an increased chain mobility and gas solubility and diffusivity, resulting in decreased mechanical and barrier properties.

The production of MFC is widely reported, resulting in MFC suspensions having different degree of fibrillation, fibre morphology, and chemistry. The degree of fibrillation is difficult to characterise and is mostly described by indirect techniques such as the rheology of MFC suspensions or the optical properties of MFC films. When working with MFC, it is of interest to be able to compare the quality of the MFC used with what is reported in the literature. For this reason, a first objective of this thesis is to compare the degree of fibrillation of different MFC grades, using indirect techniques on suspensions and self-standing films made from different pulps and with different intensity of mechanical treatment. This comparison also has tvhe objective of determining what MFC grade would be best suited for the production of barrier layers. Due to the high viscosity of MFC suspensions at low solid content causing issues upon application on a base by coating (drying, partial destruction of the base fibre network), pure MFC layers have been rather deposited on board using the recently developed process of wet lamination, involving a filtration step. It aims at getting a better understanding of the possible barrier performance that can be offered by such technique and the influence of possible defects in the MFC layer. The second strategy investigated in this thesis for the production of a MFC-comprising layer on paper or board is its use as filler in a coating formulation, which is introduced thereafter.

I.3. MFC-based nanocomposites

MFC composite is a wide area of research. According to SciFinder research engine, on the 30th of August 2016, among the 6,227 scientific publications comprising the concepts "cellulose nanofiber", "microfibrillated cellulose", or "nanofibrillated cellulose", 1,252 are closely associated with the concept "composite". As a matter of comparison, 465 are closely associated with the concept "coating" and 163 are closely associated with the concept "barrier".

The two main ways to produce a nanocomposite comprising MFC are by using the thermoplastic properties of the matrix (e.g. extrusion, thermopressing) or by removal of the solvent (e.g. solvent casting, filtration-pressing, water-based coating). While it is possible to use the first way to apply a layer on paper or board for food packaging using extrusion coating, concerning composites this thesis focuses on water-based coating. As a consequence, the materials to be mixed with MFC must be usable in aqueous media, be it under the form of solution, dispersion, or latex. This section will describe the use of MFC as fillers in a hydrosoluble polymer matrix, and the addition of a layered silicate dispersion to a hydrosoluble polymer or MFC.

The main way to characterise the formulation of a composite in solid state is to give the mass fraction of each component with the unit wt%. For example a composite can be made of 80 wt% polymer matrix and 20 wt% filler. The formulation can also be given in volume with the unit vol%. For example, assuming a density of 1 g/cm^3 for the matrix and 2 g/cm^3 for the filler, a composite with 20 wt% filler will be made of 89 vol% polymer matrix and 11 vol% filler. Another unit, used in this study because it is the standard in paper coating, is to express the amount of filler in pph: part per hundred. It refers to the mass of filler relative to the mass of the matrix, the amount of matrix being always 100 pph. The previous example of 20 wt% filler is equivalent to 25 pph filler. It is especially convenient when using multiple fillers, in order to change one polymer:filler ratio without changing the others. For example, 10 pph of filler(2) can be added and the formulation becomes 100 pph polymer matrix + 25 pph filler + 10 pph filler(2), while in wt% it would become 74.1 wt% polymer matrix + 18.5 wt% filler + 7.4 wt% filler(2).

I.3.1. MFC as filler in a hydrosoluble matrix

I.3.1.1. Poly(vinyl alcohol) (PVOH)

Poly(vinyl alcohol) (PVOH) is a good candidate to be used with MFC in water-based barrier coating as it is water-soluble, compatible with cellulose, and has a low oxygen transmission rate of 20 cm^3.µm/(m².d.bar) at 23°C 0%RH (Lange and Wyser, 2003). It is considered as a safe material and does not cause issues for food packaging. It is non-toxic by oral administration, do not accumulate in the body, and presents no adverse effect, making it even suitable for pharmaceutical and biomedical applications (Marin et al., 2014). It is also biodegradable, biocompatible, potentially biobased, and offers an interesting compatibility with starch. Starch is water-soluble, high barrier to oxygen, biobased, and biodegradable, but films are more brittle and more sensitive to humidity compared to PVOH. In addition, PVOH:MFC composites have been found to bring better water vapour and oxygen barrier properties than starch:MFC composites (Guezennec, 2012).

In order to produce PVOH, ethylene first reacts with acetic acid to produce vinyl acetate. Vinyl acetate is converted to poly(vinyl acetate) by free radical vinyl polymerisation, which is

thereafter hydrolysed with methanol in alkaline conditions to convert the acetate groups to alcohol groups (Klatte and Zacharias, 1999). Ethanol can be produced by fermentation of sugar and can be converted to ethylene or acetic acid. Methanol can be produced by gasification of biomass. As a result, poly(vinyl alcohol) has the potential to be a partially or fully biobased polymer (Abbott, 2015; Harmsen et al., 2014).

The properties of this polymer are strongly influenced by its degree of polymerisation and its degree of hydrolysis, i.e. the percentage of alcohol groups obtained from the hydrolysis of the acetate groups of poly(vinyl acetate). Our study will be focused on PVOH being considered as "fully hydrolysed", meaning that the degree of hydrolysis is superior to 97%. Fully-hydrolysed PVOH shows a sharp increase in crystallization tendency resulting in a reduction of cold-water solubility. The degree of polymerisation of PVOH is commonly comprised between 250 and 45,000. PVOH is soluble in water, but a high dissolution temperature is required. In water, in the range of 40 to 60°C, PVOH pellets start to swell and can be completely dissolved when a temperature of 90°C is maintained. PVOH is hydrophilic and fully-hydrolysed PVOH films can have water content at equilibrium of 5 to 15 wt% between 20%RH and 90%RH. Its glass transition temperature is in the range of 40 to 80°C and its melting point is in the range of 180 to 240°C (Klatte and Zacharias, 1999).

PVOH is biodegradable in aerobic and anaerobic conditions, contrary to the usual barrier coating solutions (Matsumura et al., 1993). However, it has to be noted that the PVOH-degrading microorganisms are not ubiquitous within the environment (Shimao, 2001). Its use in combination with MFC for barrier coating allows the possibility of producing a 100% biodegradable packaging.

Poly(vinyl alcohol) has a good affinity with several biopolymers, giving the opportunity to produce partially-biobased biodegradable blends that are reported to have improved ductility, and mechanical and thermal resistance using starch (Dean et al., 2008; Hejri et al., 2012) or xylan (X. Chen et al., 2015; Wang et al., 2013). PVOH:starch blends are also reported for barrier applications (Jansson, 2006; Javed et al., 2016; Kisku et al., 2014), but to our knowledge the influence of the PVOH:starch ratio in such composites has not been reported.

I.3.1.2. Properties of PVOH:MFC films

PVOH:MFC composite self-standing films are mainly studied for the ability of the MFC to reinforce the PVOH matrix. Most of the publications report a progressive increase of tensile strength and Young's modulus with the MFC content, coupled with a decrease of ductility (Castro et al., 2014; Liu et al., 2013; Oishi and Hotta, 2014; Wang and Sain, 2007). This reinforcement is attributed to the good compatibility between microfibrillated cellulose and poly(vinyl alcohol), a good dispersion of the cellulosic filler in the matrix, and the high mechanical resistance of the nanofibres previously reported.

PVOH:MFC composites have been obtained by in situ production of bacterial cellulose. PVOH has been added to the bacterial cellulose development medium at concentrations ranging from 0 to 6 wt%, along with glyoxal at 10% of PVOH mass for cross-linking. The crosslinked PVOH films have a strain at break of about 1.2% that is reduced down to less than 0.1% in the case of a 14 wt% MFC loading. PVOH films immersed in water during 48 hours swelled by +200% while composites swelled by +150%, which is explained by a decrease of free volume and chain mobility upon addition of MFC.

The films have been tested during humidity cycles: 0% and 90%RH alternatively during 500 min. The decrease in storage modulus and the increase in strain with increasing relative humidity are much lower for samples comprising MFC. In addition, the effect of humidity is completely reversible. FTIR and DSC analyses indicate that the presence of MFC could increase PVOH crystallinity up to a given concentration, after which it decreases, attributed to the ability of MFC to act as nucleation agent (Castro et al., 2014). A similar increase of crystallinity has been observed upon addition of either bacterial cellulose or non pre-treated MFC in PVOH. The crystallinity index of PVOH increased from 46% to 71% with 2 wt% MFC, but decreased to 44% with a MFC content of 10 wt% (Yuwawech et al., 2015).

Liu and co-workers (2013) covered a wider range of MFC content, from 1 wt% to 60 wt%, and the mechanical resistance improvement was maintained in the whole range, along with a decrease of elongation from 248% for PVOH to 19% with 60 wt% MFC. An effect on the thermal behaviour could also be observed with a progressive increase of the temperature of maximal degradation, during a thermogravimetric analysis (TGA) experiment, from 288 to 331°C at 60 wt% MFC (Liu et al., 2013).

The mechanical behaviour was not as straightforward in the case of PVOH:MFC composites studied by Zimmerman and co-workers (2004). The addition of 1 wt% MFC decreased the mechanical properties, which was attributed to the requirement of a higher filling threshold in order to obtain a MFC network in the composite. At 10 wt%, however, the mechanical resistance could be improved (Zimmermann et al., 2004).

I.3.1.3. Application to paper coating

I.3.1.3.1. Viscosity of MFC-comprising coating colours

The high viscosity of the MFC suspensions was not an issue concerning the production of self-standing composite films due to the low concentrations involved, usually inferior or equal to 5 wt% in water. However, the use of more concentrated suspensions for coating evidences a high influence of the addition of MFC in PVOH on the viscosity of the resulting formulation. At 15 wt% total solid content, the viscosity of a PVOH:MFC coating colour increases from 218 mPa.s to 876 mPa.s with 5 wt% MFC, and to 2,280 mPa.s with 15 wt% MFC. With a ten-fold increase at 15 wt% MFC, viscosity gets close to the highest values allowing its processability by rod or blade coating (Guezennec, 2012). Dimic-Misic and co-workers (2013) studied the use of MFC as a partial substitute of carboxymethyl cellulose (CMC) in coating colours for rheology modification, inducing a higher particle mobility and improving strength properties on the paper surface while avoiding flocculation.

I.3.1.3.2. Barrier of composite coatings

PVOH:MFC coatings have been prepared at laboratory scale by Guezennec (2012). Using 5 wt% MFC in a PVOH matrix, a 10 g/m² coating on board led to a slight decrease in water vapour transmission from 2.5 to 2 g/m² at 23°C 50%RH, along with a more significant reduction of oxygen transmission from 2,500 to 340 cm^3/(m².d.bar) at 23°C 0%RH. However, increasing the MFC content to 10 or 15 wt% increased both water vapour and oxygen transmission, e.g. an OTR higher than 15,000 cm^3/(m².d.bar) was obtained with 15 wt% MFC, attributed to pinholes in the layer. At pilot scale a similar 10 g/m² coating of PVOH led to an OTR of 600 cm^3/(m².d.bar), attributed to drying

defects described in the following section. The addition of MFC allowed avoiding this defect leading to a low OTR of 5 $cm^3/(m^2.d.bar)$. No significant differences were found between the laboratory and pilot scale coating of PVOH:MFC composite formulations in terms of water vapour barrier (Guezennec, 2012).

Stora Enzo has a patent application from 2011 about the coating of a cellulose fibre substrate with a dispersion comprising microfibrillated cellulose and colloidal particles of a polymer for reduced WVTR. In this patent, PVOH is cited as a possible polymer, along with more than 15 others (Heiskanen et al., 2011). Akzo Nobel Chemicals International has a similar pending patent, from 2011, specifying the use of MFC in a coating formulation comprising an anionic polymer which can be PVOH. Starch is also mentioned in both cases (Malmborg et al., 2011).

I.3.1.3.3. Improvement of the layer quality

Using MFC in a water-based formulation is reported to improve the layer formation by reduction of defects that can appear at the surface during drying. Borregaard tested the effect of Exilva® MFC on the mud-crack resistance of an exterior PVC paint. Without MFC cracks appear from a paint thickness of 0.36 mm, while the use of 0.38 wt% MFC in the formulation allows the production of layers up to 1.5 mm without visible cracking (Exilva, 2016). Another patent depicts the reduction of cracking of an acrylic paint by addition of MFC produced by homogenization (Van Engelen et al., 2014a). Closer to our application, Schmidt and co-workers (2015) published a patent about the use of TEMPO-oxidised MFC in a receiving layer for digital printing comprising a hydrosoluble polymer (PVOH) and pigments. The use of 0.05 wt% MFC in the curtain coating formulation reduced the amount of cracks by about 50% compared to the standard MFC-free formulation. An increase of machine speed leads to a faster drying that causes an increase in the number of cracks. With MFC reducing the amount of cracks, an increase of machine speed by 5 to 10% could be performed without degrading the layer quality, while without MFC at this increased machine speed a number of defects are formed (Schmidt et al., 2015). This time with a barrier application, Guezennec (2012) observed a blistering phenomenon after drying of a PVOH solution coated on board with a Soft-Tip blade, due to the evaporation of internal water through an already dried PVOH surface. The addition of 5 wt% non-chemically modified MFC allowed the complete disappearance of this defect, as shown in Figure 11 (Guezennec, 2012).

PVOH:MFC coating has also been studied from a non-papermaking point of view. A porous Bioglass® scaffold has been dip-coated into an aqueous solution of PVOH and MFC in order to strengthen the material. This type of glass is brittle and a PVOH:MFC coating is able to serve as crack bridging agent while bringing a tenfold increase in tensile strength (Bertolla et al., 2014).

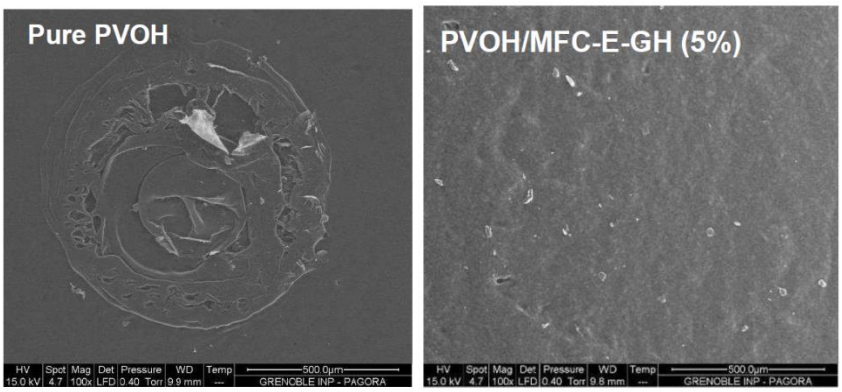

Figure 11 - Scanning electron microscopy (SEM) analysis of a board coated with PVOH (left) and PVOH:MFC (right) (Guezennec, 2012). The left picture evidences the drying defect (blistering) that vanishes upon addition of MFC.

I.3.1.4. Other uses of MFC in a coating colour

The barrier properties of starch:MFC composite coatings are reported by Martins and co-workers (2013). Using MFC produced by enzymatic pre-treatment and grinding at 20 pph, zinc oxide, and starch, composite coatings of about 3 g/m² have been performed by size-press on an AKD-treated paper, for anti-bacterial properties. The base paper had an air permeability of 11.5 nm/(Pa.s) that was reduced to 10.8 and 4.0 nm/(Pa.s) by starch coating and starch:MFC composite coating, respectively. The addition of zinc oxide antibacterial particles to the composite coating increased the air permeability to 9.2 nm/(Pa.s) (Martins et al., 2013).

Heiskanen and co-workers (2011) produced MFC with an enzymatic treatment followed by refining at 25 wt% and mixed it with a commercial latex Cartaseal TXU. A 15 g/m² layer of this composite coating on paper reduced the WVTR at 23°C 50%RH by 24% compared to the same basis weight of latex only. In addition, the grease barrier properties after converting, i.e. folding and creasing, were improved (Heiskanen et al., 2011). MFC:hydrosoluble polymer composite coatings also have other applications than barrier properties. The use of MFC has been investigated in combination with anionic starch for coating on newsprint paper. This composite coating has been found to greatly reduce the linting and dusting tendency of the papers, these two materials having a synergistic effect (Song, 2010).

I.3.2. Polymer-Clay composites

I.3.2.1. Structure of layered silicates (clays)

When a gas molecule diffuses in a homogeneous polymer, the diffusion pathway is straight. The tortuosity, i.e. the ratio between the actual pathway of the molecule and a straight diffusion, is thus equal to 1. Solid impermeable particles can be introduced in a polymer in order to force the gas molecules to bypass them, increasing the tortuosity and reducing the permeability of the filled polymer.

Layered silicates, or nanoclays, are inorganic impermeable platelet-like pigments with the distinctive feature of having a diameter much greater than their thickness. This allows them to be

especially effective concerning the ability to increase the tortuosity inside a material. The most common nanoclay found in the literature is montmorillonite. The commonly used nanoclays belong to the family of the 2:1 phyllosilicates; they consist of an aluminium or magnesium hydroxide octahedral sheet sandwiched between two silicon oxide tetrahedral sheets, as shown in Figure 12. The isomorphic substitution of these cations, e.g. Al^{3+} to Mg^{2+}, generates negative charges that are counterbalanced by the presence of exchangeable cations between the clay layers, usually Na^{+}. The layered silicates are compatible with hydrophilic polymers, and can also become compatible with hydrophobic polymers by ion exchange with alkylammonium cations having an alkyl chain of at least 12 carbons (Sinha Ray and Okamoto, 2003).

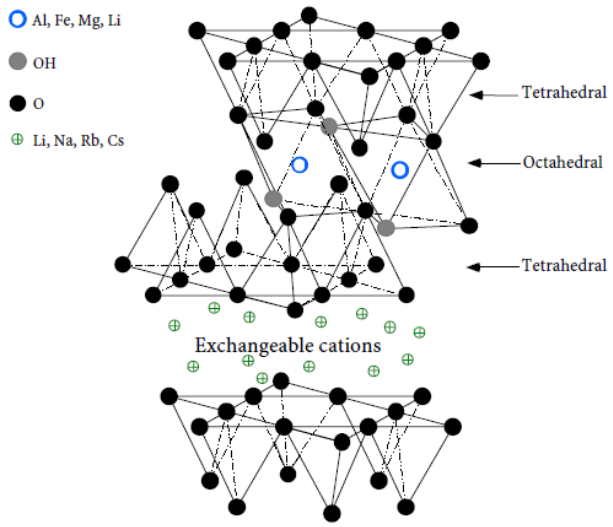

Figure 12 - Structure of 2:1 layered silicates such as montmorillonite (Giannelis et al., 1999).

The phyllosilicates have a multi-scale organisation, as shown in Figure 13. At the finest scale layered silicates are in the form of thin circular sheets: platelets having a thickness of 1 nm and a width of 10 nm to 1 µm, resulting in an aspect ratio width/thickness of 10 to 1,000. Five to ten platelets are stacked perpendicularly to the z direction, resulting in a primary particle having a thickness around 10 nm. On a larger scale, clay aggregates having a size of 0.1 to 10 µm are formed by the association of primary particles oriented in all the directions (Chivrac et al., 2009).

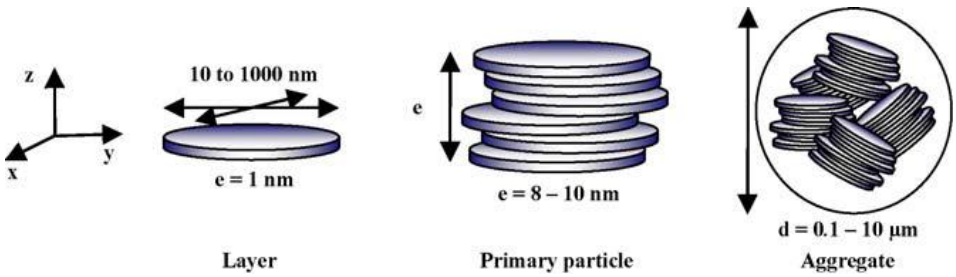

Figure 13 - Multi-scale organisation of layered silicates (Chivrac et al., 2009).

The distance between two clay layers in a stack is regular and referred to as the inter-layer spacing, or d_{001}, usually determined by X-ray diffraction (XRD). Layered silicates swell in presence of humidity due to the hydration of the intercalated cation and inter-particle capillary phenomena. This results in an increase of the inter-layer spacing, e.g. from d_{001} = 9.6 Å for anhydrous montmorillonite with sodium as counter-ion (MMT-Na) to 12 Å in ambient conditions (Chivrac et al., 2009).

Unmodified layered silicates cause no hazard toward human health. Sodium montmorillonite is intended to be in contact with food without any restriction (BYK Additives & Instruments, 2015), and layered silicates can be used as fertilizer or for wine clarification. Also, the presence of montmorillonite or its compositional elements has been evidenced on Mars (Clark et al., 2007).

I.3.2.2. Barrier properties of polymer-clay composites

Polymer-clay composite is an extensive area of research due to the ability of the layered silicate particles to act as reinforcing agent thanks to their high aspect ratio, allowing a large polymer-clay surface for stress transfer, and their ability to deflect evolving cracks. In addition, the clay platelets are able to force gas molecules to follow a tortuous path thus reducing the diffusion through the matrix. Choudalakis and Gotsis (2009) present a number of models for the prediction of the permeability of polymer-clay composites. All models have in common to take into account the volume fraction and aspect ratio of the filler (Choudalakis and Gotsis, 2009). As an example, one of the first model consider an increased diffusion pathway of gas molecules equal to the average number of particles encountered multiplied by the half of the platelet width (Barrer and Petropoulos, 1961). With a constant volume fraction, an increase of aspect ratio leads to an increase of tortuosity due to higher particle width and/or an increased amount of particles encountered, as illustrated in Figure 14.

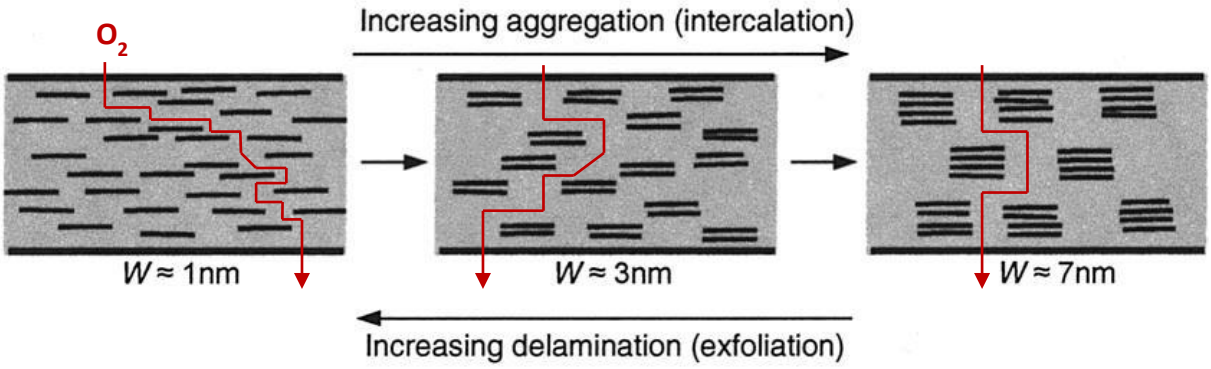

Figure 14 - Effect of platelet dispersion on the permeability of a composite. Red lines are a schematic representation of the oxygen diffusion pathway, depending on average stack thickness W. Adapted from (Bharadwaj, 2001).

The dispersion state plays an important role concerning barrier improvement. A stack of several clay layers will not be more efficient for the increase of diffusion pathway than a single layer with a similar thickness. The presence of stacks leads to taking into account thicker particles with a

lower aspect ratio and thus lower potential for barrier reinforcement. As a consequence, the dispersion of layered silicates in a matrix in order to obtain optimal properties is a key challenge. The dispersion state of layered silicates in a polymeric matrix is illustrated in Figure 15.

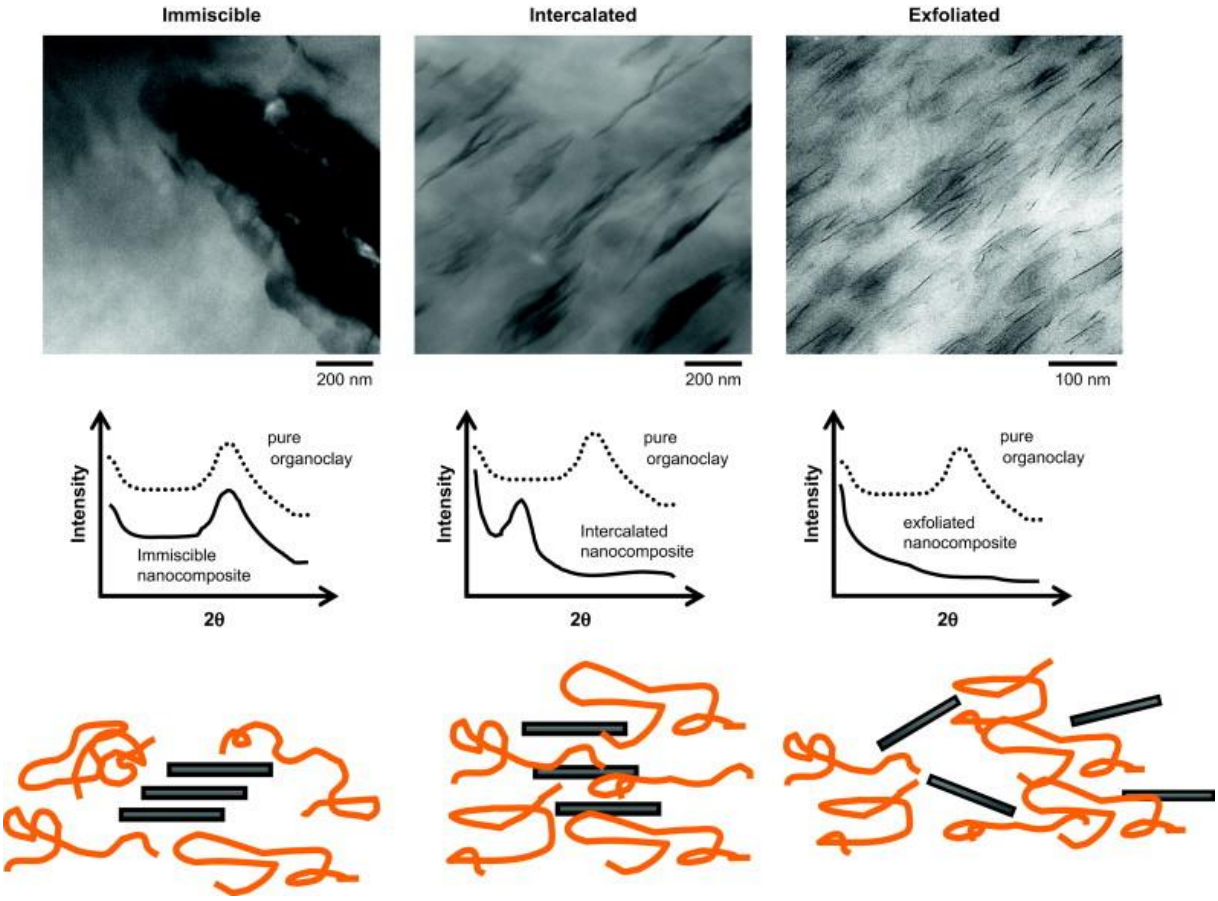

Figure 15 - Three dispersion states of layered silicates in a polymeric matrix (Paul and Robeson, 2008). TEM pictures showing the dispersion from aggregates to single layers (top), general trend of XRD spectra representing a shift in d_{001} peak toward lower angles (middle), and illustration of the dispersion of the clay in a polymer from a micro-composite to an exfoliated state (bottom).

I.3.2.3. PVOH:clay composites

Nanoclays are naturally compatible with PVOH. Montmorillonite has a large surface area covered with electronegative oxygen and hydroxide species, and PVOH has a strong tendency to hydrogen bond to itself and to other species containing highly electronegative substituents (Grunlan et al., 2004). According to Podsiadlo and co-workers (2007), mixtures of PVOH and montmorillonite have two unique properties. The first one is the effectiveness of the hydrogen bonding between the alcohol groups of PVOH and the SiO_4 tetrahedrons on the surface of layered silicates, revealed by atomic modelling and described as velcro effect. The second one is the ability of Al atoms located along the edges of the platelets to be involved in an especially stable six-membered ring structure with PVOH (Podsiadlo et al., 2007). The covalent bonding between PVOH and montmorillonite has been observed by nuclear magnetic resonance (NMR), X-ray photoelectron scattering (XPS), and

Fourier transform infrared spectroscopy (FTIR) with an Al-O-C band at 848 cm^{-1}, which has also been found in another publication in addition to physisorption (Walther et al., 2010).

The two former studies have in common the formation of nearly-ideal structures with the objective of mimicking the brick-and-mortar structure of natural nacre. Podsiadlo and co-workers (2007) used the layer-by-layer (LbL) technique for the formation of thin films of 300 PVOH:Montmorillonite bi-layers having a thickness of approximately 5 nm. This structuration allows an in-plane orientation of the platelets and an effective stress transfer by the large PVOH:Montmorillonite contact surface, leading to a reinforcement of the PVOH matrix with a tensile strength ranging from 40 to 150 MPa and a Young's modulus ranging from 1.7 to 13 GPa. In the meantime, the elongation at break is reduced from 30% to 0.7% (Podsiadlo et al., 2007). The successive steps of dipping and rinsing required for the LbL technique are highly time-consuming. The second publication, from Walther and co-workers (2010), first mixes a montmorillonite suspension with a diluted PVOH solution in order to fix a 1 nm thick PVOH layer on the platelets by physisorption and covalent bonding. The excess of PVOH is removed by centrifugation and the 15 wt% suspension of PVOH-coated platelets can be used for the formation of films by filtration, doctor-blading, or application with a paint brush. A layered structure similar to LbL can be obtained. A strong mechanical reinforcement is also found, along with an oxygen permeability of 321 cm^3.µm/(m².d.bar) at 80%RH. Another study by Grunlan and co-workers (2004), using a modified PVOH, found an oxygen permeability reduced from 6 to 1 cm^3.µm/(m².d.bar) at 35%RH with 3 wt% montmorillonite, 1 cm^3.µm/(m².d.bar) being the detection threshold of the apparatus. At 55%RH, the oxygen permeability is increased from 21 to 80 cm^3.µm/(m².d.bar) with 3 wt% montmorillonite, but a further addition to 20 wt% allows it to be reduced to 1 cm^3.µm/(m².d.bar). The increase of oxygen permeability at low clay content is attributed to the disruption of PVOH crystallinity and the occupation of hydroxyl groups that would normally be involved in hydrogen bonding with other PVOH chains. From 10 wt% clay, the increase of diffusive pathways may become predominant (Grunlan et al., 2004).

Clegg and co-workers (2014) also used the mixing-centrifugation strategy in order to study the adsorption of PVOH on montmorillonite. From 0.02 to 0.5 g_{PVOH}/g_{Clay}, almost all PVOH is adsorbed on the clay. After that, free PVOH begins to develop. The XRD analysis of PVOH:Montmorillonite composites obtained by such process shows a progressive increase of inter-layer spacing, the last observable d_{001} being close to 40 Å at 9 g_{PVOH}/g_{Clay} compared to 12 Å for pristine montmorillonite. After that, the XRD peak is situated at an angle lower than the threshold of the device, suggesting that the layers were very well dispersed (Clegg et al., 2014). Similar results were found by Strawhecker and Manias (2000) for PVOH:Montmorillonite cast films at ratios 0:100, 20:80, 40:60, 60:40, and 80:20. However, here even at 20 wt% montmorillonite the inter-layer spacing could not be observed, as shown in Figure 16. The analysis of the properties of PVOH:Montmorillonite composites has been focused on montmorillonite contents inferior to 10 wt%. The analysis of the films crystallinity by XRD and differential scanning calorimetry (DSC) showed the apparition of a second peak upon addition of montmorillonite, evidencing that a new crystalline structure having a different melting temperature is formed. As previously seen, the addition of clays improves the mechanical resistance of the composites. In addition, the water vapour permeability of PVOH could be reduced from 480 to approximately 168 g.µm/(m².d) using montmorillonite at 2 wt%. An increase in montmorillonite content to 4 wt% or 6 wt% did not lead to further improvement (Strawhecker and Manias, 2000).

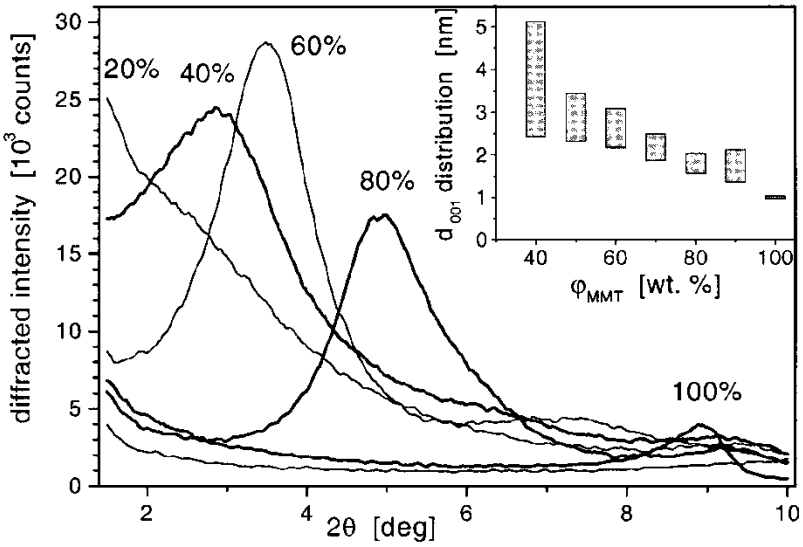

Figure 16 - XRD analysis of PVOH:Montmorillonite composites evidencing an increase of d_{001} with an increase of PVOH content (Strawhecker and Manias, 2000).

Liu and co-workers (2014) produced PVOH:Clay composites using 5 wt% of unmodified and organomodified montmorillonite. The XRD analysis showed a good dispersion of the unmodified montmorillonite with no apparent d_{001} peak, but a d_{001} peak was observed in the case of organomodified montmorillonite showing a worse dispersion coming from the worse compatibility with PVOH. The organomodified clays also had a lower efficiency concerning the mechanical reinforcement of the matrix. Compared to pristine PVOH, PVOH:montmorillonite (unmodified) demonstrated a water vapour permeability reduced from 2,720 to 2,040 g.µm/(m².d.hPa) at 100%RH (cup method, the cup being filled with deionised water). In addition, the solubility, water vapour uptake ratio, and swelling ratio of the films comprising montmorillonite was lower than for the pristine PVOH, which is attributed to the strong cohesion between the polymer and the clay platelets (Liu et al., 2014). This is in accordance with the diminution of water uptake observed by Thomassin and co-workers (2006) upon addition of montmorillonite in PVOH for a reduction of methanol permeability. Also, the reduction of PVOH chain mobility has been evidenced by an increase in glass transition temperature for modified PVOH:Clay composites (Grunlan et al., 2004).

I.3.2.4. MFC:clay composites

Microfibrillated cellulose has also been used as a matrix for layered silicates. Due to the larger dimensions of non-chemically modified MFC, the cellulose microfibrils are not intercalated in the clay galleries. It is evidenced by a constant d_{001} peak in MFC:Montmorillonite composites independently of the filler content (Carosio et al., 2015; Liu et al., 2011). A detrimental effect was observed in such composites in terms of mechanical properties (Sehaqui et al., 2010). The tensile strength and Young's modulus decreased linearly with the filler content, from 124 MPa and 8.7 GPa at 50 wt% montmorillonite to 30 MPa and 4 GPa at 89 wt% montmorillonite, respectively, showing

that the interfacial adhesion is insufficient for an effective load transfer between MFC and montmorillonite (Liu et al., 2011).

MFC:Montmorillonite composites have a layered structure with a preferential in-plane orientation of the clays, as observed in SEM pictures of cryo-fracture surfaces and evidenced by 2D-XRD. Despite the lack of mechanical reinforcement, the addition of layered silicates led to an oxygen barrier improvement in humid conditions (23°C 95%RH) from 17,600 cm^3.µm/(m^2.d.bar) for pristine MFC to 3,460 cm^3.µm/(m^2.d.bar) with 50 wt% montmorillonite. At 23°C 50%RH the permeability is much lower with values of 47 and 44 cm^3.µm/(m^2.d.bar) for MFC and MFC:Montmorillonite films, respectively (Liu et al., 2011). With application as fire retardant, a close permeability of 39 cm^3.µm/(m^2.d.bar) was found by Carosio and co-workers (2015) for a similar formulation. Another work using kaolin instead of montmorillonite reports that clay and MFC do not bind well, as evidenced by a diminution of film density. Despite that, the addition of kaolin at 5 wt% allowed obtaining an halved water vapour permeability (Spence et al., 2011b).

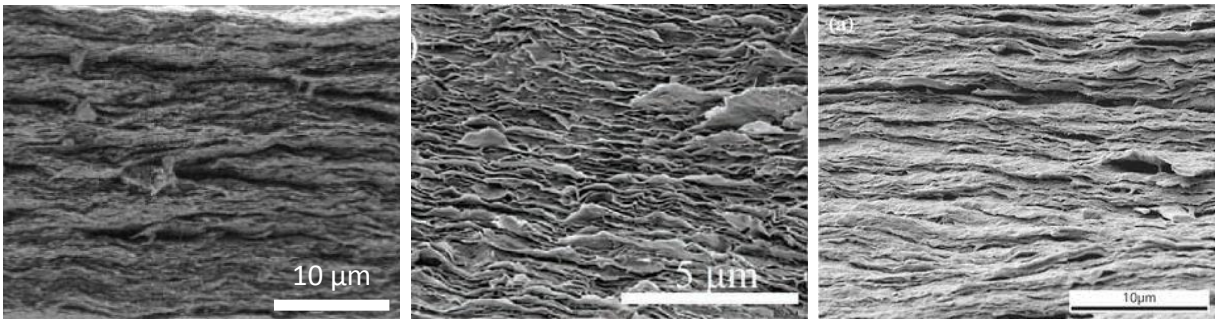

Figure 17 - Cross-section of MFC:Clay composite films observed by SEM at ratio 100:0 (Spence et al., 2011b) (left), 80:20 (Liu and Berglund, 2012) (middle), and 50:50 Clay (Ho et al., 2012a) (right).

In order to obtain a better interaction between MFC and clays, Ho and co-workers (2012a) used trimethylammonium-modified MFC having a cationic charge, instead of the anionic O^- and COO^- found in unmodified cellulose that lead to anionic repulsion with the clays. Comparing different layered silicates such as montmorillonite, kaolin, and mica, montmorillonite displayed the best interaction level being the only layered silicate with platelets folded around the cationic MFC (Ho et al., 2012a). Composites with 50 wt% montmorillonite had a slightly higher permeability that cationic MFC, suggesting that the montmorillonite folding around the micro-fibres is not in favour of improved barrier properties. On the contrary, a mica content of 50 wt% allowed a reduction of permeability from 750 to 220 g.µm/(m^2.d.hPa) at 23°C 85%RH, while the improvement in the case of unmodified MFC is only from 640 to 570 g.µm/(m^2.d.hPa). As a comparison, the cationic MFC:Mica composite had a water vapour permeability of 40 g.µm/(m^2.d.hPa) at 23°C 50%RH. Over the 0 to 85 wt% range of mica content investigated, the water vapour uptake decreased linearly and 50 wt% of filler has been found to be the optimal content in terms of mechanical and barrier properties (Ho et al., 2012b).

The use of TEMPO-oxidised MFC led to different interactions with layered silicates. An increase in montmorillonite d_{001} with the oxidised MFC content could be observed but could not be

attributed to nanofibres intercalation. Despite having a narrow range of fibres with small diameters, the size of TEMPO-oxidised MFC is still too high to penetrate the clay galleries (Wu et al., 2012). Another study report a similar d_{001} between pristine montmorillonite and 30 wt% montmorillonite in TEMPO-oxidised MFC, evidencing the absence of intercalation (Wang et al., 2014). Oxidised MFC and clay showed a good compatibility with an optimum of 5 wt% montmorillonite in terms of mechanical properties. Contrary to other results reported, the strain at break is increased at this filler content from 3.2 to 7.6%. The tensile strength and Young's modulus are more than doubled, suggesting that with this fine oxidised MFC the load transfer is more effective than with non-modified MFC. MFC:Clay interactions could be observed by FTIR, evidencing oxidised MFC:Montmorillonite hydrogen bonding and Al-O-C covalent bonds. The oxygen barrier is improved in a similar manner as previously seen (Wu et al., 2012). TEMPO-oxidised MFC are also reported to act as dispersing agent for kaolinite thanks to their amphiphilic characteristics, being as effective as a non biosourced sodium polyacrylate. Using only 0.2 wt% of oxidised MFC relative to the clay mass, aggregation could be avoided until a solid content of 34.5 wt% compared to 28.3 wt% without MFC, and the viscosity of the suspension at this critical concentration could be reduced from 1,433 mPa.s to 10 mPa.s (Ming et al., 2016). Kaolin is also reported to improve the water vapour and oxygen barrier of TEMPO-oxidised MFC, but without improvement concerning the mechanical properties (Honorato et al., 2015).

In addition of barrier and mechanical reinforcement, the use of MFC:clay composites with 50 wt% clay led to improved heat resistance, including a better thermal stability evidenced by dynamic mechanical analysis (DMA), fire-retardant property with an increased time to ignition by cone calorimetry, and a self-extinguishing ability (Carosio et al., 2016; Liu et al., 2011).

I.3.2.5. PVOH:MFC:clay composites

The combination of poly(vinyl alcohol), microfibrillated cellulose, and layered silicates is not widely reported. According to the authors, the publication described afterwards is the first on the subject and dates back to 2014. A PVOH:MFC matrix at ratio 1:1 was prepared with a montmorillonite loading ranging from 0 to 50 wt%. Clay aggregation could be observed by SEM from a content of 10 wt%. An increased clay loading did not improve the tensile strength; it led to an increase of Young's modulus with a decrease of elongation at break. This is attributed to the aggregation of the fillers, the clay aggregates acting as stress concentrators and having low load transfer efficiency. The water vapour permeability could be reduced from 2,200 to 1,720 g.µm/(m².d.hPa) with 5 wt% montmorillonite. Increasing the clay content to 25 wt% or 50 wt% led to a similar improvement with a water vapour permeability of 1,250 g.µm/(m².d.hPa). The addition of poly(acrylic acid) (PAA) as a crosslinker was found to improve the clay dispersion. The water vapour permeability was almost the same with and without PAA except at 50 wt% where the better dispersion of the clay allowed a further improvement, in comparison with the aggregates found without PAA. In addition, a higher elongation at break has been found at 50 wt% clay with PAA, which is explained by a reduction of the amount of stress concentrators with better dispersed platelets. The effect of aggregation was not found concerning the oxygen permeability, which decreased progressively with the clay content. PVOH:MFC composites had an oxygen permeability of 0.5 cm^3.µm/(m².d.bar) at 0%RH and 6,702 cm^3.µm/(m².d.bar) at 90%RH. The addition of 50 wt% montmorillonite did not lead to any change at 0%RH. However, at 90%RH it could be decreased to 188 cm^3.µm/(m².d.bar), that is to say by a factor 35 (Spoljaric et al., 2014).

Another study used TEMPO-oxidised MFC with a PVOH:MFC ratio of 3:7, and a montmorillonite content of 50 wt%. The use of PVOH compared to a MFC:Montmorillonite composite increases both the tensile strength and the elongation at break, and the use of TEMPO-oxidised MFC compared to a PVOH:Montmorillonite composite made the d_{001} montmorillonite peak disappear evidencing an improved dispersion. The combination of oxidised MFC and layered silicates in PVOH also led to improved fatigue resistance in tension mode at 0.5 Hz. Signs of interactions between the three components are found by FTIR with the Al-O-C peak at 839 cm^{-1} and a shift in the hydrogen bond peaks around 3,300 cm^{-1} which may be ascribed to the adsorption of PVOH on the surface of the clays and oxidised MFC (Wang et al., 2014).

No other scientific article on the subject was found. However, three patents deal with PVOH:MFC:Clay composites for barrier properties. The first one uses carboxymethylated MFC with PVOH, montmorillonite, a crosslinking agent, and a silane coupling agent. With a PVOH:MFC:Clay ratio preferably of 80:100:50, OTR below 0.1 $cm^3/(m^2.d)$ were found at 23°C 0%RH (Nishioka and Kobayashi, 2016). The other two patents are from the same company, Nippon Paper, and describe a multi-layer material having both vapour barrier and gas barrier properties under high humidity. It is composed of a paper base, a water vapour coating, and a gas barrier coating. The water vapour coating comprises a pigment and a binder such as styrene butadiene. The gas barrier comprises poly(vinyl alcohol), a pigment having an aspect ratio superior to 100 such a kaolin, and a cellulose derivative such as modified MFC. An example of gas barrier formulation is carboxymethylated MFC:PVOH:Kaolin at ratio 50:50:100 (Okamoto et al., 2015, 2014).

I.3.3. Alternatives to PVOH and clays

The former section focuses on the use of MFC with poly(vinyl alcohol) and layered silicates that are the materials used during this thesis, but alternatives can be found in the literature. Instead of PVOH, using cationic chitosan allows decreasing the filtration time required to form MFC:clay sheets by generating MFC flocculation (Liu and Berglund, 2012). Preferring a negatively charged carboxymethyl cellulose leads to a higher transparency indicating better clay dispersion, but it also leads to weaker polymer-clay interactions that impact the mechanical properties (Liu and Berglund, 2013). Using starch allows producing materials with an increased bio-based fraction but plasticization is necessary to avoid brittleness, for example with glycerol. Upon addition of clays, starch shows an improved behaviour towards water and water vapour with a reduction of water solubility, water uptake, and water vapour permeability (Slavutsky et al., 2012). The combination of MFC and layered silicates with CMC or starch is also reported in a patent with application to board coating for food packaging applications (Kunnas and Siren, 2014).

MFC and layered silicates are not inherently compatible with hydrophobic polymers but they can be modified. Acetylated MFC and organo-modified montmorillonite have been found to double the crystallinity of poly(lactic acid) at only 1 wt% and demonstrated a significant improvement of the oxygen barrier (Trifol et al., 2016). Such polymer has the advantage of having a better water resistance than the ones previously mentioned, but the drawback of not being directly applicable to water-based barrier coating.

Cellulose nanocrystals (CNC) have been investigated as an alternative to layered silicates in a MFC matrix for producing a fully biodegradable material from renewable resources. Using TEMPO-

oxidised CNC, the oxygen permeability at 23°C 90%RH of MFC-based cast films could be reduced from about 14 to 7 cm^3.µm/(m^2.d.bar), which is almost as efficient as using clays that reduced the oxygen permeability to 5 cm^3.µm/(m^2.d.bar) (Bardet et al., 2015). CNC have also been found to improve the water vapour barrier of PVOH films by 66% (Paralikar et al., 2008).

I.3.4. Conclusion on MFC-based nanocomposites

Using MFC as filler in a coating colour is a strategy allowing the production of suspensions with higher solid contents than using sole MFC. With application to water-based barrier coating, MFC can be combined with a hydrosoluble polymer or other materials than can be in solution, dispersion, or as latex in water. PVOH is found of interest as it is hydrosoluble, barrier to oxygen, compatible with cellulose, biodegradable, and potentially partially or fully biobased. MFC can improve the mechanical resistance of PVOH films at the cost of a reduced ductility. It can also increase PVOH crystallinity by acting as nucleating agent and reduce swelling in water. However, MFC increases the viscosity of PVOH solution, which may force to dilute the suspensions in the case of a high MFC content. It leads to PVOH:MFC suspensions having a solid content of about 15 wt%, which is more convenient for coating than using 2 wt% MFC suspensions. The addition of MFC in a PVOH solution was also found to improve the drying and layer formation. It resulted in more easily obtainable defect-free layers: an important parameter in order to avoid the formation of holes by which gas can diffuse easily. PVOH:MFC composite films have been produced in this thesis using a specifically designed process of coating-peeling involving conditions closer to coating that the usual solvent casting method: concentrated suspensions, film formation using a laboratory coating machine, and infrared drying. This study focused on the influence of the degree of polymerisation and degree of hydrolysis of PVOH that are rarely analysed, and on the comparison between highly fibrillated MFC grade and a less fibrillated MFC grade. The improvement of layer quality offered by the addition of MFC in PVOH is not well understood. In this thesis, a drying kinetic experiment has been designed in order to study the effect of MFC on the drying speed of PVOH under controlled conditions, along with the boundary times between different drying domains.

The combination of MFC with PVOH allows the formation of more convenient coating colours formulations compared to sole MFC, having better mechanical properties and layer formation than sole PVOH, but is still sensible to humidity. Layered silicates (clays) can be introduced in such formulation in order to improve the gas barrier properties by increased the diffusion pathway of gas molecules inside the composites. They can be well dispersed up to 20 wt% in PVOH, which is essential in order to obtain preferably individualised platelets, being more efficient than stacks or aggregates. The gas barrier improvement is especially effective in humid conditions, and layered silicates can reduce the water and water vapour sensibility of PVOH, which can be explained by a strong matrix-filler cohesion. This also results in tougher films with lower ductility. The dispersion of layered silicates in a MFC matrix is more difficult: microfibrils are too large to be intercalated in the clay galleries. It results in an insufficient interfacial adhesion that is not in favour of a good stress transfer, and may result in stack or aggregates that are less efficient in terms of barrier improvement. PVOH:MFC:Clay formulations could be used to obtain well-dispersed clay in PVOH while having the improvements in terms of mechanical properties and layer formation due to the presence of MFC. This thesis aims at developing PVOH:MFC:Clay composites for barrier applications, when they are mostly reported for synergistic mechanical reinforcement. This study specifically focused on the clay

dispersion in PVOH and the influence of MFC and layered silicates on the dispersion of each other. The upscaling from cast films using diluted suspensions to coated boards using concentrated suspensions has also been investigated.

I.4. Crosslinking

The low solid content of MFC suspensions and the moisture sensitivity of the resulting films remain the main locks for the use of MFC in barrier coating. In addition to the formation of a multi-layer or composite material, the moisture sensitivity can be reduced by crosslinking.

The reactivity of the hydroxyl groups of cellulose, and especially the C-6 OH linked to a primary carbon, offers a variety of possibilities for crosslinking reactions. Cellulose can for example be crosslinked by dialdehydes, polycarboxylic acids, or epichlorohydrin (Rojas and Azevedo, 2011). Fully-hydrolysed poly(vinyl alcohol) mainly consist in a carbon backbone bearing hydroxyl groups, thus crosslinking agents similar to those used for cellulose are reported (Marin et al., 2014). Alternatives to this covalent bonding strategy can be found, with the formation of bridges by hydrogen bonding with metal oxides or multi-valent cations such as ammonium zirconium carbonate (AZC) (Song, 2011) or Al^{3+} (Shimizu et al., 2016), or with the formation of an insoluble network using a pre-polymer (Siqueira, 2012).

A reduction of water and water vapour sensitivity can be obtained by crosslinking by creating bridges between polymer chains and thus reducing both the swelling capacity and number of hydroxyl groups available for bonding with water. The crosslinking of LbL PVOH:Clay films by glutaraldehyde reduced its moisture sensitivity, allowing to obtain a similar tensile strength at 42%RH and at 97%RH (Podsiadlo et al., 2007). Chemically crosslinked PVOH shows especially good properties in the wet state as the covalent bonds created cannot be cleaved and replaced by water-polymer hydrogen bonds, contrary to what happens without crosslinking. As a result, Shi and Yang (2015) were able to produce insoluble citric acid crosslinked PVOH fibres by electrospinning, whereas non-crosslinked fibres dissolve instantly in water (Shi and Yang, 2015). The improvement of MFC-based films in the wet state is also reported to be improved by crosslinking: the crosslinking of oxidised MFC with multi-valent cations, such as Al^{3+} as counter-ions, allowed films to be handled after 1h soaking in water, whereas non-crosslinked samples could not, and resulted in a reasonable wet tensile strength of about 25 MPa (Shimizu et al., 2016).

An improvement of behaviour in wet or humid conditions can also be obtained by chemical modification. As example, a mild esterification leading to the obtaining of alkyl chain with different length on MFC led to a decreased water uptake and improved wet strength (Sehaqui et al., 2014). However, this strategy is outside the framework of this thesis and will not be further discussed; mainly because such modification has to be performed off-line and/or with the use of solvent, whereas the three strategies described below could be implementable on-line by modification of a coating colour formulation.

I.4.1. Covalent bonding with citric acid

Citric acid (CA) is a naturally occurring polycarboxylic acid, present in fruits such as citrus fruits or pineapple. It is obtained industrially from the fermentation of sugar by microorganisms - *Aspergillius Niger* (Grewal and Kalra, 1995). As shown in Figure 18, citric acid bears three carboxyl groups and each one can react with a hydroxyl group in acidic media by Fisher esterification, preferably in the presence of a catalyst such as sodium hypophosphite. Another pathway for the esterification is by dehydration of citric acid forming a highly reactive cyclic anhydride intermediate

(Olsson, 2013), as shown in Figure 19. It requires the elimination of water and curing with an activation temperature around 150°C.

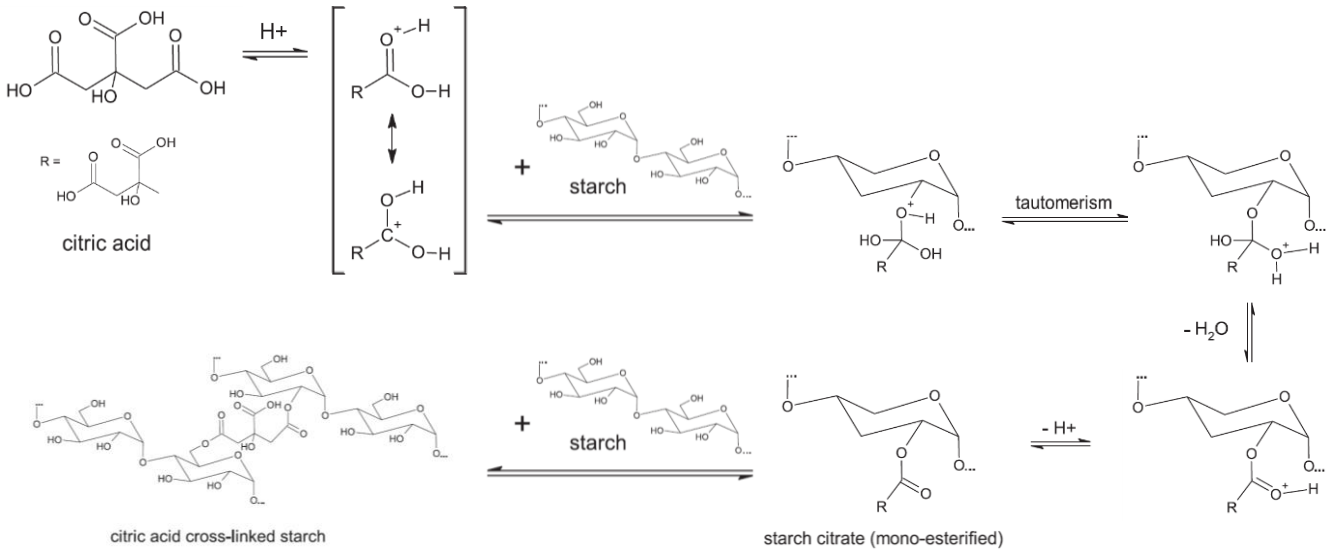

Figure 18 - Schematic illustration of the crosslinking of starch with citric acid by Fisher esterification (Olsson et al., 2013b).

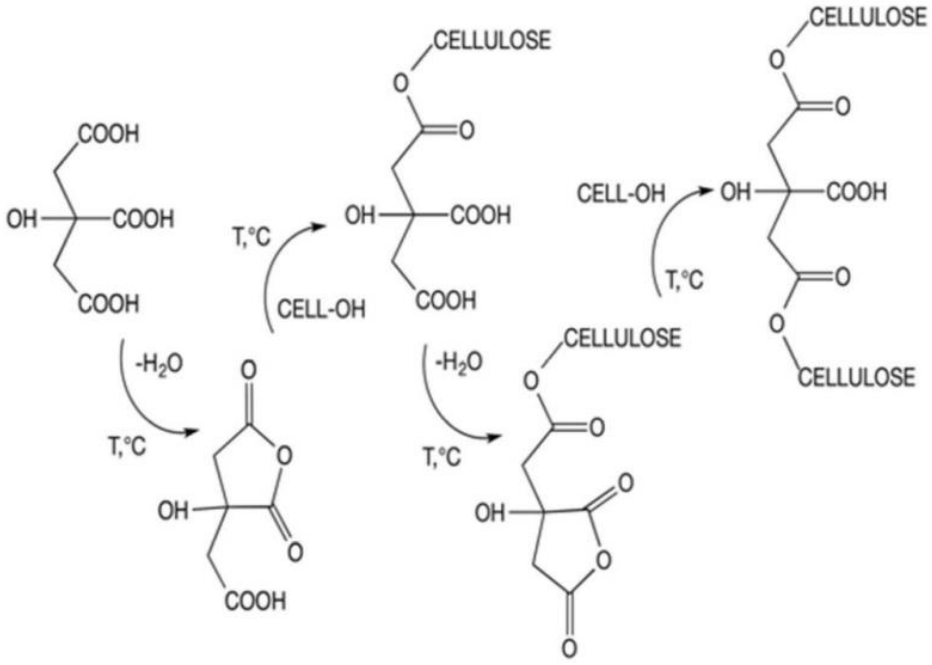

Figure 19 - Schematic illustration of the crosslinking of cellulose with citric by formation of cyclic anhydride intermediates (Quellmalz and Mihranyan, 2015).

Inspired from the textile industry using citric acid for cotton fabric finishing imparting qualities of easy care, e.g. wrinkling resistance, Caulfield (1994) soaked paper sheets in a citric acid solution with sodium hypophosphite as catalyst. After drying and curing at 180°C for 90 seconds, the crosslinked papers exhibited great improvements in mechanical properties with a wet tensile strength multiplied by 3 or 5 with 4% or 10% of citric acid, respectively. A satisfying behaviour in humid conditions has also been demonstrated with an improved creep resistance under humidity cycles between 50%RH and 90%RH. For paper-making applications, citric acid crosslinking has also the advantages of producing base hydrolysable bonds, important for the recycling of crosslinked materials, and the ability to delay the curing of the material in the production process (Caulfield, 1994). To our knowledge, only one publication deals with the cross-linking of microfibrillated cellulose with citric acid. Quellmalz and Mihranyan (2015) used citric acid for crosslinking microfibrillated cellulose filtration membranes. Films were soaked overnight in a 16 wt% citric acid solution in the presence of 1 wt% catalyst, and cured in a hot-press for 10 minutes at 160°C. The wet strength was greatly improved with an increase in wet tensile strength from 2.3 to 13.7 MPa. The treated membrane had the ability of to filter 20 nm gold particles present in water, whereas a non-treated membrane let it pass due to the formation of micro-cracks (Quellmalz and Mihranyan, 2015).

In the case of PVOH, citric acid is used to make it insoluble. Shi and Yang (2015) prepared citric acid crosslinked PVOH fibres by electrospinning and an optimal curing temperature of 140°C was found. It made the fibres insoluble while avoiding coloration observed upon curing at 160°C, attributed to the formation of unsaturated acids. An increase in PVOH crystallinity upon curing is also reported. PVOH has also been crosslinked with citric acid as films with application to food packaging by Birck (2014). The mechanical resistance and glass transition temperature have been increased with the polycarboxylic acid content and curing time, but at 40 wt% of citric acid the films were too brittle to be considered for food packaging application (Birck, 2014).

Citric acid crosslinking has been more widely studied with other polymers, such as starch, with promising results in terms of permeability. It is added after starch gelatinisation and cooling down, as the combination of acidic medium and high temperature can result in starch hydrolysis. An increasing amount of citric acid up to 20 wt%, with curing at 150°C, led to a reduction in water vapour diffusion coefficient (D) compared to pristine starch: from 14.8×10^{-14} to 0.76×10^{-14} m²/s at 50%RH and from 20.8 to 4.05 m²/s at 90%RH. The moisture sorption was also decreased and the water vapour barrier improved (Olsson et al., 2013a). This type of formulation has been applied to paper coating at different pH and with different drying temperatures. An optimum at pH = 4 was found in terms of water vapour and oxygen barrier, attributed to a better crosslinking than at pH 5 to 6.5 and a lower starch hydrolysis than at pH 2 to 3. A WVTR at 23°C 50%RH of 15.6 g/(m².d) is obtained with this formulation applied by double coating for a total basis weight of 15.4 g/m². It is equivalent to a permeability of 11.8 g.µm/(m².d.hPa), considering a film of equivalent thickness with a density of 1.45 g/cm^3. In a similar manner, an oxygen permeability of 48 cm^3.µm/(m².d.hPa) is obtained (Olsson et al., 2013b). Citric acid has also been found to act as a dispersant for clay particles in the case of plasticised starch:clay composite coating, slightly improving the water vapour barrier (Olsson et al., 2014). The use of citric acid for the crosslinking of carboxymethyl cellulose, hydroxyethyl cellulose, hydroxypropyl cellulose, and alginate is also reported (Coma et al., 2003; Demitri et al., 2008; Stone et al., 2013).

I.4.2. Hydrogen bonding with ammonium zirconium carbonate

Ammonium zirconium carbonate (AZC) is found under the form of an alkaline solution containing anionic zirconium species with bridging hydroxyl groups and carbonate groups bound to the zirconium. It has applications in paper surface coating; it promotes adhesion by forming hydrogen bonds with hydroxyl-bearing polymers and covalent bonds with carboxyl-bearing polymers (Moles, 2002). The binding of paper with a surface sizing polymer, such as starch, resulted in improved performance and a reduced dusting and linting by addition of AZC (Wolff et al., 1996). It is non-toxic and does not require curing for crosslinking. A possible mechanism of the interaction between starch or cellulose and AZC is found in Figure 20. It first consists in hydrogen bonding between starch and the ammonium ions of the AZC solution, and the formation of new hydrogen bonds upon drying after release of carbon dioxide and ammonia. This reaction can also lead to AZC self-crosslinking (Song, 2011).

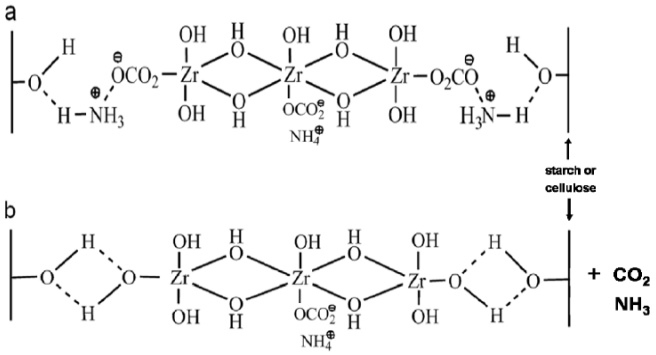

Figure 20 - Starch or cellulose crosslinking with ammonium zirconium carbonate (AZC) (Song, 2011).

The crosslinking of starch sizing by AZC has been found to improve the behaviour of the sized board towards water and humidity. Despite having no effect on the water transmission rate of the material, the sized boards exhibited lower moisture content, lower water absorbency (Cobb method), and improved compressive strength and burst strength. In particular, the burst strength was less humidity-dependent than in the case of non-crosslinked starch (Jo et al., 2012). In the case of hemicellulose (galactoglucomannan) self-standing films plasticized with sorbitol, AZC crosslinking also reduced water solubility. While pure hemicellulose films dissolved easily in water, AZC-crosslinked films were only fractionated into flakes that remained undissolved after 30 minutes. It also lowered the moisture content of the films and allowed to maintain their mechanical properties over a wider humidity range. An effect on the barrier properties was also observed with an halved oxygen and a slightly reduced water vapour permeability at 54%RH and 74%RH (Mikkonen et al., 2013). The crosslinking could not be verified by chemical analysis. However, indirect methods could be used such as a rheological study for measuring the increase in viscosity of an AZC-crosslinked polymer solution (Song et al., 2011). Another study investigates the solubility and barrier properties of AZC-crosslinked PVOH:Xylan blends plasticized with glycerol. A decrease of solubility could be observed and the polymer blend remained degradable in soil. However, similarly to Mikkonen and co-workers (2013), there was no significant effect on the water vapour permeability (X. Chen et al., 2015).

I.4.3. Self-crosslinking of polyamidoamine epichlorohydrin

Polyamidoamine epichlorohydrin (PAE) is a cationic electrolyte used for improving the wet resistance of paper (Ahola et al., 2008). Its chemical structure and main self-crosslinking reaction is presented in Figure 21. Self-crosslinking of PAE occurs upon curing at 105°C, mainly by formation of 2-propanol bridges from the azetidinium ring (AZR) (main self-crosslinking reaction) and also by reaction of the AZR with the carboxyl end for the formation of an ester bond (secondary crosslinking reaction). The AZR also reacts on the carboxyl groups of hemicelluloses present in wood fibres or in carboxymethyl cellulose (CMC) (Siqueira, 2012). The wet-tensile index of a HBKP (hardwood bleached kraft pulp) paper with 0.056 mmol/g of carboxyl groups could be improved from 1 to 12 N.m/g using 6 mg/g of PAE. In the case of a linter pulp with no carboxyl group the improvement is only from 0.5 to 0.8 N.m/g using 4 mg/g of PAE, evidencing the role of the 2-propanol bridges between PAE and the pulp for improving the wet resistance (Obokata and Isogai, 2007). Combining PAE with carboxymethylated MFC has been found to lead to a synergistic reinforcement at the wet state (Ahola et al., 2008). In the case of a water-soluble polymer such as starch, upon heating the starch molecules are entrapped in the network formed by PAE self-crosslinking. This allows a reduction of the swelling and dissolving of starch in water (Song, 2011).

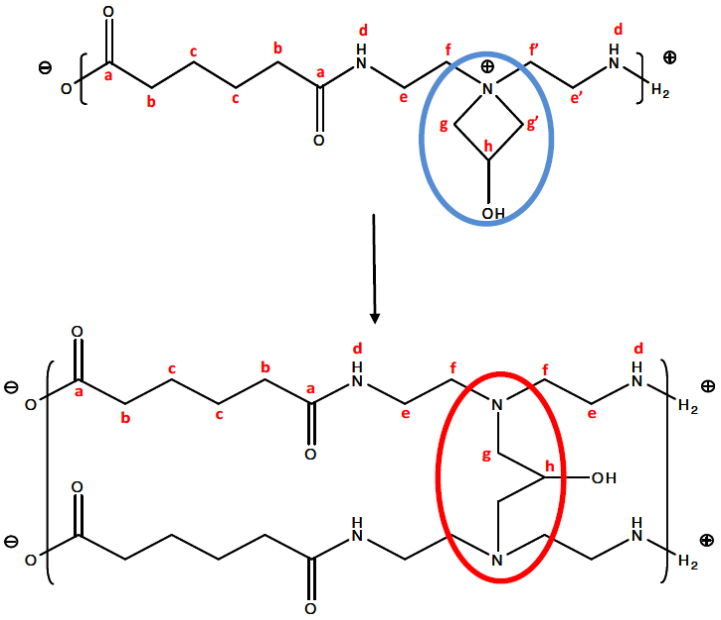

Figure 21 - Main PAE self-crosslinking reaction (Siqueira, 2012).

I.4.4. Conclusion on crosslinking

In this section, three different crosslinking strategies have been described using chemicals of low toxicity: covalent bonding using citric acid, hydrogen bonding using AZC, and formation an insoluble network using PAE as a pre-polymer. It was found to improve the general behaviour of cellulose, PVOH, or starch in wet or humid conditions, in terms of mechanical properties, swelling, and barrier properties. In addition in the case of PVOH, crosslinking can also turn the films insoluble in water. Citric acid, AZC, and PAE are not reported for the crosslinking of the same materials: citric

acid is mostly reported for starch of cotton fibres crosslinking, AZC for starch crosslinking with application to surface sizing, and PAE for the crosslinking of cellulose fibres for improving paper wet strength. Such products seem promising for improving the properties of the PVOH:MFC or PVOH:MFC:Clay composites described previously, but few study report both the use of such chemicals on PVOH and cellulose, and especially PVOH and MFC. This thesis aims at comparing the effect of chemical crosslinking on PVOH and MFC using citric acid, AZC, and PAE, in order to determine what crosslinking strategy would be best suited for improving the wet and humid behaviour of PVOH:MFC composite films with application to water-based barrier coating.

I.5. Conclusion

The objective of this study is to develop more sustainable barrier packaging solutions using microfibrillated cellulose (MFC). This literature review chapter presented the problematic of barrier food packaging and the potential of developing more sustainable solutions based on biosourced and biodegradable MFC. Nowadays, food is most of the time stored in a packaging for ease of transportation, storage, and in order to preserve it from degradation thus avoiding food spoilage. Paper-based packaging is more sustainable than plastic packaging in terms of source and end-of-life, but it lacks gas barrier for food protection. This gas barrier can be obtained using petro-sourced lattices, non-recyclable wax, or fluorinated products potentially hazardous for human health. MFC can be produced from wood fibres without chemical treatment and forms dense, tough, oxygen-barrier films. Many different mechanical treatments and chemical pre- or post-treatments exist resulting in a large number of MFC grades. Even in the case of non-chemically modified MFC, the size of the fibrils can vary enormously resulting in properties depending on the intensity of the treatment, and the influence on barrier properties is not well understood. In this study, it will be essential to begin with investigating the effect of the degree of fibrillation on the properties of MFC films or composites.

The high viscosity of MFC suspensions at low solid content (usually 2 wt%) makes them difficult to apply directly using common water-based coating processes. A strategy for the application of a 100% MFC layer on board is to include a filtration step, removing a large fraction of water before drying. Such process has not been widely studied, especially for barrier applications, and will be investigated in this thesis. A strategy for the application of MFC in water-based barrier coating is to use it as filler in a coating colour formulation. It can be combined with a hydrosoluble polymer, such as poly(vinyl alcohol) (PVOH) that is also barrier to oxygen, biodegradable, and potentially partially or fully biobased. Such materials are mostly reported in the form of self-standing films and deserve to be developed in the field of barrier coating. In such formulations, MFC is reported to bring a mechanical reinforcement, upon successful dispersion, and to improve the layer quality. This last point is not well understood and worth further investigations.

PVOH is also sensible to water and humidity; the properties of PVOH:MFC composites can be improved by addition of platy pigments: layered silicates, also named clays. Upon dispersion in a PVOH matrix, layered silicates are responsible for a distribution of gas impermeable platelets oriented normal to the permeation axis, forcing diffusing gas molecules to bypass them and thus reducing permeability. The interactions between layered silicates and the matrix also bring a mechanical reinforcement and reduce the water and humidity sensibility. Similar effects are obtained using MFC as a matrix, with a more difficult dispersion in the form of films due to the larger size of microfibrillated cellulose compared to polymer chains. From these observations, mixtures of PVOH, MFC, and layered silicates, rarely described in the literature, seem to have a great potential for the formation of gas barrier layers by water-based barrier coating. Such layers could be further improved, especially in terms of water and humidity resistance, using a crosslinking strategy.

This thesis aims at developing the use of microfibrillated for the formation of barrier layers on top of paper or board, with application to food packaging. Due to the inconvenience of using pure MFC suspensions of low solid content for coating, two other layer formation strategies are investigated: MFC as the main component using a process including a filtration step (Chapter III), and MFC as filler in a coating colour formulation (Chapter IV and VI). In Chapter III, before producing

barrier layers on board, the degree of fibrillation of different MFC grades produced by enzymatic pre-treatment will be compared by indirect methods, e.g. suspension rheology and self-standing films optical properties. This aims at determining what indirect methods describe best the quality of MFC suspensions, and at selecting which MFC grades would be best suited for the following formation of barrier layers. A selected MFC grade is then laminated on board at different basis weights in order to investigate the opportunities given by this innovative technique in terms of adhesion of the MFC layer, and oxygen and grease barrier. Chapter IV focuses on PVOH:MFC composite films produced with a process mimicking blade coating. While most of the studies report the effect of the MFC ratio, here the effect of the PVOH grade (degree of polymerisation, degree of hydrolysis) and MFC grade (degree of fibrillation, pulp origin) are also investigated. It was found of interest to better understand the improvement given by the addition of MFC in terms of PVOH layer formation, using a laboratory infrared drying bench for determining the drying kinetics of PVOH or PVOH:MFC suspensions as such and coated on board. Crosslinking is an interesting strategy for improving the properties of PVOH:MFC composites in wet or humid conditions, but most of the times either the crosslinking of PVOH films or MFC films (or similar hydroxyl-bearing polymers such as starch) is reported. In addition, looking for non-toxic water-based compounds reduces the possible choices. The effect of crosslinking on both PVOH and MFC films has thus been investigated using citric acid, AZC, or PAE. Chapter V focuses on the addition of layered silicates (clays) to PVOH:MFC barrier layers when such composites are mostly reported for their mechanical properties, with a specific attention to the dispersion of the filler and the production process for obtaining well-dispersed fillers. The original aspect of this chapter also lays into the upscaling from cast films to coated boards, which involves working with more concentrated suspensions and influences the dispersion state of the fillers.

To summarise, this thesis is divided in three chapters: the first one deals with MFC suspensions and films, with the production of a MFC barrier layer on board using an innovative technique involving a filtration step, the second one deals with PVOH:MFC composites produced using a process mimicking blade coating with in addition the study of PVOH:MFC drying and PVOH or MFC crosslinking, and the third one deals with PVOH:MFC:Clay films produced by solvent casting and their upscaling to the production of a composite barrier layer on board using a coating technique.

Chapter II: Materials and Methods

Chapter II: Materials and Methods

II.1. Materials

II.1.1. Microfibrillated cellulose

Several grades of microfibrillated cellulose (MFC) have been produced at Centre Technique du Papier (CTP) from two different pulps: a birch kraft pulp from Stora Enso, Finland, and a softwood sulphite pulp from Domsjö, Sweden. The pulps have been pre-refined at 3.5 wt% to 25 Schopper-Riegler degrees (°SR), enzymatically treated with endoglucanase FiberCare R at 0.1 kg/t during 1 hour at 50°C and pH 5, post-refined to 80°SR, diluted to 2 wt%, and mechanically treated by high-shear homogenization on a pilot scale homogenizer from GEA Niro-Soavi. The homogenization consisted in a first pass at 500 bar, a second pass at 1,000 bar, and 4 subsequent passes at 1,500 bar giving a total of 6 passes. The MFC grades, obtained using this process, are named KB in the case of the birch kraft pulp, and D in the case of the softwood sulphite pulp. The birch kraft pulp has also been treated using a similar process except that the first pass at 500 bar has not been performed, the homogenization being a first pass at 1,000 bar and 4 subsequent passes at 1,500 bar. Suspension samples have been withdrawn just before the first homogenization pass (MFC 0P), and after each pass in the homogenizer (MFC 1P, 2P, 3P, 4P, and 5P). Another MFC grade produced by strong refining of a softwood kraft pulp has been purchased from the University of Maine, USA, in 2014; it is thereafter referred to as MFC UM. All MFC suspensions were stored at 4°C in a cold room. A summary of the different MFC grades used in this study can be found in Table 7.

Reference	Source	Pre-treatment	Mechanical treatment
UM	Kraft softwood	No pre-treatment	Refining
D	Sulphite softwood	Enzymatic	Refining + Homogenization 6 passes
KB	Kraft hardwood	Enzymatic	Refining + Homogenization 6 passes
0P	Kraft hardwood	Enzymatic	Refining
1P	Kraft hardwood	Enzymatic	Refining + Homogenization 1 pass
2P	Kraft hardwood	Enzymatic	Refining + Homogenization 2 passes
3P	Kraft hardwood	Enzymatic	Refining + Homogenization 3 passes
4P	Kraft hardwood	Enzymatic	Refining + Homogenization 4 passes
5P	Kraft hardwood	Enzymatic	Refining + Homogenization 5 passes

Table 4 - Microfibrillated cellulose grades used for the study.

II.1.2. Poly(vinyl alcohol)

Four grades of poly(vinyl alcohol) (PVOH) have been supplied by Kuraray Europe under the names of Poval 6-98, 26-88, 30-98, and 28-99. In this thesis they are named PVOH 6-98, PVOH 26-88, PVOH 30-98, and PVOH 28-99. The poly(vinyl alcohol) pellets have a dry matter content of 98 wt%. Their degree of polymerization, molecular weight and degree of hydrolysis (substitution of acetate groups to alcohol groups) have been given by the supplier are reported in Table 5.

Reference in the study	Commercial name	Degree of polymerisation	Molecular weight (g/mol)	Degree of hydrolysis (%)
PVOH 6-98	Poval 6-98	1,000	47,000	98.4 ± 0.4
PVOH 26-88	Poval 26-88	3,300	160,000	87.7 ± 1.0
PVOH 30-98	Poval 30-98	3,300	150,000	98.4 ± 0.4
PVOH 28-99	Poval 28-99	3,300	145,000	99.4 ± 0.4

Table 5 - Properties of the four PVOH grades used in this study.

II.1.3. Layered silicate

Four grades of layered silicates (clays) have been used: a bentonite Cloisite-Na from Byk additives (C), a bentonite Nanofil 116 from Rockwood additives (N), a laponite Laponite RD from Rockwood additives (L), and a kaolinite (china clay) Barrisurf HX from Imerys (K). The layered silicate powders have a dry matter content of 94 wt%. The thickness, diameter, cationic exchange capacity (CEC), and density of the platelets have been copied from supplier's technical data sheet and can be found in Table 6.

Layered silicate		Thickness of the platelets (nm)	Diameter of the platelets (nm)	CEC (meq/100g)	Density (g/cm^3)
Type	Name				
Bentonite	Cloisite-Na	1	300 - 1,000	93	2.86
	Nanofil 116	1	100 - 500	116	–
Laponite	Laponite RD	1	25	95	2.57
Kaolinite	Barrisurf HX	20	15,000 - 20,000	2.5	2.72

Table 6 - Source and properties of the layered silicates.

II.1.4. Crosslinking agents

Three chemicals have been used for PVOH and MFC films crosslinking: citric acid (CA) from Univar Sweden AB, Sweden, ammonium zirconium carbonate (AZC) from Sigma-Aldrich, USA, and polyamidoamine epichlorohydrin (PAE) Kymene™ from Solenis, USA. Their chemical structure can be found in Figure 22.

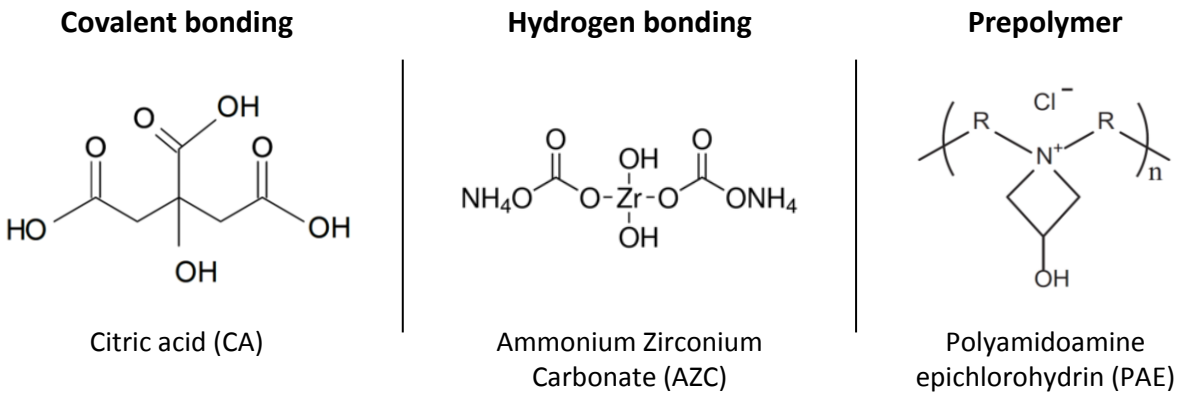

Figure 22 - Chemical structure of the chemicals used for the crosslinking of PVOH and MFC films. CA (KEGG, 2015), AZC (Sigma Aldrich, 2015), PAE (Siqueira, 2012).

II.1.5. Base board

Coating and lamination trials have been performed on a 270 g/m² solid bleached board (SBB) Performa Natura from Stora Enso, Finland, having a pigment-coated side and an uncoated side.

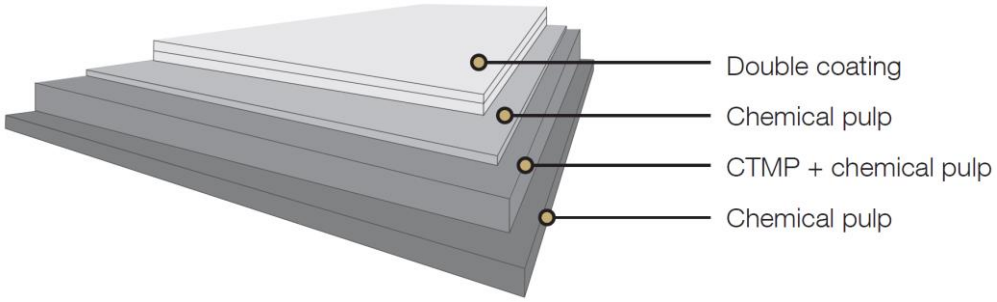

Figure 23 - Structure of the Performa Natura board used in this thesis, with pigment coating on the top side (Stora Enso, 2014).

II.2. Methods

II.2.1. Sample production

II.2.1.1. Production of self-standing films

II.2.1.1.1. MFC handsheets

MFC handsheets, or nanopapers, have been produced using a Rapid-Köthen device with a method adapted from Guezennec (2012), itself adapted from Sehaqui and co-workers (2010). A 0.5 wt% MFC suspension is prepared by dilution of a 2 wt% MFC suspension that has been mechanically stirred during 30 minutes at 500 to 1,000 rpm. The desired amount of 0.5 wt% MFC suspension, usually around 314 g in order to produce 50 g/m² dry films, is poured in a handsheet former and vacuum filtrated through a 0.65 µm cellulose ester membrane (DAWP29325, Merck Milipore, Germany). The wet MFC cake formed is covered on the top side by a cover paper (savoyeux) and a blotting paper. A 5 kg roll is passed two times to remove the excess water. The membrane is peeled off the MFC wet cake and a cover paper is applied on the bottom side. The cover paper/MFC cake/cover paper complex is dried at 93°C under depression (diaphragm applying a pressure of 100 kPa) during 10 to 15 minutes, while being covered by a carrier board. Finally, the cover papers are peeled off the MFC dry film. During all the experiment, the 0.5 wt% MFC stock suspension remains under mechanical stirring. Part of the MFC handsheets production has been performed by Bernard Alphand at CTP, Grenoble, France.

Figure 24 - Rapid-Köthen apparatus for the production of MFC handsheets.

II.2.1.1.2. MFC films by casting

MFC self-standing films have also been produced by solvent casting. A 1 wt% MFC suspension is prepared by dilution of a 2 wt% MFC suspension that has been mechanically stirred during 30 minutes at 500 to 1,000 rpm. The desired amount of 1 wt% MFC suspension, usually 75 g in order to produce 50 g/m² dry films, is poured in a polystyrene petri dish (EL49.1, Carl Roth, Germany) having an inner surface of 150 cm² and put to dry in a controlled atmosphere room at 23°C 50%RH during 3 days.

II.2.1.1.3. Composite films by coating-peeling

PVOH:MFC composite self-standing films have been produced by coating-peeling from concentrated suspensions. A 2 wt% MFC suspension is mechanically stirred during 30 minutes at 500 to 1,000 rpm. The desired amount of 2 wt% MFC suspension is diluted to 0.4 to 1.5 wt%, depending on the formulation, and mechanically stirred in a beaker during 10 minutes. The desired amount of PVOH pellets is added to the diluted MFC suspension under stirring. The beaker is then put in a bain-marie in order for the PVOH to solubilise under slow stirring during 1 hour at 95°C. The suspension is then cooled down to around 60°C. The dry content of the suspension, ranging from 10 to 25 wt%, is determined in order to obtain a viscosity of 500 to 2,000 mPa.s after PVOH solubilisation and cooling down to 60°C, as required for its processing.

PVOH:MFC:clay composite self-standing films have also been prepared by coating-peeling from concentrated suspensions. In this case, the day before the experiment, the clays are first diluted to 5 wt% and mechanically stirred overnight. The clay suspension is added to the formulation right after the 1 hour PVOH solubilisation, and the slow mechanical stirring at 95°C is continued during 3 to 4 hours before cooling down to 60°C. Variations from this procedure are presented in V.1.2, page 149.

The process of coating-peeling from concentrated suspensions is presented in Figure 25. It consists in a first step of coating on a base prepared specifically for this process. The base is made of a 2 mm thick aluminium plate covered by a 50 µm thick auto-adhesive polypropylene film. The polypropylene film has an adhesion in the correct range for the concentrated suspension to spread, but also for the film formed after drying to be removable by peeling. This base is coated using an Elcometer laboratory coating machine, and the wet coating thickness is determined using an applicator having a gap that can be monitored using a micrometric screw. The coated base is then dried by infrared during 10 to 15 minutes. After cooling down to ambient temperature, the composite self-standing film of about 20x30 cm can be peeled off the base.

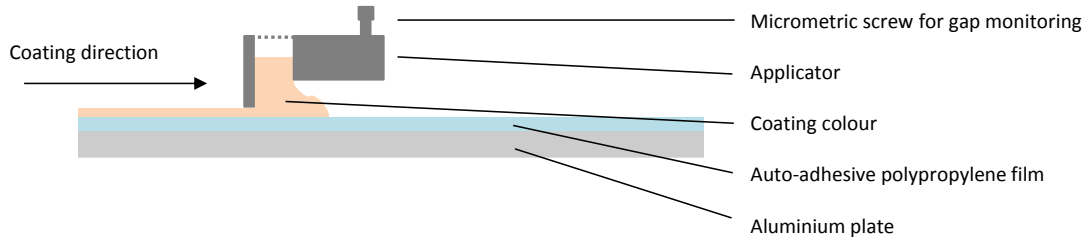

Figure 25 - Process of coating-peeling for the production of self-standing composite films.

II.2.1.1.4. Composite films by casting

PVOH:MFC:clay self-standing films have been produced by solvent casting as described in Figure 26. The day before the experiment, the clays are diluted to 5 wt% and mechanically stirred overnight. A 2 wt% MFC suspension is mechanically stirred during 30 minutes at 500 to 1,000 rpm. The desired amount of 2 wt% MFC suspension is diluted to 0.1 to 0.2 wt%, depending on the formulation, and mechanically stirred during 10 minutes in a round-bottom flask mounted with a

condenser. The desired amount of PVOH pellets is added to the diluted MFC suspension under magnetic stirring. The suspension is put in a bain-marie at 95°C during 1 hour for the PVOH to solubilise. After that, the desired amount of clay suspension is added and stirring at 95°C continues during 4 hours in order for the clays to disperse correctly. The suspension is then cooled down to ambient temperature and cast in polystyrene petri dishes as described in II.2.1.1.2, page 78. The 4 hours of additional stirring at 95°C are performed even if the clay content is equal to zero. The suspensions have a total solid content of 5 wt% before being poured in petri dishes.

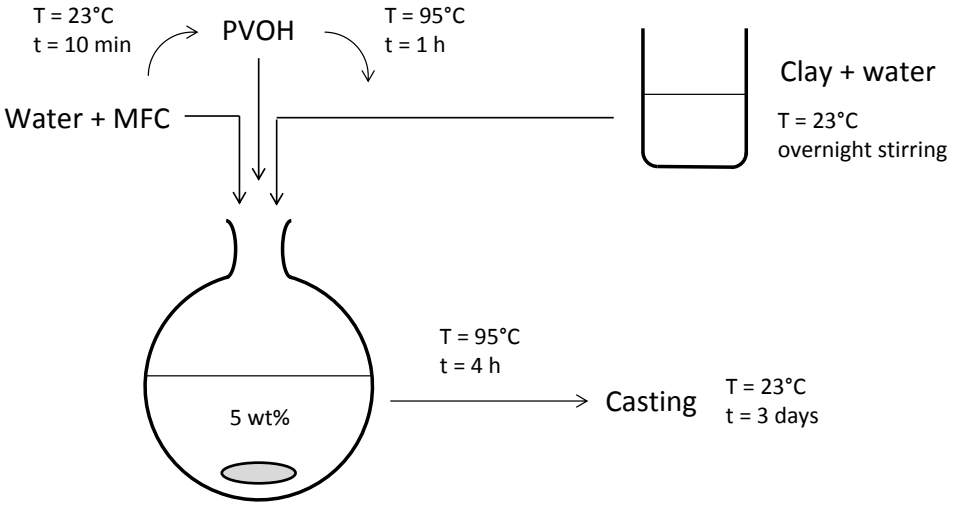

Figure 26 - Process of solvent casting for the production of self-standing composite films.

II.2.1.1.5. Crosslinking

Crosslinking agents have been added to PVOH and MFC self-standing films as described in Figure 27 with 5 wt% of crosslinking agent. The crosslinking agents used are citric acid (CA), ammonium zirconium carbonate (AZC), and polyamidoamine epichlorohydrin (PAE). In the case of MFC, a 2 wt% suspension is mechanically stirred during 30 minutes at 500 to 1,000 rpm, diluted to 1 wt%, mixed with the desired amount of crosslinking agent, and cast in polystyrene petri dishes as described in II.2.1.1.2, page 78. In the case of PVOH, the desired amount of PVOH pellets is dispersed in a beaker with deionised water and solubilised at 95°C during 1 hour in a bain-marie, leading to a 5 wt% solution. After cooling down to ambient temperature, the solution is mixed with the desired amount of crosslinking agent and cast in polystyrene petri dishes according to II.2.1.1.2, page 78. In the case of PAE crosslinking agent, a thermal post-treatment of the cast films has been performed in an oven at 105°C during 10 minutes. In the case of CA crosslinking agent, a thermal post-treatment of the cast films has been performed in an oven at 150°C during 10 minutes. Thermally-treated and untreated films without crosslinking agents have also been produced for comparison.

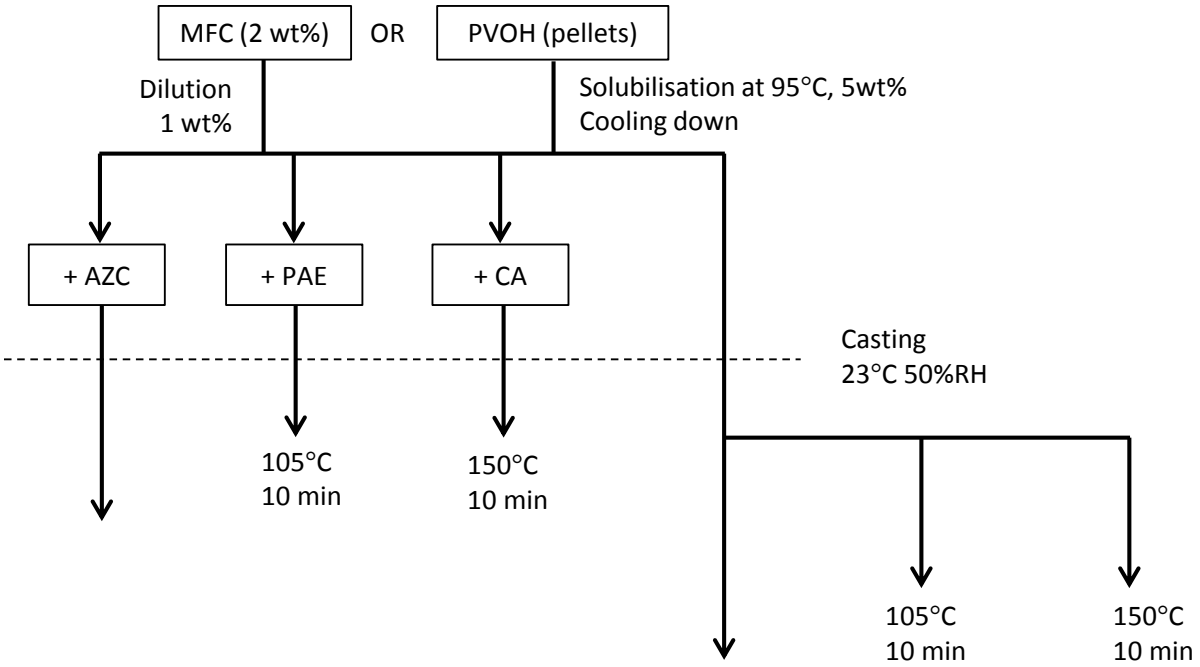

Figure 27 - Process for producing cross-linked PVOH and MFC self-standing films.

II.2.1.2. Production of a top-layer

II.2.1.2.1. Wet lamination of MFC

MFC films have been applied as a top layer on a paper or board as described in Figure 28, in the framework of a patent by Guerin and co-workers (2016a).

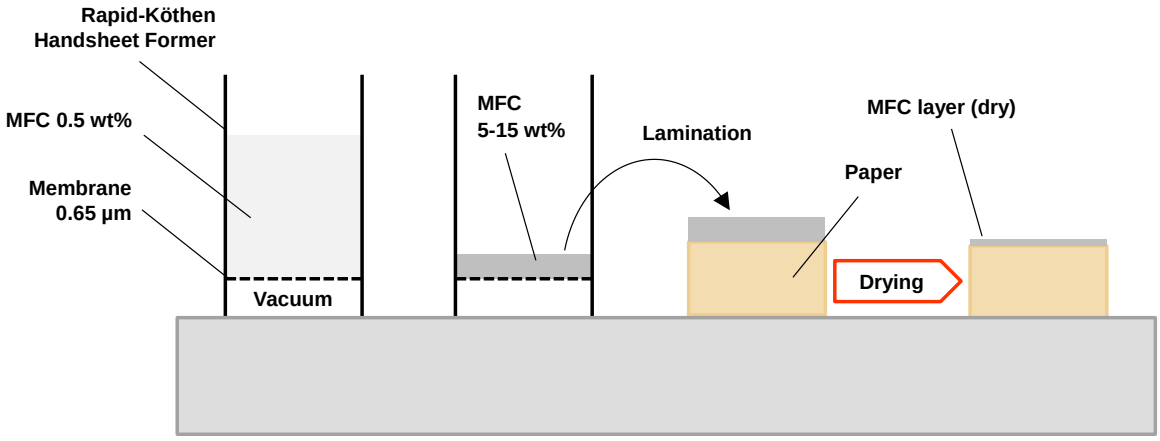

Figure 28 - Simplified process of wet lamination.

A MFC wet cake is produced by filtration of a 0.5 wt% MFC suspension through a 0.65 µm membrane using a Rapid-Köthen handsheet former as described in II.2.1.1.1, page 78. The MFC wet cake is covered by a board sample (top side). The membrane/wet MFC cake/board sample complex is

turned over, covered by a blotting paper, and a 5 kg roll is passed two times in order to remove water on the membrane side. The membrane is then peeled off the MFC wet cake, a cover paper is placed instead (bottom side), and the cover paper/MFC wet cake/board sample complex is put to dry at 93°C under depression during 10 to 15 minutes. Finally, the cover paper is peeled off the MFC dry top-layer that remains stuck on the board sample. During all the experiment, the 0.5 wt% MFC stock suspension remains under mechanical stirring.

II.2.1.2.2. Composite coating

PVOH:MFC:clay composite coating has been performed on board using an Elcometer laboratory rod coater shown in Figure 29. A PVOH:MFC:clay suspension is prepared as described in II.2.1.1.3, page 79, except that the beaker and bain-marie are replaced by a jacketed reactor serving the same purpose. A 270 g/m² board is placed on the Elcometer, pigment-coated side up, and a wired-rod is mounted. 15 mL of suspension are applied in front of the wired rod and coated on the board upon advance of the wired rod. The coated board is then dried by infrared during 2 minutes. The type of wired rod and coating speed are monitored in order to obtain a dry coat weight of 10 g/m².

Figure 29 - Elcometer laboratory coater used for composite coating.

II.2.2. Specific characterisations

II.2.2.1. Drying kinetics

The drying kinetics of PVOH:MFC suspensions have been investigated using the experimental setup described in Figure 30. First, a 18 wt% PVOH:MFC suspension is prepared similarly to II.2.1.2.2, page 82. The suspension is kept under magnetic stirring in a bain-marie at 40°C and used for this experiment on the same day. 10.75 g of suspension is poured into a 15.7 cm in-diameter Teflon mould that has been weighed, in order to obtain a film having a dry basis weight of 100 g/m^2, and then spread with a spatula. The mould is then placed under the dryer on a metal frame that is fastened to a balance (Mettler PE360, accuracy 1 mg in the range from 0 to 60 g and 1 cg in the range

from 60 to 360 g). The heat flux delivered by the lamps is monitored thanks to a radiant heat flux sensor supplied by Captec (Lille, France) fixed at one edge of the bench. It should be noted that the heat flux at this location is lower than in the centre of the dryer, where the sample is placed. The temperature at the bottom of the mould is measured by a thin Cu-Cn thermocouple (type T) that is manufactured at the laboratory. These three signals (mass, heat flux and temperature) are collected by a data acquisition system during the experiment at a rate of 1 measurement per second.

The measurement of the heat flux generated by the infrared lamp shows that the initial flow of 930 W/m^2 at t_0 increases to 1400 W/m^2 during the first two minutes due to heating of the lamps. It continues to increase slowly up to 1600 W/m^2 during the ten following minutes. In order to begin each experiment at the same point, i.e. infrared lamps cold, two experiments were spaced by at least 45 minutes of cooling down under ambient air flow.

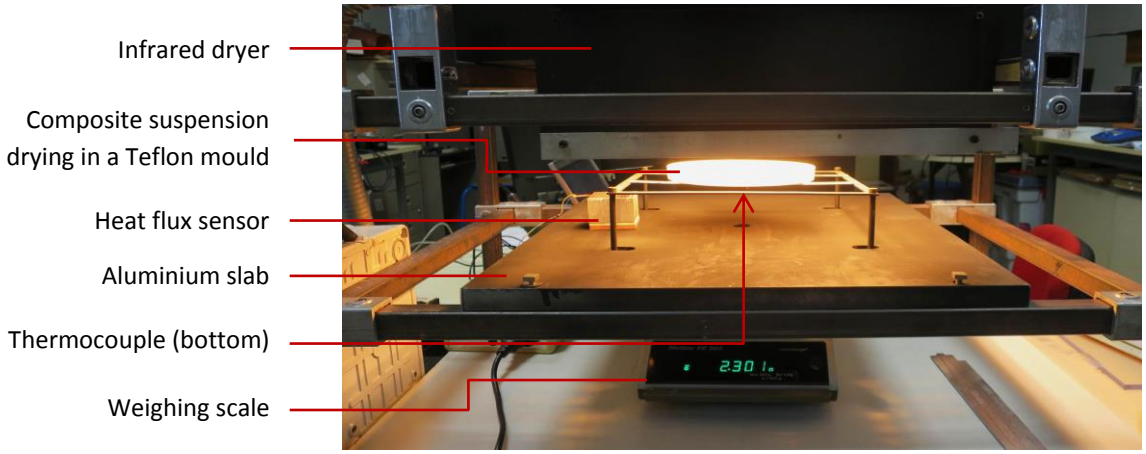

Figure 30 - Experimental setup for the analysis of the drying kinetics of a composite suspension.

A similar measurement has been performed on 15x15 cm boards coated with the same PVOH:MFC suspension, using the coating process described in II.2.1.2.2, page 82. In this case, the thermocouple is placed at the bottom of the coated board.

II.2.2.2. Water resistance

The water resistance of PVOH and MFC films, with or without thermal or chemical treatment, has been investigated by magnetic stirring in deionised water. Samples of 20 mm diameter, cut from films produced by casting according to II.2.1.1.5, page 80, are weighted after equilibrium at 23°C 50%RH. 70 mL of deionized water are poured into a 100 mL pot and placed under magnetic stirring at 400 rpm. The 20 mm diameter sample is added in the pot at t = 0 and its physical integrity is followed during 3 hours, as shown in Figure 31. The number of pieces present in the pot after 2, 5, 10, 15, 20, 35, 60, 120, and 180 min is noted. Experiments have been performed in duplicates. After 3 hours of stirring in deionized water, if the film is still in one piece, it is put between two blotting papers and pressed 2 times with a 10 kg smooth metal roll in order to remove the excess water. After that, the humid film is weighted ($m_{f,w}$), stored at 23°C 50%RH for 1 day for equilibrium, and weighted again

($m_{f,23°C\ 50\%RH}$). The evolution of the mass of the sample before the experiment ($m_{i,23°C\ 50\%RH}$), just after the experiment ($m_{f,w}$), and after re-equilibrium with the ambient ($m_{f,23°C\ 50\%RH}$) allows determining the water absorption (m_{ads}, %) and mass loss (m_{loss}, %) according to the following equations:

$$m_{ads} = \frac{m_{f,w} - m_{f,23°C\ 50\%RH}}{m_{f,23°C\ 50\%RH}} \quad (Eq.10)$$

$$m_{loss} = \frac{m_{i,23°C\ 50\%RH} - m_{f,23°C\ 50\%RH}}{m_{i,23°C\ 50\%RH}} \quad (Eq.11)$$

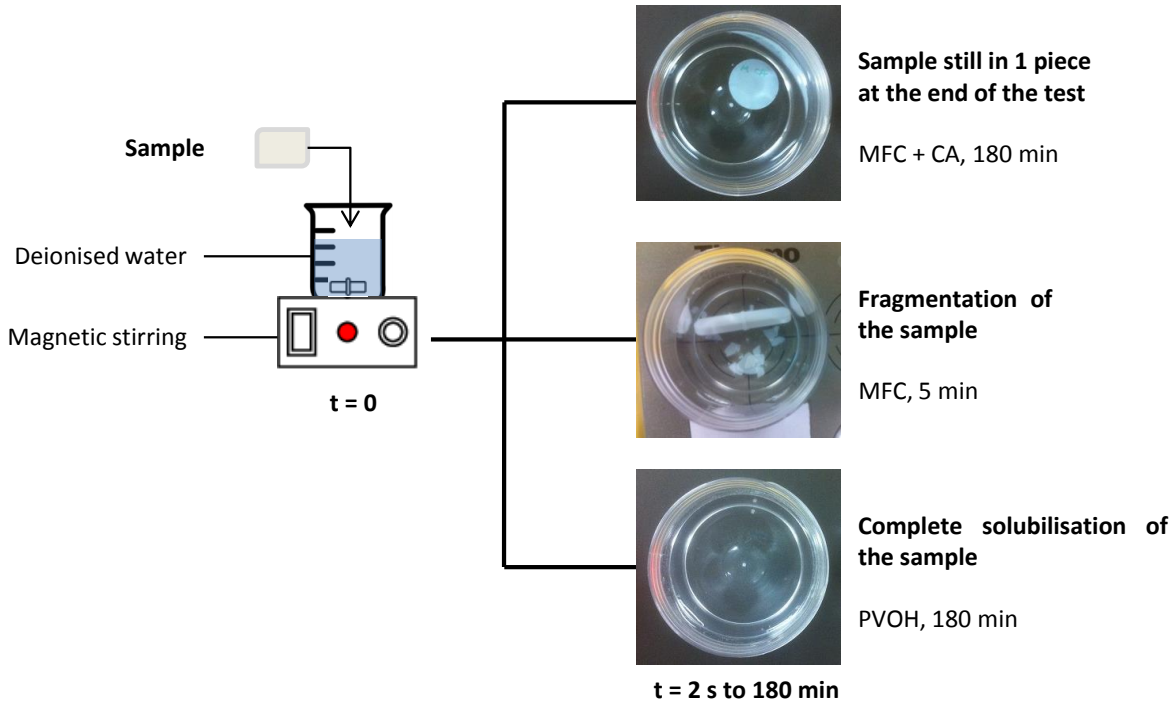

Figure 31 - Water resistance test for PVOH and MFC samples.

II.2.3. Other analyses

II.2.3.1. Suspension characterisation

The viscosity of composite suspensions has been measured with a Brookfield viscosimeter, using different sizes of rotational spindle according to the viscosity range, and at a rotational speed of 100 rpm.

The rheological behaviour of MFC suspensions has been determined with a control stress rheometer AR-1000 from TA Instruments, at 20°C, using plate-plate geometry with a gap of 1 mm. The 2 wt% MFC suspension was mechanically stirred during 30 min at 500 to 1,000 rpm before testing. The flow procedure consisted in a decreasing shear rate from 2,000 to 0.02 s^{-1} followed by an increasing shear rate from 0.02 to 2,000 s^{-1}, with five steps of 90 seconds per decade.

The morphology of the residual macro-fibres present in MFC suspensions has been measured with a pulp inspector MorFi from Techpap, France. The lengths and widths are determined by image analysis of a flowing diluted suspension. With a detection threshold of 5 µm, elements having a length inferior to 80 µm are considered as "fines" and elements having a length superior to 80 µm are considered as "fibres". MorFi analyses have been performed by François Cottin at CTP, Grenoble, France.

The particle size distribution of Cloisite-Na aggregates in PVOH solutions has been measured with a flow particle image analyser FPIA-3000 from Sysmex, Japan. Similarly to the pulp inspector, the suspension flows in from of a camera performing image analysis, determining the area and diameter of the elements in suspension.

II.2.3.2. Structural characterisation

The solid content of composite suspension and the dry coat weight of coated boards have been determined with a thermo-balance LJ16 from Mettler Toledo, USA, heating at 120°C to 160°.

The basis weight of the samples has been measured by weighting discs of 70 cm² using a precision balance (± 0.1 mg).

The thickness of the samples has been measured with a precision micrometer MI.20 from Adamel Lhomargy, France, with a precision of 1 µm. Measurements were performed on a 16 mm² area under a pressure of 100 ± 10 kPa.

The surface topography of composite films and coated board has been analysed with a Topo3D apparatus belonging to Techpap Sas. The measurement principle of Topo3D is based on enhanced white light vertical scanning interferometry. The scanned surfaces were 1380 µm long per 1044 µm large. The lateral resolution was 0.94 µm and the vertical resolution is 0.02 µm Ra. Topo3D analyses have been performed by Geneviève Cortot at CTP, Grenoble, France.

II.2.3.3. Microscopic analysis

Optical microscopy observations were performed using an optical microscope AXIO Imager M1m from Zeiss, Germany, in transmission mode. In the case of MFC suspensions, fibres have been coloured with Congo Red. Parts of the optical microscopic observations have been performed by Christelle Boucherand at CTP, Grenoble, France.

Scanning Electron Microscopy (SEM) micrographs of surfaces were obtained from a Quanta 200 ESEM from FEI, USA, with an acceleration voltage from 10.0 to 15.0 kV and a magnification of x600 to x1300. The surface of the samples was sputter coated with a thin layer of gold prior to analysis. SEM analyses have been performed by Caroline Duprat at CMTC, Grenoble, France.

The surface of composite films has been analysed using a field emission gun-scanning electron microscope FEG-SEM Ultra-55 from Zeiss, Germany. The working distance was 6 to 10.9 mm for an accelerating voltage of 3.00 kV at a magnification of x600 to x20,000. FEG-SEM analyses have been performed by Caroline Duprat and Valerie Meyer at CMTC, Grenoble, France.

II.2.3.4. Optical and mechanical properties

The optical properties of the films have been measured with a hazemeter haze-gard plus from Byk Additives & Instruments, Germany, according to ASTM-D1003. This apparatus gives the total transmittance (transmitted intensity of visible light divided by the incident intensity), haze (fraction of visible light diffused through the sample at an angle superior to 2.5°), and clarity (fraction of visible light transmitted through the sample at an angle inferior to 2.5°) of the samples.

Tensile tests were carried out at 23°C 50%RH after at least 24 hours of conditioning. Measurements were performed on a dynamometer MTC 100 from Noviprofibre SA, France, equipped with a load cell of 500 N according to the standard ISO 1924-2, with a crosshead speed of 10 mm/min on samples 15 mm long with a tested length of 100 mm. At least 5 replicates were tested per reference.

Scott bond adhesion tests have been carried out on MFC-laminated boards using an internal bond tester pendulum IBT-10A from IDMtest as described in TAPPI T 569 pm-00. A 2.54x2.54 cm sample is fixed by its non-laminated side on an aluminium platen using double coated tape. An L-shaped aluminium platen is fixed on top of the laminated side using double coated tape. This sandwich is pressed under a load of 500 N during 30 seconds. A pendulum impacts the top inside surface of the platen, causing it to rotate and split the paper specimen in the z-direction. The energy absorbed by the impact is used to determine the internal strength. Five replicates have been performed for each sample tested.

II.2.3.5. Barrier properties

The oxygen transmission rate (OTR) of the samples was measured with an Ox-Tran 2/21 ML from Mocon, USA, at 23°C 0%RH as described in ASTM F1927. One side of the sample is exposed to an oxygen flux (side A) and the other side to a nitrogen flux (side B). Oxygen molecules diffusing from side A to side B are identified by a coulometric detector. OTR measurements using the MOCON apparatus have been performed by Genevieve Cortot at CTP, Grenoble, France.

OTR has also been measured with an apparatus from Presens, Germany, equipped with pst6 detectors. The sample is placed between two hermetic chambers sealed with grease, one has been flushed by dry oxygen (23°C 0%RH) or equilibrated in a conditioned room (23°C 50%RH) (side A), and the other has been flushed with nitrogen (side B). A fluorescence sensor is used in order to determine the increase of oxygen partial pressure side B, corresponding to the permeation of oxygen from side A through the sample. When not specified, measurements presented are performed with this Presens apparatus.

The water vapour transmission rate (WVTR) of the samples was determined as described in ISO 2528:1995. Samples have been put on dishes containing calcium chloride ($CaCl_2$) anhydrous salt, in order to have a dry inner atmosphere (side B), and the system was hermetically closed by wax. The dishes were stored at constant temperature and humidity (23°C 50%RH or 85%RH) (side A) and weighed 2 to 3 times per day during 5 days. The slope of the increase of weight, normalised by the sample area, enables the determination of WVTR. Six replicates are performed for each formulation tested.

Dynamic vapour sorption, DVS, was carried out on PVOH:MFC:clay films at 23°C over a range of relative humidity from 0%RH to 95%RH using a controlled atmosphere microbalance apparatus Dynamical Vapour Sorption system from Surface Measurement System Ltd., UK. After equilibrium at 0%RH, 7 mm discs are continuously weighted while being exposed to different levels of relative humidity by an air stream of a specific relative humidity. Steps in relative humidity were equal to 10%RH from 0%RH to 90%RH, with an additional step at 95%RH. At each relative humidity step, water vapour sorption ($Sorp$ in g/g) has been calculated using the following equation:

$$Sorp = \frac{m_w - m_d}{m_d} \quad (Eq. 12)$$

where m_w (g) is the sample mass equilibrated at the corresponding relative humidity, and m_d (g) is the dry sample mass measured upon equilibrium at 0%RH. The solubility coefficient (S in mol/(m^3.Pa)) has been calculated from the water vapour sorption using the following equation:

$$S = \frac{Sorp \cdot \frac{m_d}{M_{H_2O} \cdot V}}{a_w \cdot p_0} \quad (Eq. 13)$$

where M_{H_2O} (g/mol) is the molecular mass of water, V (m^3) the volume of the sample, a_w the water activity, and p_0 the water vapour saturation pressure at the experiment temperature.

The diffusion coefficient (D in m²/s) has been determined from the sorption isotherms during each step using a mathematical model, according to an analytical solution of Fick's law for a cylinder isolated by its sides and bottom (Crank, 1975):

$$\frac{M_t}{M_\infty} = \operatorname{erf}\left(\frac{H}{2\sqrt{Dt}}\right) + \frac{2\sqrt{Dt}}{H\sqrt{\pi}} \exp\left(\frac{-H^2}{4Dt} - 1\right) \quad (Eq. 14)$$

where M_t (g) is the quantity of water vapour that has entered the material at time t (s), M_∞ (g) the quantity of water vapour that has entered the material at infinite time (equilibrium), H the thickness of the sample, and D (m²/s) the diffusion coefficient. DVS experiments and modelling have been performed by Valentin Thoury at INRA-Montpellier SupAgro, France.

Grease absorption tests have been carried out on MFC-laminated boards using a Cobb method modified from ISO 535:1991. After weighting, the sample is fixed between a 25 cm² cylinder, on top of the MFC-laminated side, and a rigid plate. A 10 mm height of oil is applied using 25 mL of vegetable oil Isio 4 from Lesieur, France, coloured in red with 0.12 g/L of Sudan III from Alfa Aesar, USA. The oil is poured out after 30 minutes. Any remaining excess oil is removed by gentle wiping. The increase of the mass of the sample, measured with a precision microbalance (± 0.1 mg), divided by the surface of the cylinder, gives the grease absorption in g/m². A visual analysis of the sample is also performed in order to determine if there is any hole in the MFC layer where red oil stains may appear.

II.2.3.6. Other analyses

X-ray diffraction (XRD) traces of clay powders or cast composite films were obtained using a Philips X'Pert Pro diffraction system using a Cu-tube (λ = 1.542 Å), operating at 40 kV and 40 mA. The inter-layer spacing of the clays (d_{001}) has been calculated using Bragg's Law:

$$d_{001} = \frac{\lambda}{2 \cdot \sin(\theta)} \quad (Eq. 15)$$

where d_{001} is the inter-layer spacing (Å), λ the wavelength of the X-ray (Å), and θ the incident angle of the X-ray (°). XRD analyses were performed at Sheffield Hallam University, Sheffield, United Kingdom.

Differential scanning calorimetry (DSC) was performed in a TA Instruments Q200 at a heating (or cooling) rate of 5°C/min, in three steps: heating from 20°C to 250°C, cooling from 250°C to 20°C, and second heating from 20°C to 250°C. The degree of crystallinity (χ_c) of PVOH-based composite films has been determined using the following equation:

$$\chi_c = \frac{\Delta H_f(T_m)}{\alpha \cdot \Delta H_f^{\circ}(T_m^{\circ})} \quad (Eq. 16)$$

where $\Delta H_f(T_m)$ the heat of fusion of the PVOH endothermic peak around 230°C (J/g), $\Delta H_f^{\circ}(T_m^{\circ})$ the heat of fusion of 100% crystalline PVOH that is equal to 138.6 J/g according to Peppas and Merrill (1976), and α the mass fraction of PVOH in the composite. DSC analyses have been performed by Pierre Sailler at CERMAV, Grenoble, France.

Chapter III: MFC for Barrier Applications

Chapter III: MFC for barrier applications

The objective of this thesis is to develop the use of microfibrillated cellulose in barrier layers deposited on paper or board. The first strategy is to use the oxygen barrier properties of MFC films, knowing that microfibrillated cellulose comprises a wide range of materials with different size distributions and chemistry. It has been chosen to work with non-chemically treated MFC in order to avoid the use of toxic compounds, such as 2,2,6,6-tetramethylpiperidine-1-oxyl (TEMPO) or monochloroacetic acid, that are required for the TEMPO-mediated oxidation or carboxymethylation of cellulose, respectively. Even without chemical pre-treatment, the size distribution of the elements in a MFC suspension can vary greatly depending on the intensity of a potential enzymatic pre-treatment and of the mechanical treatment. The relation between the size distribution and the properties of resulting self-standing films is not fully understood, especially concerning barrier properties. This is first of all because the determination of this size distribution is hard to obtain; most of the time an idea of the degree of fibrillation is given using indirect techniques such rheological measurements.

This chapter aims at getting a better understanding of the influence of the MFC fibrillation on the barrier properties of MFC films, by comparing several MFC grades in terms of degree of fibrillation with respect to their barrier properties, and to select the most appropriate grades for the following of the study. It also aims at getting a better understanding of the potential of wet lamination to produce 100% MFC barrier layers on board, and to target key points for future developments.

The first section of this chapter begins with the evaluation of the degree of fibrillation of several MFC suspensions by indirect techniques such as measuring their rheological behaviour or the amount of residual macro-fibres. In a second section, the degree of fibrillation is characterised through the properties of MFC films and compared to what was obtained concerning the MFC suspensions in order to: (1) determine which techniques would be the best suited to assess the degree of fibrillation of a MFC grade, and (2) compare the degree of fibrillation with the barrier properties of the MFC self-standing films in order to choose the best grade for our application. In a third section, one MFC suspension has been selected to be applied as an oxygen barrier layer on board by wet lamination: a process recently patented by Guerin and co-workers (2016a) and described page 81. The adhesion of MFC layers of 10 to 40 g/m² on board has been investigated, along with the oxygen and grease barrier of the laminated boards.

III.1. MFC suspensions

In this section, 9 different MFC suspensions have been characterised in order to determine which are the most relevant parameters to compare their degrees of fibrillation. The influence of the pulp source, enzymatic pre-treatment, and intensity of the mechanical defibrillation has been investigated in terms of suspension appearance at macroscopic and microscopic scale, residual macro-fibre size distribution, and rheology.

III.1.1. Different MFC grades with different costs

The MFC grades used in this thesis are presented in Table 7. One commercial grade has been purchased from the University of Maine and the others have been produced at Centre Technique du Papier (CTP) by enzymatic pre-treatment followed by pilot-scale high-pressure homogenization.

Reference	Source	Pre-treatment	Mechanical treatment
UM	Kraft softwood	No pre-treatment	Refining
D	Sulphite softwood	Enzymatic	Refining + Homogenization 6 passes
KB	Kraft hardwood	Enzymatic	Refining + Homogenization 6 passes
0P	Kraft hardwood	Enzymatic	Refining
1P	Kraft hardwood	Enzymatic	Refining + Homogenization 1 pass
2P	Kraft hardwood	Enzymatic	Refining + Homogenization 2 passes
3P	Kraft hardwood	Enzymatic	Refining + Homogenization 3 passes
4P	Kraft hardwood	Enzymatic	Refining + Homogenization 4 passes
5P	Kraft hardwood	Enzymatic	Refining + Homogenization 5 passes

Table 7 - Microfibrillated cellulose grades used in this study.

These grades are expected to allow the use of MFC with a wide range of degree of fibrillation, especially with MFC 0P to 5P that have been produced by successive passes of a same pulp in the homogenizer. MFC D and MFC KB have been produced with the same process but with different pulps, thus allowing seeing the effect of the cellulose source; MFC UM allowed making a comparison with a non-pre-treated commercial MFC suspension. The interest in having a wide range of degree of fibrillation comes from the high energy cost required to produce this material. As shown in Table 8, each pass in the homogenizer increases the production cost by a significant amount (114 to 180 €/t). It is of interest to characterise the degree of fibrillation of these suspensions and to measure the resulting barrier properties, in order to be able to tailor the production process for the desired application. This should avoid potential unnecessary passes, reducing energy consumption.

Step	Step energy (kWh/t)	Total energy (kWh/t)	Total energy cost (€/t)
Pre-refining	48	48	3
Refining	382	430	26
Pass 1	1,477	1,907	114
Pass 2	2,332	4,239	254
Pass 3	2,318	6,557	393
Pass 4	2,271	8,828	530
Pass 5	2,274	11,102	666

Table 8 - Energy requirement for the pilot scale production of MFC 0 to 5P. Total energy represents the sum of step energy required up to the corresponding step, and total energy cost is the cost of the total energy considering an electricity cost of 0.060 €/kWh.

III.1.2. First assessment of the fibrillation of the suspensions

Contrary to chemically-pre-treated MFC, non- or enzymatically-pre-treated pulps do not have all their fibrils completely individualised (Chinga-Carrasco, 2011). It is evidenced in Figure 32 by the white colour of the suspensions due to light diffusion by macro-scale elements, whereas individualised microfibrils suspensions such as what can be obtained after TEMPO-mediated oxidation are translucent.

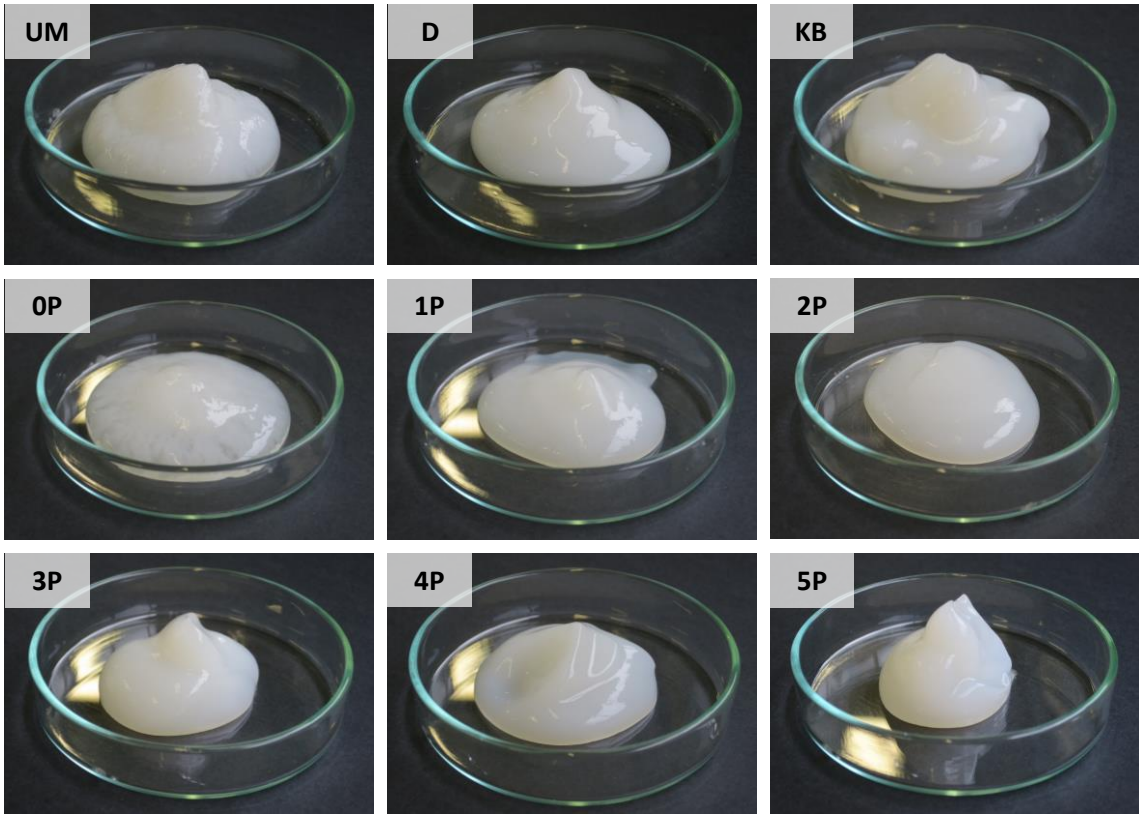

Figure 32 - Visual analysis of the MFC suspensions at 2 wt% in water. Picture width: 8 cm.

Suspensions of MFC 0P to 5P appear smoother and smoother, which is expected to come from a reduction of the size of the residual macro-fibres with increasing mechanical treatment. There is especially a major difference between MFC 0P, presenting visible flocks at 2 wt%, whereas for MFC 1P the suspensions are homogeneous. MFC UM also already appears less fibrillated with a rough surface suggesting large elements in the suspension, which can be expected due to the lack of enzymatic pre-treatment and homogenisation.

As evidenced on the optical micrographs presented in Figure 33, MFC UM has residual macrofibres having diameters of up to 50 µm, which is attributed to its light treatment compared to the other grades. Numerous large fibres can also be found in MFC 0P, while their quantity is lowering in MFC 1P and 2P. No fibres can be found in MFC D, KB, and 3P to 5P, indicating their higher quality. What can be seen on the latter optical micrographs are MFC-comprising areas, mostly in the form of bundles; this observation will thereafter be referred to as woolly areas.

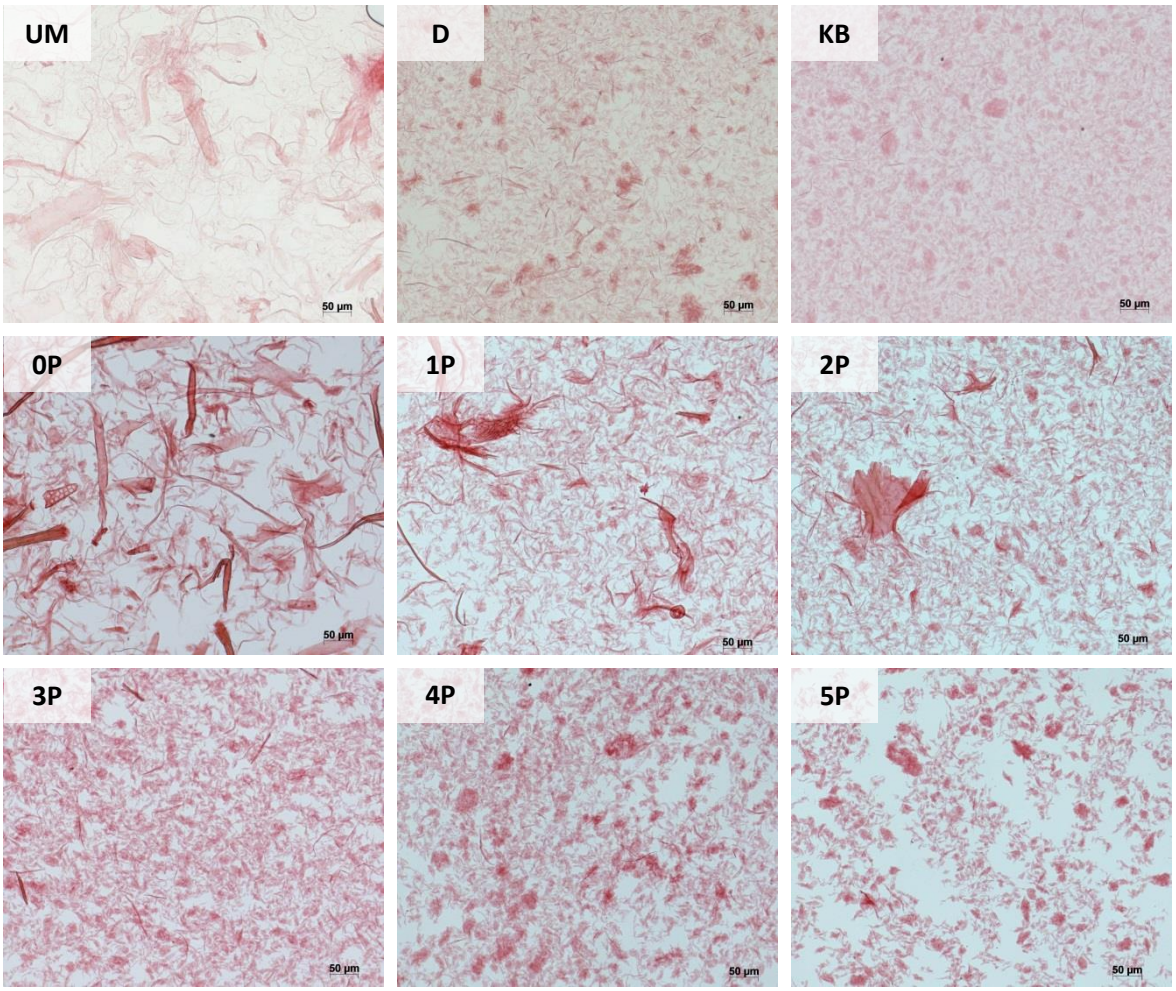

Figure 33 - Optical microscopic analysis of the MFC suspensions coloured with Congo Red. Picture width: 650 µm.

III.1.3. Size distribution of the residual macro-fibres by MorFi analysis

The size distribution of the elements in suspension has been characterised quantitatively by optical analysis using a MorFi device. The detection threshold of this apparatus is 5 µm in width, thus only allowing the observation of the residual macro-fibres. The detected elements having a size superior to 80 µm are defined as "fibres" and the ones having a size inferior to 80 µm are defined as "fines". This separation is usually made at 200 µm for wood pulps dedicated to papermaking, but has been reduced in this case due to the low fraction of large elements.

The characteristics of residual fibres in MFC suspensions are presented in Table 9. "Pulp" corresponds to birch kraft pulp, before any treatment, that has been used for the production of MFC 0 - 5P. The amount of fibres increases with refining from the pulp (30 M/g) to MFC 0P (59 M/g) corresponding to the separation of large fibres into smaller fibres, evidenced by a reduction of the mean area-weighted length from 876 to 321 µm and a tripled fine content. Then, the fibre content decreases progressively down to 3.4 M/g for MFC 5P. Fibres are not just converted into smaller fibres, but rather on fines or fibrils having a diameter inferior to 5 µm, as indicated by the decreasing amount of both fibres and fines. This is in accordance with observations by Nechyporchuk and co-workers (2015), using a similar MorFi apparatus. In the meantime, the mean area-weighted length of the elements is increasing; this could be explained by small elements being fibrillated (converted into fibrils), while larger elements remain. As a consequence, the area-weighted length cannot be used as the sole parameter to characterise the degree of fibrillation.

With these results in mind, it can be observed that MFC UM has a fibre content similar to MFC 0P, which is consistent with the fact that both pulps have only been subjected to refining. They are of similar quality; MFC UM only seems slightly more fibrillated due to its lower fibre content and higher fine content. MFC KB and D have the low fibre content characteristic of a highly fibrillated pulp, once again consistent with the similar mechanical treatment compared to MFC 5P. It can be noted that MFC D presents a high amount of fines (922 M/g) compared to MFC 5P, while having a lower fibre content, 2.2 M/g compared to 3.4 M/g, making difficult the comparison between these two suspensions. MFC KB has both a lower fibre content and fine content, suggesting it to be the most fibrillated suspension. These analyses are consistent with the microscopic observations of the suspensions.

	Fibre content (millions/g of pulp)	Fine content (millions/g of pulp)	Mean area-weighted length (µm)
UM	52.2	586	228
D	2.2	922	124
KB	1.5	114	154
Pulp	30.5	121	876
0P	58.6	368	321
1P	37.9	498	221
2P	14.9	377	232
3P	6.6	290	278
4P	4.1	211	299
5P	3.4	169	303

Table 9 - Characteristics of the residual macro-fibres present in MFC suspensions.

III.1.4. Rheological behaviour

The rheological behaviour of MFC suspensions is reported to serve as a tool for characterization of the degree of fibrillation (Nechyporchuk et al., 2016b). The viscosity of the MFC suspensions from 2,000 to 0.02 s^{-1} after 30 minutes vigorous mechanical stirring is reported in Figure 34.

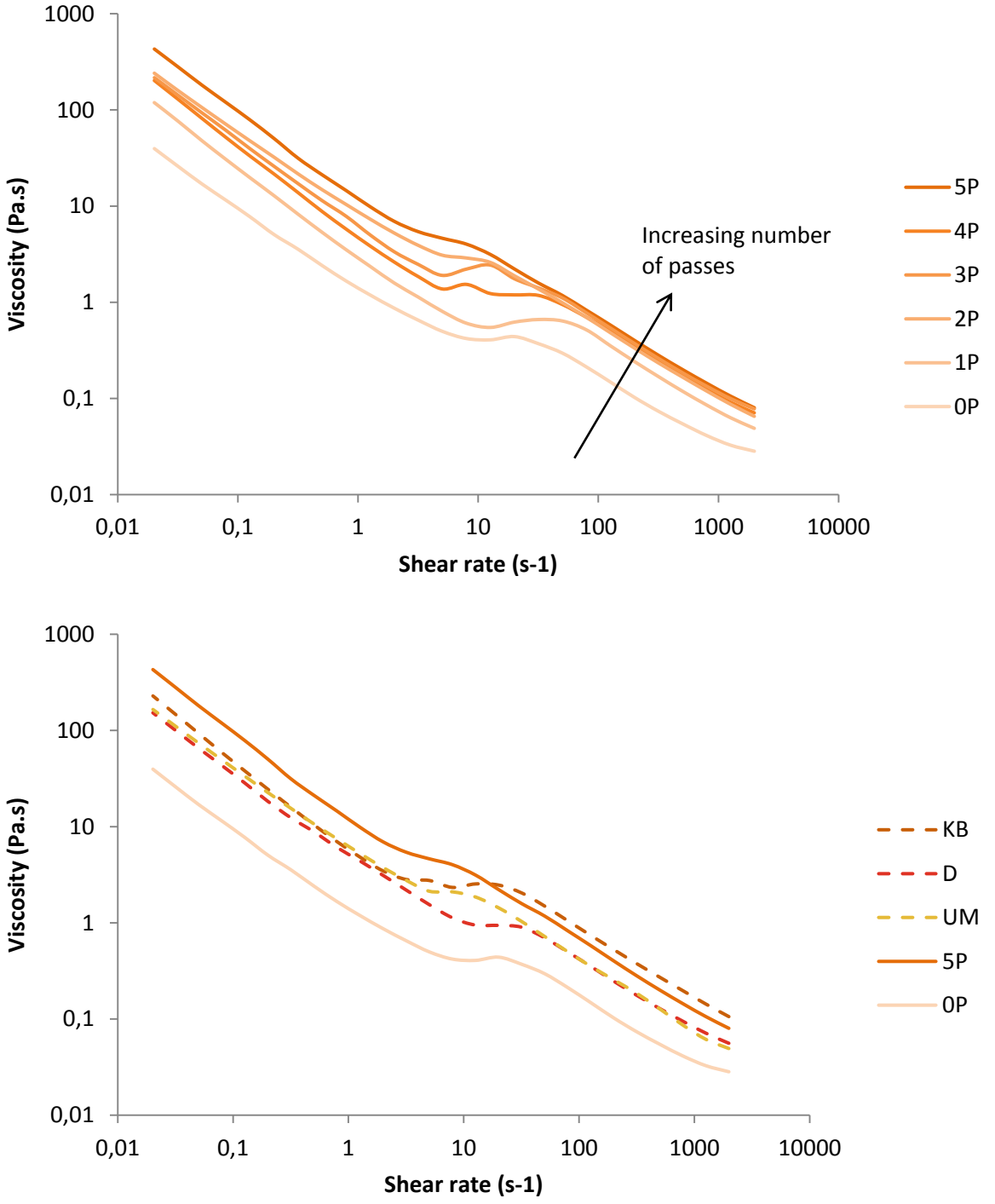

Figure 34 - Rheological behaviour of the MFC suspensions at 2wt%.

An increase in viscosity with the intensity of the mechanical treatment can be observed, especially comparing MFC 0P, 1P, and 2P. This increasing viscosity is also reported in the literature, e.g. for an increasing number of passes of a TEMPO-oxidised pulp in a homogeniser (Besbes et al., 2011). It is also reported for an increasing number of passes of a non-chemically pre-treated pulp in a grinder or a homogeniser (Grüneberger et al., 2014), with viscosities closer to the present results. At higher shear rates (50 to 2,000 s^{-1}), MFC 3P, 4P, and 5P have a similar viscosity. It can be linked to the shear-thinning behaviour of the suspensions and microscopic and MorFi analyses where few differences were found concerning the amount of residual macro-fibres.

MFC KB has been determined as the most fibrillated suspension which is supported by its higher viscosity. However, the viscosity of MFC D is surprisingly low as it would be expected to be at a level similar to MFC KB and 5P. In addition, MFC UM and MFC 0P were expected to be at a similar level, but MFC UM has a much higher viscosity: its behaviour is close to the one of MFC D.

The rheological behaviour of MFC 0P to 5P is in accordance with the microscopic and MorFi analyses. However, the comparison between the different pulps is far from a direct relation with the degree of fibrillation as characterized previously, suggesting that fibrillation comparison using viscosity should only be made with MFC suspensions produced from the same pulp.

III.1.5. Conclusion

In this section, several MFC suspensions obtained from different pulps or with different intensity of mechanical treatment have been characterised in order to assess their degree of fibrillation. At first, a visual observation of the suspension allows to divide them in two groups whether they look smooth or fibrous. The fibrous look of a MFC suspension is linked to residual macro-fibres that can be clearly observed by optical microscopy; this method allows a qualitative arrangement of the suspensions depending on the visual amount and size of the residual macro-fibres. A quantitative analysis of these macro-fibres could be achieved using a MorFi apparatus, allowing observing a reduction of fibre and fine content in the most fibrillated suspensions. All these observations are in good accordance with what could be expected according to the processes used for the MFC production. Finally, the viscosity of the MFC suspensions from kraft birch pulp increased with the intensity of their mechanical treatment as already reported in the literature. However, the comparison of MFC suspensions from kraft birch pulp with MFC suspensions from other pulps did not coincide with their expected degree of fibrillation, suggesting that viscosity comparisons should be limited to MFC produced from the same pulp.

III.2. MFC films

In this section, self-standing MFC films have been manufactured with a handsheet method from the previously described suspensions. With the similar objective of determining which parameters were relevant for comparing the degree of fibrillation of the 9 MFC grades, MFC films have been characterised in terms of macroscopic appearance, optical properties, apparent density, mechanical properties, and gas barrier properties. Another objective of this section is to select relevant MFC grades for the next parts of the study, targeting high degree of fibrillation for high oxygen barrier.

III.2.1. Influence of the residual macro-fibres on the appearance of MFC films

Self-standing films have been produced from the previously studied MFC suspensions using a Rapid-Köthen handsheet former. Differences have been found during the production of the handsheets. MFC expected to have a higher degree of fibrillation tended to lead to higher filtration and dewatering times, which is attributed to their higher specific surface area and ability to bind with water molecules. The filtration step of MFC 0P took 20 seconds compared to 40 seconds for MFC 1P, 1 minute 50 seconds for MFC 2P, and 2 minutes 30 seconds for MFC 5P, estimated from the moment when the wet cake became mat (no more water at the surface) and began to crackle on the sides. The drying time at 93°C under depression also had to be increased from 10 to 15 min in the case of MFC 5P, and the filtration membrane had to be replaced more regularly from MFC 3P to MFC 5P which was attributed to the clogging of pores by the smallest fibrils.

Pictures of the MFC handsheets are presented in Figure 35. From 0P to 5P, the films are more and more homogeneous; this is especially visible for MFC 0P with its bad formation (uneven distribution of the cellulosic elements) compared to MFC 1P to MFC 5P. A similar observation is made with MFC UM being less homogeneous.

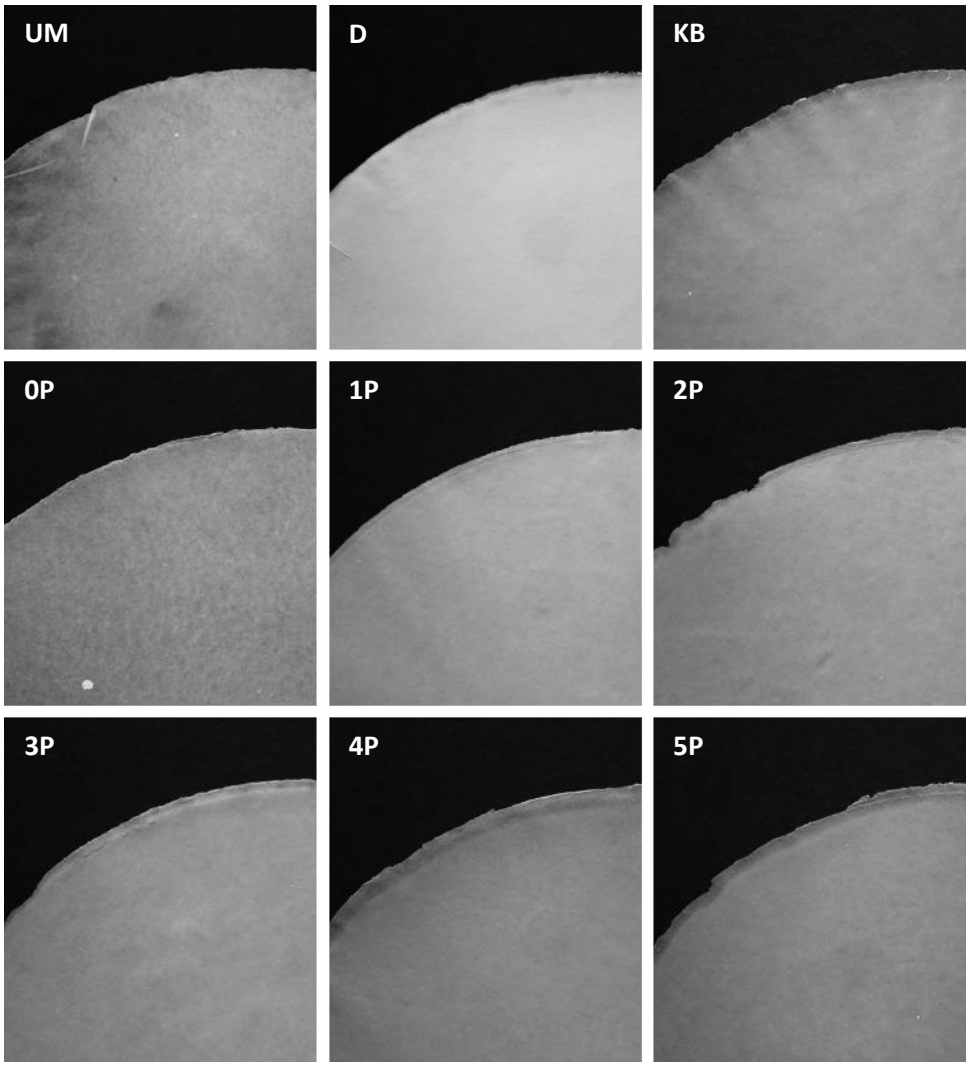

Figure 35 - Edited Pictures of MFC films manufactured with a handsheet method: contrast +50%, saturation 0%. Picture width 8 cm.

III.2.2. Optical properties of MFC films

Cellulose nanofibres have a diameter inferior to the wavelength of visible light. Therefore, dense films made from chemically pre-treated MFC suspensions such as the ones developed by Siró and co-workers (2011), without residual macrofibres, without large diameters pores, and without micrometre range roughness, should be transparent. The presence of macrofibres in the MFC grades used in this study was responsible for light diffusion, which is represented by the low clarity values (< 8%) presented in Figure 36. The full data of transmittance, haze, and clarity of the MFC films can be consulted in appendix page 199. The increase of clarity and transmittance from MFC 1P to MFC 5P is attributed to the reduction of the amount of macro-fibres responsible for light diffusion and absorption, as previously observed by MorFi analysis. It can be observed that the transmittance of MFC 0P is not lower than MFC 0P to 3P, contrary to what was expected. By looking at the pictures in Figure 35, the MFC 0P film presents light and dark areas representative of a bad distribution of the cellulosic elements caused by its higher macro-fibre content. The higher transmittance of MFC 0P is attributed to this lack of homogeneity causing light to be able to cross the material more easily through the light areas. This is in accordance with interpretations by Kangas and co-workers (2014),

explaining the higher transmittance of a MFC grade having a low degree of fibrillation due to its tendency to agglomerate.

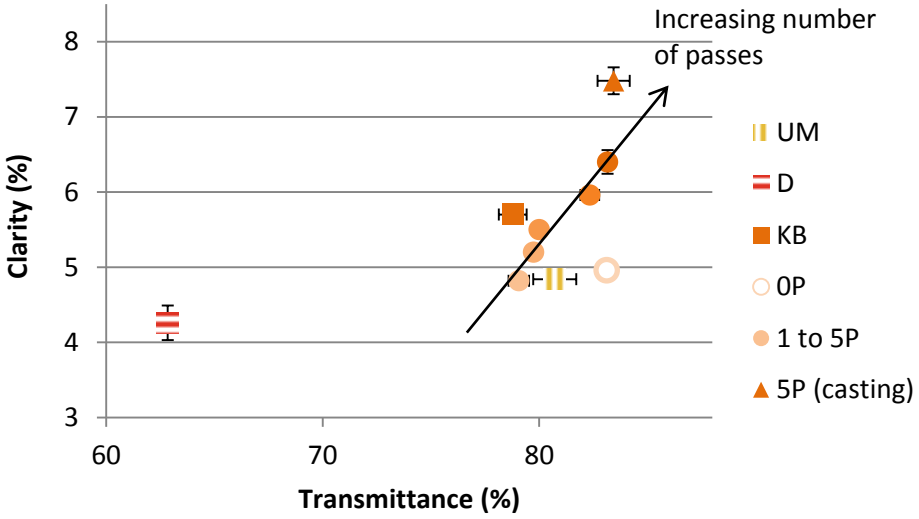

Figure 36 - Optical properties of MFC self-standing films.

Transmittance and clarity measurements appeared well suited for characterising the evolution of the fibrillation of a pulp. However, these properties were highly dependent on the MFC source. MFC D had a much lower transmittance and the lowest clarity compared to the other pulps despite its higher degree of fibrillation than for MFC 1P for example, as demonstrated in I.1, page 92. The influence of the film formation technique has also been investigated through the production and analysis of a sample made by casting of a diluted MFC 5P suspension. Higher transmittance and clarity were obtained in this case.

III.2.3. Apparent density of MFC films

All MFC films have a target dry basis weight of 50 g/m², resulting in an average basis weight of 51.5 +/- 2 g/m² after equilibrium at 23°C 50%RH. With this similar basis weight, MFC films have a different apparent thickness depending on the MFC used, coming from variations in apparent density as can be seen in Table 10. The increase in apparent density is in accordance with the degree of fibrillation assessed by analysis of the MFC suspensions, and especially the residual macro-fibre content. The density of pure non-porous cellulose with 50% crystallinity would be of 1.56 g/cm^3 (Chen et al., 2004; Diddens et al., 2008), meaning that the MFC films have an apparent porosity of 17% for MFC 5P to 38% for MFC 0P. This is expected to have a high impact on the mechanical and barrier properties of the films. Compared to the films densities found in the literature and presented on Table 3, page 42, the apparent densities of the films developed in this study are close to the highest values found for enzymatically pre-treated MFC (Belbekhouche et al., 2011; Minelli et al.,

2010). Chemically pre-treated MFC tend to have a higher density up to 1.5 or 1.6 cm^3/m^2 (Aulin et al., 2010; Fujisawa et al., 2011)

	Basis weight (g/m^2)		Apparent density (g/cm^3)		Apparent porosity (%)	
	Average	Stdev	Average	Stdev	Average	Stdev
UM	51.9	1.0	1.06	0.01	32%	0.2%
D	51.7	0.4	1.26	0.04	19%	0.6%
KB	51.4	1.6	1.27	0.04	18%	0.6%
0P	51.3	0.3	0.96	0.00	38%	0.1%
1P	50.9	0.4	1.09	0.01	30%	0.1%
2P	50.7	0.4	1.17	0.00	25%	0.1%
3P	52.4	0.1	1.24	0.01	20%	0.2%
4P	50.5	0.4	1.25	0.02	19%	0.3%
5P	52.7	0.2	1.29	0.01	17%	0.2%

Table 10 - Basis weight, apparent density, and apparent porosity for MFC handsheets.

III.2.4. Mechanical properties of MFC films

The mechanical properties of fibre-based materials in the case of a tensile test are characteristic of the binding between the fibres. In our case, the fibrillation of cellulose causes an increase in specific surface area that leads to an improved ability to form hydrogen bonds and fibre entanglement. This is verified in Table 11, where the tensile strength and Young modulus are increasing from MFC 0P to 5P with values from 77 MPa and 8.4 GPa to 127 MPa and 11.3 GPa, respectively. These values are in the range of the commonly reported tensile strength (100 to 200 MPa) and Young moduli (6 to 15 GPa) for MFC films (Arola et al., 2013; Spence et al., 2010a; Syverud and Stenius, 2009).

	Elongation at break (%)		Tensile Strength (MPa)		Young Modulus (GPa)	
	Average	Stdev	Average	Stdev	Average	Stdev
UM	3.4	1.2	91	9	6.5	0.2
D	1.7	0.5	102	12	8.8	0.3
KB	1.8	0.4	120	9	9.1	0.4
0P	1.7	0.3	77	4	8.4	0.6
1P	2.7	0.7	114	3	10.1	0.7
2P	3.0	0.2	122	8	11.5	0.4
3P	3.3	0.3	131	3	11.5	0.4
4P	3.3	0.5	137	4	12.0	0.9
5P	3.4	0.6	127	5	11.3	0.6

Table 11 - Mechanical properties for MFC films.

The elongation at break is also increasing: from 1.7% for MFC 0P to 3.4% for MFC 5P. Surprisingly, MFC D and MFC KB display a low elongation at break and lower Young modulus that could be expected compared to MFC 5P. In addition, MFC UM was expected to have a better

mechanical resistance than MFC 0P, from the assessment of the degree of fibrillation in the previous part and also from the density measurement, but its Young modulus is as low as 6.5 GPa.

III.2.5. Gas barrier of MFC films in dry and ambient conditions

The oxygen barrier of MFC films has first been characterised at 23°C 0%RH, as reported in Table 12. Due to the different densities of the film, the oxygen transmission rate (OTR) is presented instead of the oxygen permeability (OP). It represents the permeability considering a given amount of MFC rather than a given thickness of film. Otherwise, the OP would artificially decrease from MFC 0P to MFC 5P due to the decreasing thickness, even if the films had exactly the same ability to hinder oxygen mass transport (OTR). In addition, OP should describe homogeneous materials, which is not the case in the porous MFC films. OP values are still given, as it is the most relevant parameter to compare with the literature.

At 23°C 0%RH, MFC UM demonstrated a high OTR of 2,845 $cm^3/(m^2.d.bar)$, whereas in the case of MFC D and MFC KB the transmission rate was below the detection threshold of the apparatus: 0.01 $cm^3/(m^2.d.bar)$. Another apparatus has been used for the determination of OTR for MFC 0P to 5P; it was not possible to compare the values that were also close to the detection threshold of the apparatus in these conditions. The MFC films have been tested at 23°C 50%RH and the first observation was the low transmission for MFC UM. Knowing that films made from this MFC can be barrier at 23°C 50%RH, the high transmission rate obtained in dry conditions is attributed to the dimensional stability of the material. At dry state, large fibres tend to shrink which can lead to holes or defect in the material, thus giving preferential pathways for the oxygen molecules to permeate.

	OTR 23°C 0%RH ($cm^3/(m^2.d.bar)$)		OTR 23°C 50%RH ($cm^3/(m^2.d.bar)$)	
	Average	Stdev	Average	Stdev
UM	2,845	3,464	0.62	0.01
D	< 0.1	-	0.39	0.08
KB	< 0.1	-	0.78	0.19
0P	< 0,1	-	25.50	35.92
1P	< 0.1	-	0.55	0.02
2P	< 0.1	-	0.48	0.00
3P	< 0.1	-	0.39	0.07
4P	< 0.1	-	0.27	0.05
5P	< 0.1	-	0.21	0.01

Table 12 - Oxygen transmission rates (OTR) of the MFC handsheets at 23°C at 0%RH and 50%RH.

Concerning the other MFC grades, the OTR at 23°C 50%RH was higher than those at 23°C 0%RH as could be expected due to the plasticization of cellulose by water. It is especially the case for MFC 0P; this is in contradiction with what has been obtained in the case of MFC UM, which is not yet fully understood. From MFC 1P to MFC 5P the oxygen transmission progressively decreases from 0.55 to 0.21 $cm^3/(m^2.d.bar)$, corresponding to oxygen permeabilities (OP) of 26 to 8.5 $cm^3.\mu m/(m^2.d.bar)$,

respectively. Values of this order of magnitude are also reported: 47 cm^3.µm/(m^2.d.bar) (Liu et al., 2011) or 90 cm^3.µm/(m^2.d.bar) (Bardet et al., 2015). This decreasing OTR is explained by the densification of the material: as the dimensions of the fibres are reduced, a lower volume of pores is created in the film. As it is more difficult for oxygen to permeate through cellulose than through air, the reduction of total pore volume leads to a decrease of OTR. It must be noted that the OTR difference between MFC 1P to MFC 5P is still low when changes in terms of order of magnitude can easily happen, as observed by Liu and co-workers (2011) concerning the effect of the humidity.

The oxygen transmission values of MFC D and MFC KB are more difficult to understand. First of all, MFC KB has been determined to be the most fibrillated MFC grade, but it results an OTR of 0.62 cm^3/(m^2.d.bar) superior to the one of MFC 1P while being of a similar kraft birch pulp as MFC 0P to 5P. Similarly, the high degree of fibrillation of MFC D resulted in an OTR of 0.39 cm^3/(m^2.d.bar), similar to MFC 3P despite its apparent higher degree of fibrillation. The difference in oxygen barrier between MFC UM and MFC 0P is not fully understood. However, it has been concluded that in order to avoid any loss of barrier due to the dimensional stability of the material, MFC with a low degree of fibrillation should not be used for high oxygen barrier applications.

In addition to the oxygen barrier, the water vapour barrier in humid conditions (23°C 85%RH) for MFC KB, MFC D, and MFC UM has been tested and resulted in high values of about 1,200 g/(m^2.d) indistinctly from the MFC grade. Full data can be consulted in appendix page 199.

III.2.6. Conclusion

In this section, self-standing films have been produced from the previously studied MFC suspensions. The resulting films have been compared in terms of processing, appearance, optical properties, densities, mechanical properties, and oxygen and water vapour transmission rates.

The appearance of MFC UM and MFC 0P films differed from the others by having light and dark areas contrary to the other homogeneous films. This is in accordance with their high amount of macro-fibres. An increased mechanical treatment led to increased filtration times attributed to the faster formation of a dense wet MFC layer opposed to the water flow. It also resulted in an increased filtration and drying times, attributed to a higher specific surface area resulting in a higher ability to bind with water molecules. From MFC 1P to MFC 5P, the films got clearer and with an increased ability to let light pass through. This is consistent with the macro-fibres and fines responsible for light diffusion being progressively transformed into fibrils with a diameter inferior to the wavelength of visible light. Measuring the transmittance and clarity of MFC films appeared to be a suited method for the evaluation of the degree of fibrillation. However, it was highly dependent on the pulp used, making it non-consistent for the comparison of MFC 5P with MFC D and MFC UM in terms of degree of fibrillation, for example. The apparent density, tensile strength, and Young modulus followed a similar trend and appeared consistent with the treatment applied on the pulp, with an increase of these properties with the degree of fibrillation. A higher fibrillation makes possible the formation of a denser and stronger network. It also led to an increase of elongation at break in the case of MFC 0P to 5P, trend that is not in accordance with the results obtained for MFC UM and MFC D from other pulps.

All MFC films except the ones from MFC UM were high barrier against oxygen in dry conditions. The fact that MFC UM has a much better oxygen barrier at 50%RH suggests that the transmission obtained at 0%RH comes from defects that could be produced by the shrinkage of the macro-fibres upon dehydration. The oxygen transmission of the other MFC samples becomes measurable at 50%RH, which is attributed to the plasticization of cellulose by water. The barrier was dependent on the intensity of the mechanical treatment considering MFC 0P to 5P, with MFC 0P having a transmission rate almost 50 times higher than that of MFC 1P. This property was highly dependent on the pulp origin. The degree of fibrillation did not have any effect on the water vapour transmission rate at 23°C 85%RH.

III.3. Wet lamination of MFC on board

The application of MFC as a top layer on board by a coating process causes issues due to its high viscosity at low solid contents. MFC suspensions have commonly a solid content around 2 wt% and their concentration to a higher solid content results in aggregation and high viscosity making them difficult to process (Guezennec, 2012). In addition, the high water content affects the structure of paper coated with MFC and leads to low coat weights, thus requiring several passes (Lavoine et al., 2014). In this thesis, a layer of MFC 5P has been obtained on top of paper or board using a papermaking process involving a filtration step in order to decrease the water content, showing similarities with a process used by Syverud and Stenius (2009). A wet MFC cake formed by filtration, with a dry basis weight ranging from 10 to 40 g/m², is reported on paper or board and dried with it. Upon drying, the MFC layer sticks on the base. The adhesion, oxygen barrier, and grease barrier of MFC-laminated boards have been investigated.

III.3.1. Adhesion of the MFC layer

The adhesion of the MFC layer has been determined using a Scott bond test usually performed to determine the internal strength of papers or boards. This device measures the energy required for the delamination of the sample. If the adhesion of the laminated MFC layer is too low, delamination will occur at the MFC/board interface and the delamination energy will be lower than the internal strength of the board. Upon testing of MFC-laminated boards, the delamination energy was similar to what was obtained for the pristine board, independently of the MFC layer basis weight, as presented in Figure 37. A visual analysis of the samples after testing showed that the delamination always happened inside the board, and not at the MFC-board interface, as shown in Figure 37. It has been concluded that the adhesion of the MFC layer on board was higher than its internal strength, making this process suitable for packaging applications without anticipating issues in terms of adhesion of the MFC layer.

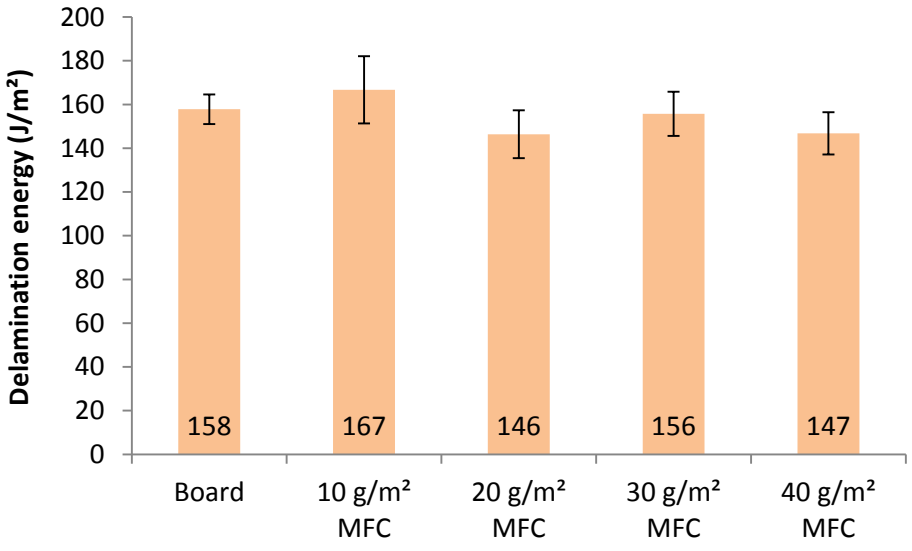

Figure 37 - Delamination energy measured on board and MFC-laminated board samples by Scott bond adhesion test.

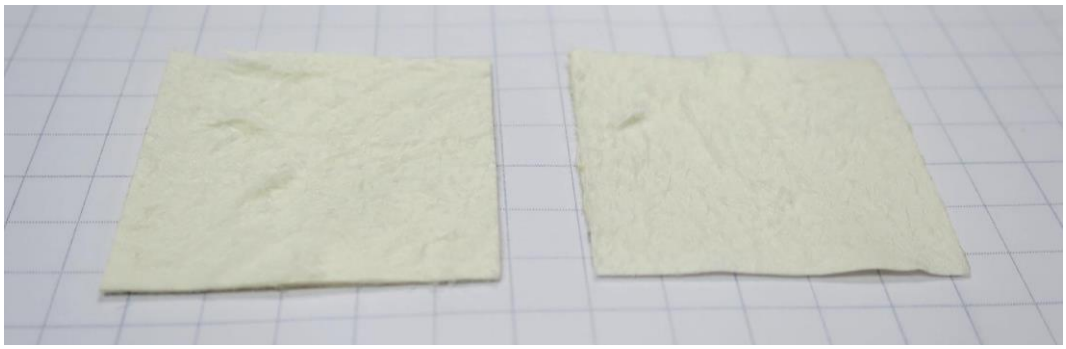

Figure 38 - MFC-laminated board sample after Scott bond adhesion test. The visible fibres on each side indicate that delamination occurred inside the board and not at the MFC-board interface. Samples width: 2.54 cm.

III.3.2. Oxygen barrier

The oxygen barrier properties of MFC-laminated boards are reported in Table 13, all four replicates are presented in order to evidence the fact that permeation should mainly come from defects in the layer. A low OTR of about 2 to 5 $cm^3/(m^2.d.bar)$ could be obtained from 10 to 40 g/m² of MFC laminated on board, while the pristine board has a transmission estimated around 12,000,000 $cm^3/(m^2.d.bar)$. However, higher values have also been measured, especially at 10 g/m² of MFC, up to about 300,000 $cm^3/(m^2.d.bar)$. This suggests that the MFC layer presents defects by which oxygen can permeate preferentially. The defects could come from a lack of coverage, i.e. holes in the MFC layer, as observed by Lavoine and co-workers (2014) on coated boards. Another explanation could be the presence residual macro-fibres having dimensions higher than the thickness of the MFC layer. The MorFi analysis in III.1.3, page 95, evidenced a reduction of the amount of macro-fibres with the number of passes in the homogeniser, but fibres in suspension having a width in the range of 56 to 75 µm remain. Such elements, when present in a layer of 10 g/m², i.e. about 8 µm, may result in areas where there is no real dense MFC network. Be it from incomplete coverage or macro-fibres defects, the intensity and frequency seems to decrease by increasing the MFC layer basis weight. It can be noted that the transmission rates of the laminated boards do not exactly match the theoretical values; the lamination process has a non-negligible impact and may probably be improved.

		Oxygen transmission rate (OTR) $cm^3/(m^2.d.bar)$			
		10 g/m²	20 g/m²	30 g/m²	40 g/m²
Replicate	1	5.3	4.0	3.8	4.6
	2	4,718	1.5	1.6	2.5
	3	4,275	3.2	3.8	3.6
	4	293,752	289	395	2.7
Theoretical		1.04	0.52	0.35	0.26

Table 13 - Oxygen transmission rate for MFC-laminated boards. The theoretical values were calculated from the permeability of MFC 5P self-standing films (page 102), considering a layer thickness equal to the basis weight of the layer divided by the density of MFC 5P self-standing films (Table 10, page 101).

III.3.3. Revelation of defects by coloured oil Cobb test

The grease barrier of MFC-laminated boards has been investigated using a modified Cobb method, consisting in measuring the increasing weight of a sample after being put in contact with coloured oil. In addition to the increase of weight representing oil absorption and thus permeability, the samples can be analysed visually in order to observe where oil has been absorbed. The base board has an opened structure allowing grease to penetrate easily. It results in high oil Cobb index (basis weight of oil absorbed) of 132 g/m², as presented in Table 14, while the board itself has a basis weight of about 270 g/m². A large stain appeared on the whole board surface tested. The appearance of MFC-laminated boards after oil Cobb test can be found in Figure 39.

	Oil Cobb index (g/m²)	
Sample	Average	Stdev
Board	132	2
Board + 10 g/m² MFC	3.6	0.8
Board + 20 g/m² MFC	1.9	0.7
Board + 30 g/m² MFC	1.2	0.1
Board + 40 g/m² MFC	1.0	0.3

Table 14 - Oil Cobb indices for MFC-laminated boards.

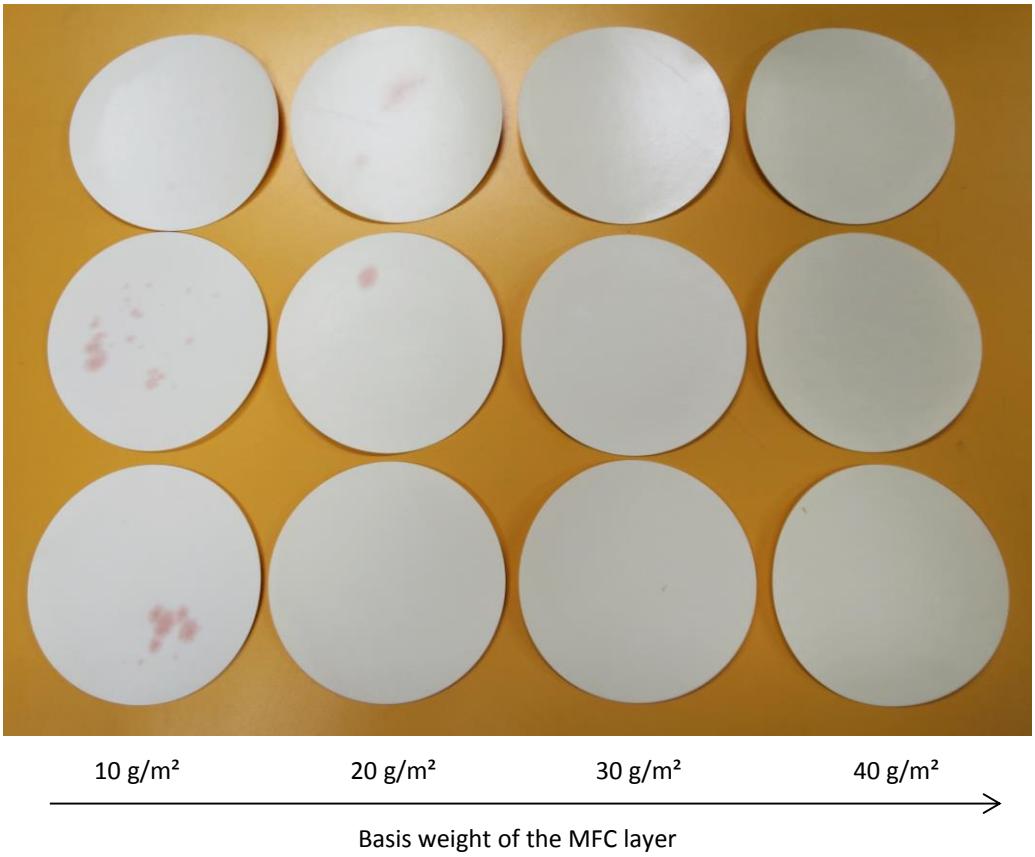

Figure 39 - MFC-laminated board samples after coloured oil Cobb test. Samples in the same column are three replicates for the same MFC layer basis weight. Sample width: 9.4 cm.

Upon lamination of a MFC layer, oil absorption decreases drastically; oil cannot penetrate the dense MFC network. However, the apparition of red stains on MFC-laminated samples after testing indicates that oil found a way through the MFC layer. Stains were mainly present on 10 g/m² MFC-laminated board samples, with some stains also appearing at 20 g/m². It matches well the oxygen barrier results that suggested defects in the layer by which oxygen could diffuse.

III.3.4. Scanning Electron Microscopy

The dispersion of the oxygen transmission rate measurements suggested the presence of defects in the MFC layers laminated on board, especially at low basis weights of 10 or 20 g/m². This has been confirmed by coloured oil Cobb tests due to the formation of small isolated red stains. These defects may be due to a lack of coverage by the MFC layer or the presence of macro-scale elements as evidenced by MorFi analysis in III.1.3, page 95. The surface of the MFC-coated board has been analysed by scanning electron microscopy in order to detect holes or macro-elements that could be responsible for defects in the layer and can be found in Figure 40.

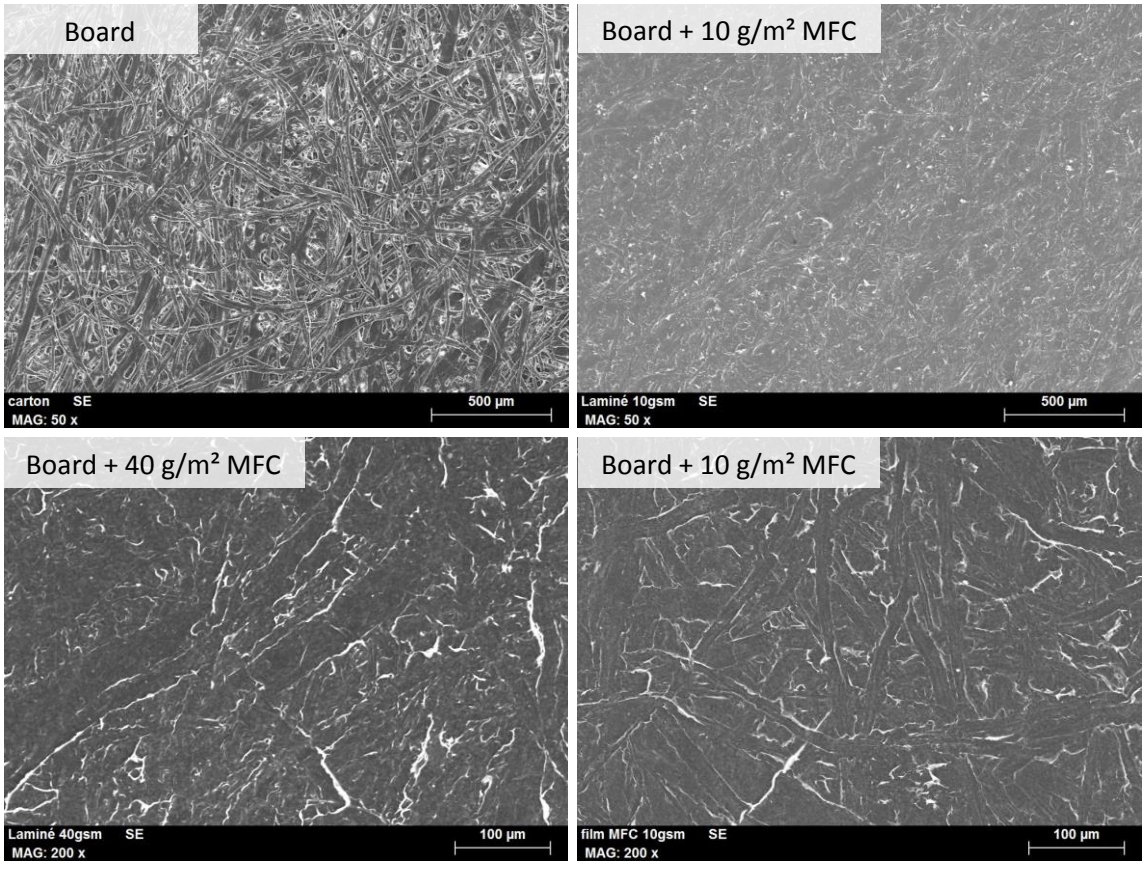

Figure 40 - SEM analysis of the surface of MFC-laminated boards.

The surfaces analysed are from the 4th replicate of each MFC layer basis weight presented in Table 14, assuring the presence of defects responsible for oxygen permeation except in the case of a 40 g/m² MFC layer. However, no hole and no especially large element have been observed on the

surfaces analysed. Even for a 10 g/m² MFC layer, the surface coverage is total and homogeneous. It shows a dense closed structure compared to the open structure of the board. The fibrous shapes observed on MFC-laminated surfaces most probably come from the replication of the fibres of the cover paper used during the production process. No significant differences were found comparing a MFC laminated layer of 10 and 40 g/m². Lavoine and co-workers (2014) also reported low barrier properties with a low basis weight of MFC coated on board, which was attributed to an incomplete coverage - holes in the layer that were observed by SEM. As the SEM pictures on Figure 14 present a complete coverage without holes, the low barrier of MFC-laminated boards with a low basis weight of MFC is more preferentially attributed to the presence of large fibre fragments.

III.3.5. Conclusion

MFC layers of 10 to 40 g/m² have been deposited on board using an innovative technique involving a filtration step forming a MFC wet cake laminated on board, similarly to what is described in a patent application by Guerin and co-workers (2016a). Adhesion between the MFC layer and board occurred during drying, without glue, and was stronger than the internal strength of the board. The lamination of a 40 g/m² MFC layer led to a low oxygen permeability, similar to what could be obtained with pure MFC films, suggesting a good coverage and layer formation. It was not the case for a lower MFC layer basis weight, especially at 10 g/m² where oxygen transmissions 100,000 times higher have been found. The dispersion of the oxygen transmission values measured for MFC layers of 10, 20, or 30 g/m², have been attributed to defects in the layer. The frequency and intensity of these defects seemed to decrease by increasing the MFC layer basis weight. Red oil Cobb tests, in addition to demonstrate the high grease barrier of MFC layers, evidenced defects in the 10 and 20 g/m² MFC layers. It was highlighted by small red oil stains remaining after testing. It supports the fact that oxygen permeation occurred due to small preferential pathways distributed in the low coat weight MFC layers, but neither holes nor macro-scale elements could be observed by scanning electron microscopy. The surfaces analysed presented a full coverage without especially large elements.

III.4. Conclusion

In order to develop new barrier using microfibrillated cellulose, this chapter aimed at getting a better understanding of the characterisation of the degree of fibrillation of MFC pulps, its influence on the barrier properties of MFC films, and to investigate the opportunity of using a wet lamination process for the deposition of 100% MFC layers on board.

The degree of fibrillation of MFC suspensions is difficult to measure and its effect on the barrier properties of MFC layers is not well understood. It is usually measured using indirect methods, but no study was found investigating which indirect methods were the most relevant. The first and second sections of this chapter were dedicated to the analysis of suspensions and self-standing films made from several MFC grades, prepared with different treatments, and from different pulps. Strong differences were found, even with only a visual analysis, especially concerning MFC UM produced by strong refining and MFC 0P produced by enzymatic pre-treatment and refining. These suspensions appeared rough (not homogeneous) at 2 wt% and resulted in non-homogeneous films. A more detailed comparison of the MFC suspensions could be performed by optical microscopy, evidencing a reduction of fibre fraction with increasing mechanical treatment from MFC 0P to 5P, and suspensions consisting more and more of woolly areas. This amount of residual macro-fibres could be quantified by MorFi analysis and was found to be consistent with the expected degree of fibrillation of the MFC suspensions. Rheological measurements were not as consistent with the expected degree of fibrillation: an increasing viscosity described well the increasing treatment of MFC 1P to MFC 5P, but comparison with MFC UM and MFC D evidenced a pulp origin dependency disturbing the sole analysis of the fibrillation. A similar effect was observed with the optical properties of MFC films, clarity and transmittance increased from MFC 0P to 5P due to the reduction of the size of the elements, but could not be compared correctly with MFC UM and D. The quantification of the macro-fibres residues in suspension and the density of self-standing films should be preferred to rheology or optical measurements for the characterisation of the degree of fibrillation of MFC suspensions. Other methods may be at least as relevant, such as fibril length measurements on multiple transmission electron micrographs (W. Chen et al., 2015) turbidity analysis (Nuopponen et al., 2016), or other methods described in a review by Kangas and co-workers (2014).

MFC films had different apparent densities depending on their degree of fibrillation, resulting in a higher apparent porosity for samples made of MFC produced with a light treatment: MFC UM and MFC 0P. It led to poor oxygen barrier properties, whereas more fibrillated MFC demonstrated low oxygen transmissions. MFC having a low degree of fibrillation should be avoided for the formation of 100% MFC oxygen barrier layers. However, the fibrillation was not found to affect the water vapour transmission in humid conditions of MFC films, which are permeable in any cases. An increased mechanical defibrillation in a homogeniser (MFC 0P, i.e. 0 pass, to MFC 5P, i.e. 5 passes) resulted in films with improved oxygen barrier, MFC 5P has thus been selected as the relevant grade to be applied on board by an innovative process including a filtration step.

Due to its high viscosity at low solid content, the deposition of a MFC layer on board using common coating techniques present several issues: wetting of the board, low coat weights, high drying energy demand. The potential of a new process of wet lamination including a filtration step for the production of 100% MFC barrier layers has been demonstrated. The deposition of 10 to 40 g/m² of MFC on board by wet lamination evidenced that the formation of thinner films, and/or

the process of wet lamination, resulted in defects in the MFC layer. These defects, revealed by red oil adsorption, appeared mostly for MFC layers of 10 and 20 g/m². They may be attributed to residual macro-fibres having dimensions in the order of magnitude of the thickness of the layer, or to holes formed during the peeling of the MFC wet cake from the membrane during the process of wet lamination. Oxygen permeability measurements showed that these defects made the MFC layer lose its oxygen barrier. At 40 g/m² no defect was revealed; it appeared as the minimum deposition required in order to obtain a defect-free oxygen barrier MFC layer on board by wet lamination with MFC 5P. The efficiency of this process, close to an industrial reality, seemed limited by the fraction of residual macro-fibres in suspension. A fractionation step or a different MFC production process allowing the removal of most macro-fibres may enable to reduce this minimum basis weight.

To conclude, this first chapter focused on 100% MFC suspensions and films for the production of oxygen barrier layer on board using a process including a filtration step. Preferential indirect methods have been evidenced for the characterisation of the degree of fibrillation of MFC grades, and one highly fibrillated grade has been selected to be applied due to its better oxygen barrier. Upon lamination on board, defects in the MFC layer have been revealed, which could be avoided by increasing the MFC layer basis weight. At 40 g/m² of MFC on board, a 100% biosourced barrier material could be obtained. The next part of this thesis investigates another technique for the use of MFC to create barrier layers: the coating strategy. It includes the study of PVOH:MFC composite films in Chapter IV, and the study of PVOH:MFC:clay composite films and coatings in Chapter V.

Chapter IV: MFC as Filler in a PVOH Matrix

Chapter IV: MFC as Filler in a PVOH Matrix

The objective of this thesis is to develop the use of microfibrillated cellulose in barrier layers deposited on paper or board. Chapter III focused on the development of 100% MFC layers of board in order to exploit its intrinsic grease and oxygen barrier properties. Another strategy for the development of MFC-based barrier layers is to use MFC as filler in a water-based barrier coating colour. Poly(vinyl alcohol) (PVOH) has been chosen as a matrix for the formulation of MFC-comprising barrier coating colours because it is a water-soluble, barrier to oxygen, biodegradable, and potentially biobased polymer (Harmsen et al., 2014; Shimao, 2001). In addition, PVOH has a higher ductility compared to starch, and starch:PVOH is reported as a promising blend allowing the material to be partially biobased (Dean et al., 2008; Hejri et al., 2012). PVOH:MFC appear as a promising blend for water-based barrier coating, but both materials can be found in many forms. In order to optimise such formulations, the most relevant PVOH and MFC grades should be used. In addition, the improvement in PVOH layer formation brought by MFC is not fully understood, and such composite layers are sensible to water and humidity due to the hydrophilicity of both components.

This chapter aims at selecting the most relevant MFC and PVOH grades for the development of MFC-comprising water-based barrier coatings. It also aims at getting a better understanding of the potential improvement in PVOH layer formation given by the addition of MFC, and to improve the behaviour of both components upon exposure to water or water vapour using different crosslinking strategies.

The first three sections of this chapter are dedicated to the investigation of the influence of the MFC grade (first section), MFC ratio (second section), and PVOH grade (third section) on the production of PVOH:MFC composite films with a coating-peeling process designed to mimic blade coating (cf. II.2.1.1.3, page 79). The objective is to obtain the best barrier properties while matching industrial expectations, especially in terms of viscosity and solid content. The fourth section is dedicated to the investigation of the drying kinetics of PVOH and PVOH:MFC coating colours, in order to measure the potential PVOH layer formation improvement given by the addition of MFC, using a laboratory infrared drying bench. Finally, the fifth section is dedicated to the development of three crosslinking strategies for improving the behaviour of PVOH and MFC films upon exposure to water or water vapour.

IV.1. Influence of the MFC grade

First, 2 pph of MFC UM, MFC D, or MFC KB have been mixed with PVOH 6-98 by adding the MFC suspension to the water used for PVOH solubilisation. Then, self-standing composite films have been produced with a coating-peeling process. The films have been tested in terms of optical, mechanical, and barrier properties in order to investigate the effect of the degree of fibrillation and source of the microfibrillated cellulose used.

IV.1.1. Self-standing films obtained by coating-peeling

The preparation of PVOH:MFC composite films is widely reported in the literature and they are mostly produced by solvent casting, consisting in the formulation of a diluted suspension of 1 to 5 wt% comprising PVOH and MFC, pouring in a petri dish, and slow evaporation of water in ambient conditions or eventually in oven at 40 to 60°C (Arola et al., 2013; Rodionova et al., 2012; Spence et al., 2010a). In order to obtain a material formed in a similar manner as a coated layer, a process of coating-peeling has been designed. It consists in three steps: coating, drying, and peeling, as described in Figure 41.

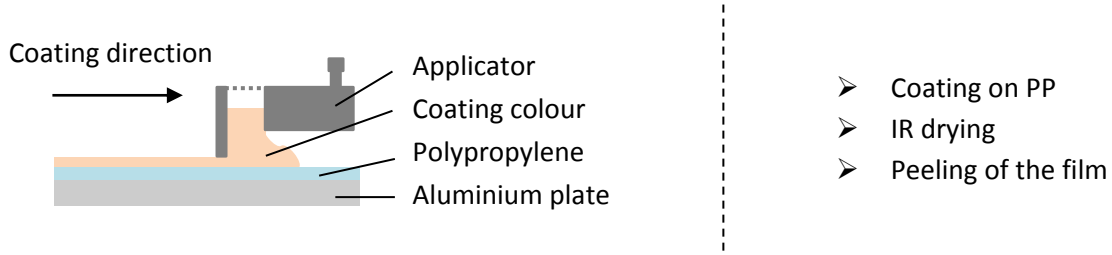

Figure 41 - Process of coating-peeling for the production of PVOH:MFC self-standing films.

A comparison between the process parameters for industrial barrier coating, the designed process of coating-peeling, and solvent casting are presented in Table 15. Coating-peeling allows working in conditions closer to industrial coating compared to solvent casting thanks to the use of suspensions with a higher solid content, higher viscosity, and infrared drying for a shorter film formation time.

	Industrial barrier coating	Coating-peeling	Solvent casting
Solid content		9 - 24 wt%	1 - 5 wt%
Viscosity	500 - 2,000 mPa.s	500 - 2,000 mPa.s	< 100 mPa.s
Drying mode	Infrared + convective + conductive drying	Infrared drying	Free drying
Film formation time	< 5 s	20 min	24 - 72h

Table 15 - Parameters for the processes of industrial coating, coating-peeling, and solvent casting.

IV.1.2. Apparent density and mechanical properties

A PVOH solution at 22 wt% with a viscosity of 1,010 mPa.s at 55°C has been produced using PVOH 6-98, a low molecular weight (47,000 g/mol) and high degree of hydrolysis (> 98%) PVOH. The addition of 2 part per hundred (pph), i.e. addition of a mass of MFC equal to 2% of the mass of PVOH, only slightly affected the viscosity of the composite suspension allowing to keep a similar solid content while remaining under 2,000 mPa.s.

The theoretical density of PVOH is 1.31 g/cm^3 (International Chemical Safety Cards (ICSC), 2015). The apparent density of PVOH 6-98 self-standing films obtained from basis weight and thickness measurements is also 1.31 g/m² (Table 16), suggesting that they present almost no porosity. The theoretical density of non-porous MFC films is 1.56 g/cm^3 as calculated from the literature (Chen et al., 2004; Diddens et al., 2008), while the one measured in the previous chapter, page 101, was of 1.06 g/m^3 for MFC UM films and 1.26 to 1.27 g/cm^3 for MFC D and MFC KB films. Due to the low amount of MFC in the composites and the density value close to the one of PVOH, a law of mixture would not predict a variation of more than 0.005 g/cm^3 upon addition of MFC. However, it can be observed in Table 16 that the PVOH + 2pph UM composite films had an apparent density as low as 1.03 g/cm^3. It has to be noted that this measurement took into account the surface roughness/porosity that can be created due to the presence of macro-elements. It also had a high impact on the mechanical properties, suggesting that there is actually an increase in internal porosity. SEM cross-section measurements on films cut by cryofracture could give more information. The lowering of both tensile strength and elongation at break for PVOH + 2 pph UM suggested that weak points were created, facilitating sample failure.

	Apparent density (g/cm3)		Tensile strength (MPa)		Elongation at break (%)		Young Modulus (GPa)	
	Average	Stdev	Average	Stdev	Average	Stdev	Average	Stdev
PVOH	1.31	0.01	59.8	2.1	72.0	27.9	3.4	0.1
PVOH + 2 pph UM	**1.03**	0.06	**48.5**	4.3	**17.7**	2.7	3.1	0.2
PVOH + 2 pph D	1.29	0.03	55.6	8.3	**26.8**	11.8	3.5	0.1
PVOH + 2 pph KB	1.28	0.01	58.6	6.5	**29.6**	7.1	3.5	0.2

Table 16 - Mechanical properties for PVOH:MFC composite films.

In the case of MFC D and KB the density and mechanical properties are not strongly affected. The most affected property is the elongation at break that decreases from 72% to about 30%. The force-elongation profiles of the tensile tests of PVOH samples presented in Figure 42 show two distinct regions. Similarly to Strawhecker and Manias (2000), the samples exhibited an initial period of plastic deformation, followed by a plateau during plastic deformations until failure. In the presence of MFC D or MFC KB, the first region is similar but the plateau that follows is shorter. It has been deducted that the MFC network inside the material could be deformed up to a certain point after which the whole sample breaks. At 2 pph MFC, this point is located in the plateau region of PVOH.

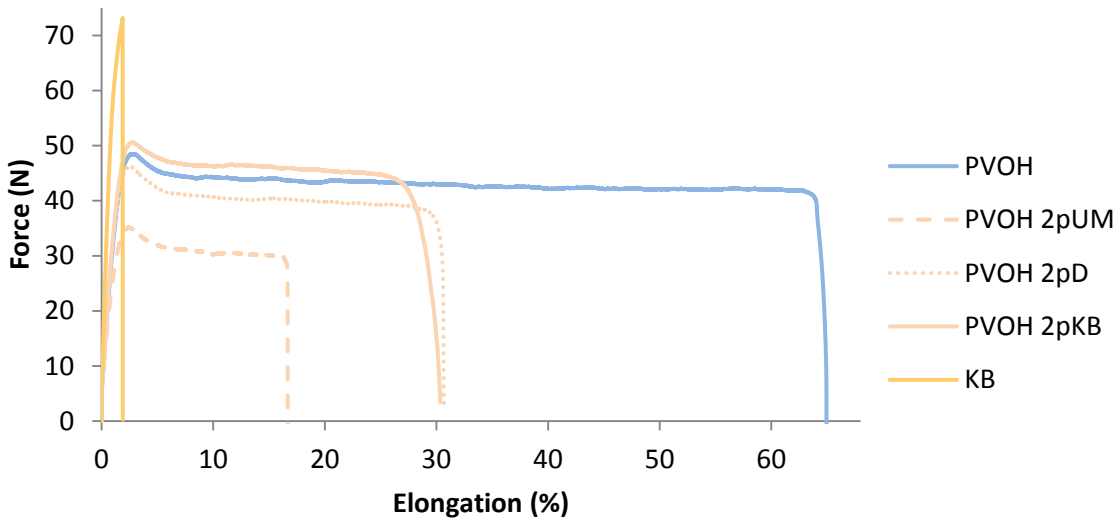

Figure 42 - Force-elongation profile during the tensile tests for MFC, PVOH, and PVOH:MFC composites. PVOH 2pMFC is equivalent to PVOH + 2 pph MFC.

IV.1.3. Optical properties

The introduction of MFC in PVOH led to significant changes in terms of optical properties. As shown in Figure 43, PVOH was completely transparent and clear while the introduction of MFC caused a blurring of the film. The blurring is homogeneous in the case of MFC D and KB, whereas in the case of MFC UM, solid elements could be observed and were attributed to the important fraction of residual macro-fibres, as described in Chapter III.

PVOH | PVOH + 2 pph D | PVOH + 2 pph UM

Figure 43 - Pictures of PVOH and PVOH:MFC self-standing films.

The blurring of the film upon addition of MFC is characterised by an increase in haze and a decrease in clarity, as reported in Table 17. The haze values are similar with MFC UM, MFC D, or MFC KB addition in PVOH despite the optically visible difference in the case of MFC UM compared to MFC D and MFC KB.

	Transmittance (%)		Haze (%)		Clarity (%)	
	Average	Stdev	Average	Stdev	Average	Stdev
PVOH	92.9	0.1	**1.6**	0.1	98.2	0.1
PVOH + 2 pph UM	92.9	0.1	11.8	1.6	**72.5**	4.1
PVOH + 2 pph D	92.8	0.2	12.3	2.3	**66.8**	7.9
PVOH + 2 pph KB	92.8	0.1	13.8	1.3	**65.8**	2.0

Table 17 - Optical properties for PVOH and PVOH:MFC self-standing films

Several parameters suggest that diffusion and scattering phenomena occurred mainly because of a surface roughness modification: the transmittance is kept constant but haze and clarity are modified, the films did not seem to have internal porosity according to the density measurements, and PVOH and cellulose having close refractive indices of 1.50 and 1.54, respectively (Mahendia et al., 2013; Nogi et al., 2005). TOPO 3D analyses evidenced this increase of surface roughness, as represented in Figure 44. Upon addition of 2 pph MFC KB, the roughness of PVOH increased from 36 ± 11 to 436 ± 63 nm.

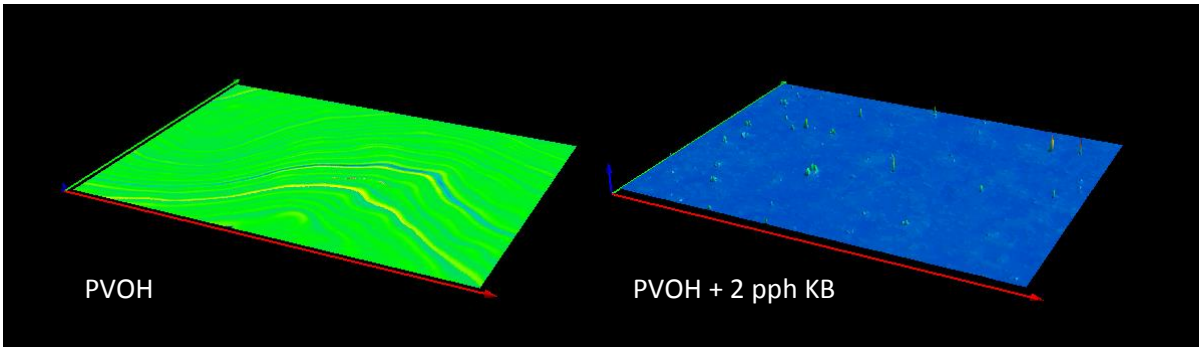

Figure 44 - TOPO 3D pictures of PVOH (left) and PVOH + 2pph KB (right) films surfaces. Surface analysed: 1380x1044 µm.

IV.1.4. Oxygen and water vapour barrier

The high barrier property of PVOH has been confirmed by analysis of the oxygen transmission rate (OTR) in dry conditions (23°C 0%RH) that was below the detection threshold of the MOCON apparatus, as shown in Table 18. Despite an apparent density reduced by 21% compared to pristine PVOH as described in IV.1.2, page 117, the PVOH + 2 pph UM composite also presented an OTR below the detection threshold of the apparatus. Although pores are formed inside the material, they are not expected to be interconnected thus keeping a continuous PVOH coverage along the sample preventing oxygen permeation. The oxygen barrier may be affected, but it could not be detected with the device used. The oxygen barrier is also preserved in the case of PVOH + 2 pph D and PVOH + 2 pph KB composites.

	OTR at 23°C 0%RH ($cm^3/(m^2.d.bar)$)	$WVTR_{65}$ at 23°C 85%RH (g/(m².d))	
		Average	Stdev
PVOH	< 0.01	178	10
PVOH + 2 pph UM	< 0.01	**307**	13
PVOH + 2pph D	< 0.01	172	27
PVOH + 2pph KB	< 0.01	154	11

Table 18 - Oxygen and water vapour barrier of PVOH:MFC composite films with different MFC grades.

More differences were found upon analysis of the water vapour transmission rate (WVTR) in humid conditions (23°C 85%RH), normalised to the target basis weight of 65 g/m² ($WVTR_{65}$) for comparison. The WVTR of 178 g/(m².d) for PVOH is lower than what was obtained for the MFC films manufactured by handsheet method. However, this value is still high considering that a PE layer of equivalent thickness would have a WVTR of about 20 g/(m².d), as calculated from Lange and Wyser (2003). It can be noted that the thickness of the samples is around 50 µm and the water vapour pressure at 23°C 85%RH is of 19.7 hPa, leading to a PVOH water vapour permeability (WVP) of 453 g.µm/(m².d.hPa). MFC UM has a strong detrimental effect on the water vapour barrier, increasing the $WVTR_{65}$ by 72%, while MFC D did not have any effect and a slight improvement has been observed with the addition of MFC KB.

IV.1.5. Conclusion

The addition of microfibrillated cellulose in poly(vinyl alcohol) changed its appearance from clear to blurry and affected the mechanical and barrier properties depending on the degree of fibrillation. The use of 2 pph of MFC UM, with a high amount of residual macro-fibres, led to composite films with a lower apparent density of 1.03 g/cm³ compared to 1.31 g/cm³ for the PVOH matrix, taking into account both internal and surface porosity. This lower apparent density is assumed to be responsible for a slight decrease of the Young modulus from 3.4 to 3.1 GPa, and especially for the formation of weak points resulting in a reduction of both the tensile strength and elongation at break from 60 MPa and 72% to 48 MPa and 18%, respectively. The water vapour barrier is affected as well with an increase in $WVTR_{65}$ at 23°C 85%RH from 178 to 307 g/(m².d), while no effect on the OTR could be observed. The more fibrillated MFC D and MFC KB mostly preserved the properties of PVOH, with almost no effect on the apparent density, tensile strength, Young modulus, $WVTR_{65}$, and no observable effect on the OTR. No significant difference between the effect of MFC D from sulphite softwood pulp and KB from kraft birch pulp has been found, except a slightly lower $WVTR_{65}$ in the case of MFC KB. The only property that was strongly affected by MFC D or MFC KB addition is the elongation at break that has been reduced from 72% to 30%. This is attributed to the lower deformation ability of the MFC, as observed concerning the films manufactured with handsheet method in Table 11, page 101, with values close to 2%.

It can be concluded that the use of MFC comprising a high amount a residual macro-fibres affects the structure of the composite films making them more porous, with weak points and lower mechanical properties, and with a lower ability to hinder the permeation of water vapour. On the

contrary, highly fibrillated MFC grades can be incorporated into the matrix without affecting its properties, except for the elongation at break, and MFC KB even slightly improved the water vapour barrier of the resulting films.

IV.2. Influence of MFC content

From the previous chapter and previous section, MFC KB has been selected as the reference MFC grade to be used as filler in a PVOH matrix. Its content has been varied from 0.5 to 20 pph in order to determine the influence of the MFC content on the processing, optical, mechanical, and barrier properties of the composites.

IV.2.1. Increased viscosity and aggregation with increasing MFC content

An increase of MFC content in PVOH had a high impact on the viscosity of the suspension, as already observed by Guezennec (2012), affecting the process of self-standing film production. The coating-peeling process requires coating colours with a viscosity below 2,000 mPa.s, preferably around 1,000 mPa.s. In order to remain in the correct range, suspensions with increasing MFC contents had to be diluted as shown in Table 19. While neat PVOH could be used at more than 20 wt%, the total solid content had to be decreased to 9 wt% when adding 20 pph MFC in order to keep a viscosity close to 1,000 mPa.s. This necessity to dilute the suspension is disadvantageous, as it implies that more energy will have to be used in order to evaporate the water from the coating colour. In addition, it could affect the structuration of the material during drying. However, using a 9 wt% suspension with a viscosity of 1,020 mPa.s is still more convenient than the use of pure MFC suspensions that, in our case, are used at a maximum of 2 wt%.

Formulation	MFC (pph)	Solid content (wt%)	Viscosity (mPa.s)	Temperature (°C)
PVOH	0	23%	1,010	55
PVOH + 0.5 pph KB	0.5	21%	360	52
PVOH + 2 pph KB	2	24%	1,430	55
PVOH + 5 pph KB	5	14%	650	51
PVOH + 10 pph KB	10	10%	640	54
PVOH + 20 pph KB	20	9%	1,020	51

Table 19 - Properties of the PVOH:MFC suspensions with a MFC KB content from 0 to 20 pph in a matrix of PVOH 6-98.

In addition, at 20 pph MFC, aggregates began to appear. Figure 45 shows a wet film of PVOH + 10 pph KB before infrared drying (A); it was as smooth and homogeneous as in the case of neat PVOH. When increasing the MFC content to 20 pph (B), gel-like particles could be found impacting the homogeneity of the suspension. Continuing to stir the suspension at 95°C during three hours after the solubilisation of PVOH allowed removing a high fraction of the aggregates. However, some were still present as can be observed in the picture of the wet layer (C). Temperature played an essential role as an overnight stirring without heating had few effects on the aggregates. These aggregates truly come from the mixing of MFC with PVOH, as they were neither found in the case of neat PVOH, nor in the case of MFC suspensions, as can be observed from a 100% wet MFC film (2 wt%) (D). Films have been produced from the PVOH + 20 pph MFC suspension with three hours of additional stirring at 95°C. The gel-like particles were responsible for whiter areas that can be mainly

observed by reflexion (F). The white colour of these areas was attributed to a higher local fraction of MFC.

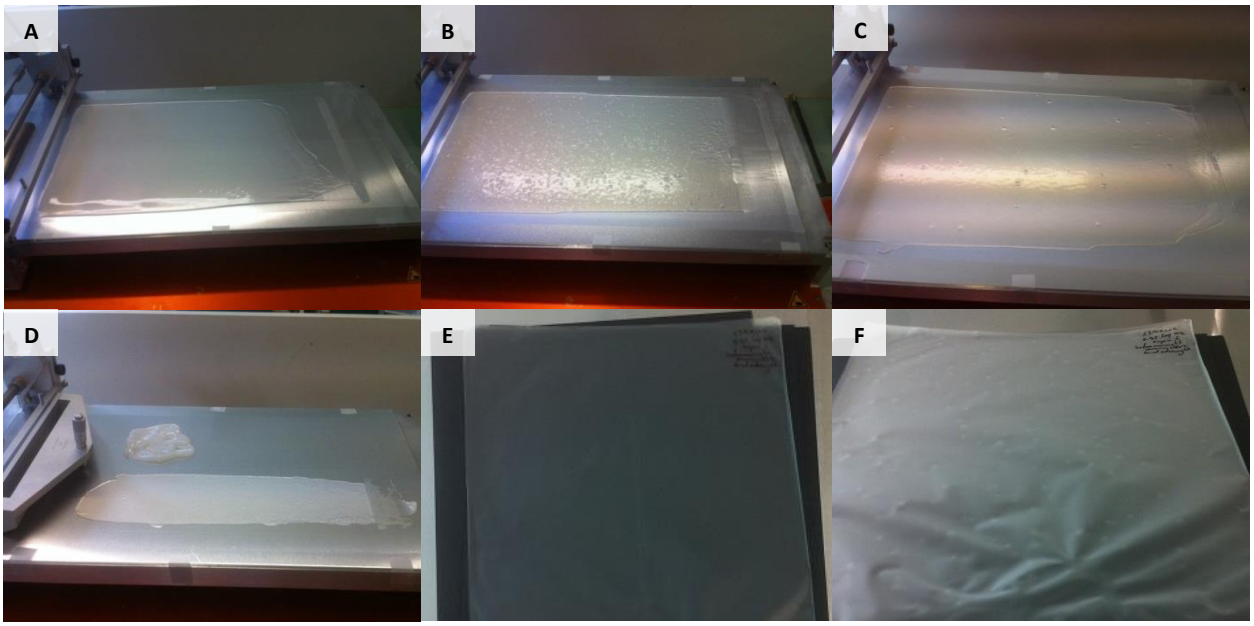

Figure 45 - PVOH + 10 pph KB wet film (A), PVOH + 20 pph KB wet film (B), PVOH + 20 pph KB after three hours at 95°C wet film (C), 2 wt% MFC wet film (D), PVOH + 20 pph KB after three hours at 95°C dry film (E & F). PVOH and PVOH:MFC films have dimensions of 20x30 cm.

The use of concentrated suspensions corresponding to what is expected for industrial coating highlighted the risk of using a high MFC content, as it requires the dilution of the suspension in order to keep a low enough viscosity. It also highlighted a limit in terms of MFC content due to the aggregation of MFC with PVOH at 20 pph MFC, leading to less homogeneous composite films.

IV.2.2. Apparent density and mechanical properties

The evolutions of the apparent density, Young modulus, tensile strength, and elongation at break with the MFC content for the PVOH:MFC composites are presented in Figure 46. Full data can be found in appendix page 200. A general trend was observed consisting in a reduction of the apparent density, Young modulus, and tensile strength up to a certain MFC content, after which the properties increase. The trend was different concerning the elongation at break as it continues to decrease along all the tested range of MFC content. A similar behaviour was observed by Zimmerman and co-workers (2004) using non chemically-modified MFC in PVOH, with a degradation of mechanical resistance at 1 wt% MFC but improvement from 5 wt%. They made the hypothesis that at low MFC content, no mechanical reinforcement was obtained because the amount of MFC was too low for network formation.

From 5 pph MFC, the apparent density starts to be significantly degraded despite the similar apparent density of 1.27 g/cm^3 for MFC KB films. This lower apparent density is expected to be

responsible for the lower Young modulus and tensile strength of the PVOH:MFC composite films with up to 10 pph MFC. However, neat MFC KB films have approximately double the Young modulus and tensile strength of neat PVOH films; MFC also acts as reinforcement, explaining the progressive increase from 5 to 20 pph MFC. It has to be noted that increasing the MFC content forced to reduce the solid content of the suspensions. The fast drying of the more and more diluted suspensions may result in a quickly immobilised structure, without possibility of reorganisation, leading to a decreasing density and mechanical resistance.

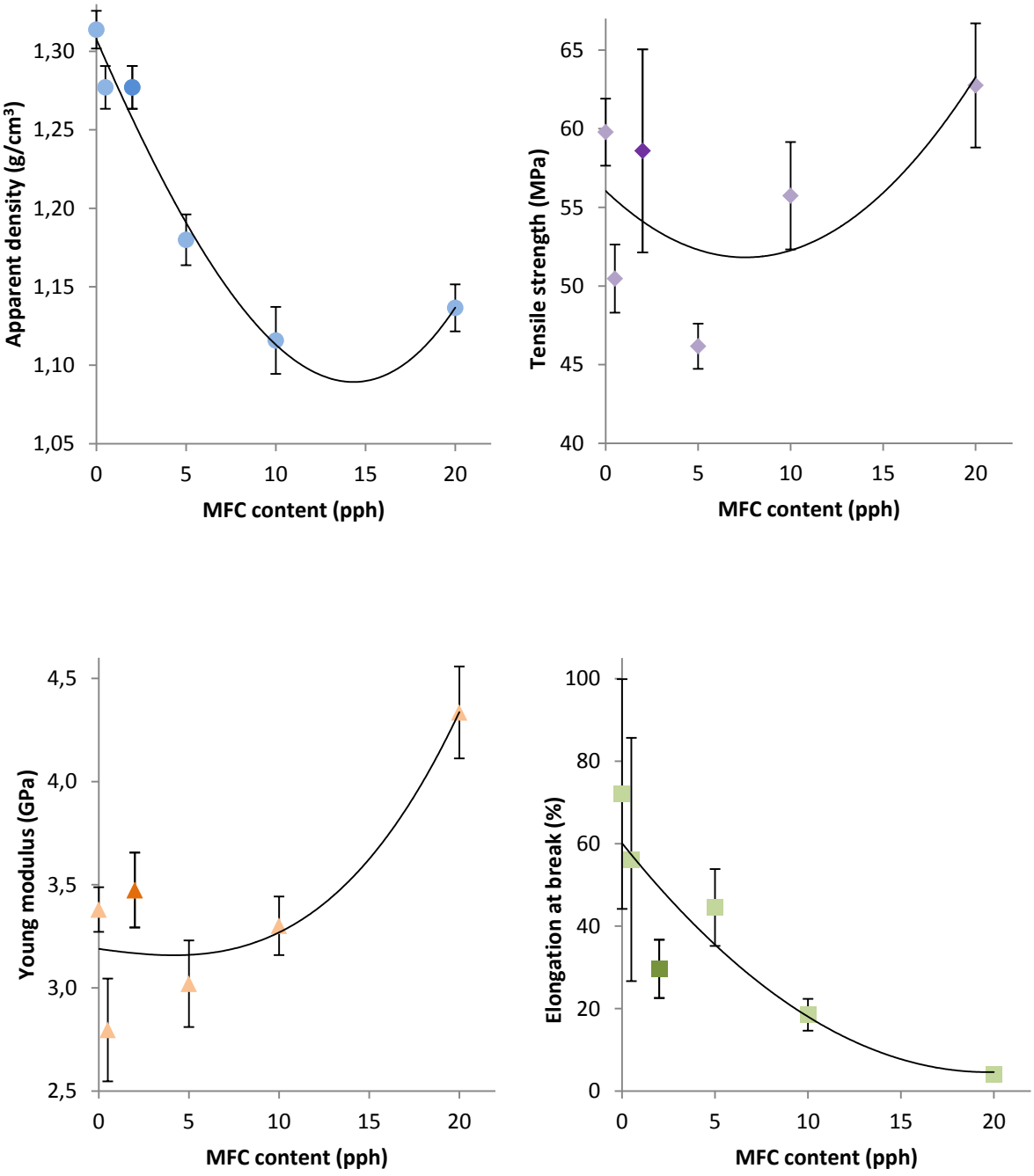

Figure 46 - Density and mechanical properties for PVOH:MFC composite films with increasing MFC KB content. Lines are only present to guide the eye.

It can be noted that a specific behaviour is observed upon addition of 2 pph MFC. Compared to what would be expected taking into account the other measurements, the PVOH + 2 pph KB composite films have a significantly higher density, tensile strength, and Young modulus while having a lower elongation at break. Similar results have been found upon production of another batch of PVOH + 2 pph MFC and mechanical testing. The reasons for this specific behaviour have not been yet determined.

IV.2.3. Optical properties

It has been observed in the previous section that the introduction of MFC in PVOH led to a blurring of the film characterised by an increase in haze while maintaining a constant transmittance. Figure 47 evidences that it continued to increase with the MFC content, with a constant transmittance from 0 to 20 pph MFC, and the haze and clarity appearing to reach a plateau at 10 to 20 pph. Full data can be consulted in appendix page 200. As a matter of comparison, a MFC KB film manufactured by handsheet method has a transmittance of 78.8%, a haze of 96.0%, and a clarity of 5.7%.

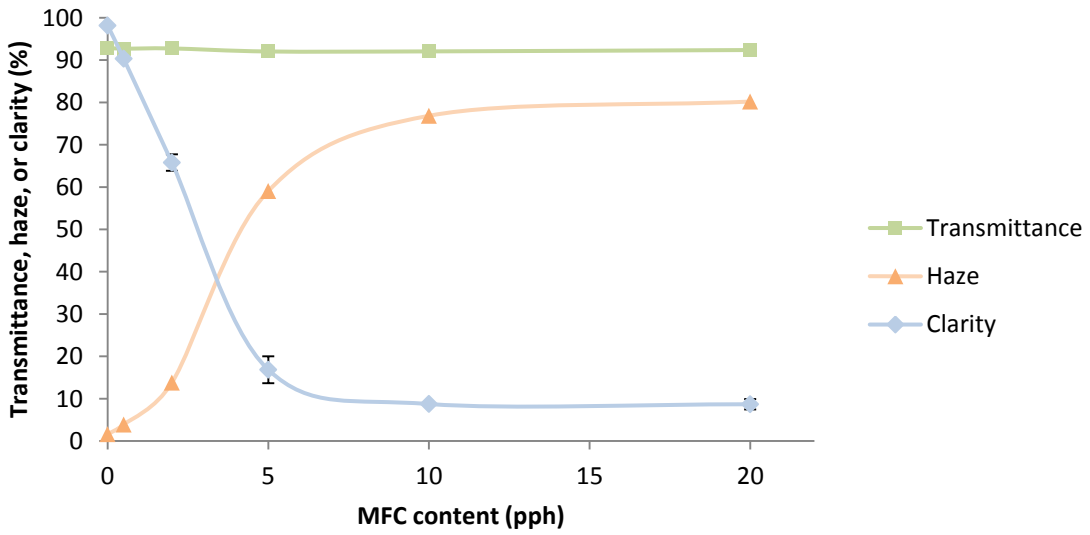

Figure 47 - Evolution of the optical properties for PVOH:MFC composite films with increasing MFC KB content.

IV.2.4. Oxygen and water vapour barrier

As all tested samples showed an oxygen transmission rate below the detection threshold of the MOCON apparatus, the comparison between the formulations in terms of barrier properties could only be made through the analysis of the $WVTR_{65}$ at 23°C 85%RH. The results are presented in Figure 48; a slight degradation occurs upon the progressive addition of MFC with a $WVTR_{65}$ at 23°C 85%RH ranging from 178 g/(m².d) for PVOH to 206 g/(m².d) for PVOH + 20 pph MFC. As previously observed concerning the mechanical properties of the composites, a specific behaviour is found at 2 pph MFC with a $WVTR_{65}$ of 154 g/(m².d), lower than that of the pristine matrix.

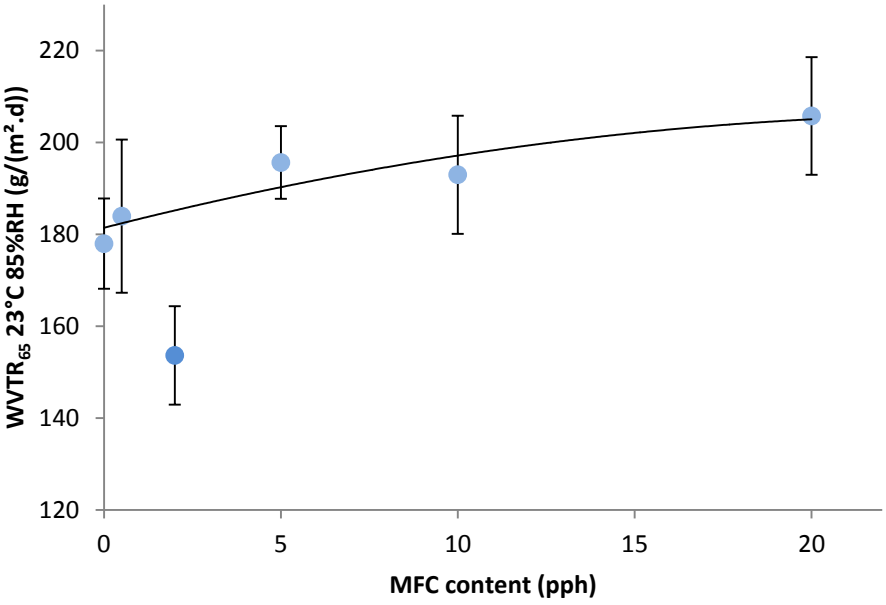

Figure 48 - $WVTR_{65}$ at 23°C 85%RH for PVOH:MFC composites with increasing MFC content.

IV.2.5. Conclusion

MFC suspensions are highly viscous and their addition in PVOH affects drastically the rheology, while a viscosity under 2,000 mPa.s is mandatory and about 1,000 mPa.s is preferable for using the coating-peeling process. In order to keep a viscosity close to 1,000 mPa.s, the PVOH:MFC coating colours had to be diluted depending on their MFC content with any further dilution leading to a higher drying requirement. In addition, aggregates appeared at 20 pph MFC, evidencing difficulties in dispersing MFC correctly. By increasing the MFC content the transmittance of the composite films was not affected while the haze increased sharply, reaching a plateau with values of 77% and 80% at 10 and 20 pph, respectively. Concerning the mechanical properties a mix between the introduction of porosity and a mechanical reinforcement by the MFC network could be observed. It resulted first in a decrease of the mechanical properties by addition of 0.5 pph, and after that a progressive improvement with values of tensile strength and Young modulus superior to those of the pristine matrix at 20 pph MFC. The elongation at break progressively decreased from 72% down to 4% at 20 pph MFC. A specific behaviour was observed with the use of 2 pph MFC with higher apparent density, tensile strength, and Young modulus compared to what would be expected. This specific behaviour at 2 pph MFC was also observed concerning the water vapour barrier in humid conditions that was improved compared to the pristine PVOH, whereas in any other case the increase of MFC content damaged progressively the barrier of the film. No comparison in terms of oxygen barrier could be drawn as all the tested samples were under the detection threshold of the apparatus.

IV.3. Influence of PVOH grade

As different grades of MFC can be found depending on their source, chemical or enzymatic pre-treatment, and intensity of mechanical treatment, different PVOH grades can be found mainly differing in terms of degree of polymerisation and degree of hydrolysis. Poly(vinyl alcohol) is produced from the hydrolysis of the acetate groups of poly(vinyl acetate) into alcohol groups. However, residual acetate groups are still present in poly(vinyl alcohol). The degree of hydrolysis is the percentage of alcohol groups among the total of alcohol plus acetate groups. A PVOH is considered "fully- hydrolysed" when its degree of polymerisation is higher than 97% (Klatte and Zacharias, 1999). In this section, four PVOH grades were combined with 2 pph of MFC KB in order to analyse the effect of the degree of polymerisation and degree of polymerisation on the process, and the mechanical and barrier properties of PVOH:MFC composites.

IV.3.1. Description of PVOH grades

In addition to PVOH 6-98 that has been used in the previous sections, three other grades were used as a matrix: PVOH 26-88, PVOH 30-98, and PVOH 28-99. In the nomenclature of the PVOH grades, the first number corresponds to the viscosity of a 4 wt% aqueous solution at 20°C and is indicative of its degree of polymerisation, and the second number corresponds to the degree of hydrolysis of the PVOH grade. The properties of the four PVOH grades can be found in Table 20.

Commercial name	Degree of polymerisation	Molecular weight (g/mol)	Degree of hydrolysis (%)
Poval 6-98	1,000	47,000	98.4 ± 0.4
Poval 26-88	3,300	160,000	87.7 ± 1.0
Poval 30-98	3,300	150,000	98.4 ± 0.4
Poval 28-99	3,300	145,000	99.4 ± 0.4

Table 20 - Properties of the four PVOH grades compared in this section.

IV.3.2. PVOH:MFC coating colour viscosity and foaming

The degree of polymerisation has a strong influence on the viscosity of hydrosoluble polymers. The PVOH grades with a degree of polymerisation of 3,300 led to more viscous coating colours that, as in the case of increased MFC contents, had to be diluted in order to remain in the appropriate viscosity range. The dilution of the PVOH:MFC suspensions and their viscosity are presented in Table 21. The fully-hydrolysed PVOH 30-98 and PVOH 28-99 were diluted to 12 to 13 wt% compared to the fully-hydrolysed PVOH 6-98 of lower degree of polymerisation that could be used at 24 wt%. The use of PVOH 26-88 with a lower degree of hydrolysis of 88% led to an even more viscous coating colour that was at the limit of what could be processed by coating-peeling. In addition, the coating colour has been difficult to produce due to a higher tendency to foam.

Formulation	Solid content (wt%)	Viscosity (mPa.s)	Temperature (°C)
PVOH 6-98 + 2 pph KB	24%	1,432	55
PVOH 26-88 + 2 pph KB	14%	2,146	50
PVOH 30-98 + 2 pph KB	13%	960	55
PVOH 28-99 + 2 pph KB	12%	1,120	52

Table 21 - Properties of PVOH:MFC suspensions with different PVOH grades.

IV.3.3. Apparent density and mechanical properties

The PVOH grade has also a great influence on the mechanical properties of the resulting composites. The lower degree of hydrolysis of PVOH 26-88 led to composite films with a lower density, as shown in Table 22. This is attributed to the steric hindrance and lack of hydrogen bonds generated by the higher amount of acetate groups compared to the fully-hydrolysed PVOH grades. A lower degree of hydrolysis also leads to a lower crystallinity (Klatte and Zacharias, 1999). It results in a lower tensile strength of 44 MPa and a much higher elongation at break of 92% compared to the values obtained with the fully-hydrolysed PVOH 30-98 and PVOH 28-99, of similar degree of polymerisation. Combined with 2 pph MFC KB, PVOH 30-98 and PVOH 28-99 have a density of 1.27 and 1.28 g/cm^3, similar to the one of PVOH 6-98. They also have a similar elongation at break of 50% and 58%, respectively, the composite films being slightly stronger with the use of PVOH 28-99. The effect of the degree of polymerisation can be observed comparing PVOH 6-98 and PVOH 30-98. The density and mechanical properties are similar, with the exception of the higher elongation at break with PVOH 30-98 of higher degree of polymerisation.

The degree of hydrolysis strongly affects the mechanical properties: a low degree of hydrolysis of 88% leads to composites with lower density and strength, but with a higher elongation that would be beneficial for the converting ability of the layer. Few differences were found comparing the degree of hydrolysis of 98% and 99%, only a slight strength gain was observed at 99% of hydrolysis. The degree of polymerisation has not been found to play a role in terms of density or mechanical resistance. However, a higher degree of polymerisation allows the composite films to have a better elongation at break.

	Apparent density (g/cm^3)		Tensile strength (MPa)		Elongation at break (%)		Young Modulus (GPa)	
	Average	Stdev	Average	Stdev	Average	Stdev	Average	Stdev
PVOH 6-98 + 2 pph KB	1.28	0.01	59	6	30	7	3.5	0.2
PVOH 26-88 + 2 pph KB	**1.08**	0.05	**44**	3	92	17	3.0	0.2
PVOH 30-98 + 2 pph KB	1.27	0.02	65	8	50	28	2.9	0.8
PVOH 28-99 + 2 pph KB	1.28	0.03	**75**	6	58	31	**4.2**	0.2

Table 22 - Density and mechanical properties for PVOH:MFC composites with different PVOH grades.

IV.3.4. Oxygen and water vapour barrier

The analysis of the water vapour transmission rate at 23°C 85%RH of the PVOH:MFC composite films with different PVOH grades presented similarities with what has been found concerning the mechanical properties. The low degree of hydrolysis of PVOH 26-88 had a high impact on the $WVTR_{65}$ of its PVOH:MFC composite, with a value of 380 g/(m².d) compared to about 135 g/(m².d) for the composites with PVOH 30-98 and PVOH 28-99, respectively, of same degree of polymerisation but higher degree of polymerisation than PVOH 26-88. This is equivalent to a water vapour permeability of 1,160 g.µm/(m².d.hPa) with PVOH 26-88 and 349 g.µm/(m².d.hPa) with PVOH 30-98. It can be noted that going from a degree of hydrolysis of 98% to 99% did not produce a significant difference. The lower degree of polymerisation of PVOH 6-98 compared to PVOH 30-98 led to a slightly higher WVTR of 154 g/(m².d). The OTR at 23°C 0%RH was found to be under the detection threshold of the apparatus for all tested composite films.

	$WVTR_{65}$ 23°C 85%RH (g/(m².d))	
	Average	Stdev
PVOH 6-98 + 2 pph KB	154	11
PVOH 26-88 + 2 pph KB	**380**	15
PVOH 30-98 + 2 pph KB	135	10
PVOH 28-99 + 2 pph KB	132	8

Table 23 - $WVTR_{65}$ for PVOH:MFC composites with different PVOH grades.

IV.3.5. Conclusion

In this section, four PVOH grades have been combined with 2 pph of MFC KB in order to assess the influence of the degree of hydrolysis and the degree of polymerisation of PVOH on the process, and on the mechanical and barrier properties of PVOH:MFC composites. The degree of hydrolysis had a strong impact on the process when going from a fully-hydrolysed to a partially-hydrolysed PVOH with a tendency to foam, making it difficult to produce bubble-free samples. In addition, the use of PVOH 26-88 led to poor mechanical resistance and water vapour barrier, attributed to the lower density resulting from its higher fraction of residual acetate groups. Comparing PVOH 30-98 and PVOH 28-99 with a degree of hydrolysis of 98% and 99%, respectively, no clear difference could be found except a slightly better mechanical resistance in the case of PVOH 28-99.

The effect of the degree of polymerisation has been observed in terms of better mechanical resistance and, more importantly, a higher elongation at break of 50% to 58% that predicts a better ability for future coating layers to withstand creasing and folding. It also led to a slightly better water vapour barrier. However, it had a strong impact on the viscosity of the coating colour. The use of a PVOH with a degree of polymerisation of 3,300 resulted in a PVOH:MFC suspension that had to be diluted to 12 to 14 wt%, while the use of PVOH 6-98 with a degree of polymerisation of 1,000 allowed working with a coating colour having a higher solid content of 24 wt%. This section highlighted the necessity of using a fully-hydrolysed poly(vinyl alcohol) grade in order to avoid getting poor water vapour barrier. In addition, despite its poor elongation at break and slight barrier improvement at higher degree of polymerisation, PVOH 6-98 has been selected for further work in order to be able to use formulations having a higher solid content.

IV.4. Drying kinetics of PVOH:MFC suspensions

MFC is reported to have a positive effect for the drying of PVOH solutions by avoiding the formation of defects (Guezennec, 2012; Schmidt et al., 2015). Guezennec (2012) also observed that a PVOH solution comprising MFC dried faster, using a thermo-balance. It has been found of interest to perform a more detailed study on the basis of this observation, using an instrumented infrared drying bench described in II.2.2.1, page 82. The heat flow generated by the infrared lamp during the experiment is measured, as well as the evolution of the temperature and mass of the drying sample. This experiment has been used to determine the drying kinetics of PVOH or PVOH:MFC suspensions in a Teflon mould and as coating on board, using PVOH 6-98 and MFC 5P.

IV.4.1. Suspension in a Teflon mould

First, 10.75 g of PVOH or PVOH + 5 pph MFC 5P suspension at 18 wt% were dried in a Teflon mould, corresponding to 100 g/m² dry. The mass loss of the suspensions during drying is shown in Figure 49. The addition of 5 pph MFC is found to accelerate the mass loss, similarly to what was observed by Guezennec (2012).

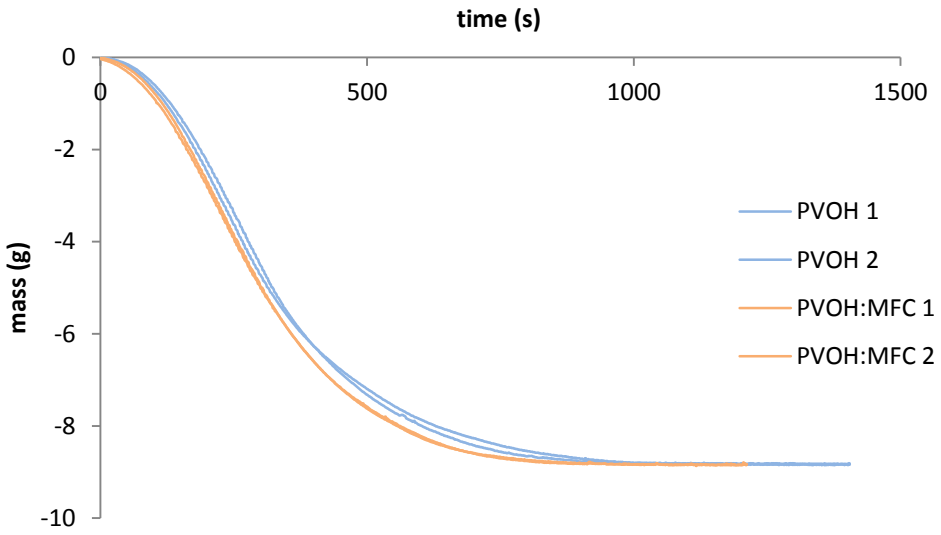

Figure 49 - Evolution of the mass loss during drying for PVOH or PVOH:MFC suspensions. Duplicate results are shown.

Similarly to what was described by Navarri and Andrieu (1993) who studied much thicker PVOH layers, the drying kinetics of PVOH-comprising suspensions display three main domains:

- Increasing drying rate corresponding to the heating of the suspension and also due here to the lamps taking time to warm up and reach the equilibrium heat flux emitted.
- Constant rate period, where the mass decreases linearly as a function of time, similar to the case of free water.

- Falling rate period when the sample is getting dry and water becomes harder to remove. It is during the third domain that the material may be damaged (bubbling).

Based on this description, the curves have been fitted using a parabolic equation, then a linear equation, and finally an exponential equation, as follows:

$$First\ domain\text{:}\ \frac{m-m_0}{m_1-m_0}=\frac{(t-t_0)^2}{(t_1-t_0)^2}\quad (Eq.17)$$

$$Second\ domain\text{:}\ \frac{m-m_1}{m_2-m_1}=\frac{t-t_1}{t_2-t_1}\quad (Eq.18)$$

$$Third\ domain\text{:}\ \frac{m-m_2}{m_3-m_2}=1-exp[-k\cdot(t-t_2)]\quad (Eq.19)$$

where m (g) is the mass loss of suspension at time t (s), m_0 (= 0 g) the initial mass loss at time t_0 (= 0 s), m_1 (g) the mass loss at time t_1 (s) corresponding to the boundary between the parabolic and linear domains, m_2 (g) the mass loss at time t_2 (s) corresponding to the boundary between the linear and exponential domains, m_3 (g) the final mass loss at the end of the experiment, and k the exponential coefficient.

The continuity of the derivative functions at t_1 and t_2 leads to two other conditions:

$$At\ \boldsymbol{t_1}\text{:}\ 2\cdot(m_1-m_0)\cdot\frac{\boldsymbol{t_1}-t_0}{(t_1-t_0)^2}=(m_2-m_1)\cdot\frac{1}{t_2-t_1}\quad (Eq.20)$$

$$which\ implies\text{:}\ m_2=m_1+2\cdot(m_1-m_0)\cdot\frac{t_2-t_1}{t_1-t_0}\quad (Eq.21)$$

$$At\ \boldsymbol{t_2}\text{:}\ (m_2-m_1)\cdot\frac{1}{t_2-t_1}=(m_3-m_2)\cdot k\cdot\exp[-k\cdot(\boldsymbol{t_2}-t_2)]\quad (Eq.22)$$

$$which\ implies\text{:}\ k=\frac{m_2-m_1}{m_3-m_2}\cdot\frac{1}{t_2-t_1}\quad (Eq.23)$$

As a result: m_0, t_0, and m_3 are determined experimentally, m_1 is determined as the experimental mass loss at time t_1, m_2 is determined from the continuity of the derivative functions in t_1, and k is determined from the continuity of the derivative functions in t_2. The only remaining variables are the boundary times t_1 and t_2. The values of t_1 and t_2 are determined in order to minimise the mean squared error between the experimental and the predicted data. An example of result is shown in Figure 50, highlighting the three domains.

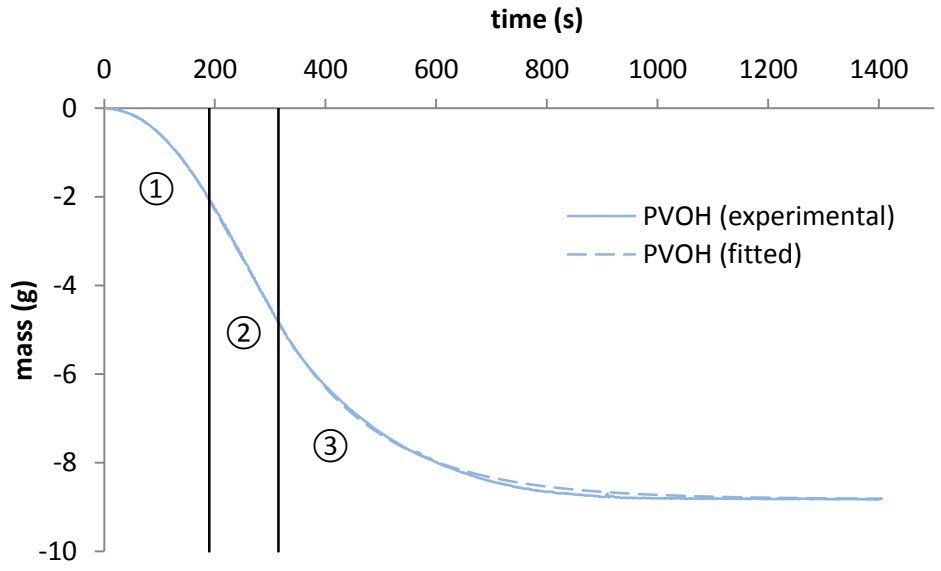

Figure 50 - Fitting of a drying curve of PVOH using the previous equations.
①, ②, and ③ indicate the parabolic, linear, and exponential domains, respectively.

The equations of the fitted curves of mass loss are then expressed in terms of water content in g_{water}/g_{dry}, and derived as a function of time in order to obtain the evaporation rate per unit dry matter in $(g_{water}/g_{dry})/s$. It allows a characteristic drying curve, as presented in Figure 51. Drying occurs from the right side to the left side of the graph, i.e. from high water contents to low water contents.

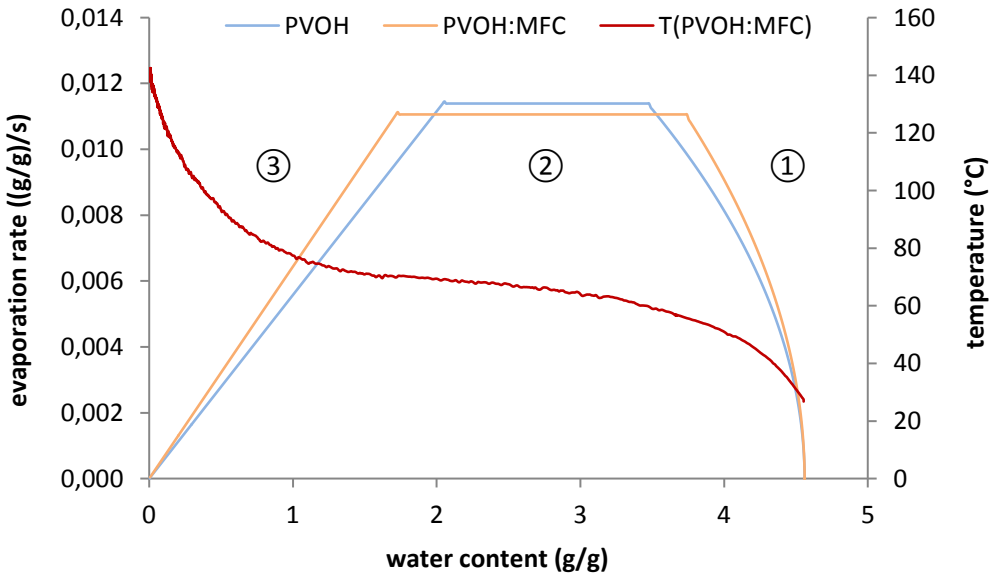

Figure 51 - Evaporation spectra for PVOH and PVOH:MFC suspensions (blue and orange curves, left axis), along with the temperature at the bottom of the Teflon mould during the PVOH:MFC experiment (red curve, right axis).

It can be observed that the domain corresponding to water evaporation at constant evaporation rate (domain ②) gets wider in the presence of MFC. It begins at higher water content and ends at lower water content, also corresponding to lower t_1 and higher t_2. The diminution of the first domain may come from a more homogenous heat repartition inside the suspension. The wider second domain means that water can be evaporated easily up to a further drying state. Upon fast drying of a PVOH solution a solid skin tends to be formed, obstructing the evaporation of solvent present underneath, as also observed in the case of conjugated polymer solutions (Breiby et al., 2003). This skin formation is responsible for blistering defects in industrial coating, resulting from water vapour piercing the skin in order to come out. The addition of MFC has been found to reduce this blistering phenomenon (Guezennec, 2012), which is in accordance with a wider second domain. Skin formation is responsible for a reduction of evaporation rate, i.e. occurs at the boundary between the second and third domains. Upon addition of MFC, this boundary is shifted towards further drying state, which is explained by MFC-hindering skin formation. It can be observed that the temperature profile during the PVOH:MFC experiment matches well the fitting of the evaporation rate: the boundary between the second and third domains correlates with faster increase of temperature. The evaporation rate is decreasing, meaning that the energy received is less and less used for evaporation and results in a faster increase of temperature. A water concentration gradient may exist, slowing down the overall drying, but could not be measured.

IV.4.2. Suspension coated on board

Similar experiments have been performed on boards coated with the same formulations as those used in the previous section. The bar coating has been performed in the same conditions for each experiment, but the amount deposited is not as reproducible as what was obtained by syringe deposition in the previous section. It can be noticed on Figure 52 that a 0.1 g difference could occur.

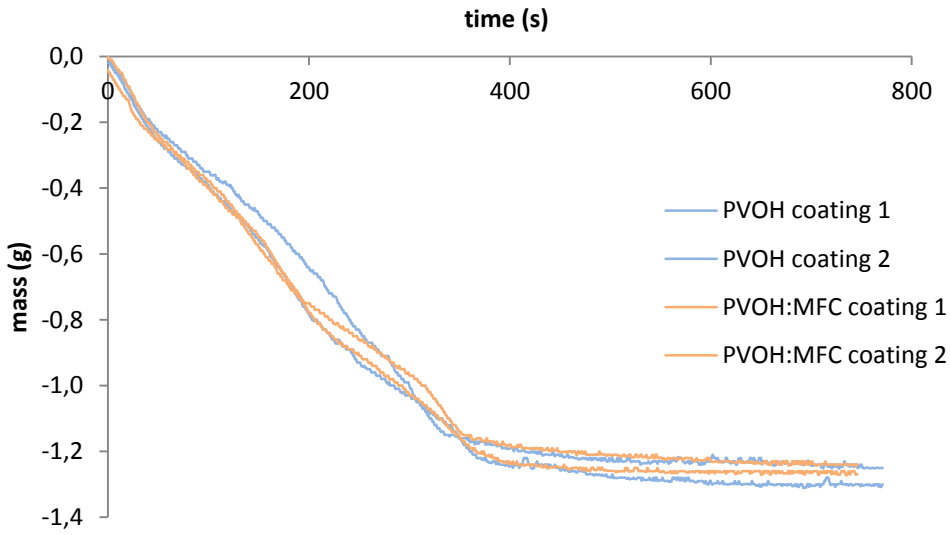

Figure 52 - Evolution of the loss of mass during drying for PVOH- or PVOH:MFC-coated boards.

It can also be noted that the curves are not as smooth as previously. This might be due to small deformations of the board or its fastening system to the frame that affect the mass measurement. Contrary to the previous section, the first parabolic domain corresponding to the heating of the suspension cannot be observed. This is explained by the much lower amount of suspension to dry: the target dry basis weight is 10 g/m² in the case of coating while it was 100 g/m² in the other experiments, corresponding to a wet thickness of about 53 and 530 µm, respectively. The heating of a 53 µm thick suspension layer is much faster than the heating of a 530 µm thick suspension layer. In addition, in the previous experiment the energy in domain ① has also been used to warm up the 260 g Teflon moulds, while in this case a lower amount of energy is required to warm up the 6 g boards. As a result, the first parabolic domain corresponding to the heating of the suspension has been neglected in this section. The curves have been fitted considering only two domains: the linear domain ② and the exponential domain ③, as shown in Figure 53. $(Eq.18)$ and $(Eq.19)$ can be applied, where m (g) is still the mass loss of suspension at time t (s), m_1 (= 0 g) becomes the initial mass loss at time t_1 (= 0 s), m_2 (g) is still the mass loss at time t_2 (s) corresponding to the boundary between the linear and exponential domains, m_3 (g) is still the final mass loss at the end of the experiment, and k is still the exponential coefficient. The condition of continuity of the derivative functions is still represented by $(Eq.23)$. As a result: m_1, t_1, and m_3 are determined experimentally, m_2 is determined as the experimental mass loss at time t_2, and k is determined from the continuity of the derivative functions in t_2. The only remaining variable is the boundary time t_2. This time t_2 has been determined in order to minimise the mean squared error between the experimental and the predicted data. It has to be noted that during the drying of the coated board, water present in the board is also evaporated. The board has a basis weight in ambient conditions of 264 ± 0.6 g/m² and a dry basis weight of 245.5 ± 0.8 determined using a thermo-balance. It results in 18.5 ± 0.9 g/m² of water, i.e. 0.42 ± 0.02 g in the 15x15 cm samples used for the drying experiment. Due to a mass loss of the board, the water content of the suspension could not be directly determined. In order to represent it at best in Figure 53, it has been considered that all evaporated water came from the suspension, thus over-estimating the dry amount of PVOH or PVOH:MFC. For example for the drying of a PVOH-coated board resulting in a final mass loss (m_3) of 1.26 g, the amount of dry PVOH deposited has been considered as:

$$m_{PVOH,dry} = 18\ wt\% \cdot \frac{1.26\ \text{g}}{(100-18)\ wt\%} = 0.28\ g_{dry} \quad (Eq.24)$$

while only 0.23 g_{dry} are theoretically deposited in order to obtain a layer of 10 g/m². The amount of water in the layer at time t is considered as the final mass loss of 1.26 g minus the mass loss at time t. The water content, being equal to the amount of water divided by the amount of dry PVOH deposited, is thus equal to 4.55 g/g at $t = 0$ and 0 g/g at final state, as it should be.

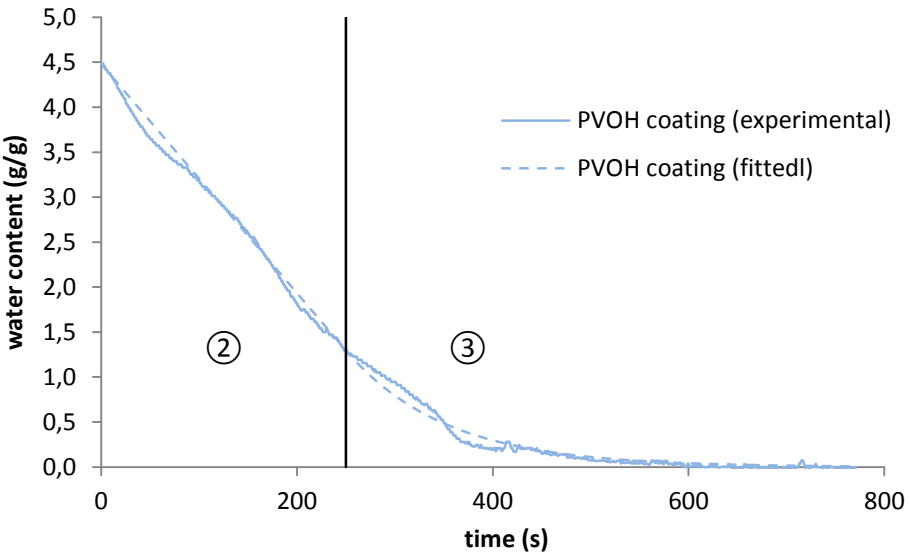

Figure 53 - Fitting of a drying curve of PVOH coated on board.
② and ③ indicate the linear and exponential domains, respectively.

The fitting of the curves was not as representative of the experimental data as in the case of syringe application in IV.4.1, page 132. In addition, the drying profiles for PVOH and PVOH:MFC coating were too similar to draw conclusions on the effect of MFC addition. The temperature profiles were also very similar, as shown in Figure 54.

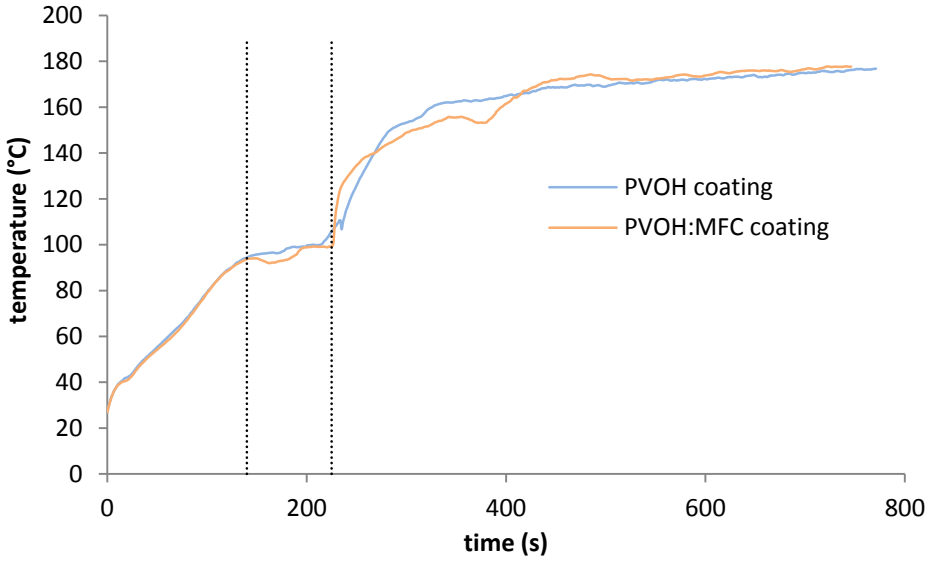

Figure 54 - Evolution of the temperature during drying of PVOH- and PVOH:MFC coated boards.
Vertical dotted lines evidence the boundaries of a domain of drying at almost constant temperature.

In particular, a domain of drying at constant temperature close to 100°C can be observed in both cases, and in the same range of time (between 140 and 225 seconds). This lack of effect upon addition of MFC may be ascribed to the lower thickness of suspension to dry. Considering that the main improvement due to the addition of MFC is avoiding or modifying the formation of a skin at the surface, using a thin suspension layer also avoids this effect due to the more homogeneous and faster drying. The effect of MFC on the drying rate of boards coated with a thin layer of suspension may only be significant upon faster and stronger drying, such as during the pilot scale blade coating performed by Guezennec (2012).

IV.4.3. Conclusion

An infrared drying bench has been used in order to study the drying kinetics of PVOH and PVOH:MFC suspensions in a Teflon mould or coated on board. The reproducibility of the heat flow generated by the infrared lamps during the experiments has been validated using a heat flow sensor. The drying of a thick layer of suspension in a Teflon mould allowed satisfying fitting of the drying curves considering three domains: a parabolic domain corresponding to the heating of the suspension, a linear domain of evaporation at constant temperature and drying rate, and an exponential domain corresponding to the suspension getting dry and water being harder to remove. The addition of MFC resulted in a wider domain of evaporation at constant drying rate, being especially efficient by delaying the time (and water content) at which the drying rate begins to decrease. The linear fitting has also been validated by the temperature profile. This effect corresponds well with an opposition to the formation of a dry skin at the surface of the suspension, obstructing the evaporation of water underneath. As a result, MFC-comprising suspensions dried faster than pristine PVOH solutions. This could not be observed when applying these formulations by coating on board, most probably due to the much thinner layer deposited resulting in a more homogeneous and faster drying. The influence of MFC on the drying kinetics of PVOH:MFC coatings on boards may be revealed using stronger drying conditions.

IV.5. Thermal and chemical treatment of PVOH and MFC films for water resistance

The objective of this part of the work is to improve the water resistance of PVOH and MFC films using crosslinking, with three different strategies: covalent bonding using citric acid (CA), hydrogen bonding using ammonium zirconium carbonate (AZC), and entrapping in an insoluble network using polyamidoamine epichlorohydrin (PAE). These strategies may involve a thermal treatment (curing) of the films that can modify their properties regardless of the addition of the corresponding chemicals. Therefore, the sole influence of the thermal treatment has been first investigated. After analysis of crosslinking by FTIR, the effect of the thermal and chemical treatment has been investigated in terms of water resistance by analysing the behaviour of the samples upon stirring in water, and in terms of water vapour permeability in humid conditions.

IV.5.1. Thermal treatment of PVOH and MFC films

Crosslinking of poly(vinyl alcohol) or cellulose with citric acid requires removal of water and an activation temperature around 150°C, while self-crosslinking of PAE requires a curing at 105°C. AZC, on the other hand, presents the advantage of not requiring such thermal treatment. Due to these differences, the effect of a thermal treatment in oven at 105°C or 150°C on PVOH and MFC cast films has first been investigated and compared with untreated samples. The duration of the treatment has been fixed to 10 minutes based on the literature (Olsson et al., 2013a; Siqueira, 2012).

IV.5.1.1. Water resistance

The water resistance of thermally-treated and untreated samples has been measured by magnetic stirring of a disc of known area in deionised water, as described in II.2.2.2, page 83. Untreated films are fragmented in a multitude of pieces in less than two minutes for PVOH, and 5 minutes for MFC. In this section the term "multitude" corresponds to more than 10 pieces from a 20 mm in diameter disc.

A thermal treatment of PVOH at 105°C or 150°C could not avoid fragmentation, but it was only fragmented into 5 to 6 pieces after 3 hours, while untreated PVOH was completely solubilised.

In the case of MFC, the fragmentation into a multitude of pieces was only delayed from 5 to 15 minutes. No significant differences between 105°C and 150°C were found in either case.

IV.5.1.2. Water vapour barrier

A much stronger effect is observed concerning the water vapour barrier in humid conditions, as reported in Table 24. The water vapour transmission normalised to a 65 g/m² film ($WVTR_{65}$) of PVOH has been reduced from 211 to 115 g/(m².d) after treatment at 105°C during 10 minutes, and to 56 g/(m².d) for a temperature of 150°C. This transmission rate of 56 g/(m².d) corresponds to a permeability of 241 g.µm/(m².d.hPa) for the PVOH film treated at 150°C. This is attributed to the fact that PVOH crystallinity increases upon curing, crystalline parts being considered impermeable to gases and improving the barrier. Increasing the curing temperature increases the crystallinity of PVOH (Peppas and Merrill, 1976), explaining the better barrier for samples treated at 150°C. In the

case of MFC films, a thermal treatment at 105°C during 10 minutes reduced the water vapour transmission rate from 1,140 g/(m².d) to 725 g/(m².d) while an increase of the temperature to 150°C did not lead to any further improvement. This is attributed to hornification, also reported by Bardet and co-workers (2015), which is an irreversible bonding between the fibres upon removal of water, resulting in a decreased inter-fibrillar space and increased hydrophobicity. This phenomenon is due to water removal rather than temperature itself, explaining the lack of difference between the barrier of MFC films treated at 105°C and 150°C.

	$WVTR_{65}$ 23°C 85%RH (g/(m².d))			
	PVOH		MFC	
Thermal treatment	Average	Stdev	Average	Stdev
-	211	13	1,139	92
10 min at 105°C	115	10	725	9
10 min at 150°C	56	4	816	14

Table 24 - Effect of a thermal treatment at 105°C or 150°C during 10 minutes on the water vapour transmission rate of PVOH and MFC films.

IV.5.2. Crosslinking of PVOH and MFC films

Citric acid (CA), ammonium zirconium carbonate (AZC), and polyamidoamine epichlorohydrin (PAE) have been used for the crosslinking of PVOH and MFC films, at a content of 5 wt%. After casting, for the crosslinking reaction to occur, CA-comprising films have been treated at 150°C and PAE-comprising films at 105°C during 10 minutes. The water resistance and water vapour barrier of the resulting films have been investigated, along with the crosslinking reaction by Fourier transform infrared spectroscopy (FTIR).

IV.5.2.1. Infrared spectroscopy

Fourier-transform infrared spectroscopy (FTIR) has been used in order to determine if crosslinking occurred. The spectra concerning citric acid are presented in Figure 55. Citric acid presents a doublet at 1,701 and 1,747 cm^{-1} corresponding to the C=O of its carboxyl groups. Upon addition of citric acid in PVOH or MFC and heating at 150°C during 10 minutes, a new peak appears at 1,713 cm^{-1} corresponding to the C=O of the ester bond formed between the carboxyl groups of citric acid and the alcohol groups of PVOH or MFC, indicating successful reaction. In the literature, this peak is found at 1724 cm^{-1} for CA-crosslinked PVOH (Shi and Yang, 2015) and 1730 cm^{-1} for CA-crosslinked MFC (Quellmalz and Mihranyan, 2015). The crosslinking of PVOH or MFC films by AZC or PAE could not be observed by FTIR, spectra can be found in appendix page 201. The observation of PAE self-crosslinking by FTIR is reported by the formation of a band at 1,260 cm^{-1} corresponding to the C-N stretching vibration of tertiary amine and C-O stretching vibrations of secondary alcohols, created by the azetidinium ring (AZR) opening and formation of 2-propanol bridges. In the presence of carboxymethyl cellulose (CMC), a C=O stretching vibration is observed at 1,742 cm^{-1} corresponding to the ester formation between the carboxyl groups of CMC and the hydroxyl end of PAE (Siqueira, 2012).

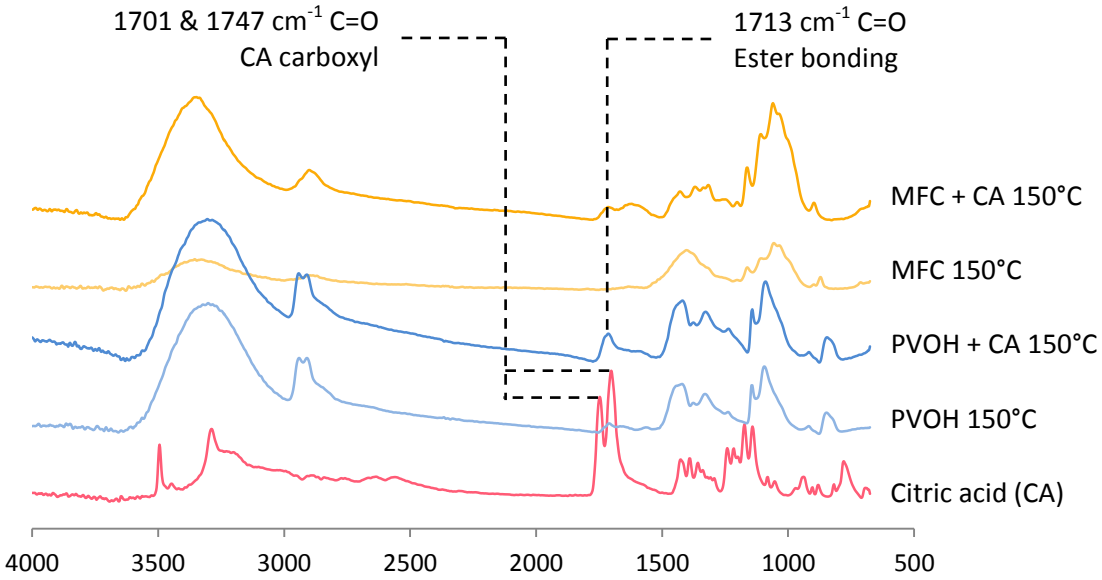

Figure 55 - FTIR spectra for citric acid (CA), PVOH or MFC treated at 150°C during 10 minutes, and PVOH or MFC + 5 pph CA treated at 150°C during 10 minutes. Ordinate represents the FTIR absorption.

IV.5.2.2. Water resistance

The use of AZC and PAE did not improve the water resistance of PVOH films. As shown in Table 25, the fragmentation is even faster than in the case of PAE compared to pristine PVOH with the same curing time and temperature.

	Number of pieces after t (hh:mm)								
Formulation	00:02	00:05	00:10	00:15	00:20	00:35	01:00	02:00	03:00
PVOH	>10	>10	>10	>10	>10	>10	>10	>10	>10
PVOH 105°C	1	2	3	3	3	5	5	5	5
PVOH 150°C	1	1	5	5	5	6	6	6	6
PVOH + AZC	8	>10	>10	>10	>10	>10	>10	>10	>10
PVOH + PAE 105°C	1	2	5	9	>10	>10	>10	>10	>10
PVOH + CA 150°C	1	1	1	1	1	1	1	1	1
MFC	1	2	4	>10	>10	>10	>10	>10	>10
MFC 105°C	1	1	8	>10	>10	>10	>10	>10	>10
MFC 150°C	1	3	5	8	>10	>10	>10	>10	>10
MFC + AZC	1	1	1	1	1	1	1	1	1
MFC + PAE 105°C	1	1	1	1	1	1	1	1	1
MFC + CA 150°C	1	1	1	1	1	1	1	1	1

Table 25 - Evolution of the number of sample pieces present under stirring in deionised water during the water resistance test.

The inefficiency of PAE crosslinking may come from the lack of carboxyl groups of PVOH. Upon heating, PAE crosslinking occurs mainly by formation of 2-propanol bridges from two azetidinium rings (AZR), but also by ester bond formation between the hydroxyl groups present on the AZR and PAE carboxyl end (Siqueira, 2012). Ester bonding can also occur in presence of carboxyl-bearing polymers, thus binding the polymer to the insoluble PAE network. This PAE-polymer bonding has been found of importance for paper wet resistance (Obokata and Isogai, 2007), and may be lacking for obtaining an improvement in PVOH water resistance. The inefficiency of AZC for PVOH water resistance has not been explained yet. However, the use of citric acid resulted in films that could stay intact under stirring in water during three hours, confirming a successful water resistance improvement by citric acid crosslinking.

In the case of MFC, the three crosslinking routes have been found effective for water resistance improvement. In any case the samples could stay intact under stirring in water during three hours, but differences were found in terms of water adsorption and mass loss as shown in Table 26. The mass loss during the test is as low as 3% and 6% using PAE and citric acid as crosslinking agent, respectively. It shows that not only the sample remains in one piece, but also the fibrils at the surface of the sample tend to remain bound to the film and not be progressively dispersed as suspended particles in water. This is attributed to the effectiveness of covalent bonding: the binding of microfibrils to the insoluble PAE network due to esterification of PAE hydroxyl groups with carboxyl groups of the hemicellulose in the MFC, and bridges between microfibrils by reaction of at least two carboxyl groups of citric acid with cellulose hydroxyl groups. AZC leads to a much higher mass loss of 17%. It only acts as crosslinking agent through hydrogen bonding that can be cleaved by water. This may make it easier for microfibrils at the surface of the samples to exit from the network and get dispersed in water. It also makes it easier for water to be adsorbed in the film as evidenced by the water sorption of 133%, compared to 85% for PAE and 53% for citric acid. The lower water absorption with the use of citric acid compared to PAE is attributed to the small size of citric acid leading to a tighter network. It has to be noted that the thermal treatment may also influence the results, especially concerning the higher water absorption in the case of AZC that could also be attributed to the lack of hornification.

	Water absorption (%)		Mass loss (%)	
	Average	Stdev	Average	Stdev
MFC + AZC	133%	18%	17%	7%
MFC + PAE 105°C	85%	0%	3%	4%
MFC + CA 150°C	53%	1%	6%	2%

Table 26 - Water absorption and mass loss for crosslinked MFC films after a water resistance test.

IV.5.2.3. Water vapour barrier

The use of a crosslinking agent had no influence on the water vapour barrier of PVOH films, even in the case of citric acid that has been found to successfully improve the water resistance, as shown in Figure 56. A significant improvement has only been found in the case of citric acid-crosslinked MFC films, with a $WVTR_{65}$ reduced from 818 to 585 g/(m².d). It can be expected that citric

acid crosslinking allows a reduction of available cellulose hydroxyl groups thus reducing its hydrophilicity, similarly to what was observed concerning the water absorption, and a reduction of chain mobility. As a result, plasticisation by water vapour may be reduced, leading to an improved barrier.

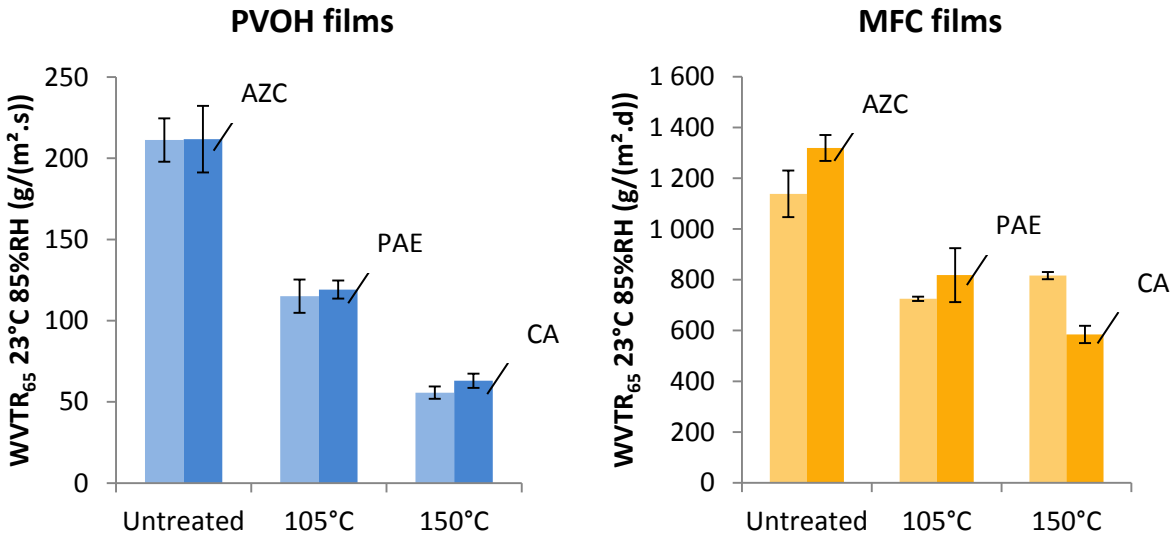

Figure 56 - Water vapour transmission ($WVTR_{65}$) for untreated and cured PVOH and MFC films, with and without the corresponding crosslinking agent. In light blue or yellow: pristine PVOH or MFC. In dark blue or yellow: PVOH or MFC with crosslinking agent.

IV.5.3. Conclusion

A thermal and chemical treatment has been applied to PVOH and MFC cast films using three different strategies. A thermal treatment alone, at 105°C or 150°C during 10 minutes, could not avoid the fragmentation of PVOH or MFC films upon stirring in water. However, the water vapour transmission of PVOH films in humid conditions could almost be reduced by a factor 4, attributed to an increased crystallinity. The water vapour barrier of MFC films was also improved, by a lower factor, attributed to hornification. FTIR analysis evidenced the formation of ester bond and thus crosslinking of PVOH or MFC by citric acid, but the effect of AZC and PAE could not be observed. This crosslinking of PVOH resulted in water-resistant films that could be stirred in water during 3 hours while remaining in one piece, but the use of AZC or PAE did not have a significant effect. In the case of MFC, all three strategies resulted in water-resistant films. The efficiency of PAE on MFC but not on PVOH may be attributed to the formation of covalent bonds between an insoluble PAE network and MFC through the carboxyl groups of hemicelluloses, whereas PVOH do not bear carboxyl groups. The use of AZC led to higher mass loss and water absorption for MFC films, which is attributed to the hydrogen bonding strategy. AZC-polymer bonds can more easily be replaced by water-polymer interactions than the covalent bonding with PAE or CA. Few effects were observed in terms of water vapour barrier.

IV.6. Conclusion

In order to develop new barrier using microfibrillated cellulose, this chapter aimed at selecting the most relevant MFC and PVOH grades for the development of MFC-comprising water-based barrier coating, at getting a better understanding of the PVOH layer formation improvement given upon addition of MFC, and at improving the behaviour of PVOH and MFC films upon exposure to water or water vapour using different crosslinking strategies.

PVOH:MFC were reported as promising blends, but mostly for mechanical properties and, to our knowledge, the role of MFC fibrillation has not been investigated. In addition, the majority of the publications dealing with PVOH:MFC composites focused on MFC, while PVOH also have different properties depending on its degree of hydrolysis and degree of polymerisation. The first, second, and third sections of this chapter were dedicated to the formulation of a PVOH:MFC composite having the best barrier while having the lowest viscosity at given solid content. Composite films have been produced by a coating-peeling process mimicking a blade coating process. Compared to the usual solvent casting method the use of suspensions with higher solid contents, required to match industrial board coating specifications, brought several issues: viscosity, foaming, and dispersion state of the MFC. Every film produced was high barrier to oxygen, with an oxygen transmission rate below the detection of the apparatus. The following barrier comparisons are thus mostly based on water vapour barrier measurements. Similarly to the 100% films described in Chapter III, a high degree of fibrillation was required in order to produce PVOH:MFC barrier layers. The use of MFC UM with a high amount of residual macro-fibres led to films having lower density, mechanical resistance, and water vapour barrier. In such formulations, MFC should not be added in more than 5 pph due to its high viscosity. The progressive addition of MFC forced to dilute the suspensions, which has a negative impact on the coating process due to higher drying energy requirement and possible wetting of the base. In addition, at 20 pph macroscopic MFC aggregates appeared. In the meantime, MFC only bring a mechanical reinforcement at MFC content superior to 5 pph, but at this MFC content the water vapour barrier is degraded. Concerning PVOH, a high degree of hydrolysis is required in order to obtain the best water vapour barrier. A low degree of polymerisation was preferred in order to reduce the viscosity of the coating colours, knowing that using a PVOH having a higher degree of polymerisation can slightly improve the mechanical resistance and water vapour barrier. As a result, the addition of MFC having a high degree of fibrillation (here MFC KB) at 2 or 5 pph in a fully-hydrolysed PVOH 6-98 having the lowest degree of polymerisation required for food contact approval, has been determined the most relevant PVOH:MFC formulation for water-based barrier coating application.

The addition of MFC in water-based coating formulations is reported to improve its layer formation, especially due to a reduction of drying-induced defects. In order to better understand this improvement, the drying kinetics of PVOH and PVOH:MFC formulations have been investigated, as a thick layer in a Teflon mould and as a thin layer coated on board. The drying of suspensions in a Teflon mould evidenced a wider domain of evaporation at constant drying rate upon addition of MFC, which resulted in a faster drying. It is expected to come from a more homogeneous heat repartition and hindering of skin formation. No effect could be observed in the case of board coating, which may be related to the much lower thickness of wet film to dry. The drying of the thin coated layer is faster and more homogeneous, no skin formation was observed with or without MFC. However, industrial coating would result in a stronger and faster drying, in which case MFC were reported to have a positive impact.

Both PVOH and MFC lack water resistance: in contact with water, PVOH is solubilised and MFC is dispersed. Crosslinking is a way to improve the properties of such hydrophilic polymers upon exposure to water or water vapour, but few study investigate both the efficiency on PVOH and on MFC. With application to PVOH:MFC composite, this chapter investigated three crosslinking strategies both on PVOH and on MFC, with the perspective of applying to PVOH:MFC composites a crosslinking strategy that is efficient in for the two components. The three crosslinking strategies are: covalent bonding with citric acid, hydrogen bonding with AZC, and formation of an insoluble network using PAE. The curing of PVOH and MFC, required for citric acid and PAE crosslinking, reduced the water vapour transmission of the films. It was attributed to an increase of PVOH crystallinity and to MFC hornification. The sole curing step was not sufficient to improve significantly the water resistance of PVOH and MFC films. Covalent bonding using citric acid was efficient for PVOH and MFC water resistance improvement, as evidenced by the films remaining intact after stirring in water during three hours. In this case, the crosslinking reaction could be observed by FTIR. AZC seemed less efficient: PVOH was not as resistant in water and MFC films had higher water absorption. PAE could not improve the water resistance of PVOH, which is expected to come from its lack of carboxyl groups. However, PAE-crosslinked MFC films could remain intact under stirring in water during three hours. Among the three crosslinking strategies investigated, covalent bonding with citric acid appeared the most adapted to improve the behaviour of PVOH and MFC films upon exposure to water. However, films were visually more brittle, which can impact the converting ability of PVOH-, MFC-, and probably PVOH:MFC-coated boards.

To conclude, this chapter was focused on the formulation of PVOH:MFC coating colours for the production of barrier self-standing films. It evidenced the necessity of using highly-fibrillated MFC and a fully-hydrolysed PVOH while showing a preferential MFC ratio of 2 pph, allowing reducing the water vapour transmission while keeping a low oxygen transmission below the detection threshold of the apparatus. The use of PVOH with a low degree of polymerisation has been chosen in order to be able to use more concentrated formulations, knowing that a better elongation and water vapour barrier can be obtained using PVOH with a higher degree of polymerisation. MFC was also found to improve the drying behaviour of PVOH solutions, the observations being in accordance with MFC hindering PVOH skin formation. Finally, among the three crosslinking routes tested, the covalent bonding strategy using citric acid was capable of greatly improving the water resistance of MFC and PVOH films, while a curing step allowed reducing the water vapour permeability in humid conditions. The PVOH:MFC composites developed in this chapter remained sensitive to humidity. The next chapter is dedicated to another strategy for improving the behaviour of PVOH:MFC composites upon exposure to water vapour, based on the addition of well-dispersed clay platelets.

Chapter V: Dispersion of Layered Silicates in PVOH:MFC Composites

Chapter V: Dispersion of Layered Silicates in PVOH:MFC Composites

The objective of this thesis is to develop the use of microfibrillated cellulose in barrier layers deposited on paper or board. Chapter IV focused on using MFC as filler in PVOH for the improvement of PVOH layer formation, with application to water-based barrier coating. After improvement of the properties of the layers by the use of highly fibrillated MFC in a fully-hydrolysed PVOH having a low degree of polymerisation, or by crosslinking with citric acid, the water vapour transmission in humid conditions remained high. Another strategy for the improvement of the barrier properties of such formulations is the addition of layered silicates, or clays, platy pigments that can increase the diffusive pathway of gas molecules and thus reduce permeability (Grunlan et al., 2004; Liu et al., 2014; Slavutsky et al., 2012). While the addition of clays in PVOH or MFC for mechanical improvement is largely reported, its effect on the barrier properties is more occasionally mentioned, and only few publications deal with three components PVOH:MFC:clay formulations. There is a need to better understand the combined impact of these two fillers, along with their behaviour in concentrated suspension as required for water-based coating.

This chapter aims at obtaining well-dispersed clays in PVOH:MFC composites and at getting a better understanding on the influence of a MFC:clay combination in PVOH, in terms of barrier and dispersion. This chapter also aims at using such formulations in conditions close to industrial coating by the use of concentrated suspensions and laboratory board coating.

Similarly to the studies performed on PVOH and MFC, the first section is dedicated to the comparison of different grades of clays, in order to select the most relevant for the following of the study. The second section is dedicated to the dispersion of clays in diluted PVOH solutions comprising MFC, in order to study the influence of both MFC and clay contents on the final properties composites produced by solvent casting. The third section is dedicated to the dispersion of clays in concentrated PVOH solutions comprising MFC, using the most promising MFC and clay contents evidenced in the previous section, in order to study the influence of the upscaling from cast films to coated boards and demonstrate the opportunity of using such formulations as barrier layers on board.

V.1. Influence of the layered silicate grade

In this first section, four layered silicate grades (clays) have been compared as fillers in a PVOH 6-98 matrix, with or without MFC KB. After evidencing the morphological differences between the layered silicate grades, their dispersion in PVOH:MFC suspensions has been investigated depending on the PVOH:MFC:clay suspension production process. The resulting films have been characterised in terms of water vapour transmission in humid conditions.

V.1.1. Visual appearance and main characteristics

Layered silicates are found under the form of a hygroscopic powder and are easily dispersible in water, as can be seen in Figure 57. In aqueous medium their dispersion state progressively increases due to the adsorption of water molecules, which is why they are also called swelling clays.

Figure 57 - Pictures of layered silicate powders (top) and suspensions (bottom).
From left to right: Cloisite-Na (C), Nanofil 116 (N), Laponite (L), and Kaolinite (K).

Layered silicates mainly differ in terms of chemical composition, crystalline structure, morphology, and Cationic Exchange Capacity (CEC). The first part of this chapter focuses on choosing he best suited layered silicate for our application by comparing four selected grades: Cloisite-Na (C) and Nanofil 116 (N) (two grades of montmorillonite), Laponite (L), and Kaolinite (K) which properties are reported in Table 27.

Layered silicate		Thickness	Diameter	CEC	Density
Type	Name	(nm)	(nm)	(m_{eq}/100g)	(g/cm^3)
Bentonite	Cloisite-Na	1	300 - 1,000	93	–
	Nanofil 116	1	100 - 500	116	–
Laponite	Laponite RD	1	25	95	2.57
Kaolinite	Barrisurf HX	20	15,000 - 20,000	2.5	–

Table 27 - Source and properties of the layered silicates.

V.1.2. Undesired formation of PVOH:clay hydrogels by physical cross-linking

The first introduction of layered silicate in a PVOH:MFC formulation has been made by addition of clay powder in a PVOH solution comprising microfibrillated cellulose. MFC has been diluted, PVOH pellets added to the diluted MFC suspension, PVOH solubilisation took place during one hour at 95 °C, and layered silicate powder has been added. The final formulation comprises 100 pph PVOH, 5 pph MFC, and 5 pph Clay, with a solid content of 5 wt%. This procedure led to large clay aggregates as can be seen in Figure 58, with a surface-weighted average diameter of 62 µm. Stirring of the layered silicates in water overnight allowed them to disperse and swell before their introduction in the PVOH:MFC suspension, this type of preparation corresponding to what is described as solvent intercalation by Chivrac and co-workers (2009). It led to the successful elimination of the powder aggregates but also the apparition of a new type of PVOH:clay aggregates, observed whether MFC were present or not. These PVOH:clay aggregates were attributed to the formation of hydrogels by physical cross-linking of PVOH molecules by the clay particles as reported by Schnexnailder and Schmidt (2009) in the case of poly(ethylene oxide) with laponite. They could be eliminated by a continuous stirring of the PVOH:MFC:clay suspension during 4 hours at 95°C after the addition of the layered silicates, as shown in Figure 58.

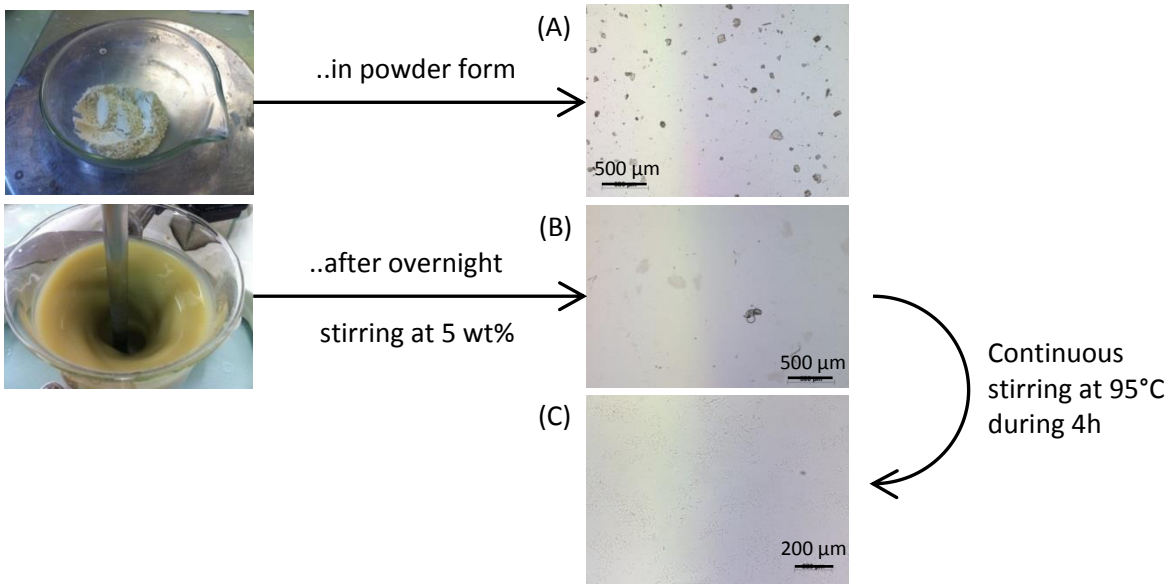

Figure 58 - Elimination of clay aggregates (A) by swelling in water before introduction in a PVOH:MFC suspension (B), and of PVOH:clay aggregates (B) by continuous stirring at 95°C during 4h (C).

The impact of clay or PVOH:clay aggregates can be observed on self-standing films obtained by casting from the corresponding formulations as presented in Figure 59. All samples have a basis weight of 65 ± 8 g/m² and a thickness of 59 ± 8 µm. As evidenced in Figure 58 for the suspensions, the addition of clay in powder (P) and in suspension without 4h at 95°C (S) led to macroscopic aggregates that could also be observed in the self-standing films and seemed to increase the

roughness of the samples. With an adapted process, composite films comprising clays with a good dispersion at macroscopic scale could be obtained.

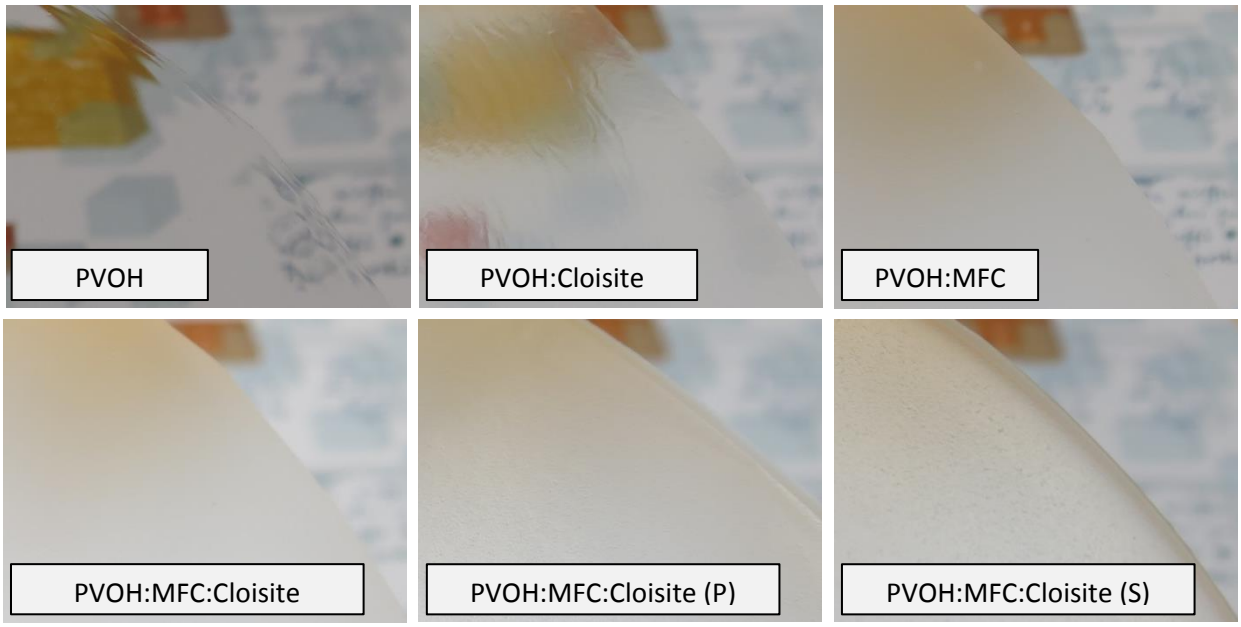

Figure 59 - PVOH, PVOH:Cloisite, and PVOH:MFC films presenting no sign of aggregation, compared to PVOH:Cloisite presenting aggregation and PVOH:MFC. (P) and (S) have Cloisite-Na and PVOH:Cloisite aggregates and are produced from the suspension observed in Figure 58 (A) and (B), respectively. Pictures width: 4 cm.

V.1.3. Effect of the clay grade on the water vapour barrier

Layered silicates have been used in order to improve the behaviour of PVOH:MFC composites in humid conditions. The Water Vapour Transmission Rate at 23°C 85%RH of the different composites are presented in Figure 60, normalised to a film of 65 g/m² for comparison ($WVTR_{65}$). The addition of 5 pph MFC KB in PVOH had no impact, and the further addition of clay increased or decreased the transmission depending on the grade used.

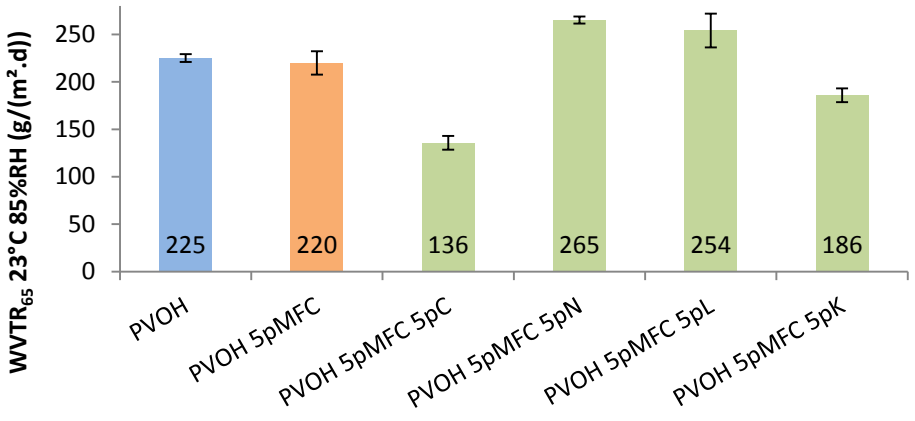

Figure 60 - Water Vapour Transmission Rate ($WVTR_{65}$) for PVOH:MFC:clay films at 23°C 85%RH.

A model for the permeability of polymer-layered silicate nano-composites is described by Bharadwaj (2001). The relative permeability of the composite is linked to the volume fraction, length, width, and angle of the particle with respect to the diffusion axis - 0° being perpendicular to the diffusion axis and 90° being parallel to the diffusion axis:

$$\frac{P_s}{P_p} = \frac{1 - \Phi_s}{1 + \frac{L}{2W} \cdot \Phi_s \cdot \frac{2}{3} \cdot (S + \frac{1}{2})} \quad (Eq. 25)$$

where P_s is the permeability of the composite, P_p the permeability of the neat matrix, Φ_s the volume fraction of layered silicate (2.1% to 2.4% PVOH + 5 pph MFC + 5 pph clay depending on clay density), L the Length (diameter) of the sheet (nm), W the width (thickness) of the sheet (nm), and S the order parameter calculated from platelets orientation θ (°) using the following equation:

$$S = \frac{1}{2}\langle 3cos^2\theta - 1\rangle \quad (Eq. 26)$$

S = 1 if the orientation of the layered silicate is perpendicular to the diffusion axis. $(Eq. 25)$ becomes:

$$\frac{P_s}{P_p} = \frac{1 - \Phi_s}{1 + \frac{L}{2W} \cdot \Phi_s} \quad (Eq. 27)$$

Using $(Eq. 27)$, the theoretical relative permeability of the PVOH:MFC:clay composites considering an orientation perpendicular to the diffu&sion axis (S = 1) is reported in Table 28 and compared to the actual relative permeability calculated from the experimental data. The experimental data are higher than the theoretical data which is expected to come from the fact that the particles in suspension are not necessarily individualized. Layered silicates should most probably be organised in stacks, reducing their overall efficiency. The clay particles may also be responsible for the formation of defects in the PVOH matrix that can have a negative impact on its permeability. However, the general trend of Cloisite-Na and Kaolinite being more efficient for the reduction of the permeability is respected, and can thus be attributed to the morphology of the particles (L / W ratio). The efficiency of the filler for an increase in diffusive pathway of gas molecules is reduced as the diameter of the particles decreases: for the same thickness of 1 nm the efficiency of the clays is given in the following order: Cloisite-Na > Nanofil-116 > Laponite. Kaolinite has a much larger diameter and thickness resulting in a L / W ratio of the same order of magnitude compared to Cloisite-Na leading to a similar theoretical relative permeability.

Layered silicate	Length (nm)	Width (nm)	Φ_s (%)	S = 1 Relative Permeability (%)	Experimental Relative Permeability (%)
Cloisite-Na	1,000	1	2.1%	8%	62%
Nanofil-116	300	1	2.1%	22%	121%
Laponite	25	1	2.4%	74%	116%
Kaolinite	17,500	20	2.3%	9%	85%

Table 28 - Theoretical and experimental relative permeability for the PVOH:MFC:clay composites.

The addition of Cloisite-Na in PVOH:MFC composite led to a significant improvement in water vapour barrier and it was thus selected for further testing.

V.1.4. Conclusion

In this section, the process for the production of composite suspensions has been adapted in order to disperse layered silicates correctly in PVOH:MFC suspensions. It includes a first swelling step by stirring clays in water overnight before their introduction in PVOH:MFC suspensions, in order to avoid the formation of clay aggregates as observed by addition of clays in powder forms. It also includes a step of continuous stirring of the PVOH:MFC:clay suspension during 4 hours after addition of clays in the PVOH:MFC suspension, in order to avoid the formation of PVOH:clay aggregates. Four layered silicate grade have been compared in terms of water vapour barrier at 23°C 85%RH. Cloisite-Na was the most effective grade for a reduction of water vapour transmission, which can be partially explained by its high diameter over thickness ratio. The experimental transmission rates obtained were higher than what would theoretically be reached according to a model by Bharadwaj (2001), which is attributed to the presence of clay stacks and possible formation of defects in the films.

V.2. Dispersion of Cloisite-Na and MFC in PVOH self-standing films for water vapour barrier improvement

This second section focuses on the use of Cloisite-Na in PVOH:MFC composites, using this time MFC 5P instead of MFC KB. There is a specific interest in the characterisation of the dispersion of Cloisite-Na and MFC in suspension and as self-standing films, but also on the synergistic dispersion effect of both fillers. The resulting films have been characterised in terms of water vapour transmission in humid conditions, differential scanning calorimetry (DSC) in order to determine the transition temperatures and crystallinity of PVOH, and dynamic vapour sorption (DVS) in order to determine the water vapour sorption and diffusion in the composite films between 0%RH and 95%RH.

V.2.1. Cloisite-Na dispersion obtained by X-Ray Diffraction

The dispersion state of layered silicates can be characterised through their inter-layer spacing (d_{001}), i.e. the distance between two platelets. An increase in d_{001} upon mixing with a polymer is characteristic of the intercalation of polymer chains in the clay galleries, which is a positive indication of dispersion. On the contrary, a steady d_{001} indicates that the polymer does not penetrate the clay galleries and that the layered silicate stacks remain isolated.

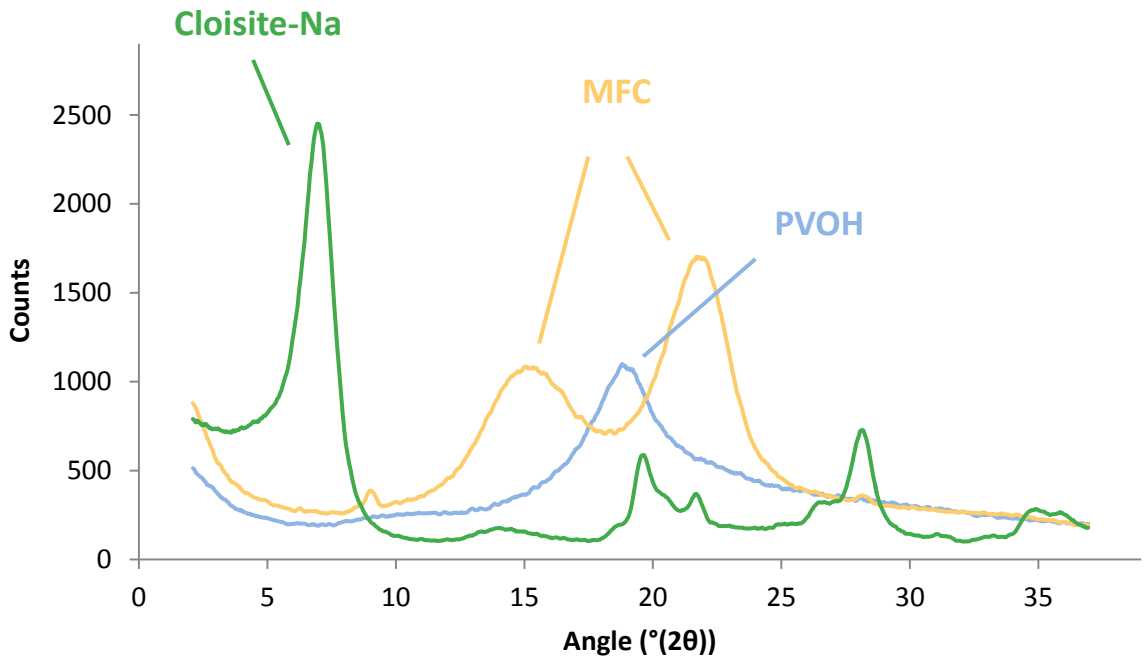

Figure 61 - XRD spectra for PVOH (cast film), MFC (cast film), and Cloisite-Na (powder).

The inter-layer spacing can be determined using X-ray diffraction (XRD). The spectra for PVOH, MFC, and Cloisite-Na are presented in Figure 61. The peaks at 15.02°(2θ) and 21.98°(2θ) for MFC and at 18.82°(2θ) for PVOH are representative of their crystallinity. Concerning Cloisite-Na, the

peak at 6.94°(2θ) is representative of the inter-layer spacing that can be calculated using Bragg's law ($Eq. 15$), page 88. A d_{001} value of 12.7 Å was obtained in the case of Cloisite-Na powder, which is consistent with the values reported in the literature: 11.6 Å according to Spoljaric and co-workers (2014) and 11.7 Å according to the manufacturer.

The progressive introduction of PVOH in the Cloisite-Na dispersion is reported to lead to an increase of d_{001} in the resulting films (Clegg et al., 2014). The composites had an intercalated structure that is demonstrated in the XRD spectra by a shift of the d_{001} peak towards lower angles. In our case there is no clear d_{001} peak anymore but instead a sloping baseline at low angles, as can be observed in Figure 62. The inter-layer spacing is not clearly identifiable because the layered silicates are highly disordered and possibly exfoliated, as also observed by Strawhecker and Manias (2000) in the case of PVOH:monmorillonite composites with a montmorillonite volumic fraction of up to 20%. This is the sign of a good Cloisite-Na dispersion that predicts an improved barrier compared to an intercalated or a micro-composite state. A d_{001} peak, if any, would be present at angles below 2°(2θ) thus corresponding to a d_{001} value higher than 44 Å. The intensity of the sloping baseline increases with the amount of clay, which is attributed to the presence of a higher amount of dispersed particles able to interact with the X-ray. Keeping the Cloisite-Na amount at 10 pph, the introduction of MFC up to 10 pph leads to an increase in the intensity of the sloping baseline as evidenced in Figure 62, which suggests that the layered silicate disorder continues to increase. It can be noted that, while there is a significant difference between 2 pph and 5 pph MFC in terms of sloping baseline intensity, increasing the MFC content to 10 pph does not seem to bring any further improvement.

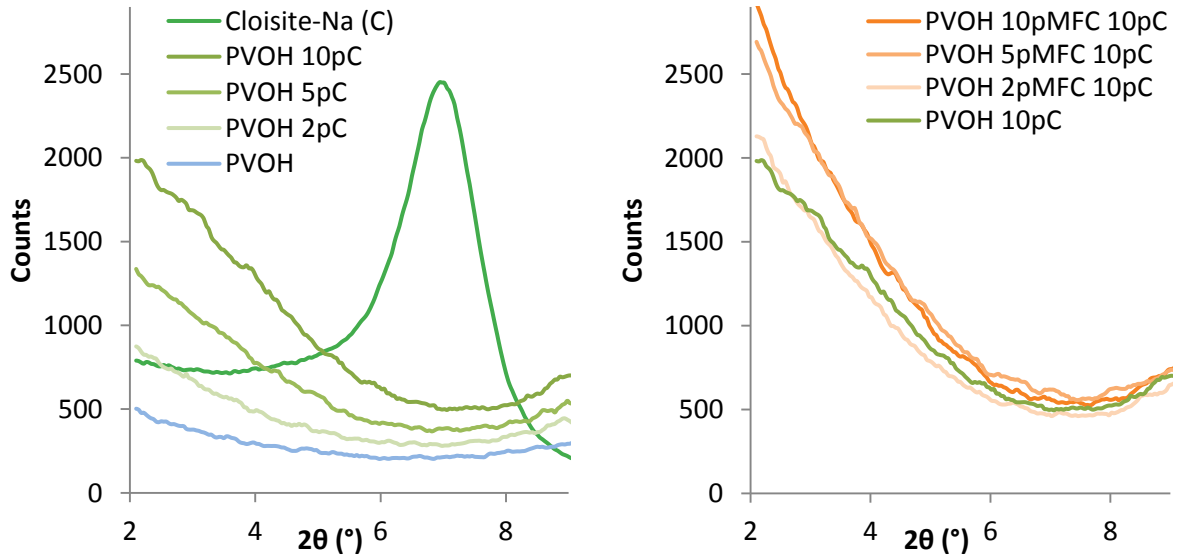

Figure 62 - XRD spectra for Cloisite-Na powder and PVOH:Cloisite composite films with an increasing amount of Cloisite-Na (left) and PVOH:MFC:Cloisite composite films at 10 pph Cloisite-Na and with an increasing amount of MFC (right).

V.2.2. Positive effect of Cloisite-Na on the MFC dispersion in PVOH evidenced by SEM

The dispersion of the fillers in the PVOH matrix has also been studied by SEM. Figure 63 shows the surface of composite films. The good dispersion of Cloisite-Na can be observed, with a surface seemingly as smooth as the one for the neat matrix. The SEM pictures show the flocculation of MFC when solely added into the PVOH matrix, but also that the further addition of Cloisite-Na reduces this flocculation phenomenon as evidenced by the smooth SEM surface of the PVOH:MFC:Cloisite composite. In addition to the improvement of the Cloisite-Na dispersion in PVOH by introduction of MFC suggested by the XRD analysis, SEM analysis evidences that the dispersion of MFC in PVOH is improved by the introduction of Cloisite-Na. To our knowledge, this is the first time that an improvement of MFC dispersion in PVOH by addition of Cloisite-Na is reported.

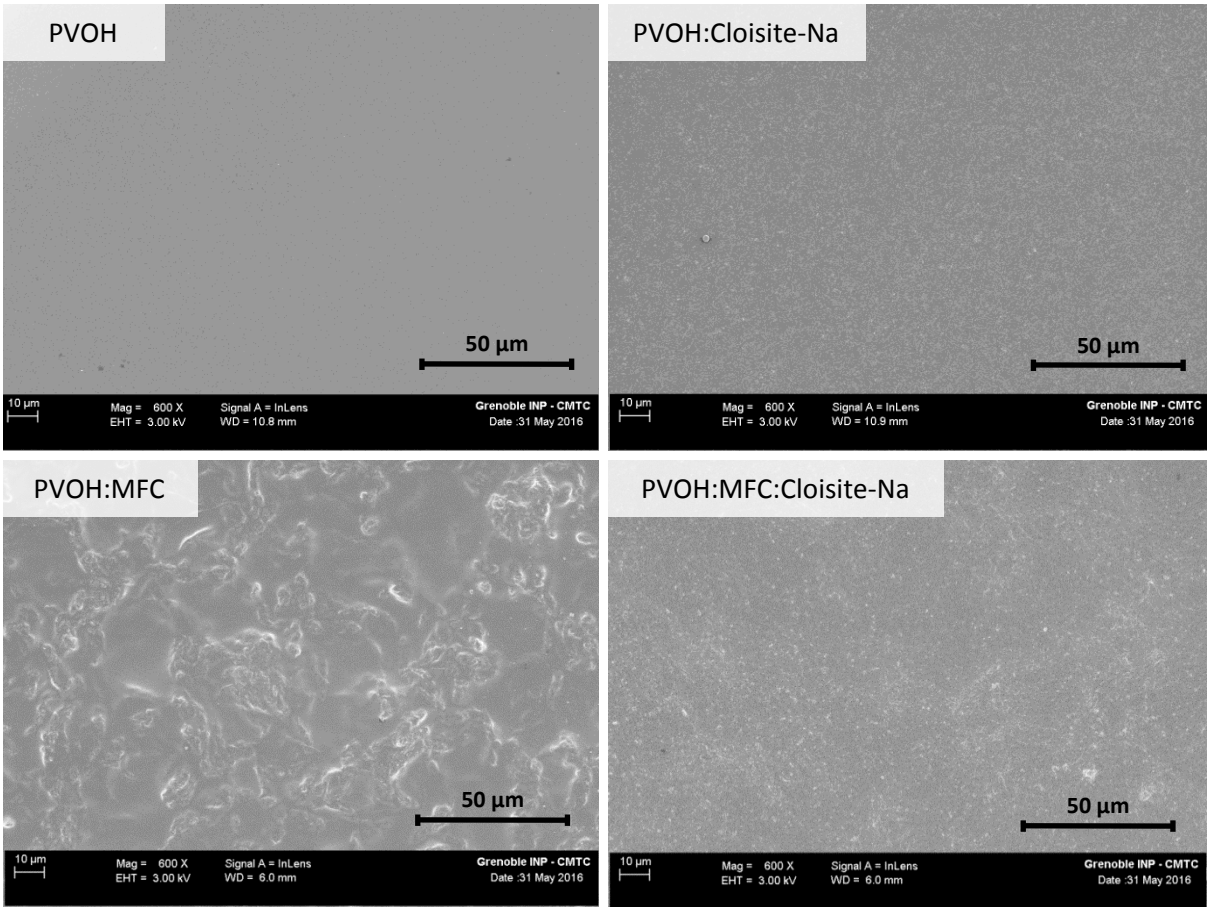

Figure 63 - SEM analysis of the surface of PVOH, PVOH:Cloisite, PVOH:MFC, and PVOH:MFC:Cloisite films. MFC content: 5 pph, Cloisite-Na content: 10 pph.

V.2.3. Use of SEM with Back-Scattered Electron for the assessment of Cloisite-Na sedimentation during casting

The use of Back-Scattered Electron (BSE) in a SEM allows the characterization of the chemical composition of the sample by acquisition of the average atomic number across each area of sample scanned. Whiter areas correspond to areas of higher average atomic number, that in our case are

representative of the Cloisite-Na. The pictures of the top and bottom surfaces of PVOH:Cloisite and PVOH:MFC:Cloisite composites are presented in Figure 64.

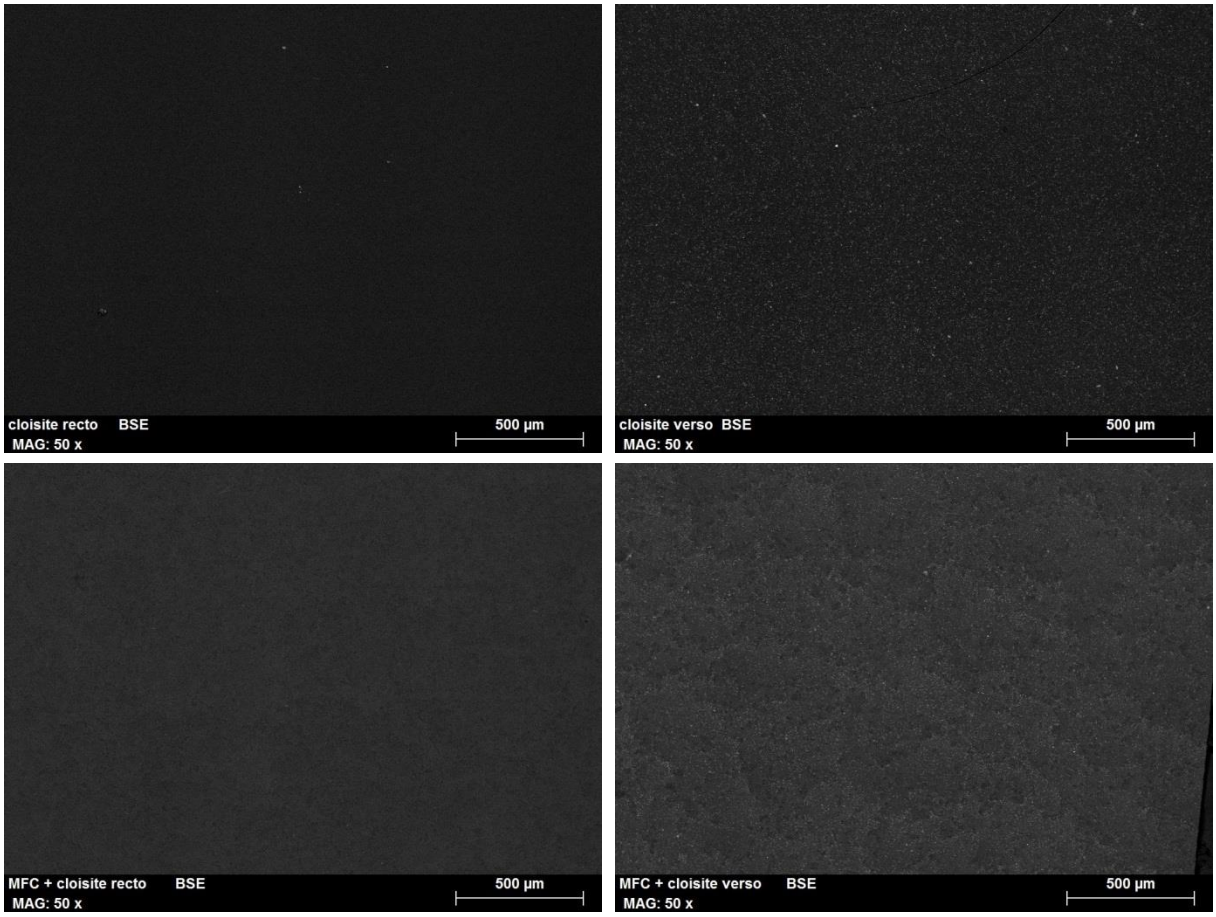

Figure 64 - SEM-BSE pictures of the top and bottom surfaces of PVOH:Cloisite and PVOH:MFC:Cloisite composite films.

In both cases the proportion of white dots corresponding to Cloisite-Na was higher on the bottom surface, which is a sign of sedimentation that could have occurred during casting of the composites. This proportion of Cloisite-Na has been qualitatively determined by the ratio of the intensity of the silicon (Si) peak corresponding to Cloisite-Na divided by the intensity of the carbon (C) peak. The peak ratios (Si/C) for the top surfaces of PVOH:Cloisite-Na and PVOH:MFC:Cloisite-Na were 11% and 8% respectively while the peak ratios for the bottom surfaces were 18% and 17%. The higher proportion of silicon element at the bottom of the films evidenced a slight sedimentation. According to the SEM-BSE pictures, the repartition of Cloisite-Na appeared more homogeneous in the PVOH:MFC:Cloisite composite compared to the PVOH:Cloisite composite where the elements corresponding to the layered silicate are concentrated in small white dots.

V.2.4. Effect of MFC and Cloisite-Na on the water vapour barrier of the self-standing films

The water vapour transmission of the samples has been tested at 23°C 50%RH and 23°C 85%RH. At 50%RH, no significant effect of either MFC or Cloisite-Na could be observed due to the high deviations of the measurements. At 85%RH, Figure 65 shows that the progressive introduction of Cloisite-Na leads to an improvement of $WVTR_{65}$ from 190 g/(m².d) in the case of PVOH to 119 g/(m².d) with addition of 10 pph Cloisite-Na, corresponding to a reduction by 37% and permeability of 351 g.µm/(m².d.hPa). This behaviour is different from the observations by Strawhecker and Manias (2000) that obtained a 60% WVP reduction upon addition of 2 wt% of Cloisite-Na in PVOH, but no further reduction by increasing the Cloisite-Na content to 4 or 6 wt%.

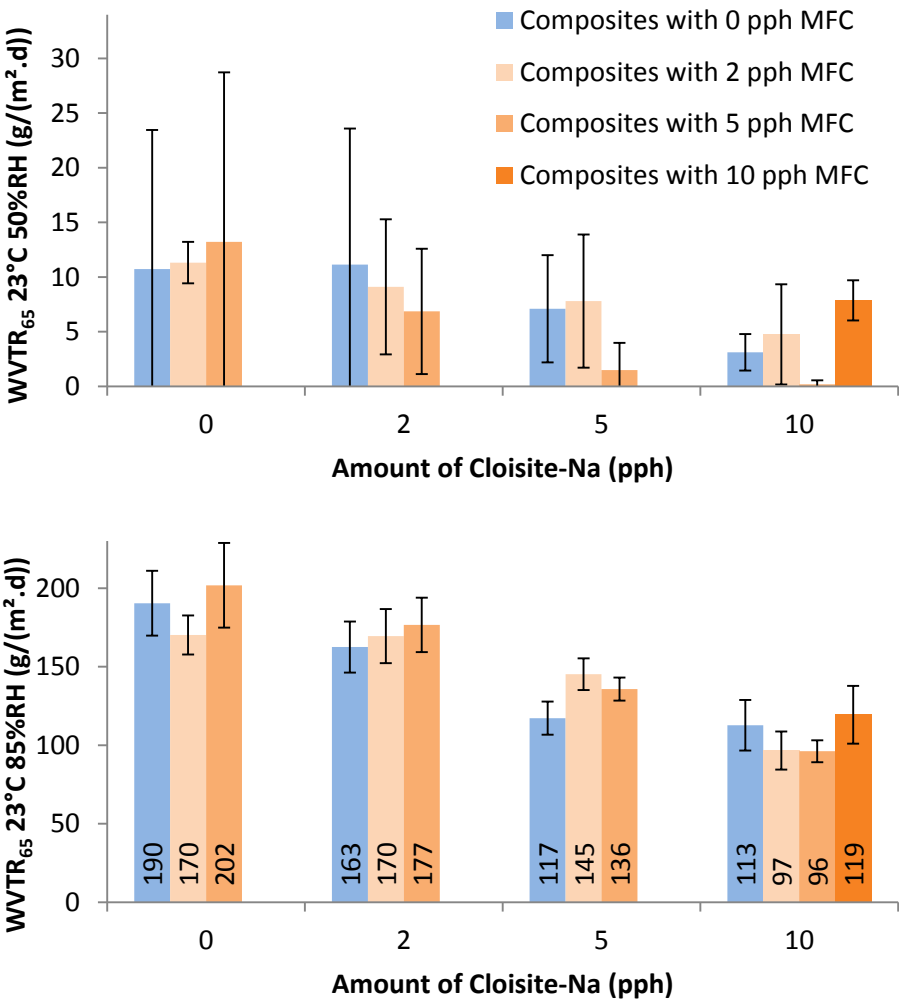

Figure 65 - Water vapour transmission for PVOH:MFC:Cloisite composites.

It can also be observed that this positive effect is almost independent of the amount of MFC. Despite dispersion improvement of MFC and Cloisite-Na in the case of PVOH:MFC:Cloisite composite films as described by SEM and XRD measurement, no synergistic effect was observed concerning the water vapour barrier. The water vapour barrier of PVOH:MFC composite films could be successfully

improved by addition of layered silicates, but no interaction between the two fillers could be observed at this level.

V.2.5. Influence of MFC and Cloisite-Na on PVOH crystallinity by DSC

Differential scanning calorimetry (DSC) experiments have been performed in order to determine if the MFC and clay fillers changed the crystallinity or transition temperatures of the matrix. Crystallites are impermeable to gases and thus affect the permeability. Similarly to the effect of layered silicates, gas has to bypass them, leading to an increased tortuosity and reduced permeability. The DSC spectra corresponding to the first heating and cooling are presented in Figure 66, PVOH being the matrix (100 pph) and fillers being MFC 5P (5 pph) and/or Cloisite-Na (10 pph). The spectra corresponding to the second heating of the samples can be found in appendix page 202.

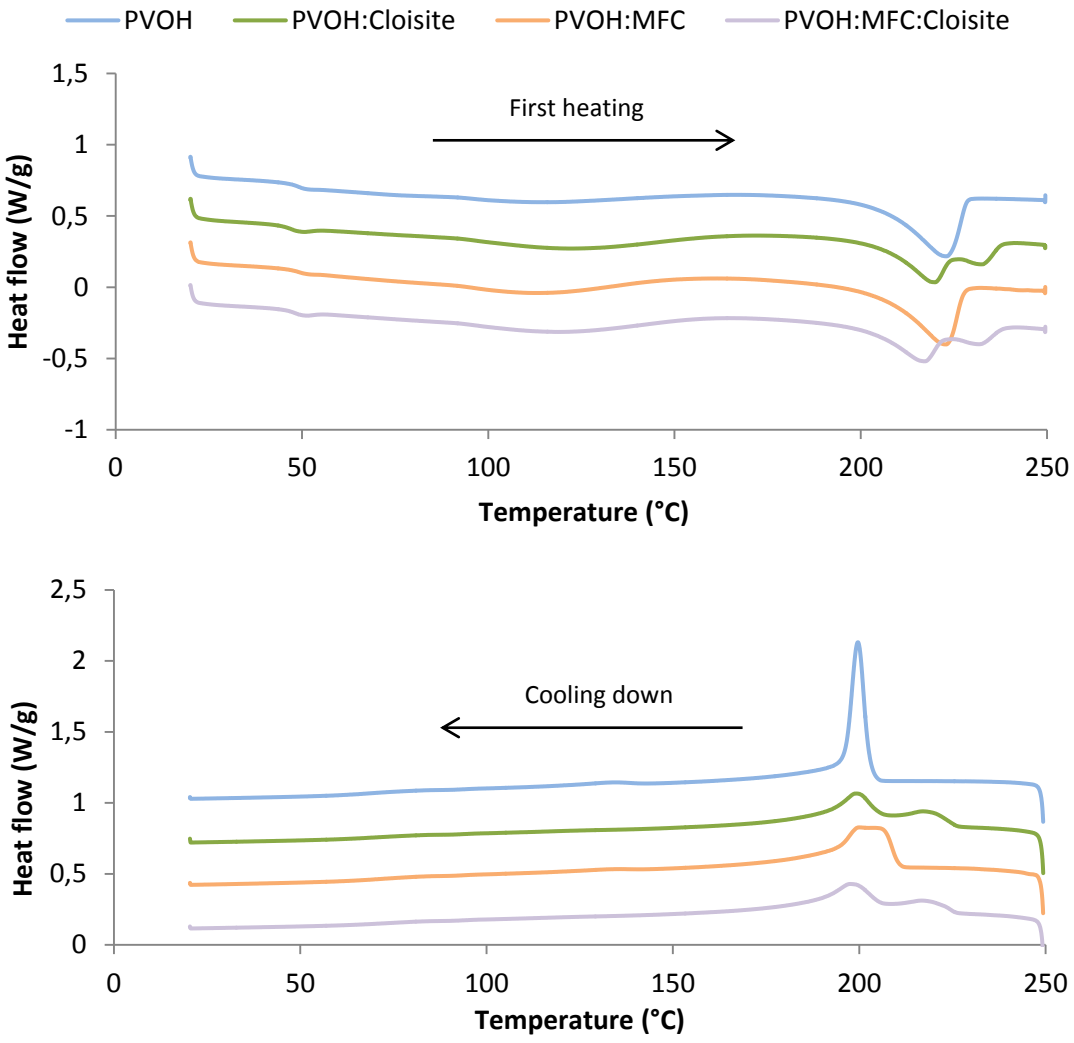

Figure 66 - DSC spectra for PVOH:MFC:Cloisite-Na composite films. First heating (top) and cooling (bottom) of samples equilibrated at 23°C 50%RH. MFC 5P is at 5 pph and Cloisite-Na at 10 pph.

In Figure 66, a first specific heat change appeared around 48°C corresponding to the glass transition temperature of the PVOH (T_g). The glass transition temperature (T_g) and melting point (T_f) upon first and second heating are reported in Table 29, along with the crystallisation temperature (T_c) upon cooling. It can be observed that $T_{g(2)}$ upon second heating was much higher than for the first heating because of the lower water content, capable of plasticizing the material, removed by evaporation during the first heating. $T_{g(2)}$ of PVOH was 72.4°C and increased with addition of fillers up to 78.1°C for PVOH:MFC:Cloisite-Na composite due to a reduction of polymer chain mobility. The shoulder observed right after $T_{g(1)}$ is characteristic of structural relaxation, or physical aging, corresponding to a compaction of the amorphous random coils over time (Montserrat et al., 1997). This structural relaxation was only observed in the case of clay-comprising composites and did not appear upon second heating. The broad endothermic peak around 120°C corresponds to water evaporation, which is shifted to higher temperatures upon addition of Cloisite-Na, indicating stronger bonding.

The endothermic peak around 220°C (T_{fA}) corresponds to the melting of PVOH crystallites. In the case of clay-comprising composites, there was also a second peak at 232°C (T_{fB}). This second peak is attributed to the formation of a second population of crystallites in the presence of clay platelets, therefore named clay-induced crystallites. The higher melting temperature indicates that they are of larger size compared to the bulk-like crystallites, contrary to the smaller spherulites observed in the case of CNC fillers in poly(ethylene oxide) by Azizi Samir and co-workers (2004). The same effect has been observed in the literature, with an increase of clay-induced crystallinity and a decrease of bulk-like crystallinity by increasing the clay content in PVOH (Strawhecker and Manias, 2000). This attribution to two crystallite populations is supported by a double exothermic peak, corresponding to crystallisation, observed at similar temperatures during the cooling of the samples. MFC has been found to facilitate PVOH crystallite formation, evidenced through a higher onset crystallisation temperature of 210°C while it begins at 202°C in the case of pristine PVOH. This is characteristic of the nucleating effect of the cellulose nanofiller, as reported in the case of MFC and CNC in poly(ε-caprolactone) by Siqueira and co-workers (2011). This effect is not present in the case of clay-comprising composites. On the contrary, the crystallisation temperature is slightly lower, corresponding to what has been observed in the case of organoclays as filler in poly(ε-caprolactone) and attributed to the clay platelets hindering the transport of polymer segments (Jimenez et al., 1997).

	T_g (°C)		T_{fA} (°C)		T_{fB} (°C)		T_{cA} (°C)	T_{cB} (°C)
Formulation	1st	2nd	1st	2nd	1st	2nd		
PVOH	48.9	72.4	222.9	222.4	-	-	199.6	-
PVOH:Cloisite-Na	46.9	74.5	220.0	216.6	232.2	232.4	199.1	217.2
PVOH:MFC	49.4	75.9	222.8	222.0	-	-	200.0	-
PVOH:MFC:Cloisite-Na	48.2	78.1	217.2	216.3	232.0	232.2	197.6	216.7

Table 29 - Glass transition (T_g), fusion (T_f), and crystallisation (T_c) temperatures for PVOH:MFC:Cloisite-Na composite films. T_g and T_f are given for the first (1st) and second (2nd) heating. T_f and T_c are given for the bulklike (A) and clay-induced (B) crystallites. MFC 5P is at 5 pph and Cloisite-Na at 10 pph.

The degree of crystallinity of PVOH in PVOH:MFC:Cloisite-Na composite films is presented in Table 30. The crystallinity of PVOH in cast films is not strongly affected by the addition of either MFC of Cloisite-Na, with values around 55%. It can be concluded that the water vapour barrier enhancement obtained upon addition of Cloisite-Na is not the result of an increased crystallinity of the matrix. The effect is stronger for the second heating by fusion of the crystallites formed during the previous step of cooling, especially for composites comprising Cloisite-Na. The decreased crystallinity of PVOH upon presence of Cloisite-Na may be ascribed to the clay platelets hindering the mobility of polymer segments, being in accordance with the higher T_g and lower T_c discussed previously. The fast crystallisation upon cooling down in DSC experiments (about 1 minute), contrary to the crystallisation occurring during drying of cast films that takes about 2 days, in addition to the absence of water, may explain the lower degree of crystallinity obtained during the second heating for PVOH:Cloisite-Na and PVOH:MFC:Cloisite-Na compared to pristine PVOH.

	Formulation	Total PVOH crystallinity (%)	Bulk-like fraction	Clay-induced fraction
First heating	PVOH	54.1	100%	0%
	PVOH:Cloisite-Na	53.6	75%	25%
	PVOH:MFC	55.2	100%	0%
	PVOH:MFC:Cloisite-Na	51.5	75%	25%
Second heating	PVOH	44.3	100%	0%
	PVOH:Cloisite-Na	36.7	79%	21%
	PVOH:MFC	41.0	100%	0%
	PVOH:MFC:Cloisite-Na	35.9	81%	19%

Table 30 - Degree of crystallinity χ_c for PVOH:MFC:Cloisite-Na composites.

The bulk-like and clay-induced fraction corresponding to the two melting peaks at 220°C and 232°C, respectively, have been determined by integration of the double peak up to 226°C for bulk-like crystallinity, and from 226°C for clay-induced crystallinity. The bulk-like versus clay-induced crystallinity fractions for PVOH:Cloisite-Na were not modified by the addition of MFC. The fraction of clay-induced crystallinity decreased on the second heating, supporting the fact that clay platelets hindering polymer mobility is involved in the lower total PVOH crystallinity upon second heating.

V.2.6. Dynamic vapour sorption

Dynamic vapour sorption experiments have been performed in order to obtain the water vapour sorption value for PVOH:MFC:Cloisite composites (MFC 5P at 5 pph, Cloisite-Na at 10 pph), and determine the water vapour diffusion coefficient from the sorption kinetics as described in II.2.3.5, page 87.

Sorption corresponds to the quantity of water in the film in g_{water}/g_{dry} calculated from $(Eq.12)$, page 87, and is proportional to the solubility coefficient according to $(Eq.13)$, page 87. The permeability is therefore proportional to the sorption, as permeability is the product of the diffusion coefficient and the solubility coefficient according to $(Eq.3)$, page 24. The sorption for PVOH:MFC:Cloisite-Na composites is presented in Figure 67 (left). Their profile is similar; slowly increasing to about 0.01 g/g at 50%RH, and increasing much faster afterwards up to about 0.35 g/g at 95%RH. The differences observed upon addition of MFC and clay are highlighted in Figure 67 (right) with the relative sorption, i.e. sorption of the composite normalised to the one of pristine PVOH. At 50%RH, the addition of fillers increased the water vapour sorption, especially in the case of MFC. From 70%RH the addition of clay was found to decrease the water vapour sorption of PVOH, whereas the sorption of PVOH:MFC composites was still above the one of pristine PVOH. Clays have been used in order to improve the barrier by increasing the tortuosity of the material and thus increasing the diffusion coefficient. Dynamic vapour sorption shows that, from 70%RH, clays could also reduce the water vapour sorption, and thus solubility coefficient, of PVOH.

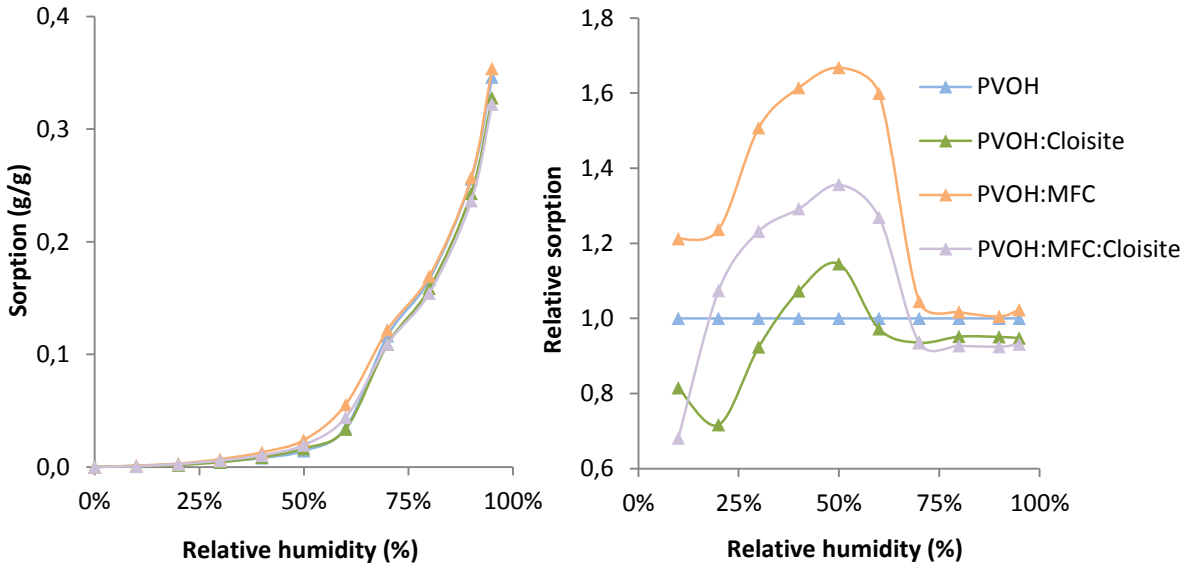

Figure 67 - Evolution of the water vapour sorption (left), and relative water vapour sorption (sorption divided by the sorption of pristine PVOH, right), for PVOH:MFC:Cloisite-Na composites from 0%RH to 95%RH.

The change of behaviour observed for water vapour sorption from 50%RH is also observed for the diffusion coefficient, as show in Figure 68. It increases sharply in the range 55%RH to 75%RH, from about 10^{-12} to 10^{-10} m²/s. This increase begins at 55%RH in the case of PVOH:MFC and

PVOH:MFC:Cloisite-Na, while it only begins at 65%RH in the case of PVOH and PVOH:Cloisite-Na. This can be linked to the higher sorption of MFC-containing composites, as shown in Figure 67. Especially, at 60%RH, PVOH:MFC has a sorption of 0.056 g/g compared to only 0.035 g/g for pristine PVOH. Water is a plasticizer for PVOH and MFC; it decreases the T_g of these materials, as seen in V.2.5, page 159, with the T_g of PVOH increasing from 49°C to 72°C after being completely dried during the DSC experiment. The much higher diffusion of PVOH:MFC at 65%RH may be ascribed to the T_g of PVOH:MFC being below the experimental temperature of 23°C due to the plasticising effect of water, as observed by Hu and co-workers (2013). At this relative humidity pristine PVOH had a lower sorption, thus a lower plasticising effect of water that may allow its T_g to be higher than the experimental temperature of 23°C. This is in accordance with the behaviour of the PVOH: Cloisite-Na and PVOH:MFC:Cloisite-Na composites. PVOH:Cloisite-Na has a sorption similar to PVOH at 60%RH and its diffusion coefficient only begins to rise at 75%RH, similarly to PVOH. PVOH:MFC:Cloisite-Na has an intermediate sorption of 0.044 g/g at 60%RH and its diffusion coefficient already begins to increase at 65%RH.

Surprisingly, the diffusion coefficient of clay-comprising composites in humid conditions was not much lower than the one of pristine PVOH: the diffusion of PVOH:Cloisite-Na is slightly lower than the one of PVOH at 75%RH, but it is slightly higher afterwards. The expected reduction of water vapour diffusion coming from the dispersion of clays in PVOH could not be observed after 75%RH, except in the case of PVOH:MFC:Cloisite-Na compared to PVOH:MFC.

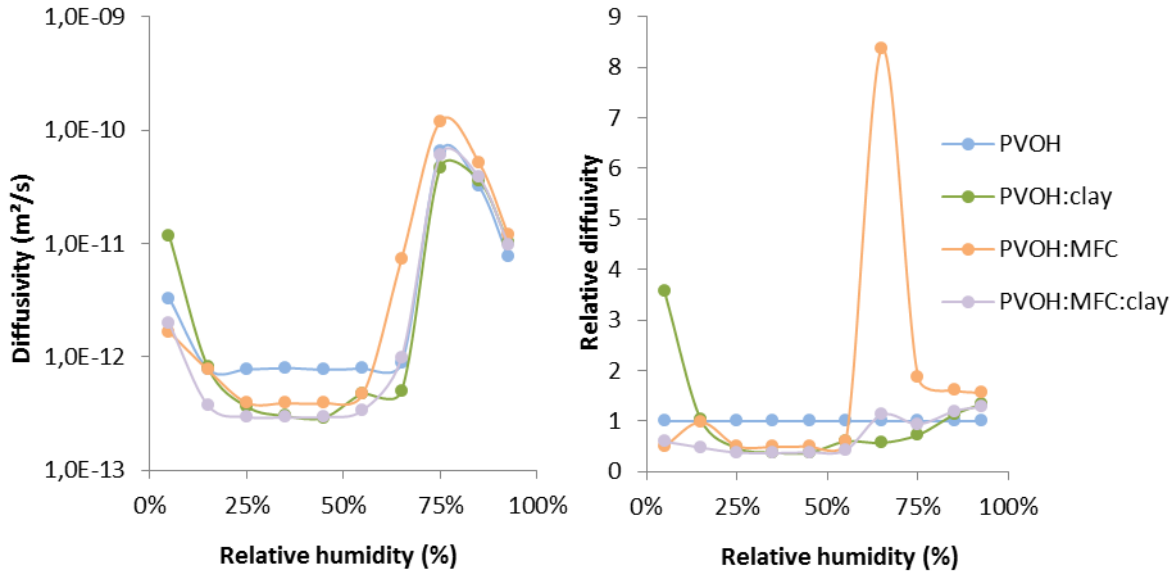

Figure 68 - Evolution of the water vapour diffusion coefficient (left), and relative water vapour coefficient (diffusion normalised by the diffusion of pristine PVOH , right), for PVOH:MFC:Cloisite-Na composites from 5%RH to 92.5%RH

The permeability of the composites has been calculated from the product of the solubility and diffusion coefficients. The values obtained are much higher than those obtained previously using the cup method, as shown in Table 31. A possible explanation is the fact that upon testing with the

WVTR cup method, one side is facing a 0%RH atmosphere, kept dry inside the cup by a dessicant. This may lead to lower water vapour sorption than with the DVS where the sample is fully equilibrated at the desired relative humidity, resulting in a lower plasticization effect and thus lower permeability for the WVTR cup method.

		Water vapour permeability (g.µm/(m².d.ha))			
Humidity	Method	PVOH	PVOH:Cloisite	PVOH:MFC	PVOH:MFC:Cloisite
50%RH	DVS	85	48	79	47
	WVTR (cup)	41	11	53	2
85%RH	DVS	29,265	31,590	47,532	32,463
	WVTR (cup)	415	248	483	264

Table 31 - Comparison between the water vapour permeability obtained by the DVS method and by the WVTR cup method.

V.2.7. Conclusion

In this section, a more detailed analysis of the MFC and Cloisite-Na dispersion in PVOH has been performed using X-ray diffraction (XRD) and field emission gun scanning electron microscopy (FEG-SEM). XRD evidenced a highly disordered state of Cloisite-Na in PVOH with no detectable d_{001} peak, sign of an intercalated and possibly exfoliated state. This was validated by FEG-SEM analysis where no aggregate could be found. FEG-SEM also evidenced a flocculation phenomenon of MFC in PVOH that disappeared upon further addition of Cloisite-Na. The use of SEM with back scattered electron (BSE) allowed observing the proportion and repartition of mineral elements (Cloisite-Na) on the top and bottom surface of the films. The higher proportion at the bottom indicates that a slight sedimentation occurred, and the repartition of mineral elements seemed to be more homogeneous in presence of MFC, suggesting a dispersing effect of the MFC on Cloisite-Na. A progressive addition of Cloisite-Na led to a progressive improvement of the water vapour barrier, with a water vapour transmission rate down to 113 g/(m².d) at 10 pph Cloisite-Na compared to 190 g/m² for pristine PVOH. MFC had little effect on the water vapour barrier; it did not bring a further improvement in presence of Cloisite-Na contrary to what could be expected due to the apparent synergistic dispersing effect observed by XRD, FEG-SEM, and SEM-BSE. Differential scanning calorimetry analysis showed that the addition of 5 pph MFC 5P and/or 10 pph Cloisite-Na did not significantly affect the crystallinity of PVOH, indicating that the barrier improvement obtained upon addition of Cloisite-Na actually come from the clay platelets and not from an increase of PVOH crystallinity. Dynamic vapour sorption experiments were expected to evidence a decrease of diffusion coefficient inside clay-comprising composites, but it has only be observed up to 75%RH, thus not being able to explain the barrier improvement. The water vapour sorption could be reduced by the presence of Cloisite-Na, but the effect is too low to explain the barrier improvement.

V.3. Application to board coating from concentrated suspensions

In this third section, based on the results of the previous sections, four PVOH:MFC:clay formulations have been selected to be coated on a 270 g/m² board: PVOH, PVOH:Cloisite-Na, PVOH:MFC, and PVOH:MFC:Cloisite-Na, using MFC 5P at 5pph and Cloisite-Na at 10 pph in a matrix of PVOH 6-98. After a description of the viscosity of the suspension, the dispersion of Cloisite-Na in PVOH has been investigated by flow particle image analysis (FPIA) on suspensions and by field emission gun scanning electron microscopy (FEG-SEM) on coated boards. Coated boards have also been characterised in terms of water vapour and oxygen barrier.

V.3.1. Increased viscosity with the higher solid content

Going from cast films to coated boards required adapting the suspension production. A solid content of 5 wt% as used in casting is too low for coating, more concentrated suspensions have been produced while maintaining a viscosity in the correct range for the coating process. The viscosity of the suspensions as used during coating is presented in Table 32. Without MFC, the introduction of 10 pph Cloisite-Na in PVOH led to an increase in viscosity of 35%. With 5 pph MFC only, the viscosity of PVOH is almost quadrupled and the further addition of Cloisite-Na has little effect. The choice of a solid content of 18 wt% has been made in order to obtain a viscosity under 2,000 mPa.s during coating. For PVOH or PVOH:Cloisite-Na suspensions higher solid contents of 20 to 25 wt% could be used while remaining in the appropriate viscosity range, thus reducing the energy required for drying.

Formulation			Properties	
PVOH 6-98	MFC 5P	Cloisite-Na	S_c (wt%)	η (mPa.s)
100			18%	392
100		10	18%	530
100	5		19%	1,560
100	5	10	18%	1,444

Table 32 - Solid content (S_c) and viscosity of the suspensions used for coating.

V.3.2. Incomplete Cloisite-Na dispersion observed with a Flow Particle Image Analyser

A Flow Particle Image Analyser (FPIA) has been used to determine the size distribution of the particles for pure Cloisite-Na in suspension in water after overnight stirring (5 wt%), and in a formulation of PVOH with 10 pph Cloisite-Na for a total solid content of 5 wt% or 18 wt%. The acquisition of the size distribution for PVOH:Cloisite-Na suspensions was made every hour from the moment when the clay was added in PVOH to the end of the stirring at 95°C during 4 hours. The results in the form of average diameter of the particles are presented in Figure 69. The Cloisite-Na particles in suspension detected by the apparatus have an average diameter of 2.1 µm, the detection range of the apparatus going from 0.5 to 40 µm. Upon addition in the PVOH solution free of any solid element, the average diameter of the particles gets higher than in the case of the Cloisite-Na suspension. This corresponds to the formation of PVOH:Cloisite-Na aggregates as observed

previously by microscopic analysis in V.1.2, page 149. As expected, these aggregates are progressively destroyed, which is evidenced by the decrease of average diameter down to a value equivalent to what was found in the Cloisite-Na suspension. By comparing the behaviour in a diluted (5 wt%) and a concentrated (18 wt%) suspension, it can be observed that the size of the aggregates formed right after Cloisite-Na addition in the concentrated suspension was more than two times higher: 15 µm compared to 6.4 µm. In addition, the reduction of the size of the aggregates was slower and after 4 hours they were still, on average, larger than for the initial Cloisite-Na particles in suspension. In concentrated suspensions to be applied to coating, the dispersion of the layered silicates appeared more difficult. The effect of MFC on the aggregates size could not be analysed with this technique due to the presence of residual macro-fibres that are also detected by the apparatus.

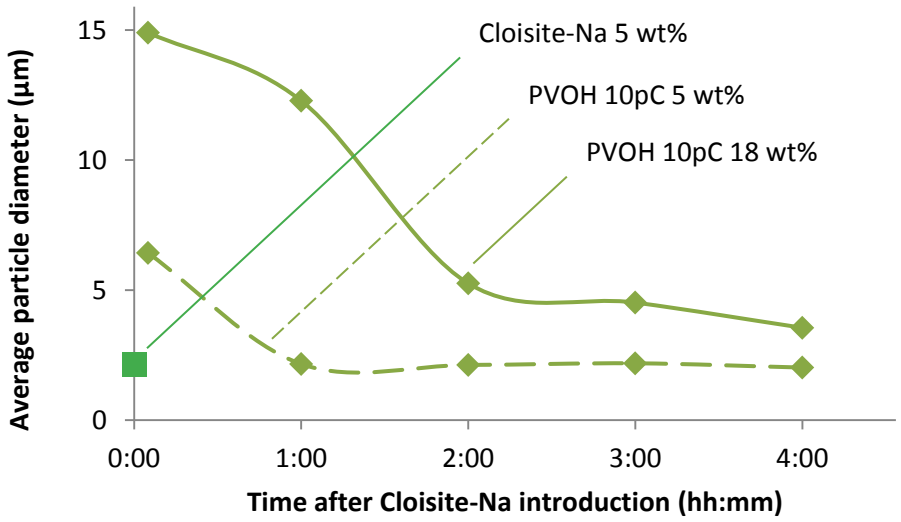

Figure 69 - Evolution of the average area-weighted diameter of the particles in suspension during 4 hours of stirring at 95°C.

V.3.3. Synergistic dispersion leading to a defect-free PVOH:MFC:Cloisite-Na coating layer

The FPIA analysis of the concentrated suspension evidenced that the PVOH:Cloisite-Na particles could not be completely destroyed. The residual aggregates were large enough to be observed at macro-scale on coated boards. Figure 70 shows the visual effect of the coatings on board. PVOH coating leads to a smooth glossy surface allowing observing the reflexion of the light source. Upon addition of Cloisite-Na, the surface remains glossy but small dots appear corresponding to the residual PVOH:Cloisite-Na aggregates. When the board is coated with PVOH:MFC or PVOH:MFC:Cloisite-Na, no aggregates could be found and the gloss disappeared, which is in accordance with the blurring that has been observed in the case of PVOH:MFC self-standing films in IV.1.3, page 118.

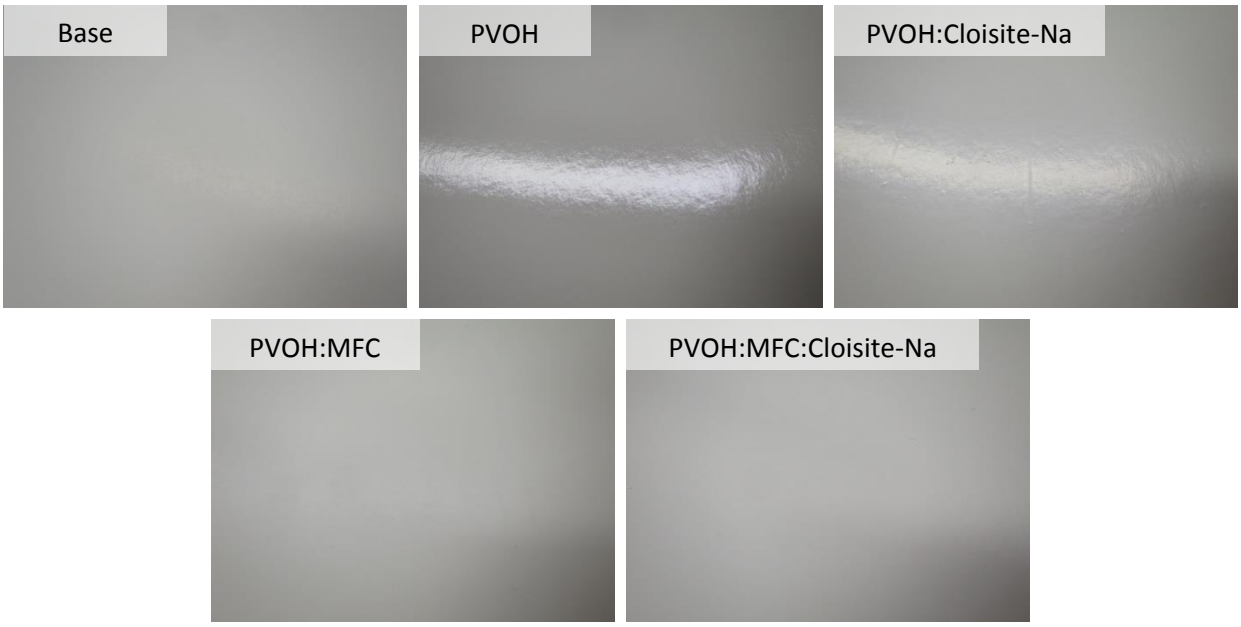

Figure 70 - Pictures of boards with, from top left to bottom right: no coating, PVOH, PVOH:Cloisite, PVOH:MFC, and PVOH:MFC:Cloisite coatings. Picture width: 10 cm.

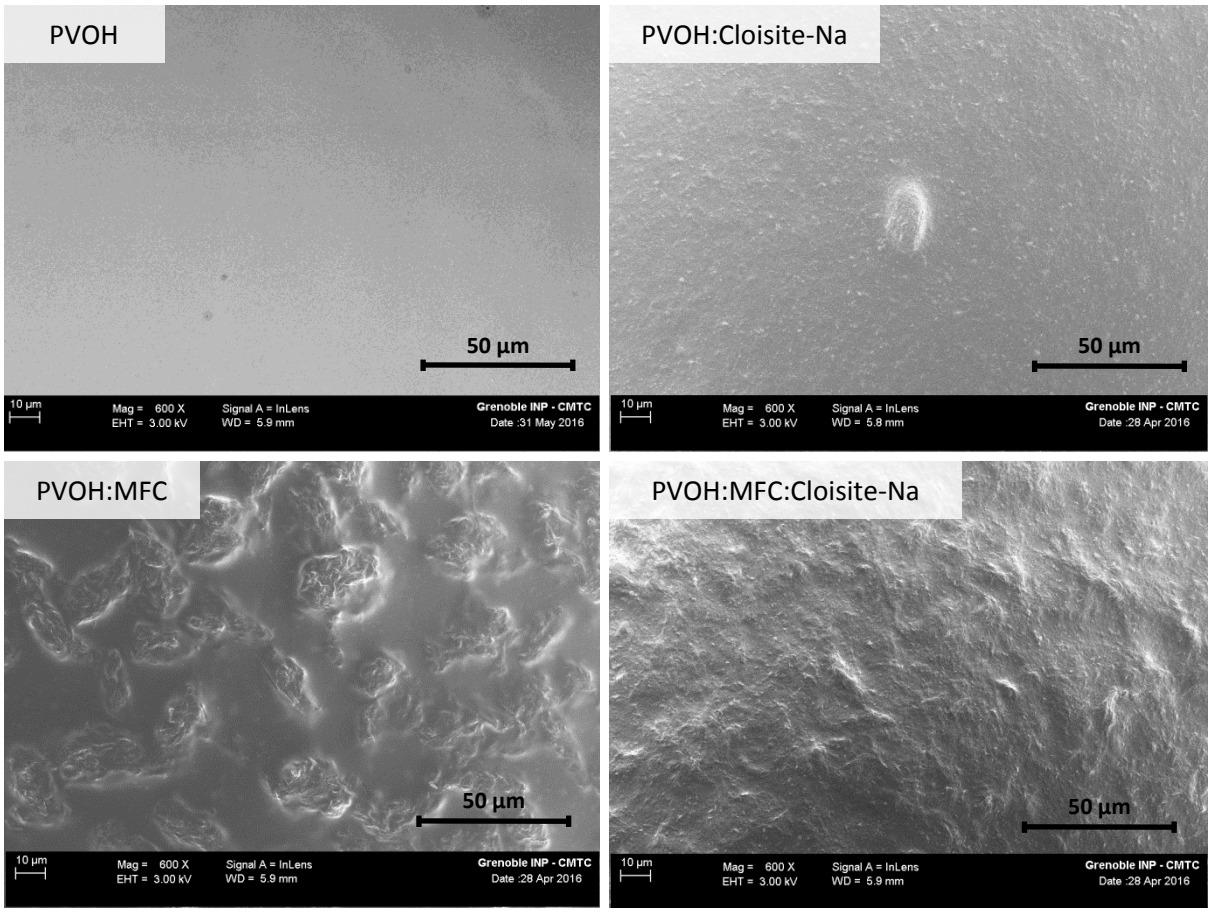

Figure 71 - SEM pictures of the surface of PVOH:MFC:Cloisite-Na composite layers coated on board. MFC is at 5 pph and Cloisite-Na at 10 pph.

The dispersion of the fillers in the coated layer has been analysed by SEM, as it has been previously made for the self-standing films in V.2.2, page 155. Figure 71 led to similar conclusions than in the case of films produced by casting from diluted (5 wt%) suspensions: PVOH had a smooth surface, MFC was flocculated, and the introduction of Cloisite-Na allowed MFC to be much less flocculated. In addition, for the coating surfaces the flocculation was stronger with larger elements and a clear separation between MFC-containing areas and smooth MFC-free areas in the case of the PVOH:MFC layer. The aggregates observed at macro-scale were present in the case of PVOH:Cloisite-Na as can be seen on the middle of the SEM picture, while no particle were found in the case of PVOH:MFC:Cloisite. In addition to the reduction of MFC flocculation by addition of Cloisite-Na already observed for the cast films, the SEM pictures of the coated layers evidence that adding MFC to a PVOH:Cloisite-Na composite led to the formation of aggregate-free layer. MFC and the layered silicate thus have a positive effect on the dispersion of each other.

V.3.4. Effect of MFC and Cloisite-Na on the water vapour barrier of the coated boards

The water vapour barrier properties of the coated boards are reported in Figure 72. The target coat weight is 10 g/m², transmission rates have therefore been normalised to this basis weight for comparison ($WVTR_{10}$).

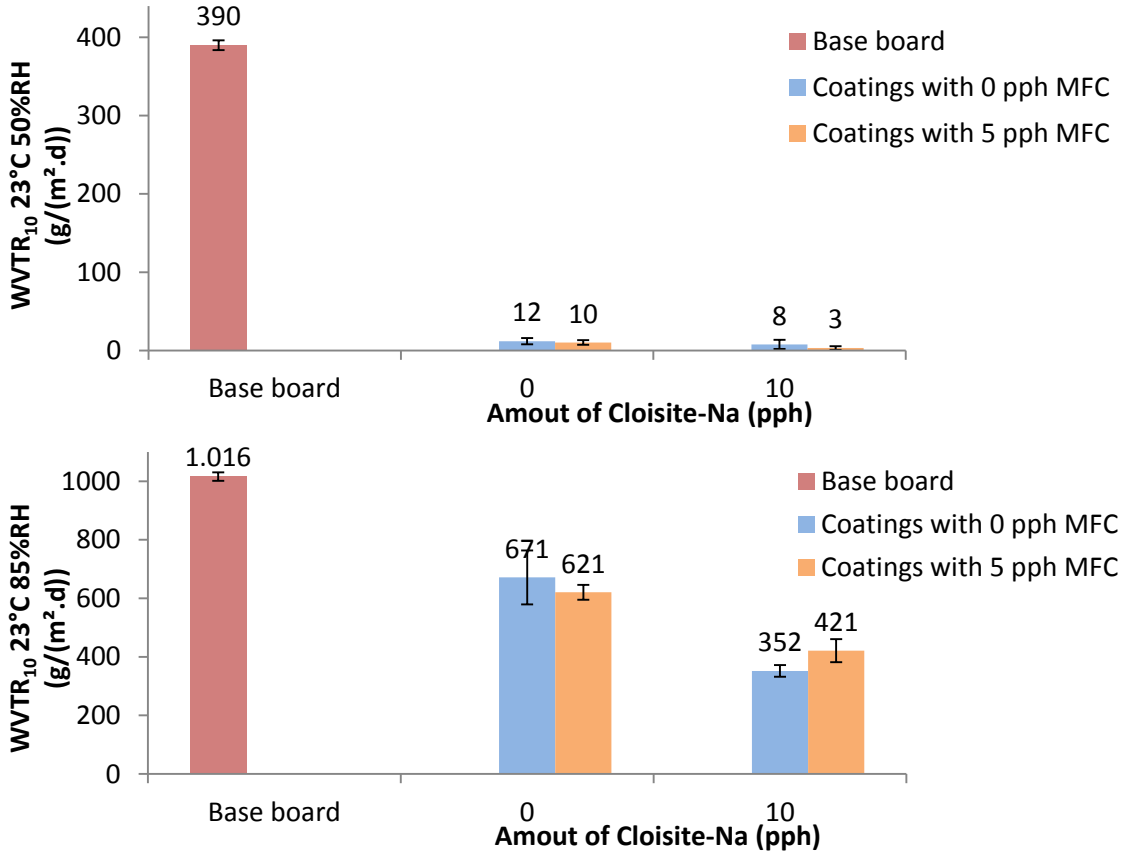

Figure 72 - $WVTR_{10}$ of PVOH:MFC:Cloisite-Na composite coatings on board. MFC is at 5 pph, Cloisite-Na at 10 pph, and the coat weight of 10 g/m².

As in the case of self-standing films, the $WVTR_{10}$ at 23°C 50%RH was satisfyingly low with values around 10 g/(m².d), especially compared to the base board that is as high as 390 g/(m².d). No clear conclusion could be drawn about the influence of MFC and Cloisite-Na due to the high standard deviation at these low transmission rates. At 23°C 85%RH, the transmission was much higher as was already observed for the self-standing films: 671 g/(m².d) for the PVOH-coated board. For comparison, PVOH cast films had a $WVTR_{65}$ of 190 g/(m².d), i.e. a $WVTR_{10}$ of 1,235 g/(m².d). Similarly, the amount of MFC does not play a significant role while the introduction of Cloisite-Na leads to an improvement of the same order of magnitude. The use of 10 pph Cloisite-Na (Φ_s = 4.3%) leads to a relative permeability of 52% while a relative permeability of 4% could be theoretically obtained according to $(Eq.\,27)$, page 151. This difference is mainly attributed to the layered silicates not being fully exfoliated. The positive synergistic effect of MFC and Cloisite-Na on the dispersion of each other in PVOH did not lead to any improvement of the water vapour barrier.

V.3.5. Oxygen barrier improvement of a PVOH:Cloisite-Na composite layer using MFC

The positive effect of MFC and Cloisite-Na on the dispersion of each other in PVOH led to a significant effect in the case of the Oxygen Transmission Rate (OTR), presented in Figure 73 after being normalised to the target thickness of 10 g/m² (OTR_{10}).

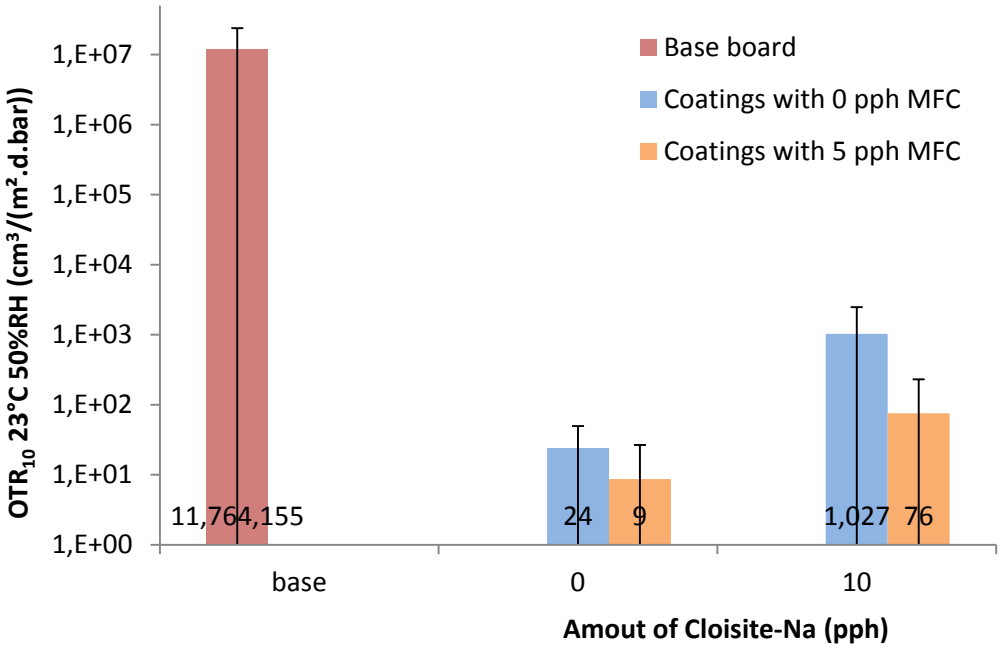

Figure 73 - Oxygen Transmission Rate for PVOH:MFC:Cloisite-Na coatings. The high error bars (± standard deviation) come from the fact that transmission is mainly due to defects in the layer.

The oxygen barrier improvement due to PVOH is on another level compared to the one obtained in the case of water vapour. At 23°C 50%RH, the PVOH coating led to an OTR reduced by several orders of magnitude: it brings an OTR of 24 $cm^3/(m².d.bar)$ that corresponds to values in the range of what is expected from a high barrier packaging: 10 to 20 $cm^3/(m².d)$ according to Syverud

and Stenius (2009). It is difficult to compare this value to the one obtained with addition of MFC due to high standard deviations, attributed to the fact that the oxygen transmission is highly dependent on small defects than can be present in the layer. However, the addition of Cloisite-Na has a detrimental effect on the oxygen barrier with an increase in oxygen transmission of two orders of magnitude: 1,030 $cm^3/(m^2.d.bar)$. This is attributed to the aggregates formed in the PVOH:Cloisite-Na concentrated suspension as observed visually and by FPIA and SEM analysis: these defects could be responsible for the creation of preferential diffusion pathways for the gas molecules. In the case of PVOH:MFC:Cloisite-Na composite coatings, these aggregates were not present and it resulted in a lower OTR of 76 $cm^3/(m^2.d.bar)$. The improvement of the layered silicate dispersion due to the introduction of microfibrillated cellulose resulted in films without aggregates, giving a significant improvement of oxygen barrier.

V.3.6. Conclusion

Going from the production of cast films to the production of coated boards required the preparation of concentrated suspensions (18 wt% compared to 5 wt% for cast films production), allowing reaching a higher coat weight with less water to evaporate. It led to more viscous suspension, especially upon addition of MFC, and also affected the dispersion state of MFC and Cloisite-Na in PVOH. Flow particle image analysis evidenced larger particles formed upon addition of Cloisite-Na suspension in PVOH for the production of concentrated suspensions compared to diluted suspensions for casting. These aggregates could not be completely broken down by mechanical stirring at 95°C, they could be observed at macroscopic scale on coated boards and at microscopic scale by scanning electron microscopy. SEM pictures also evidenced a stronger MFC flocculation in PVOH compared to cast film. However, similarly to cast films, Cloisite-Na was found to have a dispersive effect on MFC in PVOH, resulting in relatively homogeneous films. Aggregates could not be observed in the case of the PVOH:MFC:Cloisite-Na formulation, neither at macroscopic scale nor at microscopic scale, suggesting a dispersive effect of MFC on Cloisite-Na in PVOH for concentrated suspensions. Similarly to cast films, MFC had little influence on the water vapour barrier and Cloisite-Na led to an approximately halved water vapour transmission at 23°C 85%RH. Concerning oxygen barrier, PVOH and PVOH:MFC coatings were effective with an oxygen transmission rate of 24 and 9 $cm^3/(m^2.d.bar)$, respectively, but PVOH:Cloisite-Na was found quite permeable with an oxygen transmission rate of 1,030 $cm^3/(m^2.d.bar)$ attributed to the residual aggregates. The dispersive effect of MFC on Cloisite-Na allowed avoiding aggregates, which resulted in a much lower oxygen transmission rate of 76 $cm^3/(m^2.d.bar)$. Compared to neat PVOH, as shown in Figure 74, PVOH:MFC:Cloisite-Na-coated boards could thus have an improved water vapour barrier thanks to the clay platelets and keep a low oxygen transmission thanks to MFC avoiding the presence of PVOH:Cloisite-Na aggregates.

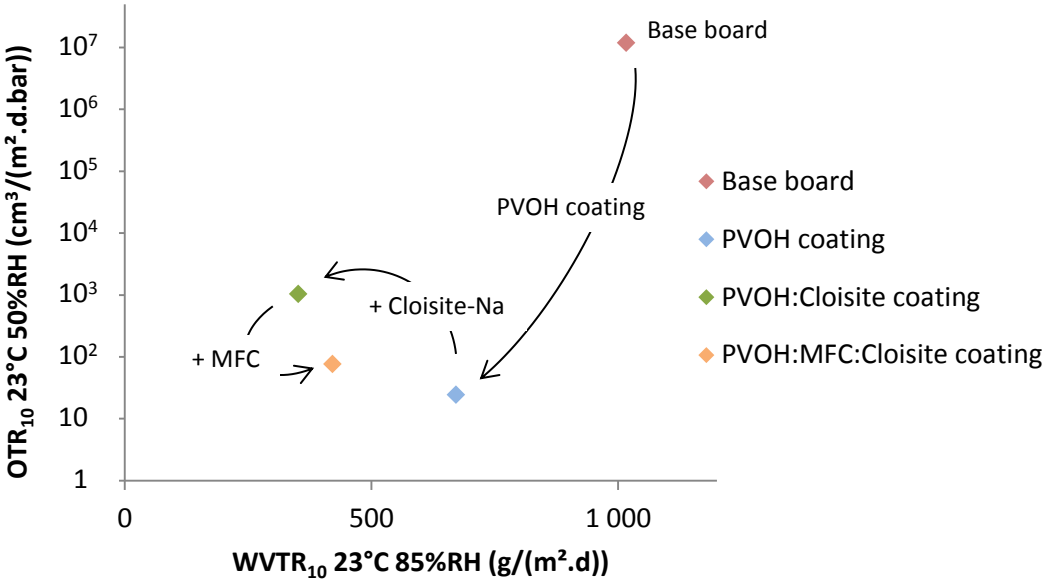

Figure 74 - Effect of MFC and Cloisite-Na on the oxygen and water vapour transmission through composite coating layers.

V.4. Conclusion

In order to develop new barrier using microfibrillated cellulose, this chapter aimed at selecting the most relevant clay grade for the development of MFC-comprising water-based barrier coating, and getting a better understanding of the impact of MFC and clay in the dispersion and barrier of PVOH:MFC:clay cast films and layers coated on board.

Four grades of layered silicates with different chemistries and morphologies have been combined with microfibrillated cellulose in a poly(vinyl alcohol) matrix. After adaptation of the suspension production process for a better dispersion of the clay, the use of Cloisite-Na allowed to significantly reduce the water vapour transmission of composite self-standing films in humid conditions compared to the other grades. For this reason, it has been studied in further details. XRD analysis of PVOH:MFC:Cloisite-Na self-standing films evidenced highly dispersed layered silicates in the composites and it was shown that the introduction of MFC seemed to slightly improve this dispersion. The effect of Cloisite-Na on the dispersion of MFC in PVOH has been observed by SEM going from flocculated MFC in PVOH to well-dispersed MFC in PVOH upon addition of Cloisite-Na. However, these dispersion improvements did not lead to an improvement in terms of water vapour barrier; only the progressive reduction of the $WVTR_{65}$ by increasing Cloisite-Na content could be observed. The use of more concentrated suspensions for coating, 18 wt% compared to 5 wt% for casting, generated more difficulties in the dispersion of the particles. It was especially shown concerning PVOH:Cloisite-Na macroscopic aggregates that could not be completely broken down at such concentration, as evidenced by analysis of the particle diameter by FPIA and by the SEM analysis. As a result, the low oxygen transmission that could be obtained with a PVOH coating went up to two orders of magnitude upon addition of Cloisite-Na. However, it could be observed that the addition of MFC to the PVOH:Cloisite-Na formulation led to an aggregate-free suspension. As a result, the oxygen barrier of the PVOH:MFC:Cloisite-Na at 23°C 50%RH is almost as satisfying as the one obtained with neat PVOH. Concerning the water vapour barrier at 23°C 85%RH, the effect of MFC and Cloisite-Na is the same as in the case of self-standing films: no visible effect of MFC and improvement upon addition of Cloisite-Na was observed. To conclude, a PVOH:MFC:Cloisite-Na layer could be obtained on board with improved water vapour barrier thanks to the layered silicates, and a satisfying oxygen barrier thanks to the dispersing effect of MFC on Cloisite-Na allowing to avoid the formation of PVOH:Cloisite-Na aggregates.

General Conclusions and Perspectives

General conclusions

Food packaging requires barrier layers to hinder the mass transport of different substances through the packaging, in order to increase shelf life and reduce food spoilage. The food packaging market evolves towards the use of more sustainable barrier solutions based on biosourced and/or biodegradable polymers. Among them is microfibrillated cellulose (MFC), which has high intrinsic oxygen and grease barrier properties and can improve the layer formation of composite coating formulations. However, MFC suspensions are highly viscous at low solid content and MFC-based layers lack of water and moisture resistance. This thesis demonstrated the opportunity of using microfibrillated cellulose (MFC) for the development of barrier layers using two different strategies:

- The application of a 100% MFC layer on board by wet lamination, bypassing the issues generated by the high viscosity of MFC suspensions thanks to a filtration step. This innovating approach is still in its early development steps and its upscaling at industrial scale requires additional research.
- The use of MFC as filler in a composite formulation for water-based barrier coating, using crosslinking and layered silicates in order to improve the behaviour upon exposure to water and moisture. This approach has been developed to fit with existing industrial coaters/dryers specifications.

This study first evidenced that indirect MFC degree of fibrillation characterisations were accurate in the cases of film densities and fraction of residual macro-fibres in suspensions. On the contrary, rheology or mechanical and optical properties were influenced by the pulp origin and could thus only be used to follow the fibrillation of a single pulp. The necessity of using highly fibrillated MFC has been demonstrated in the case of 100% MFC layers, as using MFC having low degree of fibrillation degraded the oxygen or water vapour barrier. 100% MFC layers could be applied on board by wet lamination including a filtration step, having a good adhesion without glue, and preserving the high oxygen and grease barrier properties of MFC with layers of high enough basis weights.

The necessity of using highly fibrillated MFC has also been demonstrated in the case of composite formulations consisting of MFC and poly(vinyl alcohol), a hydrosoluble polymer, with application to water-based barrier coating. The use of low MFC contents was preferred, as increasing the MFC content led to more viscous suspensions. It also resulted in layers having degraded mechanical and barrier properties. The use of a fully-hydrolysed PVOH grade with a low degree of polymerisation was preferred for low viscosity composite suspensions resulting in layers having better barrier properties. Using the appropriate MFC grade, MFC content, and PVOH grade, PVOH and PVOH:MFC suspensions were dried on a laboratory coating bench, evidencing a faster drying in the presence of MFC associated to MFC-hindering PVOH skin formation. The properties of PVOH and MFC layers could be improved upon exposure to water by citric acid crosslinking, and upon exposure to moisture by a curing step at 105°C or 150°C. The behaviours in humid conditions, of self-standing films and coated boards, were also improved by addition of layered silicates. The combined use of MFC and layered silicates had a positive effect on their dispersions, resulting in an improved water vapour barrier while avoiding the presence of layered silicates-induced aggregates that otherwise greatly damage the oxygen barrier. This dispersive effect of MFC on layered silicates was especially efficient in the case of concentrated suspensions with application to board coating.

To conclude, MFC have promising applications for the development of 100% MFC barrier layers, and as filler in a composite formulation with application to water-based barrier coating. In the first case the intrinsic barrier properties of MFC were exploited thanks to a recently developed process. In the second case MFC improved the composite layer formation, having a positive effect on drying and the dispersion of layered silicates.

Perspectives

Several perspectives to this work are given in the following paragraphs. The general objective of these perspectives is to get a better understanding of the mechanisms responsible for the materials performance, in order to improve the processes and for a relevant upscaling toward pilot and industrial scale.

In the case of MFC wet lamination, the apparition of defects in the layer at low basis weight were attributed to the presence of a small fraction of macro-fibres fragments in suspension that remained after the enzymatic pre-treatment followed by high-pressure homogenisation. The fraction of macro-fibres fragments was greatly decreased after a few passes but stagnated at a few millions elements per gram of pulp. First of all, it would be interesting to use MFC grades having different degrees of fibrillation and quantity of residual macro-fibres for wet lamination. Such MFC suspension could be produced by fractionation of MFC suspensions and or by combination of several mechanical processes during the fibrillations. This would make possible to determine the influence of the residual macro-fibres on the defects revealed by coloured oil, and on the basis weight from which they can be avoided. It may allow producing defect-free MFC barrier layers at lower basis weights. Performing MFC wet lamination on substrates of different surface topology and energy, associated to various MFC sizes and chemical compositions, would bring a better knowledge on the adhesion of the MFC layer onto a paper substrate. A better understanding of the influence of selected additives (such as citric acid, plasticizers, layered silicates) on the adhesion and barrier performance of MFC layers laminated on board would also be of interest.

The wet lamination has up to now been carried out at laboratory scale on existing and non-dedicated devices. In order to prepare the design of large scale machines, the three steps of the process should be investigated: filtration, transfer, and drying. Dewatering by filtration may be improved, e.g. using cationic chitosan leading to MFC flocculation (Liu and Berglund, 2012), as MFC filtration is slow and may determine the maximum machine speed. The strength of the wet MFC layer may be of main concern, requiring additives and/or a minimum consistency in order to pick it up and report it on a base correctly. Finally, only one drying method under vacuum at 93°C has been investigated, and it has been demonstrated that drying has an impact on the barrier properties of MFC films in the case of curing at 105°C or 150°C. Using other drying methods, such as conductive drying by hot rolls or convective drying or infrared drying, or a combination of drying methods, may enable different material structuration, barrier performance, and adhesion.

It has been demonstrated that using MFC in water-based barrier coating colours composed of PVOH and layered silicates improved both its drying and the dispersion of the mineral filler, especially in concentrated suspensions. These effects could be characterised more quantitatively, closer to industrial applications, and observed with other polymers. A laboratory drying bench has been adapted within this thesis as a preliminary study of the impact of MFC on PVOH drying. It would be interesting to investigates deeper the role of the degree of fibrillation and of the fraction of MFC in the composite suspension on its drying rate and defect-free layer formation. The drying improvement obtained upon addition of MFC has been demonstrated for thick layers and long drying times of 15 to 30 min. This study would gain in being coupled with pilot trials in order to dry coated layers in much shorter times. The qualitative determination of the effect of MFC could be performed by defect revelation using coloured oil (Cobb method), determining the number of permeable points

(blistering defects) per unit surface area and/or the surface fraction contaminated by coloured oil. The dispersive effect of MFC on layered silicates should be compared with other dispersing agents in order to determine their efficiency more quantitatively. It would also be of interest to have a more precise idea of the optimum MFC ratio for drying and dispersion improvement, in order to use as few MFC as possible and thus obtain coating colours of lower viscosity at fixed solid content.

The 3D shaping of paper-based food packaging is obtained by creasing and folding steps, glueing or heat sealing. The ductility of MFC or composite barrier layers should be compared to their ability to withstand creasing and folding without breaking. The addition of plasticizer can be required, especially if a crosslinker such as citric acid is used, and optima have to be looked for since the addition of plasticizer generally decreases the barrier performances. Crosslinking of self-standing films with citric acid at laboratory scale required a curing step at 150°C during several minutes. It is of interest to investigate if citric acid crosslinking can be activated in shorter times directly on lamination or coating machines, and to what extend these processes can be adapted for obtaining citric acid crosslinking activation. Crosslinking and layered silicates could improve the behaviour of barrier layers in wet or humid conditions. Despite no significant oxygen barrier improvement at 23°C 50%RH, such strategies can improve the oxygen barrier in humid conditions, which could be investigated.

In addition to the scientific perspective listed above, the compliance of such MFC-based layers to food packaging economic considerations and regulations should be checked. Recyclability and biodegradability should also be assessed, combined with a life cycle analysis, in order to demonstrate the sustainability of these solutions.

Literature cited

Abbott, J., 2015. Syngas from renewables, production of green methanol. Presented at the 2015 European Methanol Policy Forum, Brussels.

Abe, K., Iwamoto, S., Yano, H., 2007. Obtaining Cellulose Nanofibers with a Uniform Width of 15 nm from Wood. Biomacromolecules 8, 3276–3278. doi:10.1021/bm700624p

Ahola, S., Österberg, M., Laine, J., 2008. Cellulose nanofibrils - adsorption with poly(amideamine) epichlorohydrin studied by QCM-D and application as a paper strength additive. Cellulose 15, 303–314. doi:10.1007/s10570-007-9167-3

Andresen, M., Johansson, L.-S., Tanem, B.S., Stenius, P., 2006. Properties and characterization of hydrophobized microfibrillated. Cellulose 13, 665–677. doi:10.1007/s10570-006-9072-1

Anthierens, T., Ragaert, P., Verbrugghe, S., Ouchchen, A., De Geest, B.G., Noseda, B., Mertens, J., Beladjal, L., De Cuyper, D., Dierickx, W., Du Prez, F., Devlieghere, F., 2011. Use of endospore-forming bacteria as an active oxygen scavenger in plastic packaging materials. Innov. Food Sci. Emerg. Technol. 12, 594–599. doi:10.1016/j.ifset.2011.06.008

Arola, S., Malho, J., Laaksonen, P., Lille, M., Linder, M.B., 2013. The role of hemicellulose in nanofibrillated cellulose networks. Soft Matter 9, 1319. doi:10.1039/c2sm26932e

Aulin, C., Gällstedt, M., Lindström, T., 2010. Oxygen and oil barrier properties of microfibrillated cellulose films and coatings. Cellulose 17, 559–574. doi:10.1007/s10570-009-9393-y

Aulin, C., Ström, G., 2013. Multilayered Alkyd Resin/Nanocellulose Coatings for Use in Renewable Packaging Solutions with a High Level of Moisture Resistance. Ind. Eng. Chem. Res. 52, 2582–2589. doi:10.1021/ie301785a

Axrup, L., Heiskanen, I., Backfolk, K., 2011. A Paper or Paperboard Substrate, a Process for Production of the Substrate and a Package Formed of the Substrate. WO/2011/078770.

Azizi Samir, M.A.S., Alloin, F., Sanchez, J.-Y., Dufresne, A., 2004. Cellulose nanocrystals reinforced poly(oxyethylene). Polymer 45, 4149–4157. doi:10.1016/j.polymer.2004.03.094

Bardet, R., Reverdy, C., Belgacem, N., Leirset, I., Syverud, K., Bardet, M., Bras, J., 2015. Substitution of nanoclay in high gas barrier films of cellulose nanofibrils with cellulose nanocrystals and thermal treatment. Cellulose 22, 1227–1241. doi:10.1007/s10570-015-0547-9

Barrer, R.M., Petropoulos, J.H., 1961. Diffusion in heterogeneous media: lattices of parallelepipeds in a continuous phase. Br. J. Appl. Phys. 12, 691.

Belbekhouche, S., Bras, J., Siqueira, G., Chappey, C., Lebrun, L., Khelifi, B., Marais, S., Dufresne, A., 2011. Water sorption behavior and gas barrier properties of cellulose whiskers and microfibrils films. Carbohydr. Polym. 83, 1740–1748. doi:10.1016/j.carbpol.2010.10.036

Bertolla, L., Dlouhý, I., Philippart, A., Boccaccini, A.R., 2014. Mechanical reinforcement of Bioglass®-based scaffolds by novel polyvinyl-alcohol/microfibrillated cellulose composite coating. Mater. Lett. 118, 204–207. doi:10.1016/j.matlet.2013.12.079

Besbes, I., Alila, S., Boufi, S., 2011. Nanofibrillated cellulose from TEMPO-oxidized eucalyptus fibres: Effect of the carboxyl content. Carbohydr. Polym. 84, 975–983. doi:10.1016/j.carbpol.2010.12.052

Bharadwaj, R.K., 2001. Modeling the Barrier Properties of Polymer-Layered Silicate Nanocomposites. Macromolecules 34, 9189–9192. doi:10.1021/ma010780b

Bhattacharya, D., Germinario, L.T., Winter, W.T., 2008. Isolation, preparation and characterization of cellulose microfibers obtained from bagasse. Carbohydr. Polym. 73, 371–377. doi:10.1016/j.carbpol.2007.12.005

Biedermann, M., Grob, K., 2010. Is recycled newspaper suitable for food contact materials? Technical grade mineral oils from printing inks. Eur. Food Res. Technol. 230, 785–796. doi:10.1007/s00217-010-1223-9

Birck, C., 2014. New crosslinked cast films based on poly(vinyl alcohol): Preparation and physico-chemical properties. Express Polym. Lett. 8, 941–952. doi:10.3144/expresspolymlett.2014.95

Blum, R., Diehl, H., 2015. Barrier solutions for innovative and sustainable paper and board packaging Coating International 10-2015, 13.

Borregaard, 2014. Borregaard invests NOK 225 million in a production facility for Exilva microfibrillar cellulose. [WWW Document]. URL www.borregaard.com/New/Borregaard-invests-NOK-225-million-in-a-production-facility-for-Exilva-microfibrillater-cellulose (accessed 11.23.16).

Bras, J., Hassan, M.L., Bruzesse, C., Hassan, E.A., El-Wakil, N.A., Dufresne, A., 2010. Mechanical, barrier, and biodegradability properties of bagasse cellulose whiskers reinforced natural rubber nanocomposites. Ind. Crops Prod. 32, 627–633. doi:10.1016/j.indcrop.2010.07.018

Breiby, D.W., Samuelsen, E.J., Konovalov, O., 2003. The drying behaviour of conjugated polymer solutions. Synth. Met. 139, 361–369. doi:10.1016/S0379-6779(03)00186-3

Brundtland, G.H., 1987. Rapport Brundtland [WWW Document]. Ministère Aff. Étrangères Dév. Int. L'Odyssée Dév. Durable. URL http://www. diplomatie. gouv. fr/fr/sites/odyssee-developpementdurable/files/5/rapport_brundtland. pdf (accessed 10.17.16).

Bundersinstitut für Risikobewertung, 2016. XXXVI. Paper and board for food contact [WWW Document]. URL https://bfr.ble.de/kse/faces/resources/pdf/360-english.pdf (accessed 12.15.16).

BYK Additives & Instruments, 2015. Food Contact Regulatory Status Information - Cloisite-Na+.

Carosio, F., Cuttica, F., Medina, L., Berglund, L.A., 2016. Clay nanopaper as multifunctional brick and mortar fire protection coating—Wood case study. Mater. Des. 93, 357–363. doi:10.1016/j.matdes.2015.12.140

Carosio, F., Kochumalayil, J., Cuttica, F., Camino, G., Berglund, L., 2015. Oriented Clay Nanopaper from Biobased Component - Mechanisms for Superior Fire Protection Properties. ACS Appl. Mater. Interfaces 7, 5847–5856. doi:10.1021/am509058h

Castro, C., Vesterinen, A., Zuluaga, R., Caro, G., Filpponen, I., Rojas, O.J., Kortaberria, G., Gañán, P., 2014. In situ production of nanocomposites of poly(vinyl alcohol) and cellulose nanofibrils from Gluconacetobacter bacteria: effect of chemical crosslinking. Cellulose 21, 1745–1756. doi:10.1007/s10570-014-0170-1

Caulfield, D.F., 1994. Ester crosslinking to improve wet performance of paper using multifunctional caboxylic acids, butanetetracarboxylic and citic acid. Tappi J. 77, 205–212.

CelluComp, 2013. Applications of Curran® [WWW Document]. URL http://www.cellucomp.com/applications.html (accessed 3.26.14).

Chakraborty, A., Sain, M., Kortschot, M., 2005. Cellulose microfibrils: A novel method of preparation using high shear refining and cryocrushing. Holzforschung 59, 102–107. doi:10.1515/HF.2005.016

Chen, W., Li, Q., Cao, J., Liu, Y., Li, J., Zhang, J., Luo, S., Yu, H., 2015. Revealing the structures of cellulose nanofiber bundles obtained by mechanical nanofibrillation via TEM observation. Carbohydr. Polym. 117, 950–956. doi:10.1016/j.carbpol.2014.10.024

Chen, W., Lickfield, G.C., Yang, C.Q., 2004. Molecular modeling of cellulose in amorphous state part II: effects of rigid and flexible crosslinks on cellulose. Polymer 45, 7357–7365. doi:10.1016/j.polymer.2004.08.023

Chen, X., Ren, J., Meng, L., 2015. Influence of Ammonium Zirconium Carbonate on Properties of Poly(vinyl alcohol)/Xylan Composite Films. J. Nanomater. 2015, Article ID 810464, 8 pages. doi:10.1155/2015/810464

Chinga-Carrasco, G., 2011. Cellulose fibres, nanofibrils and microfibrils: the morphological sequence of MFC components from a plant physiology and fibre technology point of view. Nanoscale Res. Lett. 6, 1–7.

Chinga-Carrasco, G., Averianova, N., Kondalenko, O., Garaeva, M., Petrov, V., Leinsvang, B., Karlsen, T., 2014. The effect of residual fibres on the micro-topography of cellulose nanopaper. Micron 56, 80–84. doi:10.1016/j.micron.2013.09.002

Chivrac, F., Pollet, E., Avérous, L., 2009. Progress in nano-biocomposites based on polysaccharides and nanoclays. Mater. Sci. Eng. R Rep. 67, 1–17. doi:10.1016/j.mser.2009.09.002

Choudalakis, G., Gotsis, A.D., 2009. Permeability of polymer/clay nanocomposites: A review. Eur. Polym. J. 45, 967–984. doi:10.1016/j.eurpolymj.2009.01.027

Clark, B.C., Arvidson, R.E., Gellert, R., Morris, R.V., Ming, D.W., Richter, L., Ruff, S.W., Michalski, J.R., Farrand, W.H., Yen, A., Herkenhoff, K.E., Li, R., Squyres, S.W., Schröder, C., Klingelhöfer, G., Bell, J.F., 2007. Evidence for montmorillonite or its compositional equivalent in Columbia Hills, Mars. J. Geophys. Res. Planets 112, E06S01. doi:10.1029/2006JE002756

Clegg, F., Breen, C., Khairuddin, 2014. Synergistic and Competitive Aspects of the Adsorption of Poly(ethylene glycol) and Poly(vinyl alcohol) onto Na-Bentonite. J. Phys. Chem. B 118, 13268–13278. doi:10.1021/jp507772t

Coexpan, n.d. Film plastique haute barrière pour l'industrie alimentaire [WWW Document]. URL http://www.coexpan.com/fr/materiaux/haute-barriere (accessed 8.25.16).

Coma, V., Sebti, I., Pardon, P., Pichavant, F.H., Deschamps, A., 2003. Film properties from crosslinking of cellulosic derivatives with a polyfunctional carboxylic acid. Carbohydr. Polym. 51, 265–271. doi:10.1016/S0144-8617(02)00191-1

Crank, J., 1975. The Mathematics of Diffusion: 2d ed. Clarendon Press, Oxford.

Dean, K.M., Do, M.D., Petinakis, E., Yu, L., 2008. Key interactions in biodegradable thermoplastic starch/poly(vinyl alcohol)/montmorillonite micro- and nanocomposites. Compos. Sci. Technol. 68, 1453–1462. doi:10.1016/j.compscitech.2007.10.037

Demitri, C., Del Sole, R., Scalera, F., Sannino, A., Vasapollo, G., Maffezzoli, A., Ambrosio, L., Nicolais, L., 2008. Novel superabsorbent cellulose-based hydrogels crosslinked with citric acid. J. Appl. Polym. Sci. 110, 2453–2460. doi:10.1002/app.28660

Diddens, I., Murphy, B., Krisch, M., Müller, M., 2008. Anisotropic Elastic Properties of Cellulose Measured Using Inelastic X-ray Scattering. Macromolecules 41, 9755–9759. doi:10.1021/ma801796u

Dimic-Misic, K., Gane, P.A.C., Paltakari, J., 2013. Micro- and Nanofibrillated Cellulose as a Rheology Modifier Additive in CMC-Containing Pigment-Coating Formulations. Ind. Eng. Chem. Res. 52, 16066–16083. doi:10.1021/ie4028878

Dufresne, A., 2012. Nanocellulose: from nature to high performance tailored materials. De Gruyter, Berlin ; Boston.

DuPont Packaging & Industrial Polymers, Packaging World, 2012. Survey of Future Packaging Trends [WWW Document]. URL http://www2.dupont.com/Packaging_Resins/en_US/assets/downloads/Survey_of_Future_Packaging_Trends.pdf (accessed 10.18.16).

Eichhorn, S.J., Dufresne, A., Aranguren, M., Marcovich, N.E., Capadona, J.R., Rowan, S.J., Weder, C., Thielemans, W., Roman, M., Renneckar, S., Gindl, W., Veigel, S., Keckes, J., Yano, H., Abe, K., Nogi, M., Nakagaito, A.N., Mangalam, A., Simonsen, J., Benight, A.S., Bismarck, A., Berglund, L.A., Peijs, T., 2010. Review: current international research into cellulose nanofibres and nanocomposites. J. Mater. Sci. 45, 1–33. doi:10.1007/s10853-009-3874-0

European Parliament, 2011. COMMISSION REGULATION (EU) No 10/2011 of 14 January 2011 on plastic materials and articles intended to come into contact with food. Off. J. Eur. Union.

European Parliament, D.E., 2004. REGULATION (EC) No 1935/2004 OF THE EUROPEAN PARLIAMENT AND OF THE COUNCIL of 27 October 2004 on materials and articles intended to come into contact with food and repealing directives 80/590/EEC and 89/109/EEC. Off. J. Eur. Union.

European Parliament & Council, 2008. Waste Framework Directive 2008/98/EC [WWW Document]. URL http://eur-lex.europa.eu/LexUriServ/LexUriServ.do?uri=OJ:L:2008:312:0003:0030:en:PDF (accessed 10.17.16).

EUROPEN, 2014. Packaging and Packaging Waste Statistics 1998-2011 [WWW Document]. URL http://www.europen-packaging.eu//index.php?option=com_downloads&id=1474 (accessed 10.17.16).

Exilva, 2016. Application Bulletin - Paints and coatings.

Fang, Z., Zhu, H., Yuan, Y., Ha, D., Zhu, S., Preston, C., Chen, Q., Li, Y., Han, X., Lee, S., Chen, G., Li, T., Munday, J., Huang, J., Hu, L., 2014. Novel Nanostructured Paper with Ultrahigh Transparency and Ultrahigh Haze for Solar Cells. Nano Lett. 14, 765–773. doi:10.1021/nl404101p

Feldmeier, D., 2009. Kraft Food's/Oscar Mayer's Barrier Property Requirements and Associated Flexible Packaging Challenges [WWW Document]. URL http://www.tappi.org/content/events/09placesy/course_papers/feldmeier.pdf (accessed 12.3.15).

Fujisawa, S., Okita, Y., Fukuzumi, H., Saito, T., Isogai, A., 2011. Preparation and characterization of TEMPO-oxidized cellulose nanofibril films with free carboxyl groups. Carbohydr. Polym. 84, 579–583. doi:10.1016/j.carbpol.2010.12.029

Fukuzumi, H., Fujisawa, S., Saito, T., Isogai, A., 2013. Selective Permeation of Hydrogen Gas Using Cellulose Nanofibril Film. Biomacromolecules 14, 1705–1709. doi:10.1021/bm400377e

Fukuzumi, H., Saito, T., Iwata, T., Kumamoto, Y., Isogai, A., 2009. Transparent and High Gas Barrier Films of Cellulose Nanofibers Prepared by TEMPO-Mediated Oxidation. Biomacromolecules 10, 162–165. doi:10.1021/bm801065u

Future Markets, 2014. Nanocellulose - The Global Market, Forecast from 2009 to 2024.

Giannelis, E.P., Krishnamoorti, R., Manias, E., 1999. Polymer-Silicate Nanocomposites: Model Systems for Confined Polymers and Polymer Brushes, in: Granick, S., Binder, K., Gennes, P.-G. de, Giannelis, E.P., Grest, G.S., Hervet, H., Krishnamoorti, R., Léger, L., Manias, E., Raphaël, E., Wang, S.-Q. (Eds.), Polymers in Confined Environments, Advances in Polymer Science. Springer Berlin Heidelberg, pp. 107–147.

Girard, F., 2011. Barrier materials. Presented at the Formation barrier at CTP, Centre Technique du Papier, France.

Grewal, H.S., Kalra, K.L., 1995. Fungal production of citric acid. Biotechnol. Adv. 13, 209–234. doi:10.1016/0734-9750(95)00002-8

Grüneberger, F., Künniger, T., Zimmermann, T., Arnold, M., 2014. Rheology of nanofibrillated cellulose/acrylate systems for coating applications. Cellulose 21, 1313–1326. doi:10.1007/s10570-014-0248-9

Grunlan, J.C., Grigorian, A., Hamilton, C.B., Mehrabi, A.R., 2004. Effect of clay concentration on the oxygen permeability and optical properties of a modified poly(vinyl alcohol). J. Appl. Polym. Sci. 93, 1102–1109. doi:10.1002/app.20564

Guerin, D., Rharbi, Y., Huber, P., Meyer, V., 2016a. Process and Device for Manufacturing a Laminated Material Comprising a Fibrillated Cellulose Layer. WO2016174348 (A1).

Guerin, D., Zeno, E., Crowther-Alwyn, L., 2016b. Cellulose-based packaging materials for pouch cells. Presented at the 2016 E-MRS Fall Meeting and Exhibition, Warsaw, Poland.

Guezennec, C., 2012. Development of new packaging materials based on micro- and nano-fibrillated cellulose. PhD thesis, Université de Grenoble.

Guezennec, C., Girard, F., Dufresne, A., Guerin, D., 2014. The use of microfibrillated cellulose to develop a barrier packaging board. Presented at the 8th CTP-PTS International Symposium on Packaging Design and Recycling, Grenoble, France.

Hämäläinen, M., 2016. Kotkamill's new Consumer Board machine now in production [WWW Document]. URL http://www.kotkamills.com/en/news/PHPSESSID=0nnol29dindq2beq0pj8mnvsk7/body0=1718 (accessed 11.20.16).

Harmsen, P.F., Hackmann, M.M., Bos, H.L., 2014. Green building blocks for bio-based plastics. Biofuels Bioprod. Biorefining 8, 306–324.

Hassan, M.L., Mathew, A.P., Hassan, E.A., El-Wakil, N.A., Oksman, K., 2012. Nanofibers from bagasse and rice straw: process optimization and properties. Wood Sci. Technol. 46, 193–205. doi:10.1007/s00226-010-0373-z

Heiskanen, I., Backfolk, K., Axrup, L., 2011. A coated substrate, a process for production of a coated substrate, a package and a dispersion coating. WO 2011056130.

Hejri, Z., Ahmadpour, A., Seifkordi, A.A., Zebarjad, S.M., 2012. Role of nano-sized TiO2 on mechanical and thermal behavior of starch/Poly (vinyl alcohol) blend films. Int. J. Nanosci. Nanotechnol. 8, 215–226.

Henriksson, M., Berglund, L.A., Isaksson, P., Lindström, T., Nishino, T., 2008. Cellulose Nanopaper Structures of High Toughness. Biomacromolecules 9, 1579–1585. doi:10.1021/bm800038n

Ho, T.T.T., Ko, Y.S., Zimmermann, T., Geiger, T., Caseri, W., 2012a. Processing and characterization of nanofibrillated cellulose/layered silicate systems. J. Mater. Sci. 47, 4370–4382. doi:10.1007/s10853-012-6291-8

Ho, T.T.T., Zimmermann, T., Ohr, S., Caseri, W.R., 2012b. Composites of Cationic Nanofibrillated Cellulose and Layered Silicates: Water Vapor Barrier and Mechanical Properties. ACS Appl. Mater. Interfaces 4, 4832–4840. doi:10.1021/am3011737

Honorato, C., Kumar, V., Liu, J., Koivula, H., Xu, C., Toivakka, M., 2015. Transparent nanocellulose-pigment composite films. J. Mater. Sci. 50, 7343–7352.

Hu, H., Zhang, X., He, Y., Guo, Z., Zhang, J., Song, Y., 2013. Combined effect of relative humidity and temperature on dynamic viscoelastic properties and glass transition of poly(vinyl alcohol). J. Appl. Polym. Sci. 130, 3161–3167. doi:10.1002/app.39547

Huis in't Veld, J.H.J., 1996. Microbial and biochemical spoilage of foods: an overview. Int. J. Food Microbiol., Specific Spoilage Organisms 33, 1–18. doi:10.1016/0168-1605(96)01139-7

Hult, E.-L., Iotti, M., Lenes, M., 2010. Efficient approach to high barrier packaging using microfibrillar cellulose and shellac. Cellulose 17, 575–586. doi:10.1007/s10570-010-9408-8

International Chemical Safety Cards (ICSC), 2015. ICSC:NFRN1489 International Chemical Safety Cards (WHO/IPCS/ILO) | CDC/NIOSH [WWW Document]. URL http://www.cdc.gov/niosh/ipcsnfrn/nfrn1489.html (accessed 9.23.15).

Iotti, M., Øyvind, E., Ø, G., Lenes, M., 2010. Semi industrial application of MFC barrier coating, a rheological and technological study [WWW Document]. URL http://www.tappi.org/content/events/10nano/papers/25.1.pdf (accessed 5.7.15).

Isogai, A., Saito, T., Fukuzumi, H., 2011. TEMPO-oxidized cellulose nanofibers. Nanoscale 3, 71. doi:10.1039/c0nr00583e

Iwamoto, S., Abe, K., Yano, H., 2008. The Effect of Hemicelluloses on Wood Pulp Nanofibrillation and Nanofiber Network Characteristics. Biomacromolecules 9, 1022–1026. doi:10.1021/bm701157n

Jansson, 2006. Barrier and film properties of plastisol coatings, a water free coating application based on mixtures of starch, poly(vinyl alcohol) and poly(alkyl methacrylate). Nord. Pulp Pap. Res. J. 21, 690–696. doi:10.3183/NPPRJ-2006-21-05-p690-696

Javed, A., Ullsten, H., Ernstsson, M., Järnström, L., 2016. Study of starch and starch-PVOH blends and effects of plasticizers on mechanical and barrier properties of coated paperboard. Nord. Pulp Pap. Res. J. 31, 499–510. doi:10.3183/NPPRJ-2016-31-03-p499-510

Jimenez, G., Ogata, N., Kawai, H., Ogihara, T., 1997. Structure and thermal/mechanical properties of poly (ϵ-caprolactone)-clay blend. J. Appl. Polym. Sci. 64, 2211–2220. doi:10.1002/(SICI)1097-4628(19970613)64:11<2211::AID-APP17>3.0.CO;2-6

Jo, J.-Y., Min, C.-K., Shin, J.-S., 2012. Manufacture of water-resistant corrugated board boxes for agricultural products in the cold chain system. J. Korea Tech. Assoc. Pulp Pap. Ind. 44, 29–34.

Kangas, H., Lahtinen, P., Sneck, A., Saariaho, A.-M., Laitinen, O., Hellen, E., 2014. Characterization of fibrillated celluloses. A short review and evaluation of characteristics with a combination of methods. Nord. Pulp Pap. Res. J. 29, 129–143.

KEGG, 2015. KEGG COMPOUND: C00158 (Citric acid) [WWW Document]. URL http://www.genome.jp/dbget-bin/www_bget?cpd:C00158 (accessed 9.30.15).

Keski-Orvola, H., 2007. The contemporary drying of paper and paperboard coatings. Master thesis, Tampere Polytechnic.

Khwaldia, K., Arab-Tehrany, E., Desobry, S., 2010. Biopolymer coatings on paper packaging materials. Compr. Rev. Food Sci. Food Saf. 9, 82–91.

Kim, J., Kim, S.W., Park, S., Lim, K.T., Seonwoo, H., Kim, Y., Hong, B.H., Choung, Y.-H., Chung, J.H., 2013. Bacterial cellulose nanofibrillar patch as a wound healing platform of tympanic membrane perforation. Adv. Healthc. Mater. 2, 1525–1531. doi:10.1002/adhm.201200368

Kisku, S.K., Sarkar, N., Dash, S., Swain, S.K., 2014. Preparation of Starch/PVA/$CaCO_3$ Nanobiocomposite Films: Study of Fire Retardant, Thermal Resistant, Gas Barrier and Biodegradable Properties. Polym.-Plast. Technol. Eng. 53, 1664–1670. doi:10.1080/03602559.2014.919650

Klatte, F., Zacharias, E., 1999. Mowiol Brochure En Kse. Preservation 500, 13.

Kumar, V., Elfving, A., Koivula, H., Bousfield, D., Toivakka, M., 2016. Roll-to-Roll Processed Cellulose Nanofiber Coatings. Ind. Eng. Chem. Res. 55, 3603–3613. doi:10.1021/acs.iecr.6b00417

Kunnas, L., Siren, A., 2014. A material for packaging of foodstuff, and a package for foodstuff. EP2730698 (A1).

Lange, J., Wyser, Y., 2003. Recent innovations in barrier technologies for plastic packaging - a review. Packag. Technol. Sci. 16, 149–158. doi:10.1002/pts.621

Lavoine, N., 2014. Design, Processing and Characterization of innovative functional bio-nano-materials for packaging. PhD thesis, University of Grenoble, Grenoble.

Lavoine, N., Desloges, I., Khelifi, B., Bras, J., 2014. Impact of different coating processes of microfibrillated cellulose on the mechanical and barrier properties of paper. J. Mater. Sci. 49, 2879–2893. doi:10.1007/s10853-013-7995-0

Liu, A., Berglund, L.A., 2013. Fire-retardant and ductile clay nanopaper biocomposites based on montmorrilonite in matrix of cellulose nanofibers and carboxymethyl cellulose. Eur. Polym. J. 49, 940–949. doi:10.1016/j.eurpolymj.2012.12.017

Liu, A., Berglund, L.A., 2012. Clay nanopaper composites of nacre-like structure based on montmorrilonite and cellulose nanofibers—Improvements due to chitosan addition. Carbohydr. Polym. 87, 53–60. doi:10.1016/j.carbpol.2011.07.019

Liu, A., Walther, A., Ikkala, O., Belova, L., Berglund, L.A., 2011. Clay Nanopaper with Tough Cellulose Nanofiber Matrix for Fire Retardancy and Gas Barrier Functions. Biomacromolecules 12, 633–641. doi:10.1021/bm101296z

Liu, G., Song, Y., Wang, J., Zhuang, H., Ma, L., Li, C., Liu, Y., Zhang, J., 2014. Effects of nanoclay type on the physical and antimicrobial properties of PVOH-based nanocomposite films. LWT - Food Sci. Technol. 57, 562–568. doi:10.1016/j.lwt.2014.01.009

Liu, L., Chen, Y.Z., Zhang, Z.J., 2013. Preparation of the Microfibrillated Cellulose and its Application in the Food Packaging Paper. Appl. Mech. Mater. 469, 87–90. doi:10.4028/www.scientific.net/AMM.469.87

Locre, C., 2016. Les Matériaux Barrières : Définitions et Utilisations. Presented at the Formation barrier at CTP, Centre Technique du Papier, France.

Lundahl, M.J., Cunha, A.G., Rojo, E., Papageorgiou, A.C., Rautkari, L., Arboleda, J.C., Rojas, O.J., 2016. Strength and Water Interactions of Cellulose I Filaments Wet-Spun from Cellulose Nanofibril Hydrogels. Sci. Rep. 6, 30695. doi:10.1038/srep30695

Luu, W.T., Bousfield, D.W., 2011. Application of nano-fibrillated cellulose as a paper surface treatment for inkjet printing [WWW Document]. URL http://www.tappi.org/content/events/11papercon/documents/212.517.pdf (accessed 3.19.14).

Lynd, L.R., Weimer, P.J., Zyl, W.H. van, Pretorius, I.S., 2002. Microbial Cellulose Utilization: Fundamentals and Biotechnology. Microbiol. Mol. Biol. Rev. 66, 506–577. doi:10.1128/MMBR.66.3.506-577.2002

Ma, H., Hsiao, B.S., Chu, B., 2013. Highly permeable nanofibrous membranes for energy efficient water purification, in: Abstracts of Papers of the American Chemical Society. Amer Chemical Soc 1155 16th St, Nw, Washington, DC 20036 USA.

Mahendia, S., Tomar, A.K., Goyal, P.K., Kumar, S., 2013. Tuning of refractive index of poly(vinyl alcohol): Effect of embedding Cu and Ag nanoparticles. J. Appl. Phys. 113, 73103. doi:10.1063/1.4792473

Malmborg, K., Heijnesson-Hulten, A.M., Sandstroem, J., 2011. Cellulosic Barrier Composition Comprising Anionic Polymer. WO2011147823 (A1).

Marin, E., Rojas, J., Ciro, Y., 2014. A review of polyvinyl alcohol derivatives: Promising materials for pharmaceutical and biomedical applications. Afr. J. Pharm. Pharmacol. 8, 674–684.

Martins, N.C.T., Freire, C.S.R., Neto, C.P., Silvestre, A.J.D., Causio, J., Baldi, G., Sadocco, P., Trindade, T., 2013. Antibacterial paper based on composite coatings of nanofibrillated cellulose and ZnO. Colloids Surf. Physicochem. Eng. Asp. 417, 111–119. doi:10.1016/j.colsurfa.2012.10.042

Mathew, A.P., Liu, P., Karim, Z., Oksman, K., 2014. Nanocellulose and functional material for water cleaning, in: ACS National Meeting & Exhibition: 16/03/2014-20/03/2014.

Matsumura, S., Kurita, H., Shimokobe, H., 1993. Anaerobic biodegradability of polyvinyl alcohol. Biotechnol. Lett. 15, 749–754.

Mikkonen, K.S., Schmidt, J., Vesterinen, A.-H., Tenkanen, M., 2013. Crosslinking with ammonium zirconium carbonate improves the formation and properties of spruce galactoglucomannan films. J. Mater. Sci. 48, 4205–4213. doi:10.1007/s10853-013-7233-9

Minelli, M., Baschetti, M.G., Doghieri, F., Ankerfors, M., Lindström, T., Siró, I., Plackett, D., 2010. Investigation of mass transport properties of microfibrillated cellulose (MFC) films. J. Membr. Sci. 358, 67–75. doi:10.1016/j.memsci.2010.04.030

Ming, S., Chen, G., Wu, Z., Su, L., He, J., Kuang, Y., Fang, Z., 2016. Effective dispersion of aqueous clay suspension using carboxylated nanofibrillated cellulose as dispersant. RSC Adv 6, 37330–37336. doi:10.1039/C6RA03935A

Modified Atmosphere Packaging.com, 2012. Modified atmosphere packaging of fresh meat [WWW Document]. URL http://www.modifiedatmospherepackaging.com/Applications/Modified-atmosphere-packaging-fresh-meat.aspx (accessed 10.17.16).

Moles, P.J., 2002. The use of zirconium in Surface Coatings. Data Sheet 117776-1780 MEL Chem.

Mondi, 2015. Mondi presents alufree BarrierFilm for food packaging at FachPack 2015 [WWW Document]. URL http://www.mondigroup.com/products/desktopdefault.aspx/tabid-1346/345_read-28956 (accessed 8.26.16).

Montserrat, S., Cortés, P., Calventus, Y., Hutchinson, J., 1997. The use of DSC to characterize structural relaxation in thermosetting polymers. J. Therm. Anal. Calorim. 49, 79–85.

Navarri, P., Andrieu, J., 1993. High-intensity infrared drying study: part II. Case of thin coated films. Chem. Eng. Process. Process Intensif. 32, 319–325.

Nechyporchuk, O., Belgacem, M.N., Bras, J., 2016a. Production of cellulose nanofibrils: A review of recent advances. Ind. Crops Prod. doi:10.1016/j.indcrop.2016.02.016

Nechyporchuk, O., Belgacem, M.N., Pignon, F., 2016b. Current Progress in Rheology of Cellulose Nanofibril Suspensions. Biomacromolecules 17, 2311–2320. doi:10.1021/acs.biomac.6b00668

Nechyporchuk, O., Pignon, F., Belgacem, M.N., 2015. Morphological properties of nanofibrillated cellulose produced using wet grinding as an ultimate fibrillation process. J. Mater. Sci. 50, 531–541. doi:10.1007/s10853-014-8609-1

Nishioka, Y., Kobayashi, M., 2016. Gas Barrier Material, Method for Producing the Same, and Gas Barrier Film. JP2016011392 (A).

Nogi, M., Handa, K., Nakagaito, A.N., Yano, H., 2005. Optically transparent bionanofiber composites with low sensitivity to refractive index of the polymer matrix. Appl. Phys. Lett. 87, 243110. doi:10.1063/1.2146056

Nuopponen, M., Tamper, J., Kajanto, I., 2016. Method and device for monitoring the quality of nanofibrillar cellulose. WO2016001480 A1.

Nygards, S., 2011. Nanocellulose in pigment coatings: Aspects of barrier properties and printability in offset. Master thesis, Linköping University.

Obokata, T., Isogai, A., 2007. The mechanism of wet-strength development of cellulose sheets prepared with polyamideamine-epichlorohydrin (PAE) resin. Colloids Surf. Physicochem. Eng. Asp. 302, 525–531. doi:10.1016/j.colsurfa.2007.03.025

Oishi, Y., Hotta, A., 2014. The Structure and the Mechanical Properties of a Newly Fabricated Cellulose-Nanofiber/Polyvinyl-Alcohol Composite. MRS Proc. 1621, 149–154. doi:10.1557/opl.2014.141

Okamoto, M., Noda, T., Kato, M., Chatani, A., 2014. Barrier Paper Packaging Material. WO2014181560 (A1).

Okamoto, M., Okubo, Y., Kato, M., Yamashita, H., Fukunaga, M., 2015. Barrier Packaging Material Made of Paper. JP2015227517 (A).

Oksanen, T., Buchert, J., Viikari, L., 1997. The Role of Hemicelluloses in the Hornification of Bleached Kraft Pulps. Holzforschung 51, 355–360. doi:10.1515/hfsg.1997.51.4.355

Olsson, E., 2013. Effects of Citric Acid on Starch-Based Barrier Coatings. PhD thesis, Karlstads universitet.

Olsson, E., Hedenqvist, M.S., Johansson, C., Järnström, L., 2013a. Influence of citric acid and curing on moisture sorption, diffusion and permeability of starch films. Carbohydr. Polym. 94, 765–772. doi:10.1016/j.carbpol.2013.02.006

Olsson, E., Johansson, C., Järnström, L., 2014. Montmorillonite for starch-based barrier dispersion coating — Part 1: The influence of citric acid and poly(ethylene glycol) on viscosity and barrier properties. Appl. Clay Sci. 97–98, 160–166. doi:10.1016/j.clay.2014.04.040

Olsson, E., Menzel, C., Johansson, C., Andersson, R., Koch, K., Järnström, L., 2013b. The effect of pH on hydrolysis, cross-linking and barrier properties of starch barriers containing citric acid. Carbohydr. Polym. 98, 1505–1513. doi:10.1016/j.carbpol.2013.07.040

Österberg, M., Vartiainen, J., Lucenius, J., Hippi, U., Seppälä, J., Serimaa, R., Laine, J., 2013. A Fast Method to Produce Strong NFC Films as a Platform for Barrier and Functional Materials. ACS Appl. Mater. Interfaces 5, 4640–4647. doi:10.1021/am401046x

Pääkkö, M., Ankerfors, M., Kosonen, H., Nykänen, A., Ahola, S., Österberg, M., Ruokolainen, J., Laine, J., Larsson, P.T., Ikkala, O., Lindström, T., 2007. Enzymatic Hydrolysis Combined with Mechanical Shearing and High-Pressure Homogenization for Nanoscale Cellulose Fibrils and Strong Gels. Biomacromolecules 8, 1934–1941. doi:10.1021/bm061215p

Pääkkö, M., Vapaavuori, J., Silvennoinen, R., Kosonen, H., Ankerfors, M., Lindström, T., Berglund, L.A., Ikkala, O., 2008. Long and entangled native cellulose I nanofibers allow flexible aerogels and hierarchically porous templates for functionalities. Soft Matter 4, 2492–2499. doi:10.1039/B810371B

Paralikar, S.A., Simonsen, J., Lombardi, J., 2008. Poly(vinyl alcohol)/cellulose nanocrystal barrier membranes. J. Membr. Sci. 320, 248–258. doi:10.1016/j.memsci.2008.04.009

Paul, D.R., Robeson, L.M., 2008. Polymer nanotechnology: Nanocomposites. Polymer 49, 3187–3204. doi:10.1016/j.polymer.2008.04.017

Peppas, N.A., Merrill, E.W., 1976. Differential scanning calorimetry of crystallized PVA hydrogels. J. Appl. Polym. Sci. 20, 1457–1465.

Plackett, D. (Ed.), 2011. Biopolymers: New materials for sustainable films and coatings. John Wiley & Sons, Ltd, Chichester, UK.

Plackett, D., Anturi, H., Hedenqvist, M., Ankerfors, M., Gällstedt, M., Lindström, T., Siró, I., 2010. Physical properties and morphology of films prepared from microfibrillated cellulose and microfibrillated cellulose in combination with amylopectin. J. Appl. Polym. Sci. 117, 3601–3609.

Podsiadlo, P., Kaushik, A.K., Arruda, E.M., Waas, A.M., Shim, B.S., Xu, J., Nandivada, H., Pumplin, B.G., Lahann, J., Ramamoorthy, A., Kotov, N.A., 2007. Ultrastrong and Stiff Layered Polymer Nanocomposites. Science 318, 80–83. doi:10.1126/science.1143176

Pöhler, T., Lappalainen, T., Tammelin, T., Eronen, P., Hiekkataipale, P.H., Vehniäinen, A., Koskinen, T.M., 2010. Influence of fibrillation method on the character of nanofibrillated cellulose (NFC), in: TAPPI International Conference on Nanotechnology for the Forest Products Industry. pp. 27–29.

Quellmalz, A., Mihranyan, A., 2015. Citric acid cross-linked nanocellulose-based paper for size-exclusion nanofiltration. ACS Biomater. Sci. Eng. 1, 271–276.

Qvintus, P., Kangas, H., 2015. VTT Webinar: Cellulose nanofibrils (CNF) – a big hype or on the edge of a breakthrough [WWW Document]. URL https://youtu.be/Yctog3J7shk?t=25m40s (accessed 10.27.16).

Rodionova, G., Saito, T., Lenes, M., Eriksen, Ø., Gregersen, Ø., Fukuzumi, H., Isogai, A., 2012. Mechanical and oxygen barrier properties of films prepared from fibrillated dispersions of TEMPO-oxidized Norway spruce and Eucalyptus pulps. Cellulose 19, 705–711. doi:10.1007/s10570-012-9664-x

Rojas, J., Azevedo, E., 2011. Functionalization and crosslinking of microcrystalline cellulose in aqueous media: A safe and economic approach. Int. J. Pharm. Sci. Rev. Res 8, 28–36.

Scalzo, R.P., Brandenburg, J.E., Mitchell, M.L., Mitchell, P.H., Mitchell, M.G., Mitchell, C.G., Wolfe, T.J., Wolfe, A.L., 2014. Extrudable composition derived from renewable resources. WO 2014052300.

Schexnailder, P., Schmidt, G., 2009. Nanocomposite polymer hydrogels. Colloid Polym. Sci. 287, 1–11. doi:10.1007/s00396-008-1949-0

Schmidt, W., Papier, G., Schlenstedt, M., Gericke, R., Fehlker, A., 2015. Receiving Layer for Digital Printing Methods Having Nanofibrillated Cellulose. US20150140237 A1.

Sehaqui, H., Liu, A., Zhou, Q., Berglund, L.A., 2010. Fast Preparation Procedure for Large, Flat Cellulose and Cellulose/Inorganic Nanopaper Structures. Biomacromolecules 11, 2195–2198. doi:10.1021/bm100490s

Sehaqui, H., Zimmermann, T., Tingaut, P., 2014. Hydrophobic cellulose nanopaper through a mild esterification procedure. Cellulose 21, 367–382. doi:10.1007/s10570-013-0110-5

Shi, J.J., Yang, E.L., 2015. Green Electrospinning and Crosslinking of Polyvinyl Alcohol/Citric Acid. J. Nano Res. 32, 32–42. doi:10.4028/www.scientific.net/JNanoR.32.32

Shi, Z., Phillips, G.O., Yang, G., 2013. Nanocellulose electroconductive composites. Nanoscale 5, 3194–3201. doi:10.1039/C3NR00408B

Shi, Z., Zhang, Y., Phillips, G.O., Yang, G., 2014. Utilization of bacterial cellulose in food. Food Hydrocoll. 35, 539–545. doi:10.1016/j.foodhyd.2013.07.012

Shimao, M., 2001. Biodegradation of plastics. Curr. Opin. Biotechnol. 12, 242–247.

Shimizu, M., Saito, T., Isogai, A., 2016. Water-resistant and high oxygen-barrier nanocellulose films with interfibrillar cross-linkages formed through multivalent metal ions. J. Membr. Sci. 500, 1–7. doi:10.1016/j.memsci.2015.11.002

Sigma Aldrich, 2015. Ammonium zirconium(IV) carbonate solution in H2O [WWW Document]. URL http://www.sigmaaldrich.com/catalog/product/aldrich/464597?lang=fr&region=FR (accessed 9.30.15).

Sinha Ray, S., Okamoto, M., 2003. Polymer/layered silicate nanocomposites: a review from preparation to processing. Prog. Polym. Sci. 28, 1539–1641. doi:10.1016/j.progpolymsci.2003.08.002

Siqueira, E.J., 2012. Polyamidoamine epichlorohydrin-based papers: mechanisms of wet strength development and paper repulping. PhD thesis, Université de Grenoble.

Siqueira, G., Bras, J., Dufresne, A., 2010. Cellulosic Bionanocomposites: A Review of Preparation, Properties and Applications. Polymers 2, 728–765. doi:10.3390/polym2040728

Siqueira, G., Bras, J., Dufresne, A., 2009. Cellulose Whiskers versus Microfibrils: Influence of the Nature of the Nanoparticle and its Surface Functionalization on the Thermal and Mechanical Properties of Nanocomposites. Biomacromolecules 10, 425–432. doi:10.1021/bm801193d

Siqueira, G., Fraschini, C., Bras, J., Dufresne, A., Prud'homme, R., Laborie, M.-P., 2011. Impact of the nature and shape of cellulosic nanoparticles on the isothermal crystallization kinetics of poly(ε-caprolactone). Eur. Polym. J. 47, 2216–2227. doi:10.1016/j.eurpolymj.2011.09.014

Siró, I., Plackett, D., Hedenqvist, M., Ankerfors, M., Lindström, T., 2011. Highly transparent films from carboxymethylated microfibrillated cellulose: The effect of multiple homogenization steps on key properties. J. Appl. Polym. Sci. 119, 2652–2660. doi:10.1002/app.32831

Slavutsky, A.M., Bertuzzi, M.A., Armada, M., 2012. Water barrier properties of starch-clay nanocomposite films. Braz. J. Food Technol. 15, 208–218. doi:10.1590/S1981-67232012005000014

Song, 2010. Reduction of the linting and dusting propensity of newspaper using starch and microfibrillated cellulose. Nord. Pulp Pap. Res. J. 25, 495–504. doi:10.3183/NPPRJ-2010-25-04-p495-504

Song, D., 2011. Starch crosslinking for cellulose fiber modification and starch nanoparticle formation. PhD thesis, Georgia Institute of Technology.

Song, D., Breedveld, V., Deng, Y., 2011. Rheological study of self-crosslinking and co-crosslinking of ammonium zirconium carbonate and starch in aqueous solutions. J. Appl. Polym. Sci. 122, 1019–1029. doi:10.1002/app.34215

Spence, K.L., Venditti, R.A., Habibi, Y., Rojas, O.J., Pawlak, J.J., 2010a. The effect of chemical composition on microfibrillar cellulose films from wood pulps: Mechanical processing and physical properties. Bioresour. Technol. 101, 5961–5968. doi:10.1016/j.biortech.2010.02.104

Spence, K.L., Venditti, R.A., Rojas, O.J., Habibi, Y., Pawlak, J.J., 2011a. A comparative study of energy consumption and physical properties of microfibrillated cellulose produced by different processing methods. Cellulose 18, 1097–1111. doi:10.1007/s10570-011-9533-z

Spence, K.L., Venditti, R.A., Rojas, O.J., Habibi, Y., Pawlak, J.J., 2010b. The effect of chemical composition on microfibrillar cellulose films from wood pulps: water interactions and physical properties for packaging applications. Cellulose 17, 835–848. doi:10.1007/s10570-010-9424-8

Spence, K.L., Venditti, R.A., Rojas, O.J., Pawlak, J.J., Hubbe, M.A., 2011b. Water vapor barrier properties of coated and filled microfibrillated cellulose composite films. BioResources 6, 4370–4388.

Spoljaric, S., Salminen, A., Dang Luong, N., Lahtinen, P., Vartiainen, J., Tammelin, T., Seppälä, J., 2014. Nanofibrillated cellulose, poly(vinyl alcohol), montmorillonite clay hybrid nanocomposites with superior barrier and thermomechanical properties. Polym. Compos. 35, 1117–1131. doi:10.1002/pc.22759

Stone, S.A., Gosavi, P., Athauda, T.J., Ozer, R.R., 2013. In situ citric acid crosslinking of alginate/polyvinyl alcohol electrospun nanofibers. Mater. Lett. 112, 32–35. doi:10.1016/j.matlet.2013.08.100

Stora Enso, 2014. PerformaNatura [WWW Document]. URL http://assets.storaenso.com/se/renewablepackaging/DownloadDocuments/PerformaNatura-en.pdf (accessed 3.18.15).

Strawhecker, K.E., Manias, E., 2000. Structure and Properties of Poly(vinyl alcohol)/Na+ Montmorillonite Nanocomposites. Chem. Mater. 12, 2943–2949. doi:10.1021/cm000506g

Surip, S.N., Wan Jaafar, W.N.R., Azmi, N.N., Anwar, U.M.K., 2012. Microscopy Observation on Nanocellulose from Kenaf Fibre. Adv. Mater. Res. 488–489, 72–75. doi:10.4028/www.scientific.net/AMR.488-489.72

Sydney Gladman, A., Matsumoto, E.A., Nuzzo, R.G., Mahadevan, L., Lewis, J.A., 2016. Biomimetic 4D printing. Nat. Mater. 15, 413–418. doi:10.1038/nmat4544

Syverud, K., Stenius, P., 2009. Strength and barrier properties of MFC films. Cellulose 16, 75–85. doi:10.1007/s10570-008-9244-2

Taniguchi, T., Okamura, K., 1998. New films produced from microfibrillated natural fibres. Polym. Int. 47, 291–294.

Tapin-Lingua, S., 2013. Microfibrillated Cellulose and production optimization. Presented at the BioMatPack Winter Training School - Use of nanopolysaccharides in Biobased Packaging, Grenoble, France.

Tetra Pack, 2015. The environmental impact plays an important role in purchasing decisions. IPW 6–7/2015, 14.

Thomassin, J.-M., Pagnoulle, C., Caldarella, G., Germain, A., Jérôme, R., 2006. Contribution of nanoclays to the barrier properties of a model proton exchange membrane for fuel cell application. J. Membr. Sci. 270, 50–56.

Trifol, J., Plackett, D., Sillard, C., Szabo, P., Bras, J., Daugaard, A.E., 2016. Hybrid poly (lactic acid)/nanocellulose/nanoclay composites with synergistically enhanced barrier properties and improved thermomechanical resistance. Polym. Int.

Turbak, A.F., Snyder, F.W., Sandberg, K.R., 1985. Microfibrillated cellulose and process for producing it. CH 648071.

Van Engelen, G.P.F.M., Van Ingen, G.A., Meeuwissen, C., 2014a. Anti-cracking agent for water-borne acrylic paint and coating compositions. WO 2014017912.

Van Engelen, G.P.F.M., Van Ingen, G.A., Meeuwissen, C., 2014b. Plant derived cellulose compositions for use as drilling muds. WO 2014017911.

Velásquez-Cock, J., Gañán, P., Posada, P., Castro, C., Serpa, A., Gómez H., C., Putaux, J.-L., Zuluaga, R., 2016. Influence of combined mechanical treatments on the morphology and structure of cellulose nanofibrils: Thermal and mechanical properties of the resulting films. Ind. Crops Prod. 85, 1–10. doi:10.1016/j.indcrop.2016.02.036

Wågberg, L., Decher, G., Norgren, M., Lindström, T., Ankerfors, M., Axnäs, K., 2008. The Build-Up of Polyelectrolyte Multilayers of Microfibrillated Cellulose and Cationic Polyelectrolytes. Langmuir 24, 784–795. doi:10.1021/la702481v

Walther, A., Bjurhager, I., Malho, J.-M., Pere, J., Ruokolainen, J., Berglund, L.A., Ikkala, O., 2010. Large-Area, Lightweight and Thick Biomimetic Composites with Superior Material Properties via Fast, Economic, and Green Pathways. Nano Lett. 10, 2742–2748. doi:10.1021/nl1003224

Wang, B., Sain, M., 2007. Isolation of nanofibers from soybean source and their reinforcing capability on synthetic polymers. Compos. Sci. Technol. 67, 2521–2527. doi:10.1016/j.compscitech.2006.12.015

Wang, J., Cheng, Q., Lin, L., Jiang, L., 2014. Synergistic toughening of bioinspired poly (vinyl alcohol)–clay–nanofibrillar cellulose artificial nacre. ACS Nano 8, 2739–2745.

Wang, S., Ren, J., Kong, W., Gao, C., Liu, C., Peng, F., Sun, R., 2013. Influence of urea and glycerol on functional properties of biodegradable PVA/xylan composite films. Cellulose 21, 495–505. doi:10.1007/s10570-013-0091-4

Wolff, B.W., Pandian, V., Van Calcar, D., 1996. Role of Zirconium Complexes to Produce Multiple Use Paper, in: Papermakers Conference. Tappi press, pp. 121–136.

Wu, C.-N., Saito, T., Fujisawa, S., Fukuzumi, H., Isogai, A., 2012. Ultrastrong and High Gas-Barrier Nanocellulose/Clay-Layered Composites. Biomacromolecules 13, 1927–1932. doi:10.1021/bm300465d

Xiao, W., Xu, J., Liu, X., Hu, Q., Huang, J., 2013. Antibacterial hybrid materials fabricated by nanocoating of microfibril bundles of cellulose substance with titania/chitosan/silver-nanoparticle composite films. J. Mater. Chem. B 1, 3477–3485. doi:10.1039/C3TB20303D

Xylophane, 2014. Xylophane Official Website [WWW Document]. Xylophane. URL http://www.xylophane.com/ (accessed 7.11.14).

Yildirim, N., Shaler, S.M., Gardner, D.J., Rice, R., Bousfield, D.W., 2014. Cellulose nanofibril (CNF) reinforced starch insulating foams. Cellulose 21, 4337–4347.

Yuwawech, K., Wootthikanokkhan, J., Tanpichai, S., 2015. Effects of two different cellulose nanofiber types on properties of poly (vinyl alcohol) composite films. J. Nanomater. 2015, 69.

Zhao, H.-P., Feng, X.-Q., Gao, H., 2007. Ultrasonic technique for extracting nanofibers from nature materials. Appl. Phys. Lett. 90, 73112.

Zheng, Q., Cai, Z., Gong, S., 2014. Green synthesis of polyvinyl alcohol (PVA)–cellulose nanofibril (CNF) hybrid aerogels and their use as superabsorbents. J. Mater. Chem. A 2, 3110–3118. doi:10.1039/C3TA14642A

Zimmermann, T., Pöhler, E., Geiger, T., 2004. Cellulose Fibrils for Polymer Reinforcement. Adv. Eng. Mater. 6, 754–761. doi:10.1002/adem.200400097

List of figures

List of tables

Appendix

Appendix for Chapter III

	Transmittance		Haze		Clarity	
	Average	Stdev	Average	Stdev	Average	Stdev
UM	80.7	1.0	97.9	0.2	4.8	0.1
D	62.8	0.4	99.0	0.2	4.3	0.2
KB	78.8	0.6	96.0	0.1	5.7	0.1
0P	83.1	0.4	97.5	0.1	5.0	0.1
1P	79.1	0.5	97.5	0.3	4.8	0.1
2P	79.7	0.2	97.0	0.1	5.2	0.0
3P	80.0	0.2	96.4	0.1	5.5	0.1
4P	82.3	0.4	95.0	0.2	6.0	0.1
5P	83.2	0.3	93.7	0.2	6.4	0.2
5P (casting)	83.4	0.7	88.2	1.0	7.5	0.2

Table 33 - Optical properties of MFC self-standing films

	$WVTR_{65}$ 23°C 85%RH (g/(m².d))	
	Average	Stdev
KB	1,230	54
D	1,114	112
UM	1,179	64

Table 34 - Water vapour transmission rate (WVTR) of MFC handsheets at 23°C 85%RH

Appendix for Chapter IV

	Apparent density (g/cm3)		Tensile strength (MPa)		Elongation at break (%)		Young Modulus (GPa)	
	Average	Stdev	Average	Stdev	Average	Stdev	Average	Stdev
PVOH	1.31	0.01	60	2	72	28	3.4	0.1
PVOH + 0.5 pph KB	1.28	0.01	50	2	56	29	2.8	0.2
PVOH + 2 pph KB	1.28	0.01	59	6	30	7	3.5	0.2
PVOH + 5 pph KB	1.18	0.02	46	1	45	9	3.0	0.2
PVOH + 10 pph KB	1.12	0.02	56	3	19	4	3.3	0.1
PVOH + 20pph KB	1.14	0.01	63	4	4	1	4.3	0.2

Table 35 - Density and mechanical properties for PVOH:MFC composites.

	Transmittance		Haze		Clarity	
	Average	Stdev	Average	Stdev	Average	Stdev
PVOH	92.9	0.1	1.6	0.1	98.2	0.1
PVOH + 0.5 pph KB	92.7	0.2	3.9	0.1	90.3	0.3
PVOH + 2 pph KB	92.8	0.1	13.8	1.3	65.8	2.0
PVOH + 5 pph KB	92.0	0.2	59.1	4.5	16.8	3.2
PVOH + 10 pph KB	92.1	0.1	76.8	1.4	8.7	0.2
PVOH + 20pph KB	92.4	0.4	80.2	5.4	8.7	1.2

Table 36 - Optical properties of PVOH:MFC composites with increasing MFC content

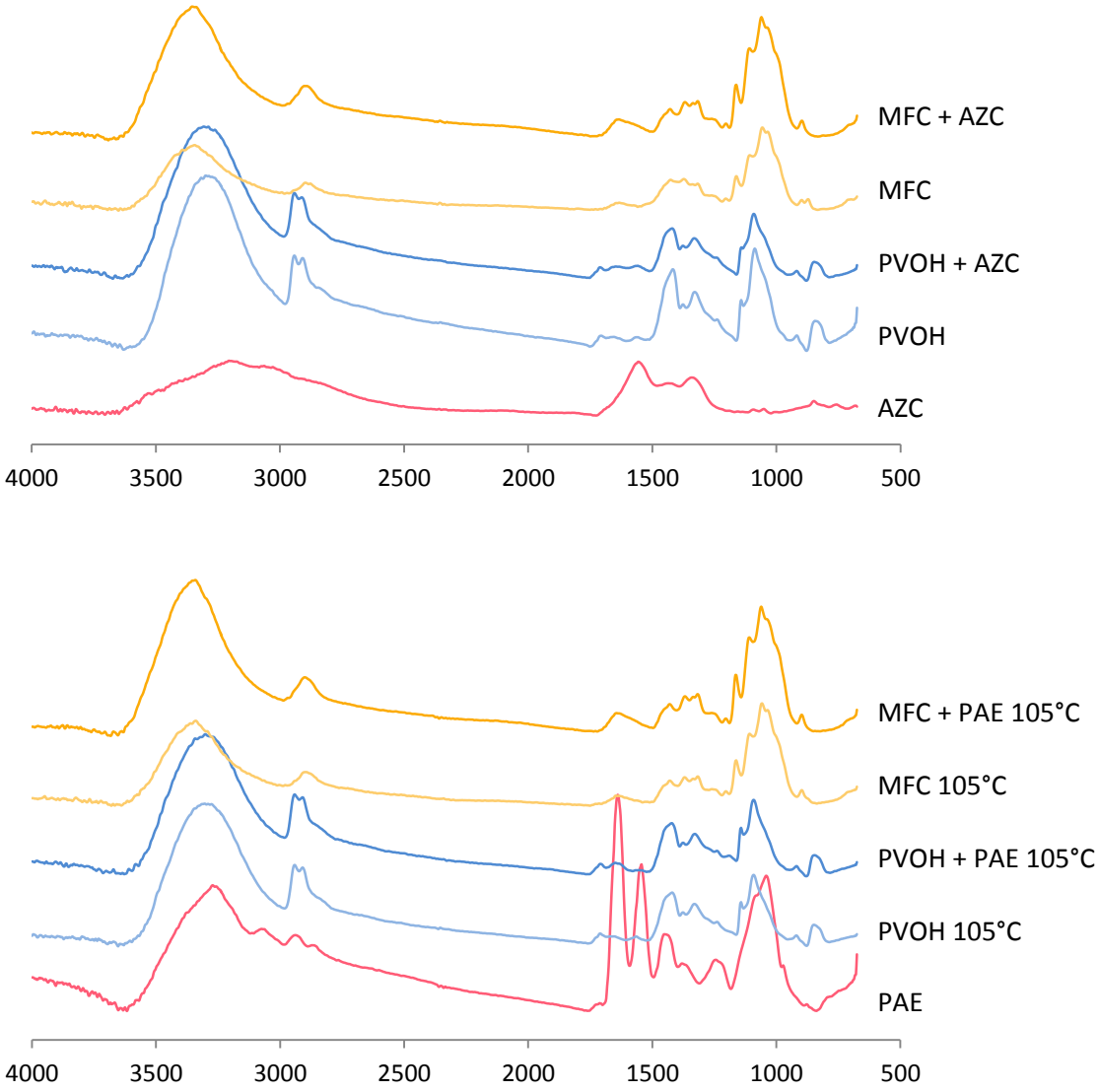

Figure 75 - FTIR spectra corresponding to the crosslinking of PVOH and MFC by AZC and PAE.

Appendix for Chapter V

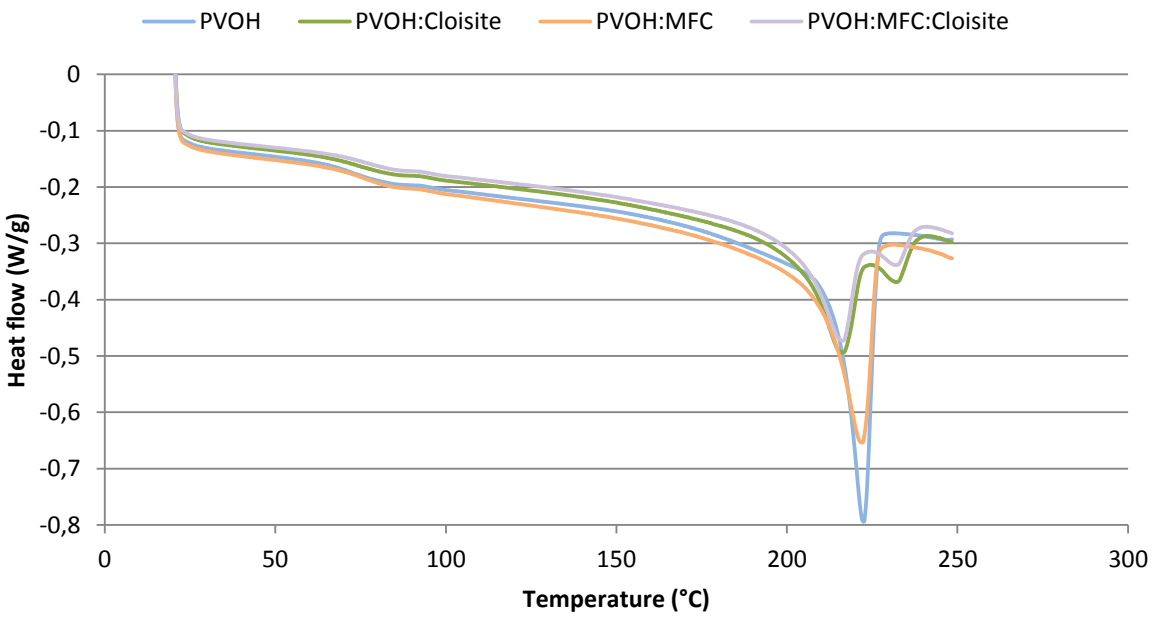

Figure 76 - DSC spectra of the second heating of PVOH:MFC:Cloisite composite films. MFC 5P is at 5 pph and Cloisite-Na at 10 pph.

Résumé étendu

Résumé étendu

Notre mode de consommation rend nécessaire le transport et le stockage de nos aliments. L'emballage alimentaire est un moyen de transporter la nourriture de façon pratique. C'est aussi un moyen de la protéger contre différents mécanismes de dégradation, afin d'augmenter leur durée de consommation et ainsi réduire la gâche alimentaire. Cette protection contre les gaz, l'eau, les aromes, ou les huiles minérales par exemple, est obtenue grâce à des matériaux barrières capables d'entraver la perméation de ces substances à travers l'emballage. Pour cette raison, les emballages alimentaires sont principalement faits de plastiques et peuvent contenir une couche d'aluminium. Les papiers-cartons sont perméables, mais peuvent être utilisés comme support d'une couche barrière appliquée par couchage ou lamination. Que ce soit sous forme d'emballage plastique ou de couche sur papier-carton, les solutions actuelles de barrière pour l'emballage alimentaire sont principalement issues de ressources non renouvelables et/ou posent des problèmes de fin de vie (matériaux non recyclables, non biodégradables). L'utilisation de biopolymères est largement étudiée dans le but d'apporter des solutions plus durables. La cellulose est le biopolymère le plus largement disponible et permet d'obtenir des microfibrilles de cellulose (MFC) par traitement mécanique des fibres végétales, éventuellement prétraitées. La structure du bois jusqu'à la molécule de cellulose, et en passant par les microfibrilles de cellulose, est présentée sur la Figure 77.

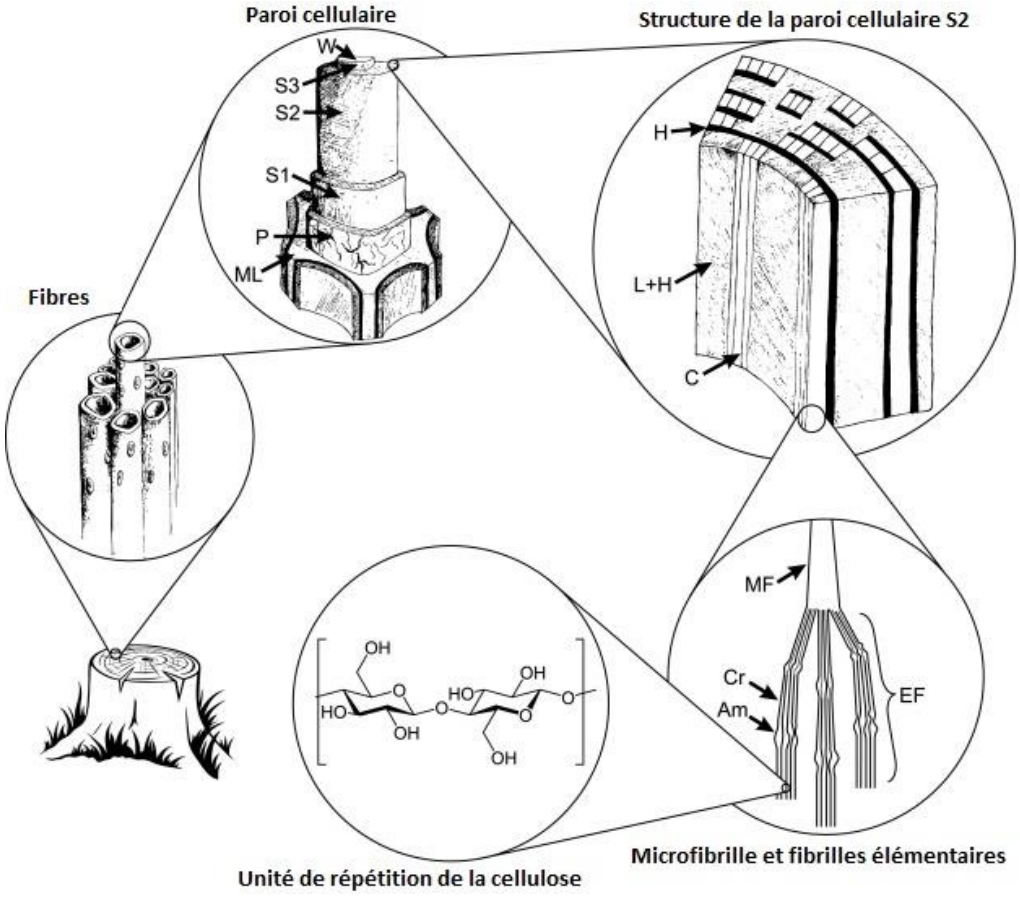

Figure 77 - Structure hiérarchique du bois jusqu'à la molécule de cellulose (Nechyporchuk et al., 2016a). MF: microfibrille, EF: fibrille élémentaire, Cr: partie crystalline, Am: partie amorphe.

Les MFC sont des éléments de diamètre nanométrique qui permettent de former des films denses et hautement barrière à l'oxygène et à la graisse. Leur application en couche barrière sur carton permet de produire des matériaux d'emballage alimentaire barrières, biosourcés, recyclables, et biodégradables, mais leur utilisation est limitée par certains facteurs. Les MFC sont sensibles à l'humidité et à l'eau, limitant les performances barrières en conditions humides. Les suspensions de MFC ont une haute viscosité à faible taux de matière sèche. La grande quantité d'eau présente dans la suspension dégrade le réseau fibreux du carton lors du couchage d'une suspension de MFC, et rend difficile le séchage de telles couches sur des coucheuses industrielles.

Dans ce contexte, cette thèse a comme but de développer des solutions d'emballage alimentaire barrière plus durables. Pour cela, deux types de matériaux ont été considérés:

- Une couche barrière 100% MFC laminée à l'état humide sur carton.
- Une couche barrière composite comprenant des MFC comme additif dans une sauce de couchage base aqueuse appliquée sur carton. La couche barrière est principalement constituée d'un polymère hydrosoluble et biodégradable: l'alcool polyvinylique (PVOH).

La première partie se concentre sur la formation de couches barrières 100% MFC. La deuxième partie se concentre sur la formulation de couches barrières comprenant des MFC en tant qu'additif dans une sauce de couchage base aqueuse. La troisième partie se concentre sur l'amélioration de couches barrières PVOH:MFC par ajout de particules minérales lamellaires, ou argiles plates.

Partie I : MFC pour applications barrières

Cette première partie se concentre sur la formation de couches barrières 100% MFC. De par la variété des traitements chimiques, enzymatiques, et mécaniques pouvant être utilisés pour la production de MFC, le terme "microfibrilles de cellulose" regroupe un large panel de matériaux de morphologies et de chimies différentes. En particulier, comme on peut le voir sur la Figure 78, l'utilisation d'un prétraitement chimique permet d'obtenir des microfibrilles totalement individualisées. Au contraire, une suspension de MFC n'ayant pas subi de prétraitement chimique comprend encore des résidus de fibres. Dans cette thèse, il a été choisi d'utiliser des MFC dont la nature de la cellulose n'a pas été modifiée par un prétraitement chimique. Cela permet d'éviter l'utilisation de produits toxiques, et devrait faciliter l'aptitude au contact alimentaire de couches barrières pour l'emballage comprenant ces MFC. Un prétraitement enzymatique est tout de même appliqué afin de faciliter la fibrillation. L'intensité du traitement mécanique utilisé pour la production des MFC est un point clé quant à leur industrialisation. Intensifier le traitement mécanique permet d'obtenir des MFC de meilleure qualité mais engendre des coûts énergétiques qui, s'ils sont trop élevés, risquent de freiner l'utilisation des MFC à l'échelle industrielle.

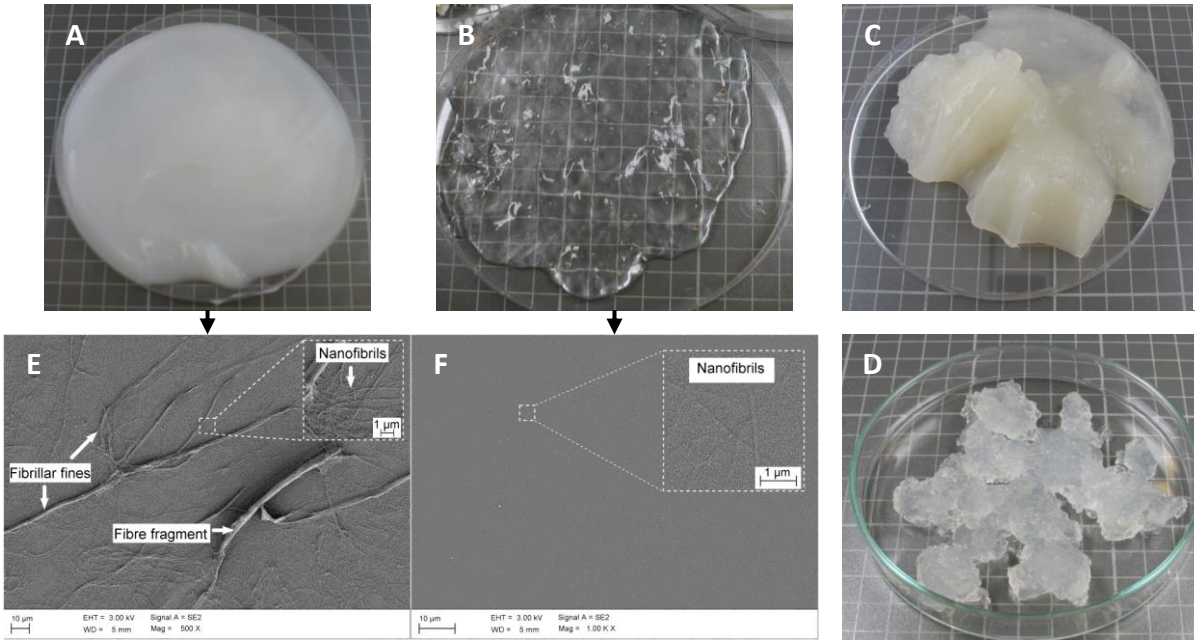

Figure 78 - Apparence de suspensions de MFC non modifiées chimiquement (A) et prétraitées chimiquement. Les prétraitements sont: oxydation TEMPO (B), carboxymethylation (C), quaternisation (D) (Pöhler et al., 2010). Images de microscopie électronique à balayage de suspensions de MFC séchées sur une lame de verre sans prétraitement (E), largeur d'image : 235 µm, et avec un prétraitement d'oxydation TEMPO (F), largeur d'image : 115 µm (Chinga-Carrasco, 2011).

Le premier objectif de cette thèse est de déterminer l'influence du degré de fibrillation de différents grades de MFC sur leurs propriétés barrières. Les grades de MFC utilisés sont :

- MFC UM : MFC commerciales, achetées auprès de l'Université du Maine, produites par fort raffinage d'une pâte kraft de résineux.
- MFC D et KB : MFC produites à l'échelle pilote par prétraitement enzymatique et 6 passages dans un homogénéiseur d'une pâte sulfite de résineux et de kraft de feuillu, respectivement.
- MFC 0P, 1P, 2P, 3P, 4P, 5P : MFC produites à l'échelle pilote par prétraitement enzymatique et 0, 1, 2, 3, 4, et 5 passages dans l'homogénéiseur, respectivement, d'une même pâte de kraft de feuillu.

La détermination de la distribution de taille des éléments en suspension est difficile dans le cas des MFC de par leur polydispersité et leur grande longueur par rapport à leur diamètre. Le degré de fibrillation de ces suspensions a donc été caractérisé par des méthodes indirectes: analyse visuelle, microscopie optique (Figure 79), morphologie des fragments macroscopiques (MorFi), et rhéologie. Des méthodes indirectes ont aussi été appliquées à des films de MFC de 50 g/m² : densité, propriétés optiques, et propriétés mécaniques. Les propriétés barrières à la vapeur d'eau et à l'oxygène de films de MFC ont aussi été déterminées.

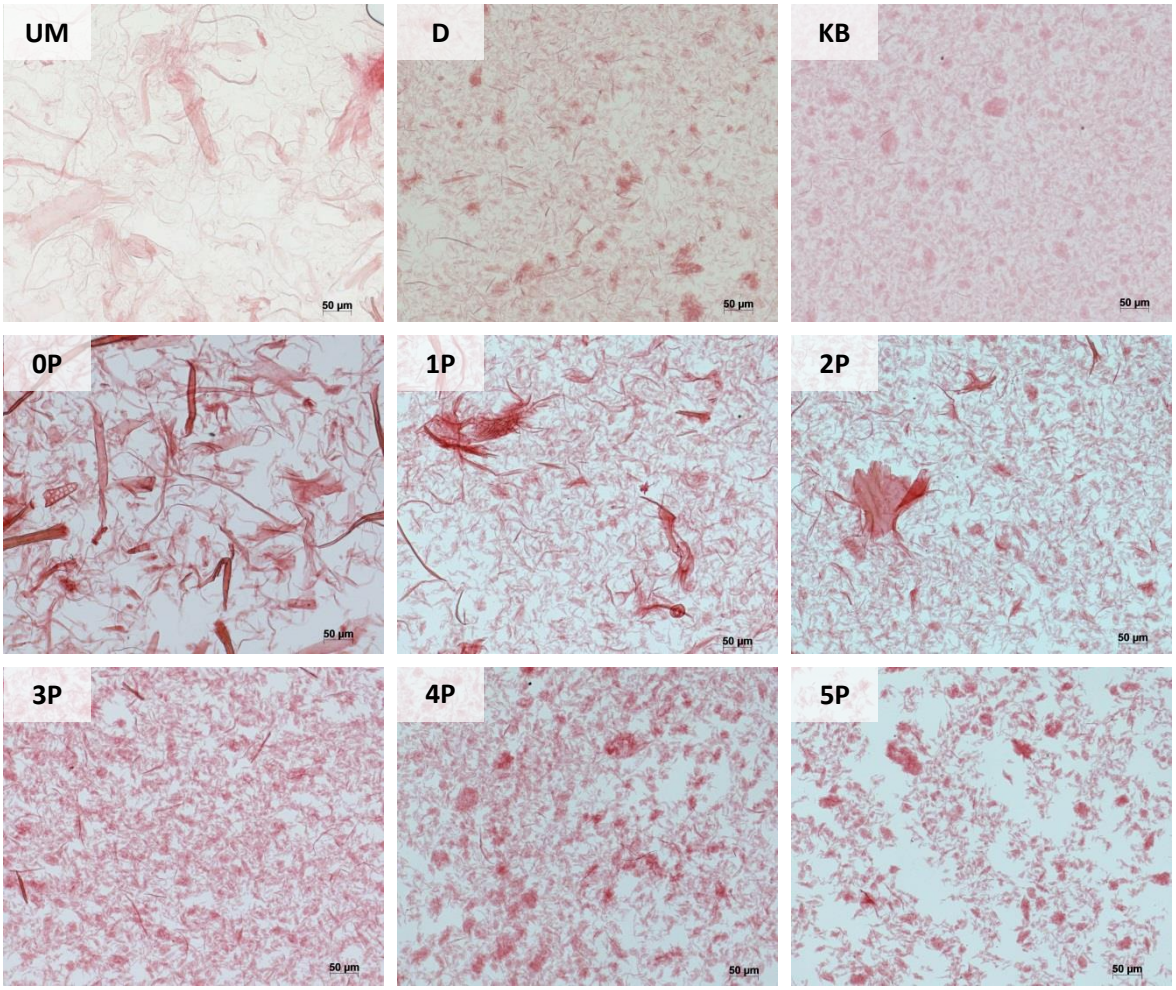

Figure 79 - Images de microscopie optique de suspensions de MFC colorées avec du Rouge Congo. Largeur d'image : 650 µm.

De grandes différences ont été observées dès l'analyse visuelle des suspensions pour ce qui est des MFC UM et 0P, qui n'ont pas subi de traitement à l'homogénéiseur. Ces suspensions présentaient un aspect granuleux à 2% de matière sèche et ont produit des films non homogènes, tandis que les autres suspensions présentaient un aspect lisse et ont produit des films homogènes. L'analyse microscopique des suspensions a montré la présence de résidus macroscopiques de fibres dans les MFC 0P. La fraction de résidus macroscopiques a diminué par une augmentation de l'intensité du traitement mécanique depuis les MFC 0P jusqu'aux MFC 5P. Cette quantité de résidus macroscopiques a pu être quantifiée par une technique d'analyse optique MorFi, et a été cohérente pour chaque grade de MFC avec le degré de fibrillation attendu d'après leur mode de production. Les analyses rhéologiques n'ont pas été aussi cohérentes. La viscosité des suspensions augmente bien avec le taux de fibrillation des MFC 0P aux MFC 5P, mais la comparaison avec les MFC UM et MFC D a montré une dépendance au type de pâte utilisé, ce qui empêche la seule analyse du degré de fibrillation. Le même effet a été observé pour ce qui est des propriétés optiques des films de MFC : la transparence et la clarté ont augmenté progressivement des MFC 1P aux MFC 5P, mais ces résultats ne permettent pas de comparer leur taux de fibrillation avec les MFC UM et MFC D. La quantification des résidus macroscopiques en suspension ou de la densité de films autoportés est donc préférable à une analyse rhéologique ou des mesures de propriétés optiques afin de caractériser le degré de fibrillation d'une suspension de MFC. D'autres méthodes sont aussi proposées dans la littérature, comme des mesures de longueur des microfibrilles sur plusieurs images de microscopie électronique à transmission (W. Chen et al., 2015), des analyses de turbidité (Nuopponen et al., 2016), ou d'autres méthodes décrites dans une revue de la littérature par Kangas et al. (2014).

Les films de MFC avaient des densités apparentes dépendantes de leur taux de fibrillation, correspondant à une porosité apparente plus élevée pour les grades de MFC ayant subi un traitement mécanique léger : MFC UM et MFC 0P. Cela a engendré une perméabilité à l'oxygène élevée pour ces deux grades, tandis que les autres ont permis la production de films à haute barrière. L'utilisation de MFC ayant un faible taux de fibrillation devrait être évitée pour la formation de couches barrières 100% MFC. Le taux de fibrillation n'a pas eu d'influence sur la barrière à la vapeur d'eau, les films de MFC étant très perméables dans tous les cas. Une augmentation du degré de fibrillation des MFC 1P aux MFC 5P a produit une amélioration progressive de la barrière à l'oxygène. Ces dernières ont donc été sélectionnées pour être appliquées en couche barrière 100% MFC sur carton.

La dépose d'une couche 100% MFC sur carton est un défi à cause de la haute viscosité des MFC à faible taux de matière sèche : les suspensions de MFC contiennent en général 98% d'eau. Une application par couchage mouille le papier, ce qui détériore sa structure, et ne permet que d'obtenir des poids de couche très faibles (Lavoine et al., 2014). De plus, le séchage de l'eau est consommateur d'énergie. Une technique alternative a été utilisée dans cette thèse afin d'éviter ces soucis : la lamination humide. D'une façon similaire à Syverud et Stenius (2009), un matelas humide de MFC 5P est formé par filtration au travers d'une membrane sur un appareil Rapid-Köthen. Ce matelas humide est ensuite reporté sur un carton et séché, comme montré sur la Figure 80. Ce procédé permet à la couche de MFC d'adhérer au carton sans nécessiter de colle.

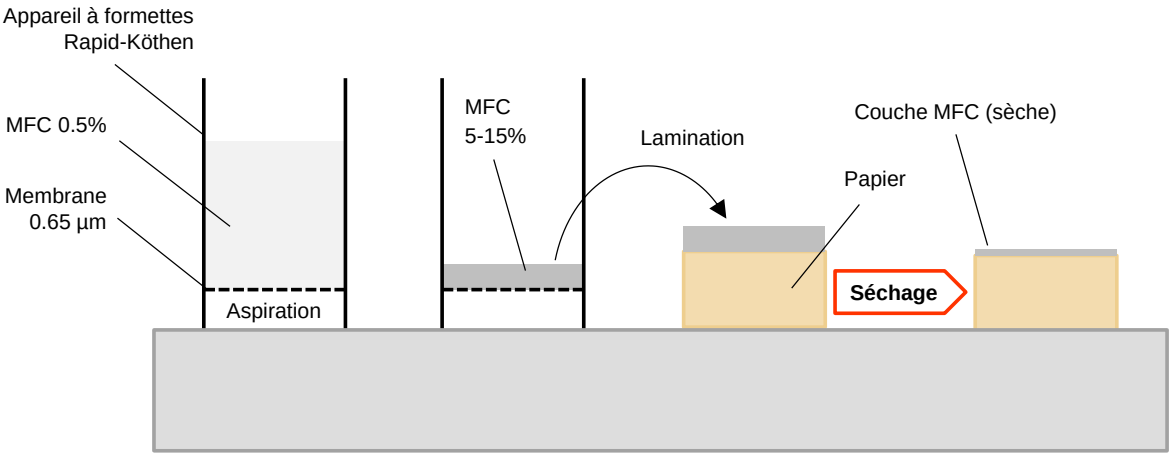

Figure 80 - Procédé simplifié de lamination humide.

La lamination de films de MFC 5P de 10 à 40 g/m² a montré que la formation de films plus fins (8 à 31 µm, contre 38 µm pour les films autoportés décrits précédemment), et/ou le procédé de lamination humide, engendre des défauts dans la couche de MFC. Ces défauts apparaissent principalement pour des poids de couche de 10 ou 20 g/m², comme on peut le voir sur la Figure 81.

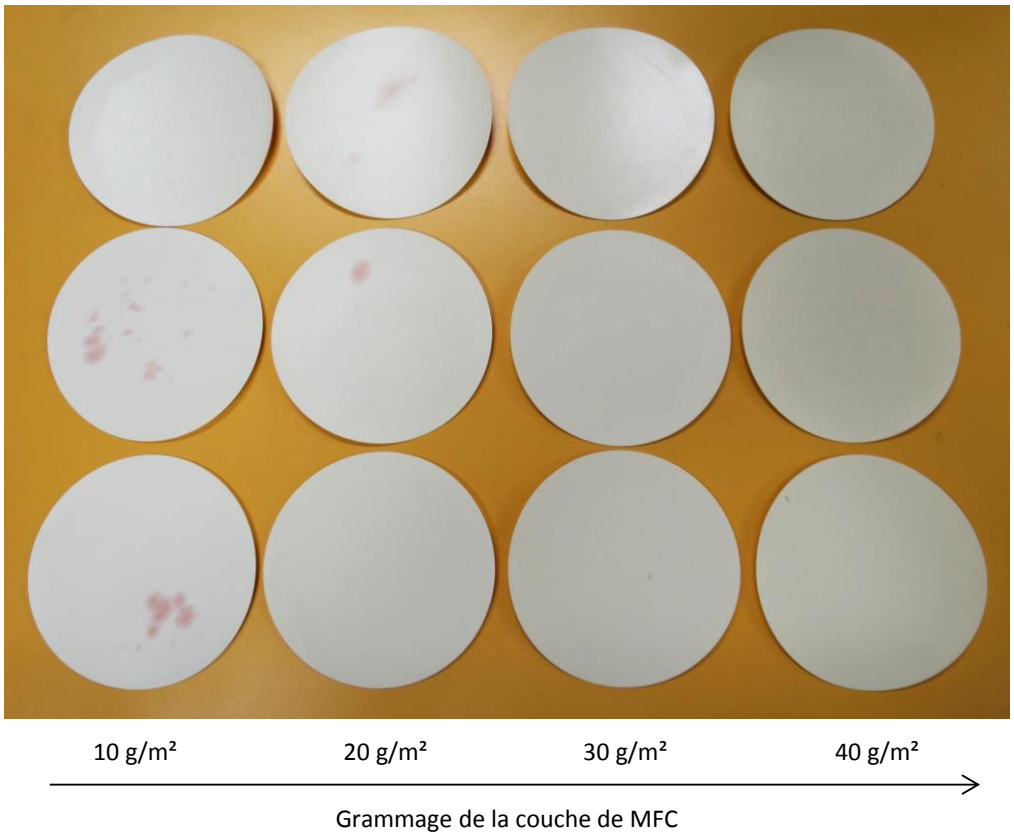

Figure 81 - Échantillons de cartons laminés MFC après mise en contact avec de l'huile colorée pendant 30 min. Les échantillons d'une même colonne sont des réplicats pour un même poids de couche de MFC. Largeur d'un échantillon : 9.4 cm.

Après contact avec de l'huile colorée, des tâches apparaissent lorsque la couche de MFC présente des défauts car l'huile peut y pénétrer et contaminer le carton. Ces défauts peuvent être attribués à la présence de résidus macroscopiques dont les dimensions peuvent être de l'ordre de grandeur de l'épaisseur de la couche de MFC, ou bien à des trous dans la couche qui peuvent être apparus lors du décollement du matelas humide de MFC de la membrane filtrante. Les mesures de perméabilité à l'oxygène montrent que ces défauts font perdre à la couche de MFC son caractère barrière. À 40 g/m² de MFC, aucun défaut n'a pu être révélé. Cela semble être le grammage minimum pour pouvoir obtenir une couche sans défaut, hautement barrière à l'oxygène par lamination humide de MFC 5P. L'efficacité du procédé de lamination humide semble limitée par la présence de résidus macroscopiques dans les suspensions de MFC. Une étape de fractionnement ou une adaptation du procédé de production des MFC pourrait permettre d'éliminer la plupart de ces éléments, et donc de réduire le grammage minimum de MFC à déposer afin de former une couche barrière sans défaut.

Cette partie était consacrée à l'étude de suspensions et films de MFC, dans le but de produire des couches barrières sur carton par un procédé incluant une étape de filtration. Des méthodes préférentielles de caractérisation du degré de fibrillation ont été mises en évidence, et un grade de MFC hautement fibrillé a été choisi pour être appliqué sur carton par lamination de par sa bonne barrière à l'oxygène. Les couches laminées ont présenté des défauts, révélés par exposition à l'huile colorée, affectant la barrière à l'oxygène. Une augmentation du poids de couche à 40 g/m² a permis d'éviter ces défauts et donc d'obtenir un matériau barrière 100% biosourcé. Les deux parties suivantes s'intéressent à l'autre stratégie pour l'utilisation des MFC dans des couches barrières : leur application en tant qu'additif dans une sauce de couchage.

Partie II : MFC en tant qu'additif dans une matrice PVOH

Cette seconde partie se concentre sur la formulation de couches barrières comprenant des MFC en tant qu'additif dans une sauce de couchage base aqueuse. L'alcool polyvinylique (PVOH) est un bon candidat pour être associé aux MFC dans ce type de couches barrières : c'est un polymère hydrosoluble, compatible avec la cellulose, et qui a une bonne barrière à l'oxygène. C'est un matériau qui ne pose pas de problème vis-à-vis de l'emballage alimentaire, non toxique, et qui peut même être utilisé pour des applications pharmaceutiques et biomédicales. Le PVOH est également biodégradable et peut potentiellement être produit à partir de ressources renouvelables, bien que ce ne soit principalement pas le cas pour des raisons économiques. L'utilisation d'amidon est une alternative biosourcée au PVOH, présentant des propriétés similaires, mais une étude précédente a montré que les couches amidon:MFC étaient plus cassantes et plus perméables à la vapeur d'eau que les couches PVOH:MFC (Guezennec, 2012).

Dans cette étude, l'ajout de MFC en tant qu'additif dans une matrice PVOH est donc étudié. La formation de couches composites autoportées comprenant des MFC est habituellement faite par coulée-évaporation, i.e. formulation d'une dispersion composite diluée qui est versée dans une boite de pétri et séchée par évaporation libre de l'eau sur une durée de plusieurs jours. Afin de se rapprocher des conditions de formation utilisées en couchage industriel, un dispositif de formation de films autoportés par couchage-pelage a été mis en place, comme décrit sur la Figure 82. Il s'agit de former une couche composite humide par un dispositif de couchage, et de sécher cette couche par infra-rouge sur une durée de quelques minutes. Plusieurs grades de PVOH et de MFC ont été étudiés, les MFC étant ajoutées à différents ratios. Le but est de mieux comprendre quels types de matériaux et de formulations sont les plus pertinentes pour une application en couchage barrière.

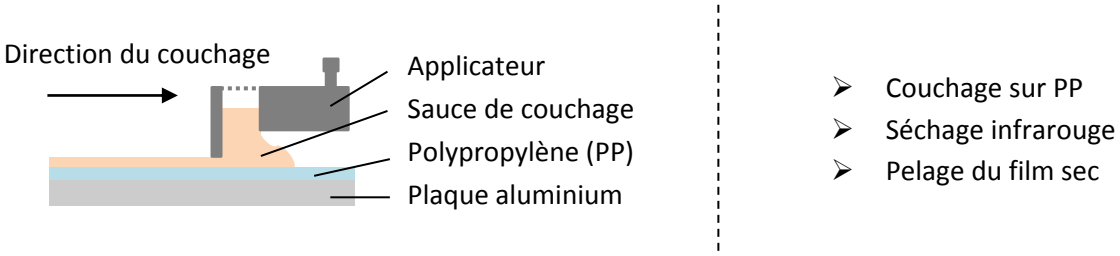

Figure 82 - Procédé de couchage-pelage pour la production de films autoportés PVOH:MFC.

L'utilisation des MFC ayant une plus grande quantité de résidus macroscopiques a été comparée aux MFC D et MFC KB hautement fibrillées et issues de pâtes différentes. Indépendamment du grade de MFC utilisé, les composites sont devenus flous en comparaison avec le PVOH transparent, comme montré sur la Figure 83, ce qui s'est traduit par une diminution de clarté à transmittance constante. L'introduction de 2 pph de MFC UM dans du PVOH (i.e. une masse sèche de MFC égale à 2% de la masse sèche de PVOH) a engendré une diminution de densité qui a dégradé les propriétés mécaniques et barrières. Au contraire, l'ajout de MFC D ou MFC KB ayant peu de résidus macroscopiques a permis de conserver la densité, la résistance mécanique, et les propriétés barrières

du PVOH. L'utilisation de MFC hautement fibrillées est donc aussi nécessaire dans le cas d'une utilisation des MFC en tant qu'additif, afin d'éviter de dégrader les propriétés des composites.

PVOH | PVOH + 2 pph D | PVOH + 2 pph UM

Figure 83 - Images de films autoportés de PVOH et de PVOH:MFC. D : MFC hautement fibrillées par traitement enzymatique et homogénéisation. UM : MFC faiblement fibrillées par fort raffinage.

L'ajout de MFC dans du PVOH augmente la viscosité des suspensions. L'utilisation de MFC KB à des taux de 0.5 à 20 pph dans du PVOH a conduit à diminuer le taux de matière sèche des suspensions de 24% à 9% afin de rester dans une gamme de viscosité correcte pour un procédé de couchage. De plus, des problèmes de dispersion des MFC apparaissent à 20 pph. Pour ce qui est des films composites, un renforcement mécanique n'est observé qu'à des taux de MFC supérieurs à 5 pph, et à ce taux de MFC les propriétés barrières de PVOH sont dégradées. Un faible taux de MFC semble préférable pour la formation de couches barrières, afin d'obtenir une faible viscosité et une conservation des propriétés mécaniques et barrières du PVOH. Pour ce qui est du grade de PVOH, il a été préférable de travailler avec un PVOH complètement hydrolysé, i.e. avec un taux de groupements alcool supérieur à 98%, et ayant un faible degré de polymérisation, afin d'obtenir une meilleure barrière à la vapeur d'eau tout en ayant une suspension de faible viscosité.

L'introduction des MFC dans du PVOH a présenté peu d'intérêt pour l'amélioration des propriétés des couches composites. Son utilité est en revanche reportée dans la littérature pour ce qui est d'améliorer le séchage de la couche lors d'un couchage à l'échelle pilote, évitant la formation de défauts lors du séchage (Guezennec, 2012; Schmidt et al., 2015). Cette observation n'a pas été approchée scientifiquement. Une étude a donc été réalisée afin d'étudier le séchage du PVOH en présence de MFC, à l'aide d'un banc de séchage infra-rouge de laboratoire instrumenté. L'évolution de la masse de suspension, de la température, et du flux infra-rouge émis sont analysés durant l'essai.

Les essais de séchage ont montré que l'ajout de MFC à du PVOH à hauteur de 5 pph permet de sécher plus rapidement, dans le cas d'une couche épaisse déposée dans un moule en Téflon. Les courbes de séchages ont présenté trois domaines : ① une augmentation de la vitesse de séchage qui correspond à l'échauffement de la suspension, ② une période de séchage à taux d'évaporation constant, et ③ une diminution de la vitesse de séchage correspondant à l'échantillon devenant sec. Ces domaines ont été modélisés en cinétique de séchage parabolique, linéaire, puis exponentielle, respectivement. La dérivation des équations obtenues permet de tracer le taux d'évaporation d'eau en fonction de la fraction d'eau dans la suspension, montré sur la Figure 84. Cela a permis de

montrer qu'en présence de MFC, la suspension atteint plus rapidement le domaine de séchage à taux constant, qui est le domaine dans lequel le séchage est le plus rapide. Ce domaine dure également jusqu'à un état de séchage plus avancé que pour le PVOH seul.

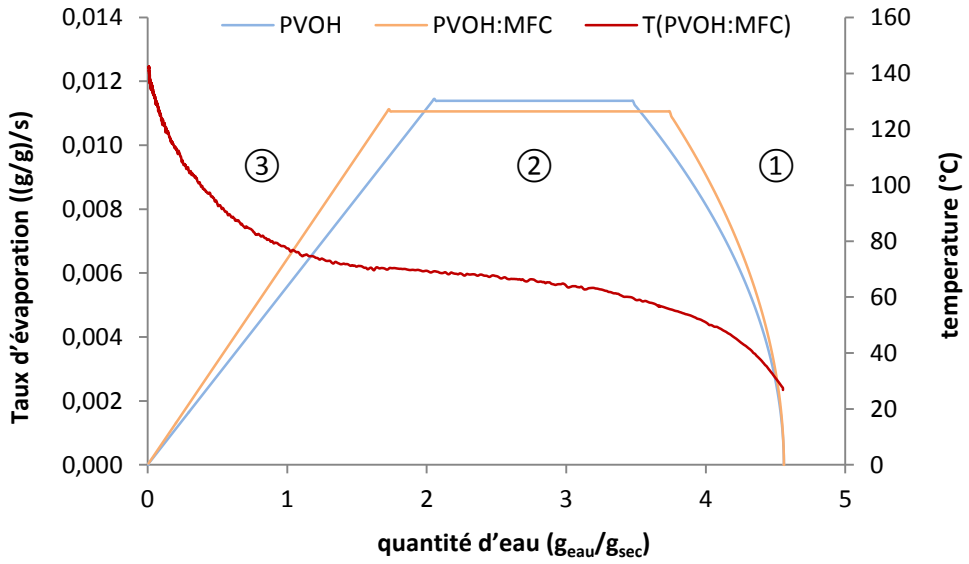

Figure 84 - Courbes d'évaporation de suspensions PVOH et PVOH:MFC (courbes bleue et orange, respectivement, ordonnée de gauche). Évolution de la température sous le moule en Téflon pendant l'expérience de séchage PVOH:MFC (courbe rouge, ordonnée de droite).

Cela est cohérent avec l'attribution de l'effet positif des MFC sur le séchage du PVOH dû au fait que les MFC retardent l'apparition d'une peau en surface, qui ralentit le séchage de l'eau présente sous cette peau. La formation d'une peau à la surface du PVOH peut aussi être responsable de défauts dans la couche, l'eau devant casser la peau afin de pouvoir sortir. Cette étude a montré l'influence positive des MFC sur le séchage du PVOH dans des conditions maîtrisées, et appuie l'hypothèse que cette amélioration vient d'une entrave à la formation d'une peau de PVOH en présence de MFC. Aucun effet n'a été observé dans le cas du séchage de cartons couchés, probablement à cause des épaisseurs de couches humides plus faibles. L'amélioration devrait être révélée lors d'un séchage plus fort de ces couches de faible épaisseur.

Le PVOH et les MFC manquent de résistance à l'eau : en milieu aqueux, le PVOH se solubilise et les MFC se dispersent. La réticulation est un moyen d'améliorer la résistance à l'eau, cependant peu d'études analysent l'impact d'un agent de réticulation à la fois sur du PVOH et sur des MFC. Trois stratégies de réticulation ont été étudiées afin d'améliorer la résistance à l'eau de films de PVOH et de MFC : la formation de liaisons covalentes grâce à l'acide citrique, de liaisons hydrogène grâce à de l'ammonium zirconium carbonate (AZC), et d'un réseau insoluble grâce à de la polyamidoamine epichlorhydrine (PAE). Un traitement thermique à 105°C ou 150°C est nécessaire dans le cas de la réticulation par l'acide citrique et la PAE, respectivement. Ce traitement thermique à lui seul a permis d'améliorer la barrière à la vapeur d'eau des films de PVOH et de MFC en atmosphère humide, ce qui est attribué à une augmentation de la cristallinité du PVOH et à un phénomène d'hornification pour

les MFC. En revanche, le traitement thermique seul ne permet pas aux films de PVOH et de MFC d'être résistants à l'eau. La réticulation par formation de liaisons covalentes grâce à l'acide citrique a permis aux films de PVOH et MFC de rester intacts pendant trois heures d'agitation magnétique dans de l'eau déionisée, comme décrit sur la Figure 85.

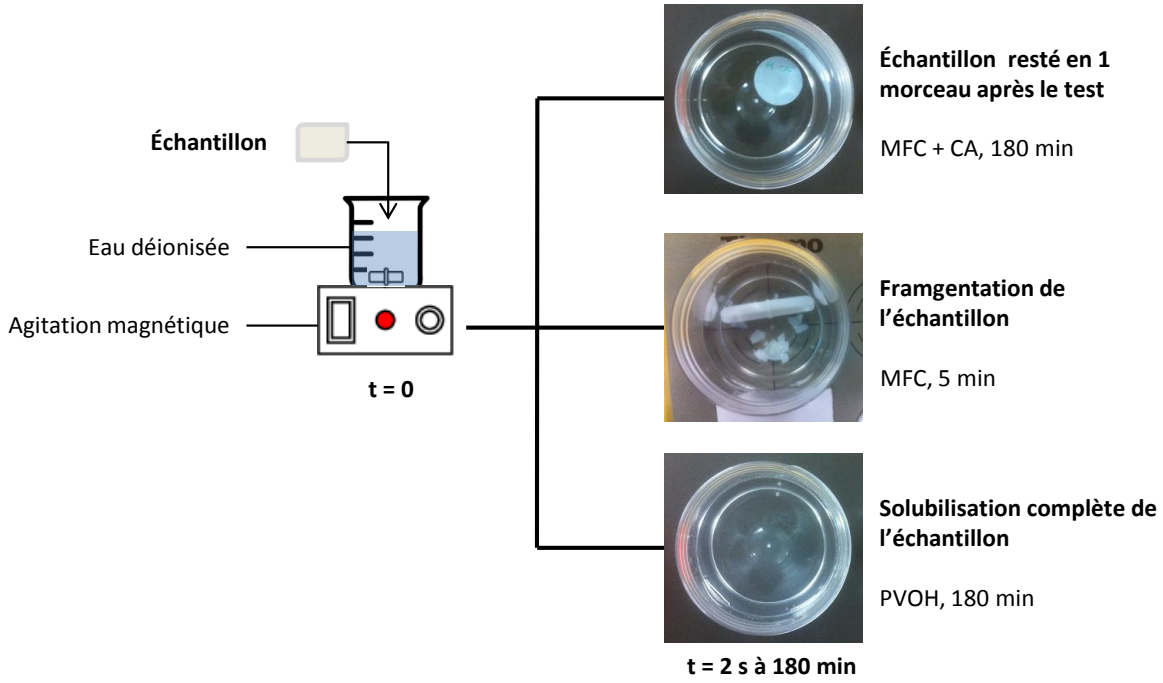

Figure 85 - Test de résistance à l'eau d'échantillons PVOH et MFC, réticulés ou non.

Les deux autres stratégies n'ont fonctionné que sur les MFC, et pour les MFC la réticulation par l'acide citrique a engendré la plus faible absorption d'eau. Contrairement à l'effet du traitement thermique, la réticulation en elle-même n'a pas eu d'influence sur la barrière à la vapeur d'eau des films de PVOH et de MFC. Une stratégie de réticulation par liaisons covalentes grâce à l'acide citrique apparait donc comme un bon moyen d'améliorer la résistance à l'eau à la fois du PVOH et des MFC, et d'améliorer aussi leur barrière à la vapeur d'eau grâce au traitement thermique associé. Cette stratégie parait prometteuse pour l'amélioration des propriétés de couches barrières composites PVOH:MFC.

Cette partie était concentrée sur la formulation de couches barrières comprenant des MFC en tant qu'additif dans une formulation pour application à du couchage base aqueuse. Il a été préférable d'utiliser un faible taux de MFC hautement fibrillées, associées à un PVOH totalement hydrolysé ayant un faible degré de polymérisation. Cela permet d'obtenir des viscosités plus faibles tout en optimisant la barrière. Les MFC n'améliorent pas les propriétés mécaniques et barrières du PVOH de façon significative, mais ont permis d'améliorer son séchage. Enfin, la résistance à l'eau et la barrière à la vapeur d'eau de films de PVOH et de MFC ont pu être améliorés par réticulation grâce à l'acide citrique. La barrière à la vapeur d'eau des couches développées n'est pas encore suffisante pour une application emballage alimentaire. La partie suivante étudie une autre stratégie pour améliorer la barrière à l'état humide : la dispersion de particules lamellaires minérales (argiles plates).

Partie III : Dispersion d'argiles plates dans des composites PVOH:MFC

Cette partie se concentre sur l'amélioration de couches barrières PVOH:MFC par ajout de particules minérales lamellaires, ou argiles plates. Lorsqu'une molécule de gaz diffuse dans un polymère homogène, le chemin de diffusion est droit. La tortuosité, i.e. le ratio entre le chemin de diffusion d'une molécule de gaz et une ligne droite, est donc égale à 1. Des particules imperméables peuvent être introduites dans un polymère, forçant les molécules de gaz à les contourner. Cela a pour effet d'augmenter la tortuosité et de réduire la perméabilité du composite. Les argiles plates sont des particules minérales lamellaires ayant la particularité d'avoir un ratio diamètre/épaisseur très élevé. Cela leur permet d'être particulièrement efficaces pour augmenter la tortuosité d'un matériau. Ces argiles plates sont compatibles avec la cellulose et le PVOH en milieux aqueux, ce qui leur permet d'être adaptées à une application de couchage barrière. Cependant, les argiles plates ont tendance à former des paquets, ce qui réduit leur aptitude à augmenter la tortuosité. Un des défis lié à leur utilisation est donc d'obtenir un bon état de dispersion, i.e. un état intercalé voir exfolié, comme présenté sur la Figure 86.

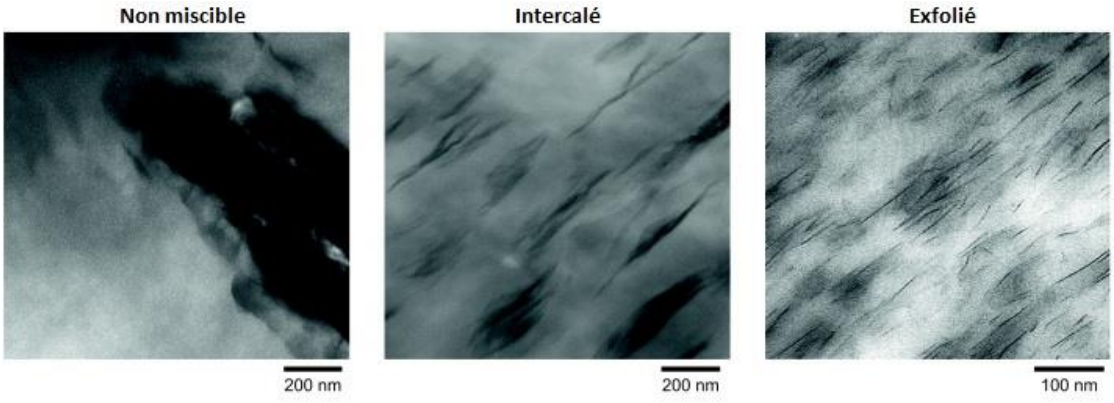

Figure 86 - Images de microscopie électronique en transmission montrant trois états de dispersion d'argiles plats dans une matrice polymère (Paul and Robeson, 2008).

Dans cette étude, quatre grades d'argiles plates de différentes chimies et morphologies ont été combinés avec des MFC dans une matrice de PVOH. Des films composites autoportés ont tout d'abord été produits par coulée-évaporation, puis une sélection de formulations a été appliquée à de couchage sur carton. La dispersion des argiles plates a été étudiée par diffractométrie de rayon X (XRD), microscopie électronique à balayage (SEM), et une technique d'analyse optique de distribution de tailles d'éléments en suspension par FPIA. Les propriétés barrières à la vapeur d'eau et à l'oxygène des films autoportés et des cartons couchés ont aussi été étudiées.

Après avoir adapté le procédé de production de suspensions afin d'obtenir une bonne dispersion des argiles plates à l'échelle macroscopique, le grade Cloisite-Na a été sélectionné pour une étude plus approfondie car apportant la meilleure barrière à la vapeur d'eau. Une analyse XRD des films composites autoportés PVOH:MFC:Cloisite-Na a mis en évidence l'état hautement dispersé des argiles plates. De plus, l'introduction de MFC a semblé améliorer leur dispersion. Un effet positif de la Cloisite-Na sur l'état de dispersion des MFC a été montré sur les images SEM, passant d'un état

floculé à un état dispersé. Cependant, ces améliorations de dispersion n'ont pas montré d'impact sur les propriétés barrières des films autoportés. L'ajout de Cloisite-Na de 0 à 20 pph dans du PVOH améliore progressivement la barrière à la vapeur d'eau à l'état humide, indépendamment de la présence de MFC.

Le passage au couchage sur carton a nécessité l'utilisation de suspensions plus concentrées : 18% de matière sèche comparé aux 5% de matière sèche des suspensions pour la production de films autoportés. Cela a généré plus de difficultés à disperser les particules en suspension. Cela a été montré en analyse d'images par des distributions de taille plus large des paquets de Cloisite-Na en suspension. Cela s'est aussi traduit par la présence d'agrégats visualisés pas SEM dans la couche de PVOH:Cloisite-Na, comme montré sur la Figure 87.

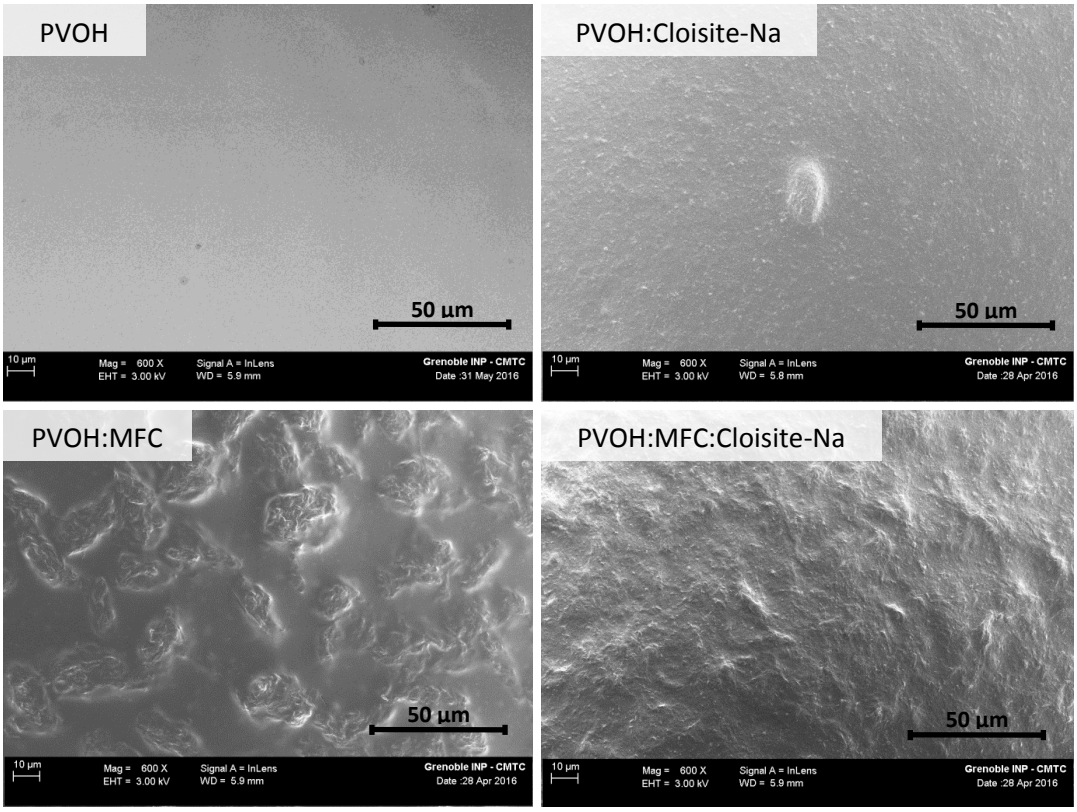

Figure 87 - Images de microscopie électronique en surface de cartons couchés PVOH:MFC:Cloisite-Na. Le taux de MFC est de 5 pph et celui de Cloisite-Na est de 10 pph, lorsque mentionné.

Ces images montrent encore une fois le passage d'un état floculé à un état dispersé des MFC par ajout de Cloisite-Na. De plus, aucun agrégat n'est présent lorsque la couche contient à la fois des MFC et de la Cloisite-Na, ce qui suggère que les MFC ont un effet dispersif suffisant sur ces argiles plates pour permettre la formation de couches sans-défauts. Les agrégats présents dans la couche de PVOH:Cloisite-Na ont été responsables d'une perte de barrière à l'oxygène. La couche de PVOH:MFC:Cloisite-Na, quant à elle, a pu conserver sa barrière à l'oxygène par l'absence d'agrégats tout en bénéficiant d'une amélioration de la barrière à la vapeur d'eau de par la présence de Cloisite-Na bien dispersée.

Conclusions et perspectives

L'emballage alimentaire nécessite des couches barrières pour empêcher la perméation de différentes substances à travers l'emballage, afin d'augmenter la durée de consommation et limiter la gâche alimentaire. Le marché de l'emballage alimentaire évolue vers l'utilisation de produits ayant un meilleur impact environnemental, en particulier en utilisant des polymères biosourcés et/ou biodégradables. Parmi ces solutions, les microfibrilles de cellulose (MFC) ont des propriétés intrinsèques de barrière à l'oxygène et à la graisse, et peuvent être introduites dans des sauces de couchage base aqueuse afin d'améliorer la formation de couche. Cependant, deux principaux verrous subsistent : les suspensions de MFC sont hautement visqueuses à faible taux de matière sèche, et les couches comprenant des MFC manquent de résistance à l'eau et à l'humidité. Cette thèse a démontré l'opportunité d'utiliser des MFC pour le développement de couches barrières par deux stratégies :

- L'application d'une couche 100% MFC sur carton par lamination humide, permettant de s'affranchir de la haute viscosité des suspensions de MFC à faible taux de matière sèche par une étape de filtration. Cette approche innovante en est à ses débuts et son application industrielle requiert encore de la recherche et du développement.
- L'utilisation de MFC comme additif dans une formulation composite de couchage barrière base aqueuse, utilisant la réticulation et des argiles plates afin d'améliorer la résistance à l'eau et à l'humidité. Cette approche a été développée afin de pouvoir être applicable le plus directement possible sur coucheuse industrielle.

Cette étude a mis en évidence l'utilisation préférentielle de la densité des films et la fraction de résidus macroscopiques présents en suspension (observés par analyse d'image de type MorFi) comme méthodes indirectes pour caractériser le degré de fibrillation, indépendamment de la source des fibres. La rhéologie des suspensions ainsi que les propriétés mécaniques et optiques des films, en revanche, n'ont été pertinentes que pour suivre l'évolution de la fibrillation d'une pâte. La nécessité d'utiliser des MFC hautement fibrillées a été démontrée dans le case de couches 100% MFC. Des MFC ayant un faible taux de fibrillation forment des films poreux et perméables à l'oxygène. Des couches 100% MFC ont pu être appliquées sur carton par un procédé de lamination humide comprenant une étape de filtration. La couche a pu avoir une bonne adhésion au carton sans nécessiter de colle. La haute barrière à la graisse et à l'oxygène des MFC a pu être conservée à la condition d'avoir un poids de couche suffisant.

La nécessité d'utiliser des MFC hautement fibrillées a aussi été démontrée dans le cas de formulations composites de MFC et d'alcool polyvinylique (PVOH), un polymère hydrosoluble, avec application à du couchage barrière base aqueuse. Cette étude a montré l'utilisation préférentielle d'un faible taux de MFC dans un PVOH totalement hydrolysé ayant un faible degré de polymérisation, pour la réalisation de suspensions de faible viscosité permettant de produire des films à la barrière améliorée. En utilisant le grade de MFC, taux de MFC, et grade de PVOH appropriés, le séchage de suspensions PVOH et PVOH:MFC a été étudié sur un banc de séchage de laboratoire. Cela a permis de montrer une amélioration du séchage en présence de MFC, associée à une aptitude des MFC à entraver la formation d'une peau en surface. Les propriétés de couches PVOH et MFC ont pu être améliorées vis-à-vis de l'eau par réticulation grâce à l'acide citrique, et vis-à-vis de l'humidité par un traitement thermique à 105°C ou 150°C. La barrière en atmosphère

humide a aussi pu être améliorée par ajout d'argiles plates, dans le cas de films autoportés comme de cartons couchés. L'utilisation combinée de MFC et d'argiles plates a eu un effet positif sur leurs dispersions. Cet effet est particulièrement efficace dans le cas de suspensions concentrées appliquées au couchage base aqueuse, permettant d'obtenir un couchage sans agrégats grâce aux MFC tout en bénéficiant d'une amélioration de la barrière grâce aux argiles plates.

Pour conclure, l'utilisation de MFC est prometteuse en tant que couche barrière 100% MFC et en tant qu'additif dans une formulation pour couchage barrière base aqueuse. La première stratégie exploite les propriétés barrières intrinsèques des MFC grâce à un procédé développé récemment. La seconde stratégie s'appuie sur la capacité des MFC à améliorer le séchage d'une solution de polymère hydrosoluble et à y disperser des argiles plates.

Ce travaille laisse place à un certain nombre de perspectives. Une amélioration du procédé de fabrication pour éviter la présence de résidus macroscopiques, ou une étape de fractionnement, pourrait permettre de produire des couches 100% MFC laminées sur carton sans défauts à poids de couche plus faible. Les différentes étapes du procédé pourraient être étudiées plus en détail en vue d'un passage à l'échelle pilote : filtration, report, séchage. La filtration pourrait être accélérée en utilisant du chitosane cationique faisant floculer les MFC (Liu and Berglund, 2012), une filtration trop lente pouvant être déterminante quant à la vitesse de la machine. Le report pourrait nécessiter un renforcement mécanique du matelas humide de MFC afin de ne pas casser. Enfin, il a été vu qu'un traitement thermique influence la barrière des films de MFC. L'utilisation d'autres méthodes de séchage (conductif, convectif, par rayonnement), ou d'une combinaison de méthodes de séchage, pourrait apporter une structuration différente du matériau, de la performance barrière, et de l'adhésion.

La capacité des MFC à améliorer le séchage du PVOH a été démontrée sur des couches épaisses avec un banc de séchage de laboratoire. Un séchage plus fort, comme celui d'une coucheuse pilote, pourrait permettre d'observer un effet sur des épaisseurs de suspensions plus fines telles que celles obtenues par couchage. Il serait aussi d'intérêt de mieux cerner la quantité optimum de MFC à ajouter afin d'obtenir une amélioration du séchage et une dispersion des argiles plates tout en ayant la viscosité la plus faible possible. Afin de produire un emballage alimentaire base carton, des étapes de rainage, pliage, et collage sont nécessaires. Il faudrait étudier plus en détails la ductilité des couches composites comprenant des MFC afin de déterminer leur aptitude à être rainées et pliées. L'ajout d'un plastifiant pourra être requis, notamment si les couches sont réticulées par de l'acide citrique. La réticulation et l'ajout d'argiles plates ont permis d'améliorer la barrière à la vapeur d'eau à l'état humide mais n'ont pas modifié significativement la barrière à l'oxygène en conditions ambiantes. La barrière à l'oxygène à l'état humide pourrait, en revanche, avoir été améliorée ; son étude serait d'intérêt. Enfin, à ces perspectives scientifiques s'ajoutent l'étude de la capacité des couches développées à être réellement appliquées, considérant les contraintes économiques et réglementaires liées à l'emballage alimentaire. De plus, ces solutions sont développées dans une optique d'amélioration d'impact environnemental ; il faudrait vérifier cette amélioration par des tests de recyclabilité, biodégradabilité, et analyse de cycle de vie.

Références

Chen, W., Li, Q., Cao, J., Liu, Y., Li, J., Zhang, J., Luo, S., Yu, H., 2015. Revealing the structures of cellulose nanofiber bundles obtained by mechanical nanofibrillation via TEM observation. Carbohydr. Polym. 117, 950–956. doi:10.1016/j.carbpol.2014.10.024

Chinga-Carrasco, G., 2011. Cellulose fibres, nanofibrils and microfibrils: the morphological sequence of MFC components from a plant physiology and fibre technology point of view. Nanoscale Res. Lett. 6, 1–7.

Guezennec, C., 2012. Development of new packaging materials based on micro- and nano-fibrillated cellulose. PhD thesis, Université de Grenoble.

Kangas, H., Lahtinen, P., Sneck, A., Saariaho, A.-M., Laitinen, O., Hellen, E., 2014. Characterization of fibrillated celluloses. A short review and evaluation of characteristics with a combination of methods. Nord. Pulp Pap. Res. J. 29, 129–143.

Lavoine, N., Desloges, I., Khelifi, B., Bras, J., 2014. Impact of different coating processes of microfibrillated cellulose on the mechanical and barrier properties of paper. J. Mater. Sci. 49, 2879–2893. doi:10.1007/s10853-013-7995-0

Liu, A., Berglund, L.A., 2012. Clay nanopaper composites of nacre-like structure based on montmorrilonite and cellulose nanofibers—Improvements due to chitosan addition. Carbohydr. Polym. 87, 53–60. doi:10.1016/j.carbpol.2011.07.019

Nechyporchuk, O., Belgacem, M.N., Bras, J., 2016. Production of cellulose nanofibrils: A review of recent advances. Ind. Crops Prod. doi:10.1016/j.indcrop.2016.02.016

Nuopponen, M., Tamper, J., Kajanto, I., 2016. Method and device for monitoring the quality of nanofibrillar cellulose. WO2016001480 A1.

Paul, D.R., Robeson, L.M., 2008. Polymer nanotechnology: Nanocomposites. Polymer 49, 3187–3204. doi:10.1016/j.polymer.2008.04.017

Pöhler, T., Lappalainen, T., Tammelin, T., Eronen, P., Hiekkataipale, P.H., Vehniäinen, A., Koskinen, T.M., 2010. Influence of fibrillation method on the character of nanofibrillated cellulose (NFC), in: TAPPI International Conference on Nanotechnology for the Forest Products Industry. pp. 27–29.

Schmidt, W., Papier, G., Schlenstedt, M., Gericke, R., Fehlker, A., 2015. Receiving Layer for Digital Printing Methods Having Nanofibrillated Cellulose. US20150140237 A1.

Syverud, K., Stenius, P., 2009. Strength and barrier properties of MFC films. Cellulose 16, 75–85. doi:10.1007/s10570-008-9244-2

Résumé

Ce travail se situe dans un contexte de développement de matériaux barrières pour l'emballage alimentaire papier-carton utilisant des microfibrilles de cellulose (MFC), ce qui donne une dimension renouvelable, recyclable, et biodégradable. Pour cela, deux stratégies ont été étudiées : l'utilisation des MFC pour la formation d'une couche barrière laminée à l'état humide sur carton, et en tant qu'additif dans une sauce de couchage barrière base aqueuse. Il a été montré que l'utilisation des MFC pour la production de couches barrières est prometteuse dans les deux cas. La lamination de MFC sur carton a permis d'obtenir de bonnes propriétés barrières à l'oxygène et à la graisse en utilisant des MFC hautement fibrillées. L'association carton-MFC a présenté une forte adhésion après séchage, permettant d'éviter l'utilisation de colle. Dans le cas du couchage composite, en vue de diminuer la viscosité et améliorer la barrière, il a été trouvé préférable d'utiliser un faible taux de MFC dans un alcool polyvinylique (PVOH) complètement hydrolysé ayant un faible degré de polymérisation. L'ajout de MFC dans une sauce de couchage composite a montré leur capacité à améliorer la cinétique de séchage du PVOH. L'utilisation combinée de MFC et de charges lamellaires a présenté un effet de synergie sur leurs états de dispersions dans une solution de PVOH, permettant leur utilisation pour l'amélioration de la barrière à la vapeur d'eau en conditions humides, tout en évitant la formation d'agrégats qui détérioreraient la barrière à l'oxygène. Ce travail a contribué à démontrer le potentiel des MFC pour la formation de couches barrières, ouvrant la voie au développement de nouveaux matériaux d'emballages plus responsables.

Abstract

This study takes place in a context of development of paper-based barrier packaging materials, using of microfibrillated cellulose (MFC) that brings renewability, recyclability, and biodegradability. Two strategies have been investigated: the wet lamination of a MFC barrier layer on board, and the use of MFC as additive in a water-based barrier coating colour. The promising use of MFC for the formation of barrier layers has been demonstrated in both cases. The wet lamination of MFC on board led to good oxygen and grease barrier properties, using highly fibrillated MFC. The board-MFC complex presented a strong adhesion after drying, without requiring glue. In the case of barrier coating, in order to obtain a low viscosity suspensions leading to high barrier layers, the use of highly fibrillated MFC mixed with a fully-hydrolysed poly(vinyl alcohol (PVOH) of low degree of polymerisation has been preferred. The addition of MFC in PVOH demonstrated its potential for improving the drying behaviour of water-barrier barrier coating colours. The combined use of MFC and layered silicates evidenced a synergistic effect on their dispersion in a PVOH solution, leading to an improved water vapour barrier while avoiding the formation of aggregates that otherwise damage the oxygen barrier. The work contributed to demonstrate the potential of MFC to be used for the formation of barrier layers, paving the way for the development of more sustainable barrier packaging materials.

Keywords

Microfibrillated cellulose, barrier, composite, coating, packaging, poly(vinyl alcohol)